ICE SHEET SOURCES OF SEA LEVEL RISE AND FRESHWATER DISCHARGE DURING THE LAST DEGLACIATION

Anders E. Carlson[1,2] and Peter U. Clark[3]

Received 22 August 2011; revised 22 September 2012; accepted 25 September 2012; published 22 December 2012.

[1] We review and synthesize the geologic record that constrains the sources of sea level rise and freshwater discharge to the global oceans associated with retreat of ice sheets during the last deglaciation. The Last Glacial Maximum (~26–19 ka) was terminated by a rapid 5–10 m sea level rise at 19.0–19.5 ka, sourced largely from Northern Hemisphere ice sheet retreat in response to high northern latitude insolation forcing. Sea level rise of 8–20 m from ~19 to 14.5 ka can be attributed to continued retreat of the Laurentide and Eurasian Ice Sheets, with an additional freshwater forcing of uncertain amount delivered by Heinrich event 1. The source of the abrupt acceleration in sea level rise at ~14.6 ka (meltwater pulse 1A, ~14–15 m) includes contributions of 6.5–10 m from Northern Hemisphere ice sheets, of which 2–7 m represents an excess contribution above that derived from ongoing ice sheet retreat. Widespread retreat of Antarctic ice sheets began at 14.0–15.0 ka, which, together with geophysical modeling of far-field sea level records, suggests an Antarctic contribution to this meltwater pulse as well. The cause of the subsequent Younger Dryas cold event can be attributed to eastward freshwater runoff from the Lake Agassiz basin to the St. Lawrence estuary that agrees with existing Lake Agassiz outlet radiocarbon dates. Much of the early Holocene sea level rise can be explained by Laurentide and Scandinavian Ice Sheet retreat, with collapse of Laurentide ice over Hudson Bay and drainage of Lake Agassiz basin runoff at ~8.4–8.2 ka to the Labrador Sea causing the 8.2 ka event.

Citation: Carlson, A. E., and P. U. Clark (2012), Ice sheet sources of sea level rise and freshwater discharge during the last deglaciation, *Rev. Geophys.*, *50*, RG4007, doi:10.1029/2011RG000371.

1. INTRODUCTION

[2] Ever since the landmark study of *Fairbanks* [1989] on the last deglacial *relative sea level (RSL)* history from Barbados, paleoclimatologists have debated the timing, rates, and ice sheet sources of sea level rise (Figure 1). In particular, *Fairbanks* [1989] identified two intervals during the last deglaciation where sea level rise accelerated, which he termed *meltwater pulses (MWPs)* 1A and 1B, that occurred at ~14.6 and 11.3 ka, respectively [*Bard et al.*, 1990]. What became readily apparent, however, was that these two intervals of more rapid ice sheet melting did not correspond with periods of reduced *Atlantic meridional overturning circulation (AMOC)* and a colder climate in the North Atlantic region such as the *Younger Dryas* cold period from ~12.9 to 11.7 ka [*Boyle and Keigwin*, 1987; *Broecker*, 1990; *McManus et al.*, 2004], which, if these events originated from Northern Hemisphere ice sheets, questioned the commonly held hypothesis that increased meltwater discharge to the North Atlantic reduced the AMOC [*Birchfield and Broecker*, 1990; *Manabe and Stouffer*, 1995; *Stocker and Wright*, 1991]. Alternatively, retreat of the Antarctic Ice Sheet (AIS) may have contributed a significant component of one or more of these MWPs [*Clark et al.*, 1996; *Peltier*, 1994], or the relationship between meltwater discharge and AMOC may not be as sensitive as climate models suggest [*Stanford et al.*, 2006; *Tarasov and Peltier*, 2005].

[3] A different mechanism that could explain reductions in AMOC and North Atlantic cold events involves the location of continental runoff discharge relative to regions of deep water formation. In another landmark study building on previous considerations [*Johnson and McClure*, 1976; *Rooth*, 1982], *Broecker et al.* [1989] suggested that routing

[1]Department of Geoscience and Center for Climatic Research, University of Wisconsin–Madison, Madison, Wisconsin, USA.
[2]Now at College of Earth, Ocean, and Atmospheric Sciences, Oregon State University, Corvallis, Oregon, USA.
[3]College of Earth, Ocean, and Atmospheric Sciences, Oregon State University, Corvallis, Oregon, USA.

Corresponding author: A. E. Carlson, College of Earth, Ocean, and Atmospheric Sciences, Oregon State University, Corvallis, OR 97331, USA. (acarlson@coas.oregonstate.edu)

8755-1209/12/2011RG000371
Paper number 2011RG000371

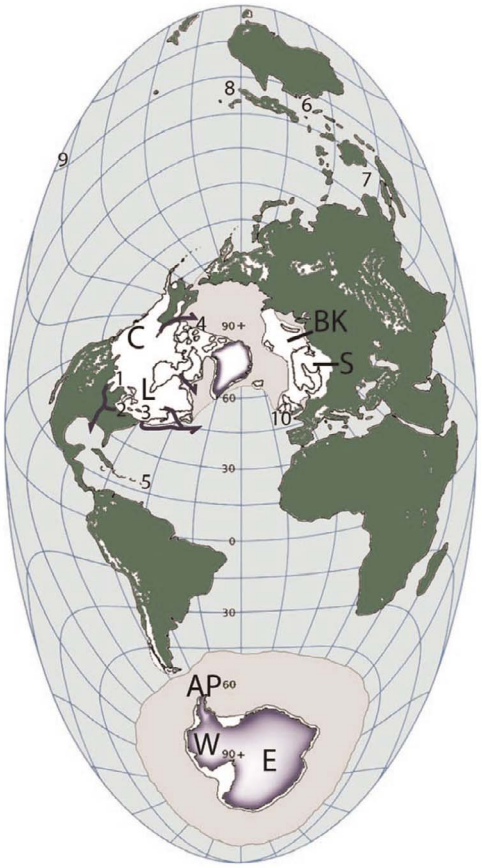

Figure 1. Ice sheet extent at the LGM [*Clark and Mix*, 2002; *Denton et al.*, 2010] with ice sheets discussed in text labeled by their first initial. Ice also covers Greenland and British Isles, but these are not labeled nor discussed as they only contributed a small fraction of the sea level change across the last deglaciation [*Clark and Mix*, 2002]. Also shown are the LIS runoff outlets (arrows), portions of the LIS discussed (numbered as follows: 1, James and Des Moines lobes; 2, Green Bay, Lake Michigan, and Lake Huron lobes; 3, New England; and 4, Canadian Arctic Archipelago), and locations of relative sea level records (numbered as follows: 5, Barbados; 6, Bonaparte Gulf; 7, Sunda Shelf; 8, New Guinea; 9, Tahiti; and 10, Ireland Coast).

of North American runoff from the Mississippi River to the St. Lawrence River (Figure 1) from retreat of the southern *Laurentide Ice Sheet (LIS)* north of the Great Lakes reduced AMOC and caused the Younger Dryas cold event. Such routing events do not necessarily cause changes in sea level and may have caused other deglacial AMOC reductions [*Clark et al.*, 2001; *Obbink et al.*, 2010; *Thornalley et al.*, 2010]. This routing hypothesis with respect to the Younger Dryas (and other cold events as well) has been questioned based on interpretations of St. Lawrence salinity proxies [*de Vernal et al.*, 1996; *Keigwin and Jones*, 1995], the southern LIS margin chronology [*Fisher et al.*, 2009; *Lowell et al.*, 2009], and ice sheet model simulations [*Tarasov and Peltier*, 2005], posing a fundamental problem of what caused deglacial AMOC reductions if not MWPs or routing events [*Broecker*, 2006; *Steig*, 2006].

[4] In the 23 years since the *Fairbanks* [1989] and *Broecker et al.* [1989] studies, a large amount of new data have become available that better constrain the timing and magnitude of sea level rise as well as ice sheet margin and runoff histories. Similarly, significant advances in climate and ice sheet modeling allow for further testing of hypotheses on the relationship between MWPs, runoff routing, AMOC strength, and abrupt climate change. Here we review the RSL records for the last deglaciation and the geologic data constraining potential ice sheet sources of sea level rise, focusing on periods of rapid sea level rise at ~19 ka and during MWP-1A, MWP-1B, and the early *Holocene*. We also examine the history of meltwater discharge and freshwater routing for Northern Hemisphere and Antarctic ice sheets and their relationship to periods of abrupt climate change such as the Oldest and Younger Dryas cold events, the *Bølling* and *Allerød* warm periods, and the *8.2 ka event*.

[5] The term "eustatic" sea level has conventionally been used to refer to a uniform global sea level change either due to changes in the volume of water in the world oceans or net changes in the volume of the ocean basins. Because these are two separate controls on sea level (albeit a change in the volume of water affects the volume of the ocean basin through *isostasy*), however, referring to sea level change without distinguishing between the controls is ambiguous. Moreover, several factors cause regional sea level to differ from the global mean on a range of time scales [*Milne et al.*, 2009], so the concept of a uniform rise of sea level is invalid. In the Birch Lecture titled "Eulogy for eustasy" presented at the 2009 AGU meeting, Jerry Mitrovica recommended that the term "eustatic" no longer be used. We follow this recommendation, and we use instead the term global mean sea level (GMSL) to refer to spatially averaged sea level that reflects the combined signals of (largely) mass and basin volume. To specifically identify the ice sheet volume contribution to GMSL, we refer to ice-equivalent sea level [*Yokoyama et al.*, 2000].

[6] Of the various factors that contribute to regional sea level variability on glacial-interglacial time scales, the *glacial isostatic adjustment (GIA)* process had the largest influence and caused sea level at nearly any location in the world's oceans to differ from the global mean during the last deglaciation [*Clark et al.*, 1978; *Lambeck and Chappell*, 2001; *Milne and Mitrovica*, 2008] (Figure 2). RSL records thus cannot be compared directly to each other without accounting for GIA effects. We further illustrate this by comparing RSL at far-field sites to ice-equivalent sea level derived from a model (Figure 3a) [*Bassett et al.*, 2005], which shows that RSL at any particular site differs relative to each other as well as to the global mean, particularly in the earlier half of the delaciation. We then adjust the RSL data for GIA (Figure 3c) using a model prediction of RSL for each site (Figure 3b) [*Bassett et al.*, 2005], which now shows good agreement between the adjusted sea level data and ice-equivalent sea level.

[7] This review discusses the major intervals or episodes of sea level rise and freshwater discharge through the last deglaciation, with a broad summary of geological data

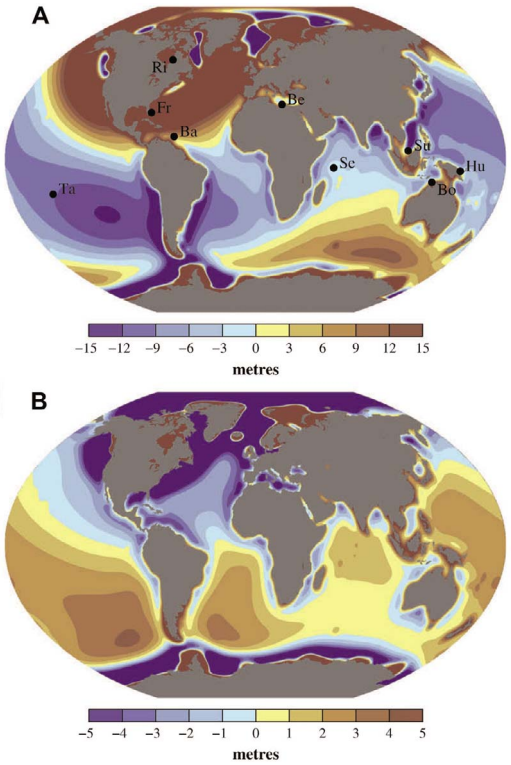

Figure 2. Predicted total RSL change minus the model eustatic (i.e., ice volume equivalent) component for a time window extending from either (a) 21 ka or (b) 6 ka to the present day. The zero contour marks where the total RSL is equal to the model eustatic value, with red and blue colors indicating sea levels that are above and below the eustatic value, respectively. The darkest red and blue colors indicate regions where the departure from eustatic sea level is greater than 15 m (Figure 2a) and 5 m (Figure 2b) (these colors are not shown on the color bar). Locations of sites referred to in this paper are shown (Tahiti (Ta), Barbados (Ba), Sunda Shelf (Su), Bonaparte Gulf (Bo), and Huon Peninsula (Hu)). From *Milne and Mitrovica* [2008], copyright 2008, with permission from Elsevier.

related to these episodes, an assessment of various hypotheses derived from that data, and a suggestion for where future progress might be made. We progress sequentially through the deglaciation starting with the end of the *Last Glacial Maximum (LGM)* and ending in the Holocene (refer to Figure 3c). Section 2 discusses RSL records that provide evidence for the first sea level rise from the LGM *lowstand* at 19–19.5 ka. Section 3 discusses the interval from 19 to 14.6 ka when sea level appears to have risen gradually but during which a major episode of ice discharge from the LIS occurred, referred to as *Heinrich event* 1. Section 4 summarizes the evidence for an episode of rapid sea level rise referred to as MWP-1A, while sections 5–7 evaluate the various lines of evidence that provide constraints on the sources of and their contributions to this event. Section 8 discusses another interval of relatively gradual sea level rise from ~14–12.7 ka as well as episodes of freshwater routing to the ocean from North America. Section 9 focuses on the various hypotheses that have been proposed for the Younger Dryas cold interval, most of which involve an increase in freshwater flux either from routing or a flood. Section 10 reviews the sea level rise during the Holocene as well as episodes on increased freshwater flux from routing or lake drainage, notably associated with the 8.2 ka cold event. Section 11 provides a general summary as well as recommendations for future research. We also include a glossary of terms at the end of the manuscript.

2. ONSET OF SEA LEVEL RISE AT 19.0–19.5 KA

[8] Several sites have reported evidence for an abrupt rise of sea level at ~19–19.5 ka that terminated the LGM

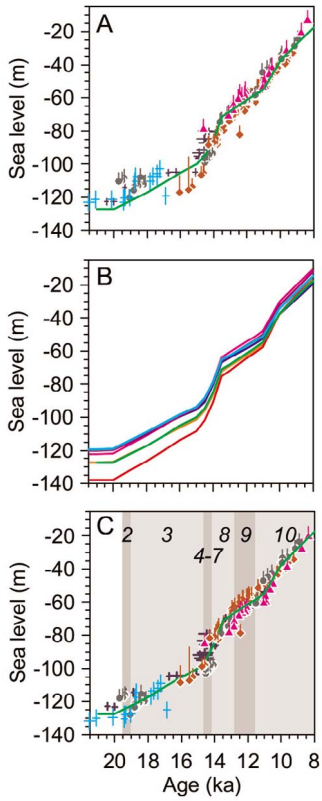

Figure 3. (a) Relative sea level data from 21.5 ka to 8 ka from Bonaparte Gulf (cyan crosses) [*Yokoyama et al.*, 2000], Barbados (gray circles) [*Peltier and Fairbanks*, 2006], Tahiti (brick red diamonds) [*Bard et al.*, 1996, 2010; *Deschamps et al.*, 2012], New Guinea (pink triangles) [*Edwards et al.*, 1993; *Cutler et al.*, 2003], and Sunda Shelf (purple crosses) [*Hanebuth et al.*, 2000, 2009]. Green line is ice-equivalent sea level history from *Bassett et al.* [2005]. (b) Predicted RSL histories for Barbados (blue line), New Guinea (magenta line), Sunda south (orange line), Sunda north (purple line), Bonaparte (cyan line), and Tahiti (red line) as compared to ice-equivalent sea level history (green line). Reprinted with permission from *Bassett et al.* [2005], copyright 2005, American Association for the Advancement of Science, http://www.sciencemag.org. (c) RSL data from far-field sites listed in Figure 3a after they have been adjusted for the ice-equivalent sea level history (green line). The numbers refer to the sections in this paper that correspond with the intervals shown by vertical gray bars.

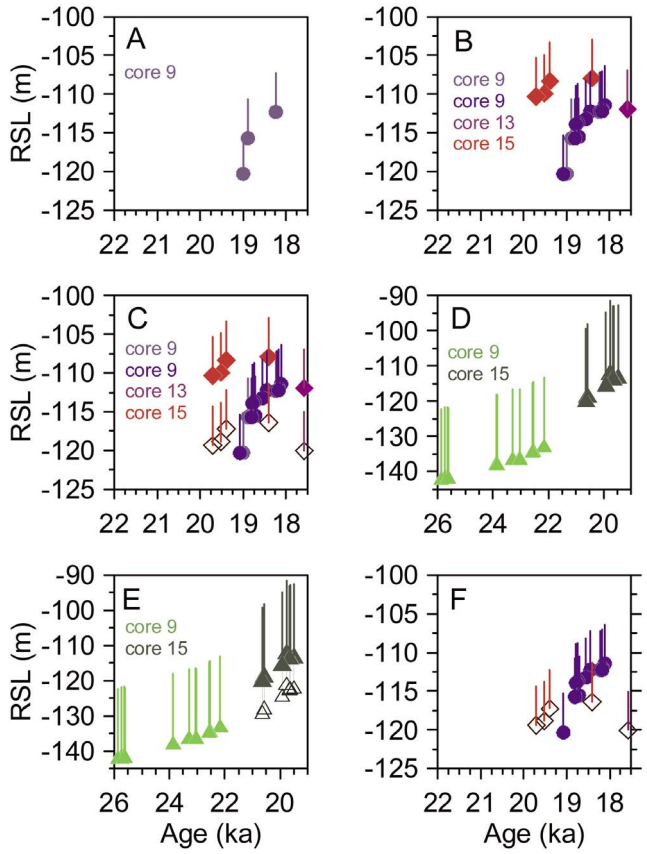

Figure 4. Relative sea level (RSL) data from Barbados constraining the 19 ka sea level event. (a) U/Th ages on the coral *A. palamata* from core 9 as published by *Bard et al.* [1990]. (b) U/Th ages on the coral *A. palamata* from core 9 published by *Fairbanks et al.* [2005] (dark blue symbols), which include replicates of those published by *Bard et al.* [1990] (light blue) as well as new ages from cores 13 and 15. (c) As in Figure 4b but now including the effects of a greater uplift rate (-0.8 m kyr^{-1}) applied to cores 13 and 15 (open symbols) as compared to the standard uplift rate that is conventionally applied (-0.34 m kyr^{-1}) (see text). (d) U/Th ages on the coral *M. annularis* reported by *Fairbanks et al.* [2005] from cores 9 and 15. (e) As in Figure 4d but now including the effects of a greater uplift rate (-0.8 m kyr^{-1}) applied to core 15 (open symbols) as compared to the standard uplift rate that is conventionally applied (-0.34 m kyr^{-1}) (see text). (f) Summary of Barbados U/Th ages on the coral *A. palmata* from core 9 with an uplift rate of -0.34 m kyr^{-1} and cores 13 and 15 with a higher uplift rate of -0.8 m kyr^{-1}. Age uncertainty is shown for all samples; where not visible, the uncertainty is less than the symbol size.

lowstand. The onset of the deglacial sea level rise at this time is consistent with the chronological constraints for onset of deglaciation of most Northern Hemisphere ice sheets [*Clark et al.*, 2009] as well as sectors of the Antarctic ice sheets [*Heroy and Anderson*, 2007; *Smith et al.*, 2010; *Weber et al.*, 2011] between 19 and 20 ka. Based on more recently dated corals from Barbados, however, *Peltier and Fairbanks* [2006] disputed the existence of this rapid rise in sea level. Here we review the sites where the event has been described and assess those data that appear to be in conflict with the event.

2.1. Barbados

[9] *Fairbanks* [1989] and *Bard et al.* [1990] reported the first dates on corals from a Barbados core (core 9) drilled into a submerged coral reef that suggested there may be a rapid rise in sea level at ~19 ka (Figure 4a). The dated corals are the reef crest species *Acropora palmata*, which are generally considered to live within 5–6 m of the water surface, although they have been reported as living to depths of 17 m [*Bard et al.*, 2010]. A simplistic interpretation of the three samples of *A. palmata* from core 9 dated by U-Th is that they indicate a rise of ~5 m within ~100 years followed by another ~3 m in ~600 years. Because there were no older samples of *A. palmata* available from the Barbados cores (Figure 4a), however, the possible full amplitude of sea level rise at this time remained unconstrained, as did the possibility that sea level began to rise at an earlier time. Moreover, given that the depth range of this species (5–6 m) is within the amount of rise suggested by the vertical offset between samples defining the initial rise, it is possible that the actual sea level rise may have been less. On the other hand, these species also have the potential to live at water depths greater than 5 m, particularly during periods of sea level rise [*Neumann and Macintyre*, 1985], indicating that the actual sea level rise may have been greater.

[10] Additional dating of *A. palmata* samples from core 9 [*Fairbanks et al.*, 2005; *Peltier and Fairbanks*, 2006] replicated the three previous ages as well as supported the suggestion that sea level rise was initially rapid and subsequently decelerated (Figure 4b). Nevertheless, the question of how much sea level rose prior to 19 ka remained unresolved by these new dates. More importantly, however, *Peltier and Fairbanks* [2006] also reported ages on *A. palmata* from core 15 which suggested that sea level was ~10 m higher than suggested by the one sample (RGF 9-27-5) constraining the start of the rise in core 9 (Figure 4b), leading *Peltier and Fairbanks* [2006, p. 3326] "to rule out the occurrence of any such sharp change of eustatic sea level back to the conventionally assumed LGM age of 21 ka."

[11] One possible explanation for this discrepancy in the sea level history between 20 and 18 ka is that the Barbados cores in question (cores 9 and 15) have experienced different uplift histories. Because Barbados is located on an accretionary prism at a convergent plate margin, it is subject to significant but variable flexure as well as faulting [*Taylor and Mann*, 1991], resulting in different amounts of uplift around the island. *Bard et al.* [2010] proposed that this tectonic setting may partly explain the amplitude of a younger episode of rapid sea level rise first recognized at Barbados and referred to as MWP-1B [*Fairbanks*, 1989] (see section 10.1.1). In particular, *Bard et al.* [2010] found that there was little or no expression of this event in their new more-complete sea level record from Tahiti, whereas the Barbados record suggested an amplitude of as much as 15 m. The event at Barbados is defined by a core gap, however, with the beginning of the event inferred from the youngest age in core 12 and the

end of the event inferred from the oldest age in the shallower core 7. Because cores 7 and 12 were drilled on opposite sides of a possible offshore extension of a tectonic structure mapped on the island (Figures 5a and 5c), *Bard et al.* [2010] suggested that core 7 on the south side of the structure may have experienced a higher uplift rate than core 12 on the north side. Accounting for these different rates would reduce the amplitude of MWP-1B at Barbados so as to be more consistent with the Tahiti data.

[12] Such a scenario of differing uplift rates relative to the presumed offshore tectonic structure could also explain the otherwise apparent discrepancy in sea level at ~19 ka suggested from Barbados cores 9 and 15. Like the two cores used to infer MWP-1B, cores 9 and 15 are found on different sides of the possible seaward extension of the tectonic structure (Figure 5a). Similarly, a greater uplift rate applied to the south side of the presumed structure would not only reduce the amplitude of MWP-1B so as to be more consistent with the Tahiti data [*Bard et al.*, 2010] but would also result in the dated corals from core 15 drilled on the south side of the fault to be at a similar paleo–sea level as suggested by those in core 9, which was drilled to the north of the fault (Figures 4c and 5c). Further support for differential uplift of these two cores is suggested by comparing U-Th ages on the coral species *Montastrea annularis.* Although this species has a greater depth range (~20 m) than *A. palmata*, there is still a distinct change in sample depth between the youngest sample in core 9 dated at 22.16 ± 0.12 ka and the oldest sample in core 15 dated at 20.63 ± 0.06 ka (Figure 4d), which largely disappears when adopting the higher uplift rate for core 15 (Figure 4e).

[13] We note that one sample from core 13 collected from the south side of the presumed tectonic structure (Figure 5a) becomes anomalously deep when a higher uplift rate is applied to it (Figure 4c). Given the consistency of all other Barbados samples when applying this higher rate, we consider this one sample to simply have lived at a water depth greater than 5 m.

[14] In summary, application of a larger long-term uplift rate to Barbados cores on the south side of a presumed offshore extension of a known onshore tectonic structure would not only make the Barbados sea level history be more consistent with the Tahiti sea level record in constraining the amplitude of MWP-1B [*Bard et al.*, 2010] but also make for a more consistent sea level history for the older part of the record (23–18 ka) derived from the Barbados cores themselves. In particular, these data suggest that sea level rose 5–10 m sometime between 19.5 and 18.8 ka (Figure 4f).

2.2. Bonaparte Gulf

[15] *Yokoyama et al.* [2000, 2001] reconstructed sea level based on microfaunal assemblages in 10 sediment cores collected from the Bonaparte Gulf on the continental shelf adjacent to northwestern Australia. Unlike the Barbados region, the Australian continental shelf is tectonically stable as well as far removed from the direct loading effects of the Northern Hemisphere ice sheets. *Yokoyama et al.* [2000, 2001] used faunal assemblages and sediment facies to distinguish four water conditions (with estimated water depths): open marine (~20 m), shallow marine (~10 m), marginal marine (<5 m), and brackish conditions (mean sea level ±3 m). From these associations, they argued that the LGM lowstand, marked by marginal marine and brackish water facies in the deeper water cores GC4 and GC5, was terminated by a rapid sea level rise of 10–15 m at ~19 ka, marked by marginal marine facies in the shallower water cores GC6, GC7, GC10, and GC11 (Figures 6a and 6b). In this regard, the sea level rise at ~19 ka suggested from Barbados corals is likely the same event as identified at Bonaparte, with the Bonaparte data first demonstrating that this event marked the termination of the LGM lowstand.

[16] *Shennan and Milne* [2003] raised several issues with the Bonaparte sea level reconstruction. First, they noted that there must be hiatuses in the sediment cores, which would complicate a presumed continuous sequence of changing sea level inferred from vertical facies changes. As explained by *Yokoyama et al.* [2003], however, this issue arose because of an erroneous statement made in *Yokoyama et al.* [2000] that no hiatuses occurred, which had been corrected and clearly illustrated in *Yokoyama et al.* [2001]. Regardless of whether hiatuses existed, however, the key to the sea level reconstruction is the dated index points, i.e., establishing brackish or marginal marine conditions at a given point in time, similar to individual index points from corals. Second, by inferring that all brackish water facies in all cores represented the LGM RSL, *Shennan and Milne* [2003] argued that the reconstructed LGM RSL differed by up to 25 m between deeper and shallower water cores. *Yokoyama et al.* [2003] pointed out that this assumption is only valid if the brackish water facies are dated to the LGM. Each of the examples of the brackish facies discussed by *Shennan and Milne* [2003] that indicate anomalously shallow LGM RSLs were undated, however, whereas those brackish facies that are dated, which are all from core GC5, consistently indicate an LGM RSL of −120 to −125 m (Figure 6). The undated brackish facies may thus represent any time that sea level approached zero at a particular core location. Third, *Shennan and Milne* [2003] noted that in core GC5, which is the key core for constraining the LGM lowstand, a hiatus before 21.3 ka followed by deposition of brackish water facies indicates that the sea level rose earlier than 19 ka and that the brackish water facies do not represent the LGM lowstand. *Clark et al.* [2009], however, showed that a RSL rise at Bonaparte Gulf would occur during a long-duration (6 kyr) LGM in response to the antisiphoning effect associated with the GIA process. Fourth, *Shennan and Milne* [2003] pointed out several inconsistencies in water depth reconstructions, indicating that the water depth constraints derived from the faunal analyses may need to be increased. This is clearly apparent, for example, in Figure 6b, where a number of sea level index points fall well below other index points from Bonaparte cores as well as index points from other far-field records. *Yokoyama et al.* [2003] acknowledged that depth uncertainties for facies other than brackish water may be larger than they first suggested. *De Deckker and Yokoyama* [2009] further addressed these uncertainties for core GC5. In particular, *Shennan and Milne* [2003] had

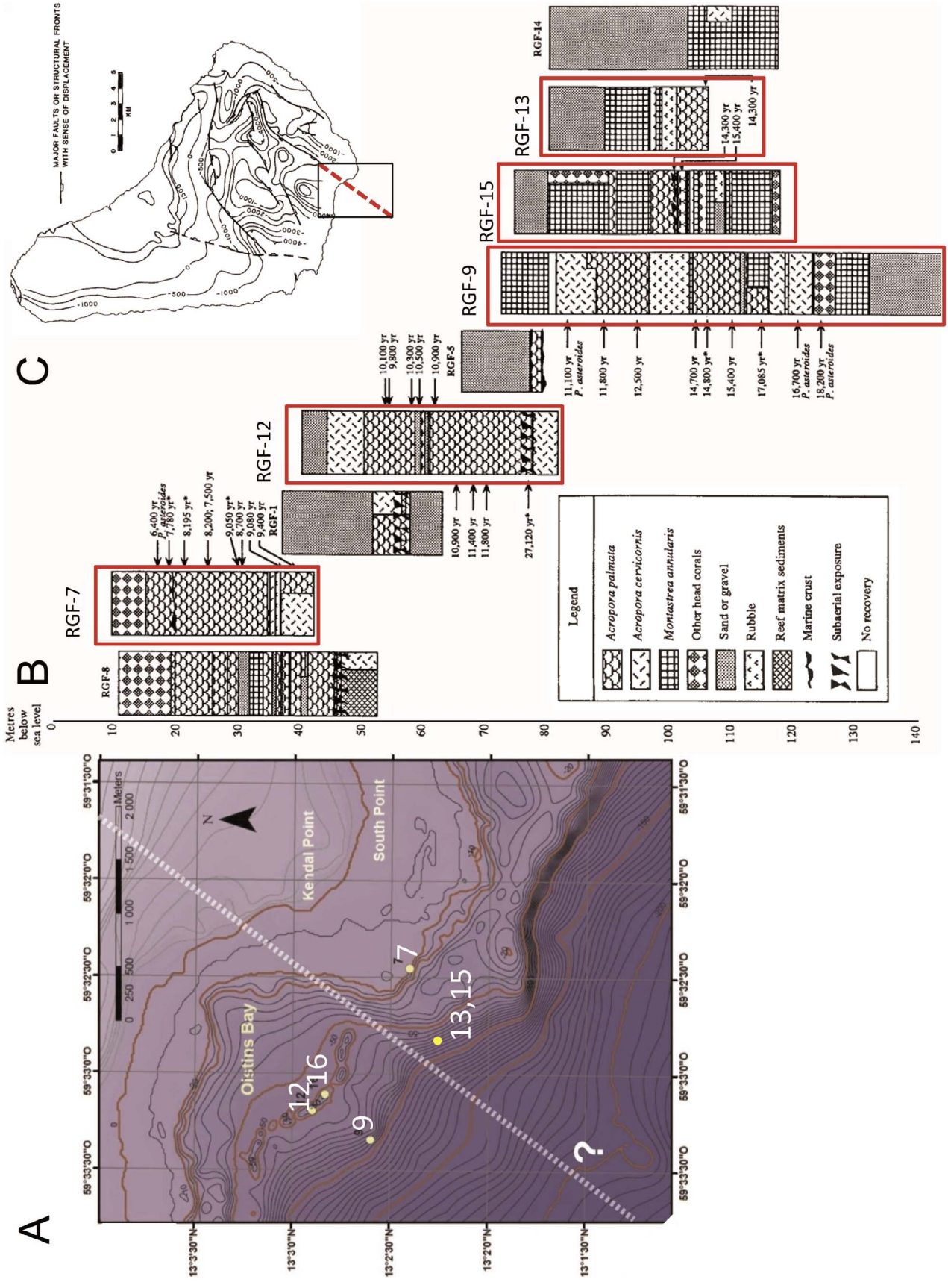
A
Oistins Bay
Kendal Point
South Point
12
16
9
7
13,15
?
Meters
N
B
RGF-7
RGF-8
RGF-12
RGF-1
RGF-5
RGF-9
RGF-15
RGF-13
RGF-14
Metres below sea level
Legend
Acropora palmata
Acropora cervicornis
Montastrea annularis
Other head corals
Sand or gravel
Rubble
Reef matrix sediments
Marine crust
Subaerial exposure
No recovery
C
MAJOR FAULTS OR STRUCTURAL FRONTS WITH SENSE OF DISPLACEMENT

Figure 5

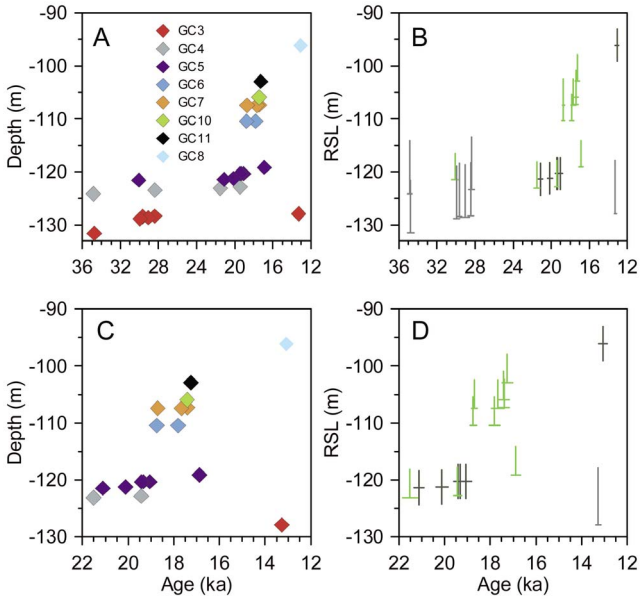

Figure 6. (a) Depth and age of samples from different cores obtained from Bonaparte Gulf constraining the 19-ka sea level event [*Yokoyama et al.*, 2000]. (b) Depth and age of samples from Bonaparte Gulf distinguished by their depositional facies (shallow marine is indicated by light blue, marginal marine is indicated by green, and brackish is indicated by dark green). (c) As in Figure 6a but for interval 22–12 ka. (d) As in Figure 6b but for interval 22–12 ka.

argued that the original published results from core GC5 conflicted with a rapid sea level rise at 19 ka in showing that the first dated sample of marginal marine facies after the brackish facies suggested a much more gradual rise than suggested by combining the dated sea level index points from other cores. However, there is a significant thickness of undated marginal marine facies below the dated horizon of that facies, and thus, the intervening sea level history could not be established from that one core. *De Deckker and Yokoyama* [2009] conducted high-resolution microfaunal analyses through this interval and found that fully marine conditions appeared in the core at an interpolated age of 18.8 ka, thus substantiating the rapid sea level rise of 5–10 m (when accounting for uncertainties in the faunal reconstructions) at ~19 ka previously reconstructed from sea level index points from several different cores [*Yokoyama et al.*, 2000, 2001].

2.3. Irish Sea

[17] *Clark et al.* [2004] described evidence from the Kilkeel site, Northern Ireland, that suggested rapid rise of sea level superimposed upon the isostatically uplifting coast of the Irish Sea following early deglaciation of the Irish Ice Sheet at >20 ka; deglaciation of the Irish Sea basin likely began ~1–2 kyr earlier [*Bowen et al.*, 2002]. Early deglaciation of the Irish Sea coast was accompanied by a high RSL due mainly to isostatic depression by the Irish Ice Sheet. The marine limit on the western margin of the Irish Sea Basin near Kilkeel is 30 m above sea level and formed between ~21 ka and 19 ka [*McCabe et al.*, 2007].

[18] Following deglaciation of the Irish Sea coast at Kilkeel, eastward flowing rivers draining the Mourne Mountains eroded several broad (~1 km wide) and deep (12–20 m) channels into existing glaciomarine sediments. These channels were graded to a RSL equivalent to or lower than present, indicating that the coast had isostatically emerged at least 30 m (the marine limit) by the time they had formed. Evidence that sea level subsequently rose is suggested by thick marine muds that now fill the erosional channels to a level ~10 m above sea level. *Clark et al.* [2004] dated five samples of the *foraminifera Elphidiun clavatum* by *accelerator mass spectrometer (AMS)* ^{14}C that were collected at four levels from the base to the top of the muds (Figure 7). The five ages indicate nearly instantaneous sedimentation of the muds, with radiocarbon ages at the base being statistically the same (at 1σ) as the radiocarbon age at the top of the sequence. Applying a standard modern *reservoir age* correction of 400 years to these five samples results in a mean calibrated age of 19.91 ± 0.16 ka. Larger reservoir age corrections, however, characterized the North Atlantic during the cold *stadial* periods of the last deglaciation, with reservoir ages of as large as 2000 years established for the *Oldest Dryas* interval [*Thornalley et al.*, 2011a; *Waelbroeck et al.*, 2001]. *Clark et al.* [2004] thus proposed that the lower end of estimates for cold period reservoir ages (1000 year correction (ΔR = 600 ± 200 years)) should be applied to the Kilkeel radiocarbon ages, yielding a corrected mean age of 19.25 ± 0.25 ka (the difference from *Clark et al.* [2004] reflects the newer calibration IntCal09) (Figure 7). *Hanebuth et al.* [2009] questioned the application of such a large reservoir age to a shallow water site subject to surface mixing and far from open Atlantic water masses. We note first that the deglaciating Irish Ice Sheet was still contributing ^{14}C-depleted meltwater to the Irish Sea and thus likely contributing to a higher reservoir age. Moreover, *Thompson et al.* [2011] used paired terrestrial and marine radiocarbon ages to document a reservoir age of ~1000 years from shallow marine sediments deposited along the Maine coast during the last deglaciation, far from the open Atlantic, providing a direct analogue of this effect.

[19] There are two possible ways to explain the sea level history suggested from the Kilkeel stratigraphy. Both of these involve initial isostatic emergence following deglaciation,

Figure 5. Details of core locations from Barbados. (a) Bathymetric map showing locations of cores 7, 9, 12, 13, 15, and 16 (reprinted with permission from *Bard et al.* [2010], copyright 2010, American Association for the Advancement of Science, http://www.sciencemag.org). The dashed white line shows the hypothetical extension of a tectonic structure mapped on Barbados (see Figure 5c), as proposed by *Bard et al.* [2010]. (b) Core logs from which samples were obtained [from *Fairbanks*, 1989]. (c) Map of Barbados showing tectonic structure from *Taylor and Mann* [1991] with possible offshore extension suggested by *Bard et al.* [2010].

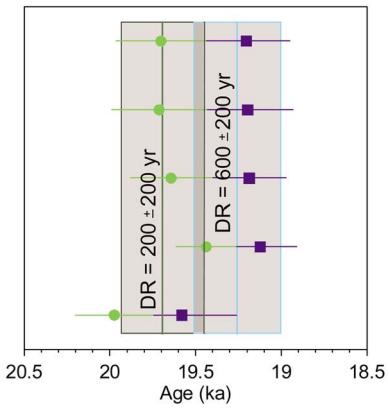

Figure 7. Calibrated radiocarbon ages on *E. clavatum* from the Kilkeel site, Northern Ireland, constraining the 19 ka sea level event [*Clark et al.*, 2004]. Green symbols are ages calibrated with a delta R of 200 ± 200 years and a 2σ error, with the mean age shown by a vertical dark green line and the average 2σ error shown by a box outlined in dark green. Blue symbols are ages calibrated with a delta R of 600 ± 200 years and a 2σ error, with the mean age shown by a vertical light blue line and the average 2σ error shown by a box outlined in light blue.

causing a RSL fall so that rivers flowing across the Mourne plain incised channels into glaciomarine sediments graded to a RSL similar to present. Sea level may then have risen due to renewed isostatic loading associated with an ice readvance or due to ice sheet melting. We discount the first possibility because there is no evidence for such a readvance, particularly of the scale needed to reverse isostatic uplift following the initial deglaciation. Instead, this early phase of deglaciation is thought to have continued with widespread ice sheet disintegration until the onset of an ice sheet readvance at ~18 ka [*McCabe et al.*, 2005]. Moreover, it is highly unlikely that any such renewed loading would cause such a rapid sea level rise as suggested by the radiocarbon constraints for near-instantaneous sedimentation in the channels. In support of a rapid ice-equivalent sea level rise, *Clark et al.* [2004] noted that the cut-and-fill nature of the channels suggests an erosional phase followed by a depositional phase, and the orientation of the channel axes suggests erosion by easterly flowing water draining the adjacent Mourne Mountains. *Clark et al.* [2004] excluded a subglacial origin for the channels because they are eroded into glaciomarine sediments that were deposited subaqueously [*McCabe*, 1986]. The orientation of the channel axes perpendicular to the coast indicates that if the channels were eroded subaqueously during high RSL by a continuation of easterly flowing streams draining the adjacent Mourne Mountains, then there should be deltas deposited by these streams at the contemporaneous sea level. The absence of any such deltas, however, suggests that this did not occur. *Clark et al.* [2004] also excluded a subaqueous origin because there is no a priori reason why subaqueous processes would initially be erosional, followed by a switch to processes that result in nearly instantaneous infilling of the channels by sediments, particularly on low slopes and at shallow water depths (~30 m). *Clark et al.* [2004] thus concluded that a subaerial origin best explains the erosional phase, which must have occurred after initial deglaciation of the Kilkeel coast and subsequent isostatic emergence. Subsequent rapid deposition of marine sediments in the channels thus requires a rapid rise in ice-equivalent sea level to flood the channels on what was otherwise still an isostatically emergent coast. The timing of local deglaciation (>20 ka) and the formation of the associated marine limit relative to the timing of channel filling (~19 ka) provides sufficient time for coastal emergence and subaerial channel erosion to occur.

[20] Although the reservoir age uncertainty introduces uncertainty in the calibrated age of the sea level event at Kilkeel, we emphasize four aspects that indicate that this event is correlative to the 19 ka sea level event identified from Barbados and Bonaparte. First, the Kilkeel stratigraphy clearly establishes that the rapid sea level rise is from ice sheet melting. Second, given the reservoir age uncertainties, the event is clearly within the age range of the 19 ka event. Third, the event has a similar amplitude (~10 m) as suggested from Barbados and Bonaparte Gulf sites, with regional variability in amplitude between sites expected from gravitational and rotational effects associated with rapid ice loss [*Clark et al.*, 2002; *Mitrovica et al.*, 2001]. Fourth, there is no other known event of rapid ice-equivalent sea level rise within the possible age range of the Kilkeel event (18–20 ka).

2.4. Sunda Shelf

[21] *Hanebuth et al.* [2009] reported 11 ^{14}C ages on organic matter from three cores that sampled sedimentary facies on the Sunda Shelf of southeastern Asia interpreted as recording shallow water, nearshore environments around the time of the LGM. A barrier bar–tidal flat facies inferred from seismic surveys suggested that sea level may have risen ~5 m during the LGM lowstand. *Hanebuth et al.* [2009] also reconstructed a sea level rise of ~10 m that they argued is equivalent to the 19 ka event, although they suggest that it may have occurred as early as 19.6 ka.

[22] Although the organic matter used for dating is terrestrial and thus is not subject to uncertainties in the marine reservoir age correction, the various materials dated (individual pieces of wood, in situ peat layers, and organic-rich bulk sediment) may have experienced either reworking or postdepositional migration of dissolved organic components. *Hanebuth et al.* [2009] argued that ages on wood and in situ fibrous peat should provide the most reliable ages, whereas reworking of plant remains on the Sunda Shelf has likely produced organic microfibers which contributed to the organic-rich bulk sediment, making them less reliable. In this regard, they noted that ages on bulk sediments may be up to 4 kyr younger than corresponding peat layers. To assess the possible impacts of postdepositional migration of dissolved organic compounds on their ^{14}C ages, *Hanebuth et al.* [2009] treated samples with an acid-leach-acid step that separates leachable from leach-resistant ("insoluble") components.

[23] Here we assess the dating results for each of their three cores with respect to constraining LGM sea level and a 19 ka event. In core 18726, there are two ages from the same horizon (−116.6 m water depth) on organic-rich bulk

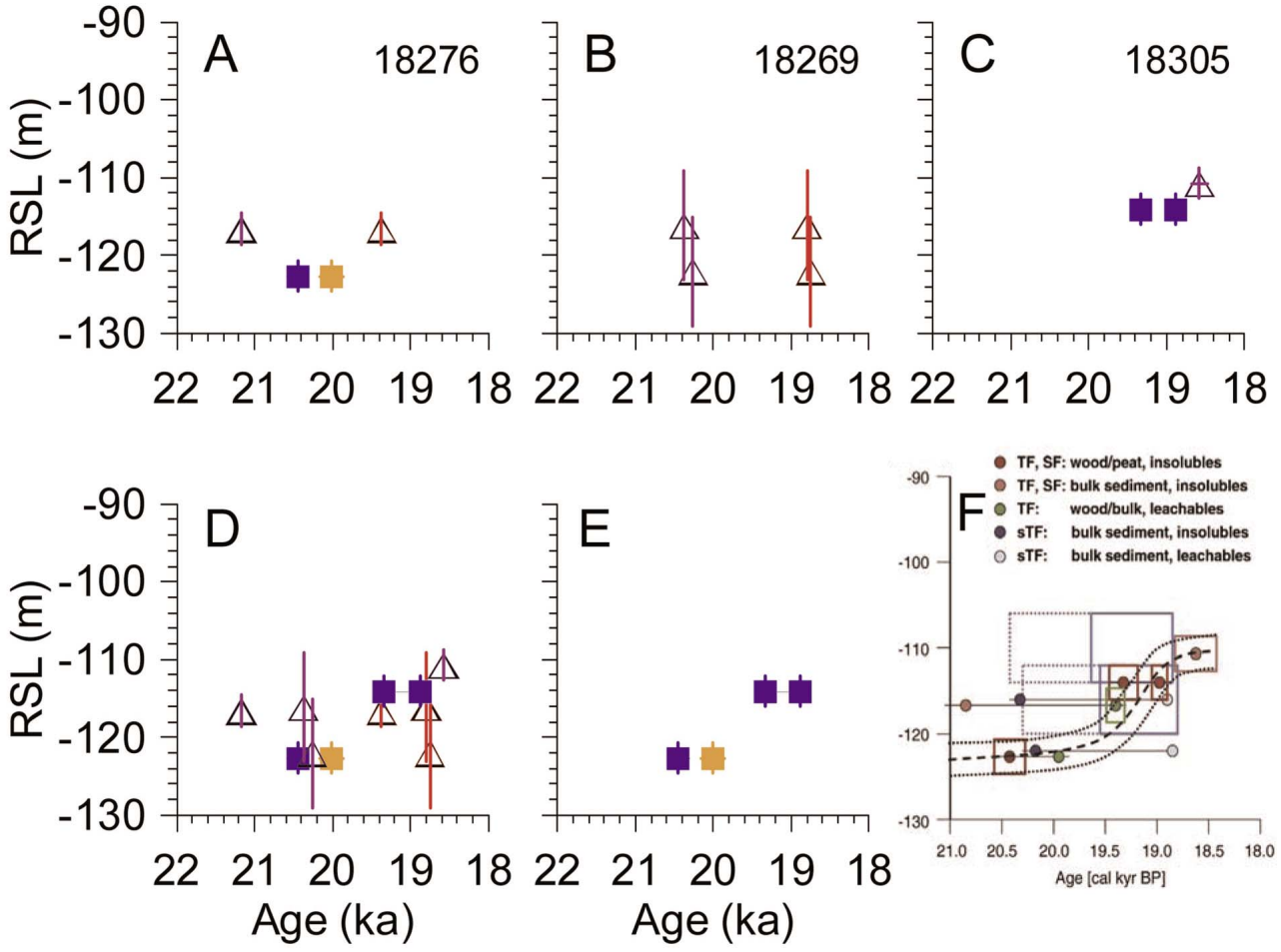

Figure 8. Calibrated radiocarbon ages constraining the 19 ka sea level event from Sunda Shelf [*Hanebuth et al.*, 2009]. (a) Data from core 18276. Triangles represent ages on bulk organic matter, and squares are ages on wood macrofossils. (b) Data from core 18269. Triangles represent ages on bulk organic matter. (c) Data from core 18305. Triangles represent ages on bulk organic matter, and squares are ages on wood macrofossils. (d) Data from all three cores. Triangles represent ages on bulk organic matter, and squares are ages on wood macrofossils. (e) The calibrated ages on wood macrofossils from cores 18276 and 18305 that provide the most reliable constraints on relative sea level. (f) Interpretation of the data by *Hanebuth et al.* [2009].

sediment, one on the leachable component and one on the insolubles. Although from the same horizon, they differ in age by ~1400 years (Figure 8a), and in the absence of any independent means of evaluating the accuracy of either age, we consider them unreliable. In contrast, two ages on wood from the same horizon (−122.7 m water depth), one on the leachable component and one on the insolubles, agree at 2σ (Figure 8a), thus providing a reliable constraint for relative sea level at ~20.2 ka. In core 18269, *Hanebuth et al.* [2009] reported two horizons with two ages each. All ages were on bulk sediment, and the differences between the ages on the leachable component versus the insolubles again are significant, with the leachables being consistently ~1400 years younger (Figure 8b). We thus also consider these as unreliable. In core 18305, *Hanebuth et al.* [2009] reported one age on the insoluble fraction of bulk organic sediment from −110.7 m water depth and two ages on wood from the same horizon (−114.1 m water depth), one on the leachable fraction and one on the insoluble fraction (Figure 8c). Given the previously documented large uncertainties in bulk organic sediment, we consider the bulk organic age in core 18305 unreliable. Because the two ages on wood only differ by 40 years at 2σ, we consider them as likely recording the time of relative sea level on Sunda Shelf at ~19 ka.

[24] In summary, radiocarbon ages on wood with differing treated fractions provide the only reliable ages for constraining relative sea level on Sunda Shelf at −122.7 m at ~20.2 ka and −114.1 m at ~19 ka (Figure 8e). *Hanebuth et al.* [2009] used these ages as well as those on bulk sediments to infer that sea level rose closer to 19.6 ka (Figure 8f), but this conclusion cannot be supported given the unreliability of the ages on bulk sediments. We also note that the

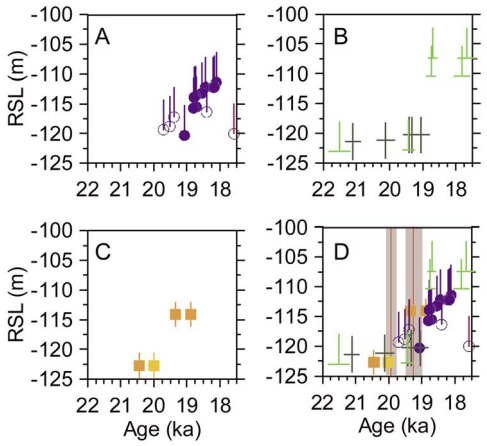

Figure 9. Summary of the data constraining the 19 ka sea level event from (a) Barbados, (b) Bonaparte Gulf, (c) Sunda Shelf, and (d) all data, including those from Kilkeel represented by mean age with a delta R of 600 ± 200 years and a 2σ error (vertical red line and gray band centered on 19.25 ka) and a mean age with a delta R of 0 years and a 2σ error (vertical red line and gray band centered on 19.9 ka). Age uncertainty is shown for all samples; where not visible, the uncertainty is less than the symbol size.

inferred rise in relative sea level of ~5 m during the LGM is consistent with the antisiphoning effect also suggested from the Bonaparte Gulf data [*Clark et al.*, 2009].

2.5. Summary

[25] In Figure 9, we summarize the most reliable data on the initial sea level rise from the LGM lowstand from the four sites where it has been documented. When combined, these data provide a robust scenario in supporting the original argument by *Yokoyama et al.* [2000] that the LGM lowstand was terminated by a rise of 5–10 m between 19.0 and 19.5 ka (Figure 9d), suggesting a rate of 8 mm yr^{-1} to 16 mm yr^{-1}. In their compilation of ages constraining the duration of the LGM of the global ice sheets, *Clark et al.* [2009] found that nearly all Northern Hemisphere ice sheet margins began to retreat from the LGM extents between 19 and 20 ka (Figure 10) in response to high northern latitude summer insolation. Although these data did not constrain the rate of ice margin retreat, they clearly indicate that the primary source of this initial rise of deglacial sea level was from widespread retreat of Northern Hemisphere ice sheets. However, there is now clear evidence that some sectors of the Antarctic Ice Sheets also began to retreat at this time [*Heroy and Anderson*, 2007; *Smith et al.*, 2010; *Weber et al.*, 2011], but their contributions to sea level rise relative to Northern Hemisphere ice sheets as well as the cause of their retreat and any attendant impact on climate remain unknown.

3. SEA LEVEL RISE AND FRESHWATER DISCHARGE FROM 19.0 TO 14.6 KA

3.1. Sea Level and Ice Sheet Records

[26] By comparison to other intervals, there are few constraints on RSL rise from far-field sites for the interval between the initial rapid rise at ~19 ka and the onset of another rapid rise beginning at ~14.6 ka (MWP-1A) (Figure 11a). The Barbados coral record is largely incomplete between ~18.12 ka (RGF 9-20-2) and ~14.54 ka (RGF 9-13-3) [*Fairbanks et al.*, 2005], with only one sample (RGF 13-8-9) at ~17.58 ka that has a large depth uncertainty owing to the possibility of a tectonic correction (section 2.1). The depth difference between the first core 9 sample following the 19 ka sea level event (RGF 9-23-5) and the first core 9 sample preceding the start of MWP-1A at ~14.6 ka (RGF 9-13-3) (and accounting for the 5 m depth uncertainty of *A. palmata* corals) suggests that RSL may have risen between ~18.78 and 14.54 ka by as little as 10 m (at 2.4 mm yr^{-1}) to as much as 20 m (at 4.7 mm yr^{-1}), with an average rate of 3.5 mm yr^{-1} (15 m rise) when using just the depth of each sample.

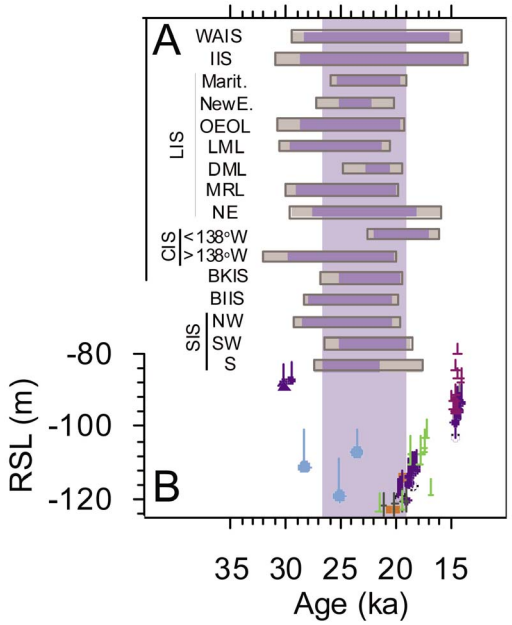

Figure 10. (a) Summary of chronologies constraining the duration of the Last Glacial Maximum for the primary global ice sheets and, where there are sufficient data, sectors of those ice sheets [*Clark et al.*, 2009]. Each horizontal blue bar represents the local LGM duration, with gray bar extensions representing age uncertainties. The vertical blue bar represents the LGM sea level lowstand, as constrained by relative sea level data shown in Figure 10b. Notation for the ice sheets and their sectors is as follows: West Antarctic Ice Sheet (WAIS), Innuitian Ice Sheet (IIS), Laurentide Ice Sheet (LIS) (with sectors for the Maritimes, New England, the Ontario-Erie-Ohio lobe, the Lake Michigan lobe, the Des Moines lobe, Mackenzie River lobe, and the northeastern sector), the Cordilleran Ice Sheet (CIS) (with sectors east and west of 138°W), the Barents-Kara Ice Sheet (BKIS), the *British-Irish Ice Sheet (BIIS)*, and the Scandinavian Ice Sheet (SIS) (with northwestern, southwestern, and southern sectors). (b) Summary of relative sea level data from Barbados (blue) [*Fairbanks et al.*, 2005], New Guinea (light blue) [*Cutler et al.*, 2003], Bonaparte Gulf (green) [*Yokoyama et al.*, 2000], and Sunda Shelf (orange and purple) [*Hanebuth et al.*, 2000, 2009].

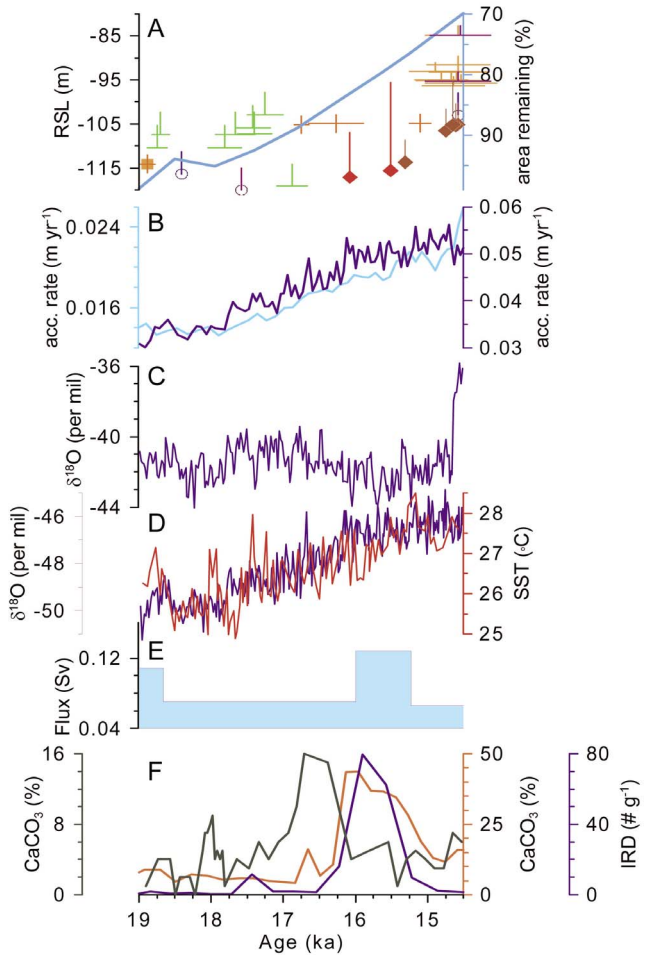

Figure 11. (a) Data constraining relative sea level between 19 and 14.5 ka. Blue circles are U/Th ages from Barbados [*Fairbanks et al.*, 2005], green symbols are calibrated ^{14}C ages from Bonaparte Gulf [*Yokoyama et al.*, 2000], and orange and purple symbols are calibrated ^{14}C ages from Sunda Shelf [*Hanebuth et al.*, 2000, 2009]. Age uncertainty is shown for all samples; where not visible, the uncertainty is less than the symbol size. Also shown is combined area loss of the Laurentide and Cordilleran [*Dyke*, 2004] and Eurasian (R. Gyllencreutz and J. Mangerud, written communication, 2010) ice sheets (light blue line). (b) Time series of accumulation rate from the EPICA Dronning Maud Land (EDML) (dark blue) and *EDC* (light blue) ice cores [*Lemieux-Dudon et al.*, 2010]. (c) North Greenland Ice Core Project (NGRIP) δ^{18}O record [*Lemieux-Dudon et al.*, 2010]. (d) EDML δ^{18}O record [*Lemieux-Dudon et al.*, 2010] (blue) and sea surface temperature record from core MD98-2181, tropical western Pacific Ocean [*Stott et al.*, 2007] (red). (e) Freshwater flux anomaly associated with routing of continental runoff through the Hudson River (filled blue time series) with age uncertainties [*Licciardi et al.*, 1999]. (f) Time series of ice-rafted debris from core MD95-2024P (orange) [*Hillaire-Marcel and Bilodeau*, 2000], core SU8118 (blue) [*Bard et al.*, 2000], and core VM23-81 (green) [*Bond et al.*, 1999].

[27] Marginal marine facies (<5 m depth uncertainty) from Bonaparte Gulf [*Yokoyama et al.*, 2000] suggest that between 18.75 ka and 17.25 ka, relative sea level rose from as little as 2.5 m (at 2 mm yr^{-1}) to as much as 12.5 m (at 8 mm yr^{-1}), with an average rate of 5 mm yr^{-1} when using just the depth of each sample (Figure 11a).

[28] Radiocarbon ages on three samples from Sunda Shelf constrain RSL between the youngest sample marking the end of the 19 ka sea level event [*Hanebuth et al.*, 2009] and the oldest sample marking the start of MWP-1A at ~14.6 ka (Figure 11a) [*Hanebuth et al.*, 2000]. These three ages are on pieces of wood or macrofibers from coastal facies (shoreline, tidal flat, and lagoonal) considered to be within 2 m of mean sea level [*Hanebuth et al.*, 2009], but since they are on material that may be reworked, their significance should be viewed with some caution. Taking these data at face value suggests that between ~19.1 and 16.7 ka, RSL rose from as little as 4.9 m (at 2.0 mm yr^{-1}) to as much as 12.9 m (at 5.4 mm yr^{-1}), with an average rate of 3.7 mm yr^{-1} when using just the depth of each sample. From ~16.7 ka to 15.1 ka, these ages suggest that RSL increased by at most 4.3 m (at 2.7 mm yr^{-1}), with no increase also being possible. RSL may then have risen 8.5 m between ~15.1 ka and 14.6 ka (at 16 mm yr^{-1}). The total possible maximum rise in relative sea level recorded at Sunda between ~19.1 ka and 14.6 ka is 20.8 m (at 4.6 mm yr^{-1}), with an average of 18.8 m (at 4.2 mm yr^{-1}).

[29] The Tahiti record has six ages that bracket the interval from 16.08 ka (15R-1 W 13–20, 117 m water depth, 10 m depth range) until the start of MWP-1A at ~14.6 ka (three samples at 105 m water depth, 5 m depth range) (Figure 11) [*Deschamps et al.*, 2012]. The large depth uncertainty (20 m) on the 15.51 ka sample (17R-2 W 0–10) precludes its use for any meaningful estimate of RSL change. These data thus suggest that during this 1500 year interval, RSL rose from as little as 2 m (at 1.3 mm yr^{-1}) to as much as 17 m (at 11.3 mm yr^{-1}), with an average rate of 8 mm yr^{-1} when just using the sample depths.

[30] In summary, the Barbados, Bonaparte, and Sunda records suggest that between ~19 ka and 14.6 ka, average RSL rose by as little as 8.3 m (at 2 mm yr^{-1}) to as much as 20.8 m (at 4.6 mm yr^{-1}), corresponding to freshwater fluxes of 0.02 *Sverdrups (Sv)* to 0.05 Sv over this ~4400 year interval. The younger Sunda ages and the Tahiti data suggest the possibility that rates may have increased after 16.0 ka to ~12 ± 4 mm yr^{-1}.

[31] Area loss estimates for the LIS and *Cordilleran Ice Sheet (CIS)* [*Dyke*, 2004] and for the *Eurasian Ice Sheet (EIS)* (R. Gyllencreutz and J. Mangerud, written communication, 2010) demonstrate that these ice sheets, which were the two largest in the Northern Hemisphere, contributed to sea level rise during this interval (~19 ka to 14.6 ka) (Figure 11a). We can derive an estimate of the contribution of these ice sheets to sea level rise by using reconstructions of the LIS that incorporated a realistic distribution of soft beds [*Licciardi et al.*, 1998] and of the EIS [*Siegert and Dowdeswell*, 2004]. Here the sea level contribution from 19 ka to 14.6 ka was ~8 m as from the LIS and ~7 m for the EIS. The

sea level contribution for the CIS can be estimated first from the well-established area-volume relationship for an ice sheet on a hard bed (log[volume] = 1.23[log[area] − 1]) [*Paterson*, 1994] as 5.5 m. If we then account for the mountainous terrain under the ice sheet, this is likely about 2.5 m. *Tarasov and Peltier* [2006] simulated a combined LIS and CIS sea level rise contribution of 14–15 m from ~19 to 14.6 ka. These estimates thus suggest that Northern Hemisphere ice sheets contributed ~17–18 m of sea level. For comparison, the ICE-5 G model predicted ~24 m from these three ice sheets over this interval [*Peltier*, 2004]. These estimates bracket the upper end of the estimates from the RSL records (maximum is 20.8 m) (Figure 11a).

[32] A greater sea level contribution from the Northern Hemisphere ice sheets than observed in the far-field RSL records between 19 ka and 14.6 ka would require that the AIS gained mass to balance the sea level budget. That this occurred is supported by Antarctic ice core records which show an increase in accumulation from ~18 ka to 14.6 ka [*Lemieux-Dudon et al.*, 2010] (Figure 11b), which would correspond to ice growth since melting margins would have been absent under the colder LGM climate and assuming there was no increased discharge from ice dynamics. One ice sheet model that was forced with Antarctic temperatures derived from ice core records simulated ice growth during the deglaciation equivalent to 3.7 m of sea level [*Huybrechts*, 2002].

[33] Regardless of the amplitude of sea level rise from the global ice sheets during this interval, the question remains as to why Northern Hemisphere ice sheets retreated while at the same time the AIS grew. In particular, the climate during this time was characterized by a strong Northern Hemisphere cooling (Figure 11c), referred to as the Oldest Dryas cold interval, and Southern Hemisphere warming (Figure 11d). These opposing climate changes are considered to be an expression of the *bipolar seesaw* that occurred in response to a reduction in the AMOC and associated meridional ocean heat transport [*Broecker*, 1998; *Clark et al.*, 2012; *Crowley*, 1992; *Mix et al.*, 1986; *Shakun and Carlson*, 2010; *Stocker and Johnsen*, 2003]. At the same time, sea surface temperatures (SSTs) in the tropical Pacific Ocean increased near-synchronously with the increase in Southern Hemisphere temperatures (Figure 11d) [*Lea et al.*, 2000; *Stott et al.*, 2007]. *Hostetler et al.* [2006] and *Clark et al.* [2007] demonstrated that an increase in tropical Pacific SSTs had a greater influence on the mass balance of Northern Hemisphere ice sheets relative to a decrease in North Atlantic SSTs, with the net effect being a negative mass balance and corresponding sea level rise. The retreat of the Northern Hemisphere ice sheets is thus an expected outcome associated with the deglacial forcing from an increase in Pacific SSTs, particularly when combined with increasing high northern latitude summer insolation and atmospheric greenhouse gases during this interval. At the same time, Southern Hemisphere warming occurred in response to the bipolar seesaw and to increasing atmospheric greenhouse gases, resulting in an increase in accumulation and corresponding volume of the Antarctic ice sheets [*Huybrechts*, 2002].

3.2. Runoff Routing

[34] In addition to the freshwater flux from the melting of ice sheets, the routing of North American runoff influenced the flux delivered to the North Atlantic. *Licciardi et al.* [1999] reconstructed the routing history of North American runoff based on radiocarbon-dated constraints on fluctuations of the LIS and on freshwater fluxes derived from ice sheet and climate model simulations. The key routing events early in the deglaciation between 19 ka and 14.6 ka involved fluctuations of the southern LIS margin and the associated routing of runoff between the Mississippi River and Hudson River. During the LGM, the ice margin blocked drainage to the east, and runoff from the southern LIS and surrounding drainage basins was directed through the Mississippi River. Following the LGM, the southern LIS margin began a gradual retreat until ~19.7 ka, when an interval of relatively rapid and widespread ice margin retreat rerouted runoff of several drainage basins from the Mississippi River to the Hudson River, with a resulting increase in the freshwater flux of 0.04 Sv (Figure 11e). Although well established from stratigraphic relations in the Great Lakes region [*Mörner and Dreimanis*, 1973], the chronological constraints on this interval of ice retreat, referred to as the Erie *Interstadial*, remain poor. *Licciardi et al.* [1999] concluded that the best constraints were from radiocarbon ages from western New York for ice-free conditions near the outlet to the Hudson River [*Muller and Calkin*, 1993] and for the age of the subsequent ice margin readvance during the Port Bruce Stadial that rerouted runoff from the Hudson River back to the Mississippi River at ~18.7 ka [*Fullerton*, 1980; *Licciardi et al.*, 1999].

[35] Following the Port Bruce readvance, the southern LIS margin began renewed widespread retreat during the Mackinaw Interstadial, again rerouting runoff of several drainage basins from the Mississippi River to the Hudson River, with a resulting increase in the freshwater flux of 0.06 Sv (Figure 11e). Radiocarbon ages from the Lake Michigan [*Monaghan and Hansel*, 1990], Lake Huron [*Gravenor and Stupavsky*, 1976], and Lake Erie basins [*Barnett*, 1985; *Calkin and Feenstra*, 1985] constrain this eastward routing event to have occurred from ~16 ka until 15.2 ka (Figure 11e), when the southern LIS margin readvanced during the Port Huron Stadial, again rerouting runoff back to the Mississippi River.

3.3. Heinrich Event 1

[36] Heinrich layers are distinguished from other *ice-rafted debris (IRD)* layers in the North Atlantic by their lithologic signature indicating a dominant source from the central regions of the LIS [*Grousset et al.*, 2001; *Gwiazda et al.*, 1996; *Hemming*, 2004; *Hemming et al.*, 1998], their increasing thickness westward toward Hudson Strait [*Dowdeswell et al.*, 1995], and their rapid sedimentation rates [*McManus et al.*, 1998]. Each layer is also associated with a large decrease in North Atlantic *planktonic* $\delta^{18}O$ that is interpreted as a low-salinity signal derived from the melting of the icebergs [*Bond et al.*, 1992; *Broecker et al.*, 1992; *Hillaire-Marcel and Bilodeau*, 2000; *Roche et al.*, 2004]. These characteristics are consistent with the hypothesis that

Heinrich layers represent the episodic release of icebergs associated with a surge from the Hudson Strait Ice Stream of the LIS [*Marshall and Koutnik*, 2006], which are conventionally referred to as Heinrich events [*Broecker et al.*, 1992].

[37] Determining the age of Heinrich event 1 (H1) from radiocarbon dating is subject to uncertainties in changing reservoir ages during the last deglaciation associated with changes in the AMOC [*Bard et al.*, 1994; *Bondevik et al.*, 2006; *Waelbroeck et al.*, 2001]. Three records of H1 are shown in Figure 11f. The chronologies for cores VM23-81 and SU8118 are based on radiocarbon, each with a standard 400 year reservoir age correction, whereas the chronology for core MD95-2024 is based on correlation of IRD layers in the core with cold periods in the *Greenland Ice Sheet Project 2 (GISP2)* ice core that was confirmed through correlations with paleomagnetic and *cosmogenic nuclide* records [*Stoner et al.*, 2000]. *Bard et al.* [1994] and *Waelbroeck et al.* [2001] demonstrated that lower-latitude sites such as core SU8118 experienced relatively constant reservoir ages through the deglaciation, whereas higher-latitude sites such as core VM23-81 experienced large changes in reservoir ages. We thus consider the age of H1 as established from core SU8118 (~16.0–15.5 ka) to be the most accurate one.

[38] The freshwater flux associated with H1 remains poorly constrained, with estimates based on modeling results or interpretation of IRD fluxes and marine $\delta^{18}O$ salinity signals ranging from 0.6 to 15 m of equivalent sea level rise over 200–500 years [*Alley and MacAyeal*, 1994; *Hemming*, 2004; *MacAyeal*, 1993; *Marshall and Clarke*, 1997]. Unfortunately, H1 occurs at a time when there are few direct constraints on RSL (Figure 11a), although if there were a substantial sea level rise from H1 that was greater than 2 m, the relative sea level record from Sunda Shelf suggests that it must have been followed by a comparable sea level fall in order to return to the level that existed prior to H1.

[39] Despite the widespread recognition that Heinrich events played an integral role in global climate change [*Cheng et al.*, 2009; *Denton et al.*, 2010; *Toggweiler*, 2008], the mechanism for the ice sheet instability that caused Heinrich events remains poorly understood, with corresponding uncertainties in understanding their specific role in climate change. Perhaps the most widely accepted mechanism involves an internal thermal oscillation of the LIS (so-called binge-purge) with a (tunable) time scale similar to the ~7 kyr interval separating Heinrich events [*MacAyeal*, 1993]. In this regard, Heinrich events are commonly thought to have triggered abrupt climate change by causing a collapse of the AMOC [*Alley and Clark*, 1999; *Broecker*, 1994; *Ganopolski and Rahmstorf*, 2001; *Menviel et al.*, 2008; *Okazaki et al.*, 2010; *Timmermann et al.*, 2005], with attendant responses in temperature, monsoons, and the carbon cycle playing a major role in driving the last deglaciation [*Anderson et al.*, 2009; *Cheng et al.*, 2009; *Denton et al.*, 2010].

[40] *Bond et al.* [1993], however, disputed this mechanism by pointing out that Heinrich events only occur following prolonged cooling intervals in the North Atlantic region, thus implicating a climatic trigger. Additional support for this scenario came from the synchronization of Greenland and Antarctic ice core records [*Barbante et al.*, 2006; *Blunier and Brook*, 2001; *Blunier et al.*, 1998], which revealed that Heinrich events not only occurred at cold times in Greenland but also at times of peak warming in Antarctica known as *A events*. This association cannot be coincidental and instead strongly suggests that Heinrich events are an integral part of the bipolar seesaw that produced the out-of-phase response between the polar hemispheres, with the changes in the AMOC that cause the seesaw somehow linked to, and possibly responsible for, Heinrich events [*Clark et al.*, 2007; *Pisias et al.*, 2010].

[41] Based on simulations with a simplified global climate model, *Shaffer et al.* [2004] first proposed that subsurface warming that develops at intermediate depths in the North Atlantic in response to a reduction or collapse of the AMOC may trigger a Heinrich event by ice shelf collapse. *Shaffer et al.*'s [2004] model simulations indicated that without an active AMOC and cooling of the ocean interior by convection, downward diffusion of heat at low latitudes warms subsurface waters to a depth of ~2500 m, within the depth range of the base of floating ice shelves that may have existed along parts of Greenland and eastern North America. Some of the heat accumulated in the subsurface is transported poleward causing a temperature inversion in the northern North Atlantic. Development of a subsurface warming following collapse of the AMOC is also clearly evident in other models [*Knutti et al.*, 2004; *Liu et al.*, 2009; *Stocker and Johnsen*, 2003; *Stocker et al.*, 2007]. *Flückiger et al.* [2006] also identified subsurface warming as possibly being important but implicated the ~1 m steric and dynamic sea level rise that accompanies a collapse of the AMOC as the primary trigger for Heinrich events, with subsequent sea level rise associated with ice sheet surging acting as a positive feedback. Recent modeling, however, indicates that ice sheets are likely to be immune to such small sea level forcing [*Alley et al.*, 2007], and sea level will fall adjacent to the ice margin where mass loss is occurring, potentially stabilizing retreat [*Gomez et al.*, 2010, 2012]. Using a parameterized conceptual model, *Alvarez-Solas et al.* [2010] also concluded that subsurface warming could produce Heinrich-like events, while *Marcott et al.* [2011] produced a *Mg*/*Ca* record on *benthic* foraminifera from an intermediate depth site that demonstrated subsurface warming at the same time as large reductions in the AMOC, with temperature increasing by approximately 2°C over a 1–2 kyr interval prior to a Heinrich event. Recent observations from Antarctica suggest that such oceanic thermal forcing would be particularly effective at causing destabilization of ice shelves [*Rignot and Jacobs*, 2002] and attendant glacier surging [*De Angelis and Skvarca*, 2003; *Rignot et al.*, 2004; *Scambos et al.*, 2004]; similar sensitivities have been identified at grounding lines of Greenland outlet glaciers [*Holland et al.*, 2008; *Motyka et al.*, 2011; *Rignot et al.*, 2010].

[42] The role of subsurface warming implies that some factor caused the AMOC to slow down prior to Heinrich events and that Heinrich events were thus responses to, rather than causes of, the shutdown of the AMOC. This conjecture is consistent with the observation first made by *Bond et al.*

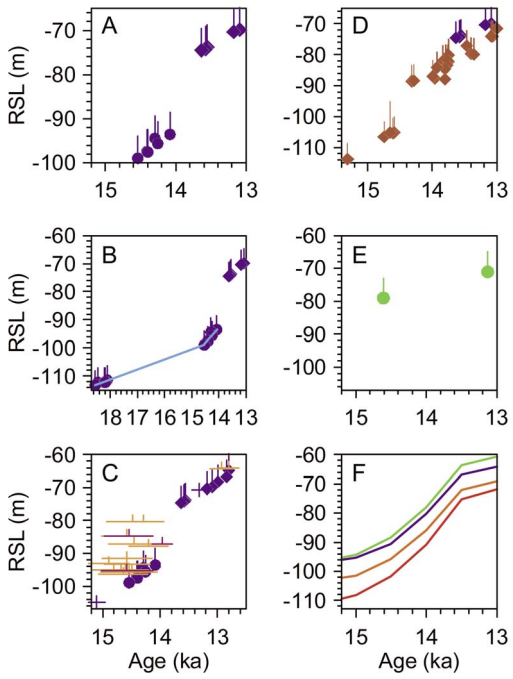

Figure 12. Summary of the data constraining MWP-1A sea level event. (a) U/Th ages on *A. palmata* corals from core 9 (circles) and core 12 (diamonds), Barbados, from *Fairbanks et al.* [2005]. (b) As in Figure 12a except extended to 18.7 ka and showing the increase in rate of sea level rise at least 14.54 ka. (c) Calibrated radiocarbon ages for relative sea level data from Sunda Shelf compared to the Barbados U/Th ages from cores 9 and 12 (blue circles and diamonds). The Sunda data are on nonmangrove wood or macrofibers (blue lines), mangrove fragments that are not in situ (orange lines), and mangrove fragments that are in situ (purple lines) [*Hanebuth et al.*, 2000]. (d) U/Th ages on corals from Tahiti [*Bard et al.*, 1996, 2010; *Deschamps et al.*, 2012] (red symbols) compared to the Barbados U/Th ages from core 12 (blue symbols). (e) U/Th ages on corals from Papua New Guinea [*Edwards et al.*, 1993; *Cutler et al.*, 2003]. (f) Predicted relative sea level histories from an Earth model [*Bassett et al.*, 2005]. Red is Huon Peninsula, New Guinea, green is Bonaparte Gulf, blue is Barbados, light blue is Sunda Shelf, and orange is Tahiti. Age uncertainty is shown for all samples; where not visible, the uncertainty is less than the symbol size.

[1993] that Heinrich events occur at the end of a long-term cooling trend, which is likely caused by a reduction in the AMOC and associated expansion of sea ice. Records of benthic $\delta^{13}C$ [*Zahn et al.*, 1997], *Pa/Th* [*Hall et al.*, 2006; *Lippold et al.*, 2009; *McManus et al.*, 2004], relative magnetic grain size [*Stanford et al.*, 2006], oceanic $\Delta^{14}C$ [*Mangini et al.*, 2010], and Nd isotopes [*Gutjahr and Lippold*, 2011; *Gutjahr et al.*, 2010] now clearly indicate that the AMOC began to decrease up to 2000 years before the Heinrich events. The reduction in the AMOC prior to H1 can be attributed to the increased freshwater flux to the North Atlantic Ocean derived from the widespread deglaciation of Northern Hemisphere ice sheets that began with the initial rapid rise of sea level at ~19 ka [*Clark et al.*, 2004, 2007; *Marcott et al.*, 2011; *Stanford et al.*, 2011a] (Figure 10) and continued thereafter (Figure 11a).

4. SEA LEVEL RISE DURING MWP-1A

4.1. Barbados

[43] *Fairbanks* [1989] first reconstructed the Barbados record of deglacial sea level rise based on radiocarbon dates, in which he identified the two periods of rapid sea level rise referred to as MWP-1A and MWP-1B. *Bard et al.* [1990] subsequently reported *U/Th ages* on Barbados samples that replicated the structure seen in the Fairbanks ^{14}C-based sea level record, thus demonstrating that it was not an artifact of the radiocarbon time scale, while at the same time improving the accuracy and precision of the chronology. MWP-1A was defined by the youngest age on *A. palmata* in core 9 (RGF 9-8-2-1, 14.24 ± 0.10 ka, −94.3 m) and the oldest age from core 12 (RGF 12-21-10, 13.73 ± 0.10 ka, −74.5 m) (Figure 12a). Although the two cores lie on the same side of the possible tectonic structure (Figure 5) and are thus not subject to the depth uncertainties discussed in section 2, the event is defined by a core break, rather than in a continuous sequence from one core, which raised the question of whether the event is an artifact of this break [*Broecker*, 1990].

[44] *Fairbanks et al.* [2005] redated samples reported by *Bard et al.* [1990], finding good agreement when accounting for newer U-Th decay constants [*Cheng et al.*, 2000], as well as dated additional samples that further resolved the sea level record surrounding the event (Figure 12a). Following on *Fairbanks* [1989] and *Bard et al.* [1990], *Stanford et al.* [2006] assigned the start of the event to the youngest age from core 9 previously dated by *Bard et al.* [1990] (RGF 9-8-2-1), which *Fairbanks et al.* [2005] redated to 14.08 ± 0.08 ka, and assigned the end of the event to the oldest age from core 12 previously dated by *Bard et al.* [1990] (RGF 12-21-10), which *Fairbanks et al.* [2005] redated to 13.63 ± 0.03 ka (Figure 12a).

[45] We point to two alternative scenarios that are equally plausible in defining the timing of MWP-1A. The first is with regard to an earlier onset for the event than 14.08 ± 0.08 ka [*Stanford et al.*, 2006], which would make it consistent with the onset age suggested from the two other records that span MWP-1A (Sunda shelf and Tahiti, discussed below). *Deschamps et al.* [2012] pointed out that the average rate of rise before 14.54 ka (RGF 9-13-3) is slower than after that time until 14.08 ka (RGF 9-8-2-1). Specifically, as discussed in section 3, for the existing ages in core 9, the long-term average rate of sea level rise from 18.78 ka (RGF 9-23-5) to 14.54 ka (RGF 9-13-3) is 3.5 mm yr^{-1}, whereas between 14.54 ka and 14.08 ka (RGF 9-8-2-1), the rate increased to 11.8 mm yr^{-1} (Figure 12b), with the 14.54 ka age only providing a minimum-limiting age for the start of the acceleration. *Weaver et al.* [2003] also noted that the youngest dated sample of *A. palamata* (RGF 9-8-2), which is generally considered as marking the start of the MWP-1A in the Barbados record, is overlain by deeper water species *Porites astroides* and *A. cervicornis* [*Fairbanks*, 1989], suggesting

that the 14.08 ka horizon was already in the process of drowning in response to rapidly rising sea level (Figure 5).

[46] During times of rapid sea level rise, coral reefs have a known tendency to "keep up, catch up, or give up" depending on the rate of sea level rise [*Neumann and Macintyre*, 1985]. The trends in sea level identified by dated samples from core 9 suggest that the coral reef was able to keep up with sea level rise until sometime after 14.08 ka, at which point it gave up. Accordingly, *Deschamps et al.* [2012] suggested that the acceleration in sea level rise that began at least at 14.54 ka, with rates that were three times higher than those of the preceding 4200 years, is related to the start of MWP-1A. During this phase of keep up, the *A. palamata* occupying the reef top may have been living below their normal 5 m depth range, so that the rate of 11.8 mm yr^{-1} is only a minimum, and it was only after 14.08 ka that the rate of sea level rise exceeded the ability of the corals to keep up, causing the reef to give up.

[47] The other possible scenario relates to the age of the end of MWP-1A inferred from the oldest coral in core 12 (13.63 ± 0.03 ka). *Hanebuth et al.* [2000] suggested that this is a maximum-limiting age since older corals may not have been sampled during coring and because there may be a 200–300 year interval between the end of the rapid rise and the time that corals could start to colonize the substrate [*Montaggioni et al.*, 1997]. As discussed below, these arguments are consistent with the RSL record from Tahiti, which places the end of MWP-1A at 14.3 ka [*Deschamps et al.*, 2012].

[48] *Fairbanks* [1989] first defined the amplitude of MWP-1A from the Barbados cores as being 24 m in less than 1000 years, presumably on the basis of the 12.5 ± 0.2 ^{14}C ka BP age (RGF 9-13-3, 98.9 m corrected depth, 14.54 ka U-Th age) in core RGF 9 and the 11.8 ± 0.2 ^{14}C ka BP age (RGF 12-21-10, 74.5 m corrected depth, RGF 12-21-10, 13.63 ± 0.03 ka) in core RGF 12, a number that was subsequently widely adopted [e.g., *Bassett et al.*, 2005; *Clark et al.*, 2002; *Peltier*, 1994, 2005]. Based on their revised age for MWP-1A from new Tahiti data (section 4.3), which ended at ~14.3 ka, *Deschamps et al.* [2012] extrapolated the RGF 12 age-depth data back to 14.3 ka and assigned that water depth (80 m) to the end of the event. Then, by assigning the onset of the event to sample RGF 15-5-3 (14.57 ka, 96.3 m water depth), they derived an amplitude of ~15 m. We note, however, that RGF 9-13-3, which is the same age (14.54 ka), occurs at a corrected water depth of 98.9 m, suggesting an amplitude of ~19 m. Neither of these estimates accounts for uncertainties, but they suggest that the amplitude is likely substantially less than the 24 m first inferred by *Fairbanks* [1989] [cf. *Kopp*, 2012].

4.2. Sunda Shelf

[49] *Hanebuth et al.* [2000] documented an episode of rapid sea level rise on the Sunda Shelf that, in timing and amplitude, confirmed the existence of MWP-1A. The record is based on calibrated radiocarbon ages measured on organic remains from shallow water (tidal flat, delta plain, and bay lagoon) sediments. Many of the ages are on mangrove remains, which grow at sea level, but because only three of these samples were from in situ mangrove roots, all remaining samples are subject to the uncertainty of having been reworked.

[50] Based on the version of the calibration software available at the time (Calib 4.0), *Hanebuth et al.* [2000] concluded that MWP-1A occurred between 14.6 and 14.3 ka, with an amplitude of ~16 m (sample KIA-5981 at 96.3 m water depth and sample KIA 5608 at 80.3 m water depth). By inferring that the youngest coral in Barbados core 9 represents the start of MWP-1A at 14.08 ka, *Stanford et al.* [2006] argued that the Sunda chronology is likely too old given that the radiocarbon ages are subject to larger uncertainties than U/Th ages, pointing specifically to [*Stanford et al.*, 2006, p. 2] "corrections for variable ^{14}C reservoir ages." All dated Sunda organic remains are terrestrial, however, and thus do not require a correction for ^{14}C reservoir ages. The ages do occur during a known radiocarbon plateau, however, introducing some uncertainty in the calibration.

[51] Figure 12c shows the Sunda ages recalibrated with *IntCal*09 calibration curve [*Reimer et al.*, 2009], including a 2σ error for direct comparison with U/Th ages from Barbados, which are also shown. The Sunda data suggest that MWP-1A likely began at least at 14.6 ka, in agreement with the acceleration seen in the Barbados data, consistent with the hypothesis that the Barbados corals in core 9 were living in increasingly deeper water as MWP-1A proceeded until they gave up [*Deschamps et al.*, 2012], as well as with the onset at Tahiti (section 4.3). The mean of the youngest calibrated ages then suggests the event ended by ~14.3 ka, although the large uncertainties on the ages and the possibility of reworking cannot preclude a younger age of ~13.9 ka. This age is older than suggested by the oldest age from Barbados core 12, which has been used to constrain the end of MWP-1A at 13.63 ka [*Bard et al.*, 1990; *Stanford et al.*, 2006], but is consistent with Tahiti [*Deschamps et al.*, 2012].

[52] *Deschamps et al.* [2012] evaluated the Sunda data from a different perspective. Specifically, they hypothesized that given the scatter and uncertainty in the ^{14}C ages (Figure 12c), MWP-1A was such an abrupt event that all the samples between 80 and 100 m water depth could be considered to be the same age. Based on this assumption, they averaged the ^{14}C ages of all samples occurring in this depth interval to derive a mean age of 12.415 ± 0.032 ^{14}C ka BP (1 SD, n = 17). This mean age for MWP-1A in the Sunda shelf record is the same as the onset of the Bølling (12.46 ± 0.15 ^{14}C ka BP) as dated in North Atlantic sediments [*Bard et al.*, 1987]. *Deschamps et al.* [2012] then used the IntCal09 calibration curve to compute a mean calendar age of the Sunda MWP-1A as 14.18–14.62 ka BP (1σ interval), or 14.14–14.94 ka BP (2σ interval). They concluded that despite the large uncertainties, this age interval does not overlap with that previously based on the Barbados record [*Peltier and Fairbanks*, 2006; *Stanford et al.*, 2006] but is consistent with the timing based on their reassessment of Barbados coral response to rapid sea level rise (section 4.1) and from the new Tahiti record (section 4.3).

4.3. Tahiti

[53] *Bard et al.* [1996, 2010] reported a RSL record based on samples from drill cores from the fringing reef of Tahiti.

The cores penetrated a hiatus in the carbonate sequence which, based on U/Th dating, corresponds to sea level lowstand prior to MWP-1A. The oldest age immediately above the hiatus places a minimum-limiting age of 13.93 ± 0.06 ka (Ta-P8-372) for the end of MWP-1A (Figure 12d), which is older than suggested from Barbados but in good agreement with the Sunda Shelf record.

[54] *Deschamps et al.* [2012] extended the Tahiti RSL record back to 16.1 ka by drilling cores from the fringing fore reef slope. They proposed that the best constraint for the onset of MWP-1A is from three coral samples dated at 14.65 ± 0.02 ka (15A-37R-1 W 19–28), 14.58 ± 0.02 ka (24A-10R-1 W 65–75), and 14.61 ± 0.03 ka (24A-10R-1 W 98–116) and occurring at a subsidence-corrected water depth of 105 m (Figure 12d). The two youngest samples are associated with vermetids, indicating growth within 5 m water depth.

[55] The occurrence of MWP-1A in the Tahiti cores is recorded by the next shallowest in situ corals from a subsidence corrected water depth of 88 m and dated to 14.28 ± 0.02 kyr BP (23B-12R-2 W 113–127) and 14.31 ± 0.04 ka (23A-13R-2 W 32–37). *Deschamps et al.* [2012] noted that these coral samples, which are also associated with vermetids, are the first datable corals to colonize the preglacial substratum after the MWP-1A sea level jump and thus [*Deschamps et al.*, 2012, p. 561] "provide the most robust constraint on MWP-1A timing and clearly indicate that the sea-level jump was complete before 14.31 kyr BP." Moreover, these two ages lie on the extension of the general trend suggested by samples from the onshore holes [*Bard et al.*, 1996, 2010] (Figure 12d), thus indicating a slower rate of sea level rise after MWP-1A. Additional evidence in support of a rapid sea level rise at this time is suggested by evidence for a major change in reef development, whereby before MWP-1A, reef growth kept pace with sea level, whereas after the event, the reef experienced widespread deepening and backstepping [*Deschamps et al.*, 2012].

[56] Given the 5 m depth uncertainty on the samples associated with the beginning and end of MWP-1A at Tahiti, *Deschamps et al.* [2012] inferred a 17 m amplitude, with lowest and uppermost bounds of 12 and 22 m accounting for depth habitat. However, *Deschamps et al.* [2012] then considered two additional approaches to constraining the amplitude. First, they evaluated the habitat zonation of the different coral species recovered in the cores. Second, they applied linear regression to the sea level data prior to and following the event. From these two approaches, they concluded that the 12–22 m amplitude range was unrealistic and instead was more likely 14–18 m, with a best estimate of 16–17 m for the amplitude.

4.4. New Guinea

[57] *Edwards et al.* [1993] and *Cutler et al.* [2003] reported RSL data from the Huon Peninsula, Papua New Guinea (Figure 12e). The oldest sample for deglacial RSL was 14.61 ± 0.05 ka (KNM 46.7) at a relative sea level of −79 m [*Cutler et al.*, 2003]. In comparison to RSL data from other sites, this sample may suggest that MWP-1A had nearly terminated by this time (Figure 12). However, a prediction from an Earth model that accounts for GIA effects suggests that this sample may have lived during MWP-1A [*Bassett et al.*, 2005], although the prediction still underestimates the RSL suggested by the sample. *Cutler et al.* [2003] applied two criteria to assess the possibility of diagenetic alteration of the dated coral: the initial δ^{234}U value and concordancy between ^{230}Th and ^{231}Pa ages. While sample KNM 46.7 fulfills the first criterion, *Cutler et al.* [2003] did not obtain a corresponding ^{231}Pa age, so the accuracy of this sample remains uncertain.

4.5. Summary

[58] The acceleration in RSL rise seen in the Barbados record starting at least at 14.54 ka is in good agreement with the start of MWP-1A at ∼14.6 ka suggested from the Sunda Shelf and Tahiti records [*Deschamps et al.*, 2012]. The Sunda Shelf and Tahiti records both suggest an age of 14.3 ka for the end of MWP-1A. The amplitude at all three sites is on the order of 16–19 m, with poorly defined uncertainty that is nevertheless likely within this range. *Clark et al.* [2002] predicted that sea level rise at Tahiti, where the amplitude (∼16 ± 2 m) is the best constrained of the three sites, would be 10–20% greater than the ice-equivalent contribution (section 7). Accordingly, this suggests that the ice-equivalent contribution was substantially less than 24 m as first inferred by *Fairbanks* [1989], and it now seems more likely that it was on the order of 14 m [*Deschamps et al.*, 2012]. A continuation of the ongoing long-term sea level rise of ∼8 mm yr^{-1} (section 3) during the 300 year duration of MWP-1A suggests that the anomalous ice-equivalent sea level rise in excess of this long-term rate was ∼11.5 m.

[59] *Stanford et al.* [2011b] combined the deglacial RSL data sets and used Monte Carlo methods to account for the uncertainties in the data. They then applied a spline to the data, accounting for all uncertainties, to derive a global sea level curve. From this, they concluded that MWP-1A occurred between 14.3 and 12.8 ka (although they also state that sea level rise began to accelerate at ∼14.6 ka and that MWP-1A [*Stanford et al.*, 2011b, p. 201] "started at around the time of the Bølling warming (14.6 ka)"). They also concluded that the event had a much broader structure than the more abrupt jump inferred from Barbados and Sunda records (the new Tahiti results were not available), with a maximum rate of rise at 13.8 ka.

[60] We note that the spline fit smoothes the sea level jump that is clearly present in the Sunda and Barbados data that have previously been used to define MWP-1A [*Fairbanks*, 1989; *Hanebuth et al.*, 2000]. *Stanford et al.* [2011b] did not address the misfit with Barbados samples that fall above their envelope but argued that because the four samples from Sunda that fall above their sea level envelope are the only data from cores 18308-2 and 18309-2, they are out of stratigraphic order. S. A. Marcott et al. (Comment on: Sea-level probability for the last deglaciation: A statistical analysis of far-field records, submitted to *Global and Planetary Change*, 2012) argued that there is no a priori explanation why being the only samples from these cores would cause them to be out

TABLE 1. Estimates of Northern Hemisphere Ice Sheet Contributions to MWP-1A[a]

Study	Method	Ice Sheet	Duration (years)	Sea Level Contribution (m)	Anomaly (m)
Licciardi et al. [1998][b]	flow-line ice sheet	LIS	1300	5.6 to 6.6	3.1 to 4.3
Peltier [2004]	ICE-5G	LIS	500	16.5	
Carlson [2009]	δ^{18}O runoff	LIS	500		4.4 to 5.3
Carlson et al. [2012]	GCM–surface mass balance	LIS	500	5.8 to 8.0	1.9 to 3.9
This study[c]	ice area-volume	LIS	800	5.7 to 7.3	3.5 to 4.9
Tarasov and Peltier [2006]	ice sheet model	LIS/CIS	500	6.3 to 9.8	4.5 to 7.6
Tarasov et al. [2012][d]	ice sheet model	LIS/CIS	500	9.4 to 13.8	5.4 to 8.8
Gregoire et al. [2012]	ice sheet model	LIS/CIS	500	9	3 to 4
Peltier [2004]	ICE-5G	CIS	500	3.6	
Carlson et al. [2012] and this study[c]	ice area-volume	CIS	800	1.0 to 1.4	0.4 to 0.6
Peltier [2004]	ICE-5G	SIS/BKIS	500	4.6	
Siegert and Dowdeswell [2004]	ice sheet model	SIS/BKIS	500	1.0 to 2.0	0
This study[c]	ice area-volume	SIS/BKIS	1000	4.1 to 5.7	−1.1 to +1.1

[a]Note the different time intervals over which these volumes are computed.
[b]Ages modified to match the new dates of *Dyke* [2004].
[c]Results based on area maps of *Dyke* [2004] and the DATED Project.
[d]Note that this study excluded LIS/CIS MWP-1A contributions that were less than 7 m.

of stratigraphic order, particularly when their ages overlap with the ages from the samples that are at greater depths in the other cores that have been used to define MWP-1A at Sunda.

[61] Marcott et al. (submitted manuscript, 2012) ran the same spline function used by *Stanford et al.* [2011b] individually through Sunda and Barbados RSL data as well as through the new Tahiti data, treating the uncertainties in the same way as *Stanford et al.* [2011b]. The spline captured the abrupt MWP-1A event in Tahiti and Barbados, where there is a clear jump between data points marking the event, but smoothed the Sunda MWP-1A data, as in *Stanford et al.* [2011b]. From this, Marcott et al. (submitted manuscript, 2012) concluded that because polynomials such as splines are by definition smoothing functions, for a noisy data set such as the combined RSL data used by *Stanford et al.* [2011b], a spline function is unable to capture an event that is well defined from the stratigraphy but where there is significant noise on the data, such as at Sunda or in the combined RSL data.

5. MWP-1A: GEOLOGICAL CONSTRAINTS ON A SOURCE FROM THE NORTHERN HEMISPHERE

[62] Due to its large size, the LIS was originally assumed to be the sole source of MWP-1A [*Fairbanks*, 1989; *Peltier*, 1994]. Other studies have suggested that the CIS and EIS also contributed to MWP-1A because of evidence for retreat of these ice sheets around the timing of MWP-1A and suggested that the entire MWP can be explained by Northern Hemisphere ice sheet retreat [*Peltier*, 2004, 2005; *Tarasov and Peltier*, 2005]. Here we review the geologic record of these ice sheets to assess their potential contributions to MWP-1A and place these comparisons in the context of ice sheet model results. We also summarize the various published estimates for sea level rise spanning the MWP-1A event (Table 1). None of these estimates reflect the shorter duration (~300 years) for MWP-1A now established from Tahiti, and so in section 5.3, we scale the estimates based on this new duration. In addition, we assume that the ongoing long-term sea level rise prior to MWP-1A that was estimated for each of the individual approaches discussed here continued through the event. We then subtract this from the total rise associated with the MWP-1A interval to derive the amount of anomalous sea level rise that occurred during MWP-1A in excess of this long-term rise. It is this anomalous rate that presumably reflects the ice sheet response to the mechanism(s) responsible for triggering MWP-1A.

5.1. North American Ice Sheet Contributions

[63] The terrestrial record of the LIS is constrained by radiocarbon dates along its southern, eastern, and northern margins around the time of MWP-1A, which can be compared with marine records of runoff through the various outlets of the LIS. Following the Mackinaw Interstadial (~16.5–15.2 ka), the southern LIS margin readvanced during the Port Huron Stadial (~15.2–14.1 ka) (Figure 13) [*Hansel and Mickelson*, 1988], which encompasses the time of MWP-1A. Port Huron Stadial moraines are traceable from the James lobe in South Dakota to the Lake Huron lobe around Lakes Erie and Ontario and are well constrained by maximum-limiting ^{14}C dates from organic material underlying and in till from the advance and by minimum-limiting ^{14}C dates overlying the deposited till [*Clayton and Moran*, 1982; *Dyke*, 2004; *Dyke and Prest*, 1987; *Mickelson et al.*, 1983]. In some cases, the ice advance caused highstands of proglacial lakes in the Great Lakes basins that indicate the presence of ice in the basin and can be dated by organic material preserved in beach deposits [e.g., *Hansel and Mickelson*, 1988].

[64] In South Dakota, the James lobe readvance occurred after 14.2 ± 0.5 ka (12.18 ± 0.36 ^{14}C ka BP, GX-5611), whereas the Des Moines lobe readvance in Iowa occurred after 14.7 ± 0.5 ka (12.61 ± 0.25 ^{14}C ka BP, ISGS-641) (Figure 14a) [*Bettis et al.*, 1996; *Clayton and Moran*, 1982]. In Wisconsin, the Green Bay lobe readvanced after 15.6 ± 0.5 ka (12.97 ± 0.20 ^{14}C ka BP, WIS-2293) [*Maher et al.*, 1998], and the Lake Michigan lobe readvanced after 16.6 ± 0.2 ka (13.47 ± 0.13 ^{14}C ka BP, ISGS-1378) [*Licciardi et al.*, 1999]. The Lake Huron lobe also readvanced after 15.7 ± 0.8 ka (12.92 ± 0.40 ^{14}C ka BP, W-430) [*Licciardi et al.*,

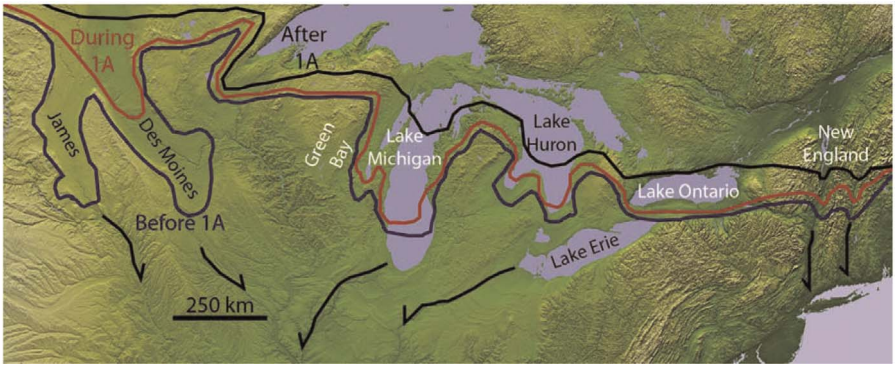

Figure 13. Map of southern LIS margin positions around the time of MWP-1A [*Dyke*, 2004]. Blue line is maximum extent during the Port Huron Stadial. Red line is a recessional ice margin position during the Port Huron Stadial. Black is the ice margin extent during the subsequent Two Creeks Interstadial. LIS lobe names are also indicated as is the routing of meltwater during the Port Huron Stadial [*Licciardi et al.*, 1999].

1999]. Advance of the Lake Michigan lobe caused the Glenwood and Calumet high lake levels in the Lake Michigan Basin that lasted from at least 14.8 ± 0.7 ka (12.65 ± 0.35 ^{14}C ka BP, W-140) to after 14.3 ± 0.5 ka (12.22 ± 0.35 ^{14}C ka BP, W-161) (Figure 14a) [*Hansel and Mickelson*, 1988]. Highstands of Lakes Erie and Ontario also show that ice was present in these basins from at least 15.5 ± 0.5 ka (12.90 ± 0.20 ^{14}C ka BP, I-3175) to 13.9 ± 0.1 ka (12.10 ± 0.10 ^{14}C ka BP, W-861) [*Fullerton*, 1980; *Licciardi et al.*, 1999; *Muller and Calkin*, 1993].

[65] The southern LIS margin retreated from its maximum Port Huron Stadial position (Figure 13) in South Dakota before 13.9 ± 0.3 ka (12.03 ± 0.21 ^{14}C ka BP, S-553) and in Iowa before 13.9 ± 0.3 ka (12.03 ± 0.20 ^{14}C ka BP, W-354) (Figure 14a) [*Bettis et al.*, 1996; *Clayton and Moran*, 1982], with both lobes retreating north into Minnesota prior to 14.0 ± 0.1 ka (12.14 ± 0.09 ^{14}C ka BP, ETH-32334) [*Lepper et al.*, 2007]. In Wisconsin and farther east, the Two Creeks Forest grew on top of till deposited during the Port Huron Stadial and constrains ice retreat to before 14.0 ± 0.1 ka (12.11 ± 0.07 ^{14}C ka BP, Beta-11558) for the Green Bay lobe and 13.9 ± 0.1 ka (12.04 ± 0.06 ^{14}C ka BP, ETH-8273) for the Lake Michigan lobe (Figure 14a) [*Kaiser*, 1994; *Larson et al.*, 1994; *Licciardi et al.*, 1999; *Mickelson et al.*, 2007]. *Rech et al.* [2012] dated mollusk shells from just below the Two Creeks Forest Bed but above lake sediment indicative of Lake Michigan lobe presence in the lake basin and obtained ages of 13.9 ± 0.1 ka (12.09 ± 0.07 ^{14}C ka BP, AA-83095) to 14.4 ± 0.3 ka (12.39 ± 0.07 ^{14}C ka BP, AA-83097). However, these shells grew on a Paleozoic carbonate terrane and thus likely contain some amount of ^{14}C-dead carbon from the underlying sediment largely composed of the local carbonate bedrock, which would shift ages older than their true age. The ice margins of the Green Bay and Lake Michigan lobes retreated ~100 km during the waning phase of the Port Huron Stadial at 14.5–14.0 ka [*Dyke*, 2004; *Hansel and Mickelson*, 1988; *Licciardi et al.*, 1999]. Farther west, the retreat distance of the Des Moines and James lobes was greater, with the ice margin at the Big Stone Moraine 250–300 km north of the Port Huron maximum extents before ~14.0 ka (Figure 13) [*Clayton and Moran*, 1982; *Lepper et al.*, 2007]. The Lake Huron lobe began to retreat as indicated by the termination of the high lake stand in Lake Ontario after 13.9 ± 0.1 ka (12.10 ± 0.10 ^{14}C ka BP, W-861) [*Licciardi et al.*, 1999; *Muller and Calkin*, 1993] with northward retreat by >50 km out of the St. Lawrence Valley before 13.4 ± 0.1 ka (11.53 ± 0.09 ^{14}C ka BP) and 13.0 ± 0.1 ka (11.05 ± 0.09 ^{14}C ka BP, WW-5383) (Figure 14a) [*Rayburn et al.*, 2011; *Rodrigues*, 1992]. The relatively limited amount of retreat of the southern LIS margin during MWP-1A constrained by this well-documented chronology thus suggests little contribution from this portion of the LIS to MWP-1A.

[66] The southeastern LIS margin is well dated by the New England *varve* chronology that is supported by several cosmogenic radionuclide ^{10}*Be* boulder ages. The New England varve chronology is anchored by six ^{14}C dates during the period of MWP-1A and indicates ~130 km of northward margin retreat at 14.5–14.0 ka from the Perry Mountain Moraine to the Littleton Moraine at 0.26–0.60 km yr^{-1} (Figure 14b) [*Balco et al.*, 2009; *Ridge*, 2003, 2004] (http://geology.tufts.edu/varves/NAVC/navcdeglac.asp). Retreat rates prior to ~14.5 ka were slower than during MWP-1A at <0.1 km yr^{-1} but continued at a similar rapid rate after MWP-1A (0.30–0.70 km yr^{-1}). Farther north, the LIS remained on the coast of Labrador during MWP-1A, showing little change in its position [*Clark et al.*, 2003; *Dyke*, 2004], which may reflect a potential increase in precipitation over this portion of the LIS in response to Bølling warming [*Carlson et al.*, 2012]. The deposition of IRD from LIS calving in the Gulf of St. Lawrence and Hudson Strait also remained low during MWP-1A, implying little change in the dynamics of the marine terminating portions of the eastern LIS [*Andrews and Tedesco*, 1992; *Bond et al.*, 1999; *Keigwin and Jones*, 1995]. From these constraints, we conclude that the eastern LIS did not contribute significantly to MWP-1A.

[67] Southern LIS meltwater during the Port Huron Stadial was predominately routed southward through the Mississippi River [*Licciardi et al.*, 1999] (section 3.2), which is recorded as a planktonic δ^{18}O decrease of ~0.6‰ and surface water δ^{18}O of seawater ($\delta^{18}O_{sw}$; temperature-corrected δ^{18}O) decrease of ~0.3‰ in the Gulf of Mexico (Figure 15d) [*Aharon*, 2006;

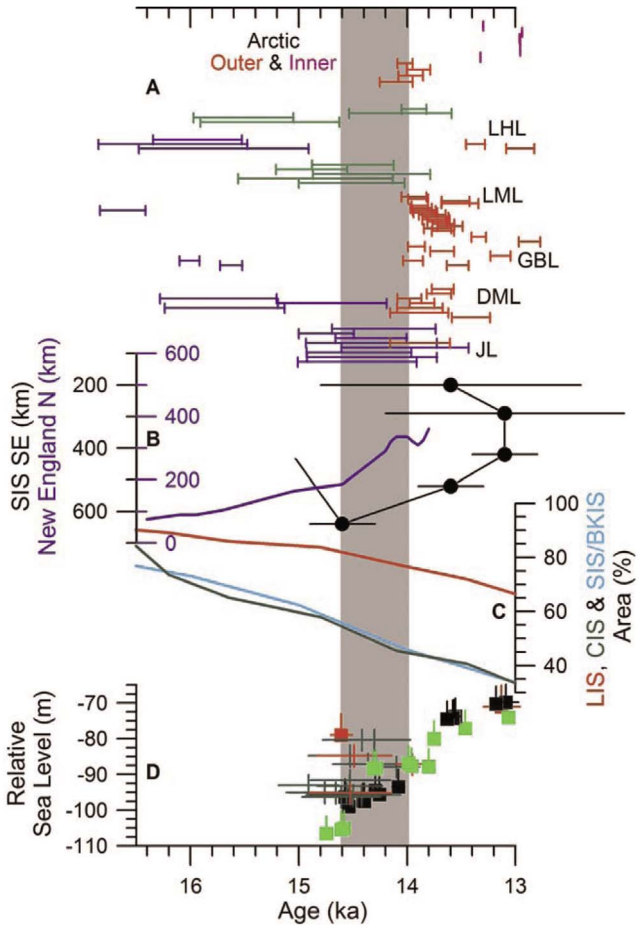

Figure 14. Northern Hemisphere ice sheet records spanning MWP-1A. (a) Radiocarbon dates that constrain the advance and retreat of the southern LIS during the Port Huron Stadial (blue maximum limiting on advance, red minimum limiting on retreat, and green showing lake level highstands and thus ice advanced in the lake basin) for the Lake Huron lobe (LHL), the Lake Michigan lobe (LML), Green Bay lobe (GBL), Des Moines lobe (DML), and James lobe (JL). Also shown are minimum-limiting dates for northwest LIS retreat in the Canadian Artic Archipelago. (b) Distance south for the southeast SIS relative to its extent at the Younger Dryas (black with symbols and uncertainties based on ^{10}Be dated moraines) [*Rinterknecht et al.*, 2006] and distance north for the southeast LIS margin relative to southern Connecticut dated by the New England varve chronology (blue line) [*Ridge*, 2003, 2004]. (c) Percent of the area remaining of the LIS (red), CIS (green), and SIS/BKIS (light blue) [*Dyke*, 2004; R. Gyllencreutz and J. Mangerud, DATED Project unpublished data, 2010]. (d) Relative sea level records. Squares are coral sea level data (red from New Guinea, light green from Tahiti, and black from Barbados) [*Edwards et al.*, 1993; *Bard et al.*, 1996; *Peltier and Fairbanks*, 2006; *Deschamps et al.*, 2012]. Crosses are mangrove sea level data from Sunda Shelf (red are in situ, and dark green are not in situ) [*Hanebuth et al.*, 2000]. Depth and age range are indicated for relative sea level data. Gray bar denotes the range in timing and duration of MWP-1A.

Flower et al., 2004]. Benthic δ^{18}O decreases as well by ~2.2‰ (Figure 15e), suggesting meltwater entering the Gulf of Mexico as a *hyperpycnal* flow [*Aharon*, 2006; *Marchitto and Wei*, 1995]. *Aharon* [2006] suggested that these Gulf of Mexico planktonic and benthic δ^{18}O decreases recorded 12.2–14.4 m of equivalent sea level rise, but he did not include the impact of low δ^{18}O values from LIS meltwater in his calculations. Using a runoff-ocean mixing model, *Carlson* [2009] found that when reduced runoff δ^{18}O from LIS meltwater was accounted for, these δ^{18}O decreases reflected ≤2.7 m of equivalent sea level rise from meltwater discharge down the Mississippi River during MWP-1A. Note, however, that the decreases in planktonic δ^{18}O and $\delta^{18}O_{sw}$ occur over a significantly longer interval than MPW-1A, only decreasing at ~12.9 ka, and therefore, hypopycnal meltwater discharge down the Mississippi River was not anomalous during MWP-1A relative to later discharge.

[68] Planktonic δ^{18}O also decreased by ~0.7‰ off of the eastern runoff outlets (Hudson and St. Lawrence Rivers) of the LIS [*Keigwin et al.*, 2005], which, if interpreted to reflect increased meltwater discharge, would be equivalent to ≤2.1 m of sea level rise [*Carlson*, 2009]. Subsequent reconstructions of water temperature using Mg/Ca in planktonic foraminifera, however, found that the δ^{18}O decrease was due to ~1.6°C of warming in the northwestern Atlantic during the Bølling [*Obbink et al.*, 2010]. After removing the effects of this warming, $\delta^{18}O_{sw}$ increases by 0.7–0.8‰ during MWP-1A (Figure 15c), suggesting a reduction in meltwater discharge to the North Atlantic through the Hudson and St. Lawrence Rivers and further implying a small contribution from this portion of the LIS to MWP-1A. Eastern outlet $\delta^{18}O_{sw}$ subsequently decreased after ~14.2 ka by ~0.8‰, but this reflects the retreat of the southern LIS during the latter part of the Port Huron Stadial (Figure 13) and routing of its meltwater runoff eastward as the eastern Great Lakes deglaciated during the Two Creeks Interstadial [*Clark et al.*, 2001; *Licciardi et al.*, 1999; *Obbink et al.*, 2010].

[69] After advancing to its LGM extent at ~29 ka, the northern margin of the LIS in the Canadian Arctic Archipelago began to deglaciate around the time of MWP-1A [*Dyke*, 2004; *England et al.*, 2009]. Radiocarbon dates on marine shells related to the marine limit from Melville and Banks Islands indicate deglaciation of McClure Strait prior to 14.1 ± 0.2 ka BP (740 year reservoir corrected to 12.18 ± 0.03 ^{14}C ka BP, UCIAMS-24770) and 14.0 ± 0.1 ka BP (740 year reservoir corrected to 12.26 ± 0.10 ^{14}C ka BP, TO-11308), respectively (Figure 14a) [*England et al.*, 2009]. However, ice remained farther south on Victoria Island until ~13.3 ka, as indicated by the oldest marine limit of 13.3 ± 0.1 ka BP (740 year reservoir corrected to 11.46 ± 0.10 ^{14}C ka BP, GSC-3511) (Figure 14a) [*Dyke*, 2004]. Similarly, the coast of mainland Arctic Canada south of the archipelago has a marine limit of 13.3 ± 0.2 ka BP (740 year reservoir corrected to 11.45 ± 0.16 ^{14}C ka BP, AECV-643Cc) [*Dyke*, 2004]. Together, these marine limits suggest only deglaciation of the outer islands of the Canadian Arctic Archipelago during MWP-1A. The breakup of ice on these outer islands before ~14.0 ka is further reflected in increased carbonate IRD deposition in the Arctic Ocean [*Darby et al.*, 2002], a

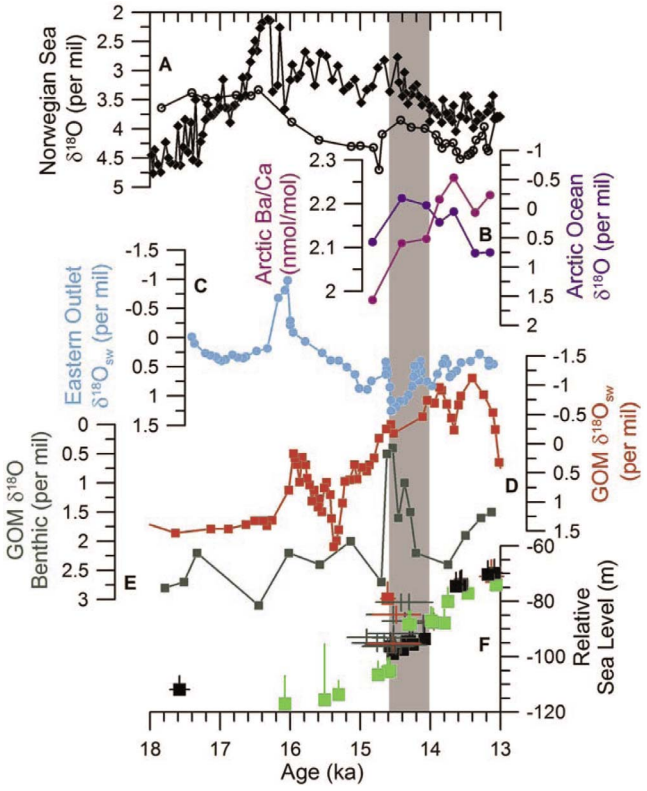

Figure 15. Runoff records during MWP-1A. (a) Norwegian Sea planktonic (solid) and benthic (open symbols) δ^{18}O [*Lehman et al.*, 1991; *Dokken and Jansen*, 1999]. (b) Arctic planktonic δ^{18}O (blue) and Ba/Ca (purple) [*Poore et al.*, 1999; *Hall and Chan*, 2004]. (c) $\delta^{18}O_{sw}$ from adjacent to the LIS eastern runoff outlets [*Obbink et al.*, 2010]. (d) Gulf of Mexico (GOM) planktonic $\delta^{18}O_{sw}$ [*Flower et al.*, 2004]. (e) GOM benthic δ^{18}O [*Aharon*, 2006]. (f) Relative sea level data. Squares are coral sea level data (red from New Guinea, light green from Tahiti, and black from Barbados) [*Edwards et al.*, 1993; *Bard et al.*, 1996; *Peltier and Fairbanks*, 2006; *Deschamps et al.*, 2012]. Crosses are mangrove sea level data from Sunda Shelf (red are in situ, and dark green are not in situ) [*Hanebuth et al.*, 2000]. Depth and age range indicated for relative sea level data. Gray bar denotes the range in timing and duration of MWP-1A.

decrease in planktonic δ^{18}O by 0.7–0.8‰ [*Poore et al.*, 1999], and an increase in Ba/Ca [*Hall and Chan*, 2004] (Figure 15b), indicative of increased iceberg and meltwater discharge. Modeling of the δ^{18}O decrease suggests that ≤0.5 m of sea level rise equivalent meltwater was discharged to the Arctic Ocean from LIS retreat during MWP-1A [*Carlson*, 2009].

[70] Estimates of the total LIS contribution to MWP-1A vary widely. Because of its size, *Peltier* [1994] assumed that all of the sea level rise originated from the LIS. Although no explanation was provided, *Peltier* [2004, 2005] revised this assumption with a contribution of 16.5 m equivalent sea level rise from the LIS and another 3.6 m equivalent sea level rise from the adjacent CIS, with the remainder coming from EIS (Figure 16a and Table 1). In their Bayesian ice sheet modeling experiments, *Tarasov and Peltier* [2005, 2006] modeled combined LIS and CIS contributions to MWP-1A of 8.1 ± 1.8 m equivalent sea level rise (Figure 16a and Table 1). More recently, *Tarasov et al.* [2012] modeled a larger combined LIS and CIS MWP-1A contribution of 11.6 ± 2.2 m of equivalent sea level rise. *Gregoire et al.* [2012] used a one-way coupling of an ice sheet and climate model to simulate a combined LIS and CIS contribution of ~9 m, assuming that the separation of the LIS and the CIS in their model corresponded with MWP-1A. The above discussed geologic records do not support the larger end of these assumed or dynamically modeled North American ice MWP-1A contributions. The area lost strictly from the LIS during MWP-1A (Figure 14c) [*Dyke*, 2004] equates to a sea level rise equivalent volume of 4.3 ± 0.5 m [*Carlson*, 2009] assuming an ice surface in equilibrium [*Paterson*, 1994], which was likely not the case during deglaciation. If ice on the eastern Canadian Arctic Archipelago and the Innuitian Ice Sheet are included [*Dyke*, 2004], the sea level rise contribution increases to 6.5 ± 0.8 m. We note, however, that the LIS area lost during MWP-1A is not anomalous relative to the following millennium (Figure 14c). Applying the same approach to the CIS area lost (Figure 14c) [*Dyke*, 2004] suggests a MWP-1A contribution of 1.2 ± 0.2 m of sea level rise from this ice sheet, but this is likely an overestimate due to the underlying mountainous terrain [*Carlson et al.*, 2012]. The aforementioned decreases in δ^{18}O adjacent to the LIS outlets imply that ≤5.3 m equivalent sea level rise was discharged from the LIS during MWP-1A [*Carlson*, 2009]. Equilibrium flow line ice sheet modeling reconstructed a LIS mass loss of 5.6–6.6 m equivalent sea level rise between 15.4 and 14 ka [*Licciardi et al.*, 1998]. Similarly, modeling of the surface mass balance response to Bølling warming simulated a 2.9 ± 1.0 m sea level rise contribution in 500 years in response to the warming, which was in addition to an ongoing sea level rise contribution of 4.0 ± 0.8 m in 500 years, yielding a total MWP-1A contribution of 6.9 ± 1.1 m from LIS surface ablation minus precipitation [*Carlson et al.*, 2012].

[71] The larger MWP-1A contributions from North America in many of the model simulations by *Tarasov and Peltier* [2005, 2006] and *Tarasov et al.* [2012] may result from their simplified climate forcing [*Tarasov and Peltier*, 2004]. Specifically, *Tarasov and Peltier* [2004] stated that "The use of a single climate proxy index based upon the Greenland Summit δ^{18}O record together with the above-defined "phase factor' is highly unlikely to allow us to capture the complexities of deglacial climate change over NA [North America]" (p. 366). They added that "The use of a downstream paleorecord (GRIP δ^{18}O) as a proxy for the time dependence of the climate forcing is a significant limitation of the current analyses" (p. 378). This suggests that there is considerable uncertainty in any attempt to associate a centennial-scale response of their ice sheet model to an actual climate change such as the centennial-scale Bølling warm period. *Marshall and Clarke* [1999] used a similar climate forcing scheme but did not attempt to correlate any individual melting event with a climate event because of the serious limitations in the use of the *Greenland Ice Core Project (GRIP)* δ^{18}O record as a proxy for climate forcing. In

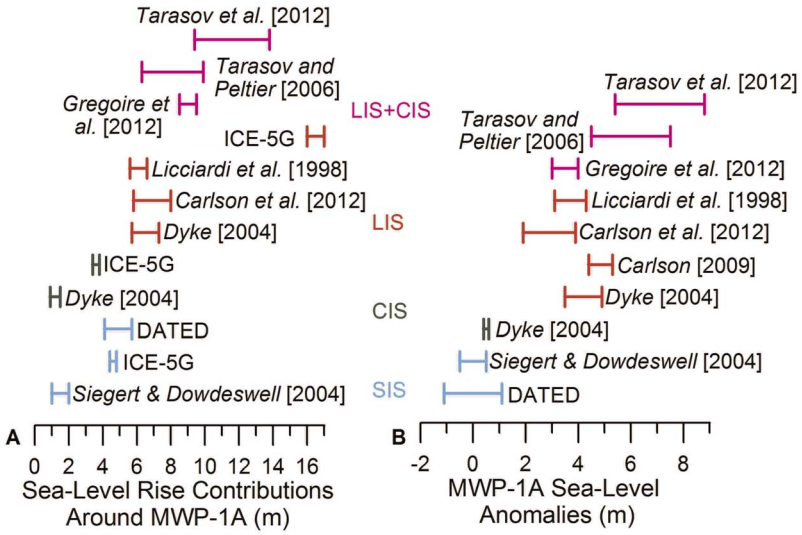

Figure 16. MWP-1A contribution estimates from Northern Hemisphere ice sheets (blue, SIS that includes the BKIS; green, CIS; red, LIS; and purple, LIS + CIS). (a) Contribution to sea level rise around the time of MWP-1A (see duration over which the volume is integrated in Table 1). (b) Anomalous sea level rise around the time of MWP-1A relative to the preceding interval of ice sheet retreat.

particular, the Summit Greenland ice core $\delta^{18}O$ records may not be directly related to temperature and precipitation over North America because changes in Greenland ice core $\delta^{18}O$ may be in response to changes in the LIS height and extent [*LeGrande and Schmidt*, 2009].

[72] Scaling of the GRIP $\delta^{18}O$ record across the entire LIS may also overestimate the degree of warming into the Bølling because the Summit Greenland ice cores exhibit the largest degree of warming into the Bølling relative to the rest of the Northern Hemisphere [*Shakun and Carlson*, 2010]. The *Tarasov and Peltier* [2004, 2005, 2006] and *Tarasov et al.* [2012] climate forcing has ~14°C of abrupt Bølling warming. This is likely larger than occurred along the southern margins of the LIS where pollen records indicated the Bølling to be cooler than the subsequent Allerød period [*Gill et al.*, 2009; *Gonzales and Grimm*, 2009; *Grimm et al.*, 2009]. In contrast, *Carlson et al.* [2012] used the climate forcing from the fully coupled National Center for Atmospheric Research *general circulation model (GCM)* transient simulation that successfully simulated changes in AMOC, Greenland, and North Atlantic climate during the Oldest Dryas and Bølling [*Liu et al.*, 2009]. This model transient simulation captured the ~10°C of mean annual warming over Greenland at the Bølling [*Severinghaus and Brook*, 1999] but simulated <4°C of summer warming along the southern margin of the LIS. The significantly larger Bølling warming in the *Tarasov and Peltier* [2004, 2005, 2006] and *Tarasov et al.* [2012] climate forcing can explain, at least in part, the larger MWP-1A contribution they simulate from the LIS relative to other estimates and simulations.

[73] A comparison between reconstructed and modeled ice streams of the LIS [*Stokes and Tarasov*, 2010] indicated that subglacial till viscosity in the *Tarasov and Peltier* [2005, 2006] model was increased prior to MWP-1A, thus allowing ice to thicken and increase in volume, with subsequent ice discharge during the MWP upon a prescribed weakening of the till viscosity [*Tarasov et al.*, 2012]. According to *Stokes and Tarasov* [2010, p. 2], "The location of fast ice flow is not prescribed but evolves freely when basal ice approaches the pressure melting point, subject to calibrated temporal controls for Heinrich events 1 and 2 and meltwater pulse 1a (i.e., two calibration parameters control a temporary increase in regional subglacial till viscosity for a few thousand years prior to these events with return to baseline viscosities at 24 ka (H2), 17.1 ka (H1) and 14.5 ka (Mwp1-a))." *Tarasov and Peltier* [2005, 2006] also applied the same method of forcing for Heinrich events in their model. Their model climate forcing (GRIP $\delta^{18}O$), however, is quite different for Heinrich events and MWP-1A as the former occurred during cold stadials whereas the latter was during the Bølling warm period. Similarly, sea level rise occurred over millennia during Heinrich events [*Clark et al.*, 2007; *Hemming*, 2004; *Siddall et al.*, 2008], whereas MWP-1A is defined by a centennial-scale jump in sea level [*Fairbanks*, 1989]. The very different climate states and sea level changes between Heinrich events and MWP-1A suggests that a change in till viscosity is unlikely to be a common contributing forcing for both MWP-1A and Heinrich events.

[74] While *Tarasov et al.* [2012] did not use a till viscosity forcing during MWP-1A, this suite of simulations allowed for uncertainties in the LIS margin chronology of *Dyke* [2004] of ±1000 years during the deglaciation up to 9 ka, when the uncertainty decreased to ±500 years. While some of the LIS margin locations during the last deglaciation may have an uncertainty of ±1000 years, during MWP-1A the southwest to eastern LIS margins are well mapped and dated (see above discussion), and an uncertainty of ±1000 years is an overestimate. Radiocarbon-dated marine limits constrain the northern LIS margin during MWP-1A and have uncertainties of less than ±1000 years. The ±1000 year margin

uncertainty will bias the simulations of *Tarasov et al.* [2012] to larger LIS MWP-1A contributions because the greater LIS retreat that occurred during the Allerød after ~14 ka (see section 8 and Figure 14c) may be included as part of the Bølling and thus contribute to MWP-1A. Southern LIS margins advanced just prior to MWP-1A and were therefore more retracted 1000 years prior to MWP-1A, also allowing for a greater MWP-1A contribution than if a more realistic margin uncertainty were employed. We note that in screening their ice sheet model simulations, *Tarasov et al.* [2012] apply an initial filter that excludes simulations that have a LIS + CIS MWP-1A contribution of <7 m of equivalent sea level rise and penalize simulations for final analysis that have a contribution of between 7 and 9.5 m, which further biases their results toward larger MWP-1A contributions from the LIS than if this initial screening and penalization was not employed. Given the above discussion of the existing data on the LIS, we suggest that the geologic record does not support such filtering.

[75] *Gregoire et al.* [2012] forced an ice sheet model of the LIS and CIS with transient deglacial climate from a GCM that had ICE-5 G topographic boundary conditions. They simulated a peak in LIS and CIS melting at ~11.5 ka due to the separation of the LIS and CIS and attendant increase in ablation area. The resulting sea level rise was ~9 m over ~500 years, with a sea level rise anomaly of 3–4 m (Figure 16) of which at least one third was sourced from the CIS. *Gregoire et al.* [2012] suggested that the separation of the LIS from the CIS may be concurrent with MWP-1A rather than at 11.5 ka as their model simulated. However, the oldest minimum-limiting ^{14}C date from the center of the confluent LIS and CIS margins indicates that these two ice sheets had largely separated before 17.0 ± 0.2 ka (13.97 ± 0.17 ^{14}C ka BP, TO-2742) [*Clague and James*, 2002; *Dyke*, 2004]. Other minimum-limiting ^{14}C dates imply that CIS retreat did accelerate during MWP-1A (Figure 14c) [*Clague and James*, 2002; *Dyke*, 2004], although its sea level rise contribution may be overestimated in *Gregoire et al.*'s [2012] ice sheet model, insofar as it does not resolve the high-relief topography of the Canadian Cordillera.

[76] In summary, multiple lines of geological and modeling evidence point to a LIS MWP-1A contribution of 6–8 m with an additional contribution from the CIS of <1 m, which agrees with the lower end of the *Tarasov and Peltier* [2006] and *Tarasov et al.* [2012] dynamic ice sheet model results and the dynamic ice sheet model results of *Gregoire et al.* [2012] if the CIS and LIS separation occurred later than suggested by existing ice margin constraints [*Dyke*, 2004] (Figure 16a and Table 1). We note that the middle to higher end of the *Tarasov and Peltier* [2006] and *Tarasov et al.* [2012] simulations may contain potential biases that lead to larger LIS + CIS MWP-1A contributions than supported by the geologic record. We also emphasize that a significant fraction of this contribution represents ongoing sea level rise at rates similar to those before and after the event, with the anomalous sea level rise contributions from the LIS and CIS to MWP-1A being a smaller volume (Figure 16b and Table 1).

5.2. European Ice Sheet Contributions

[77] *Tarasov and Peltier* [2005] and *Peltier* [2005] suggested that a large contribution to MWP-1A came from the *Barents-Kara Ice Sheet (BKIS)* part of the EIS complex, stating that [*Tarasov and Peltier*, 2005, p. 662] "Given the inferred collapse of the Barents Sea ice sheet during this interval [the Bølling]…, it follows that a substantial fraction of the remaining contribution to mwp-1a is due to Eurasian sources." However, we suggest that this was a misunderstanding by these authors in using the radiocarbon versus calibrated year chronology for the disintegration of the BKIS. One record of the demise of the BKIS comes from the ~1.0‰ decrease in planktonic δ^{18}O adjacent to the BKIS [*Jones and Keigwin*, 1988] and throughout the Norwegian Sea [*Karpuz and Jansen*, 1992] that occurred 15.0–14.0 ^{14}C ka BP (19.0–18.5 ka BP in calibrated years). This timing is supported by minimum-limiting radiocarbon dates overlying till within the BKIS LGM margin, which indicate that the onset of BKIS retreat occurred prior to 19.5 ± 0.1 ka (440 year reservoir corrected to 16.44 ± 0.08 ^{14}C ka BP, Beta-71988), whereas minimum-limiting radiocarbon dates from well within the BKIS LGM margin of 15.7 ± 0.3 ka BP (13.25 ± 0.14 ^{14}C ka BP, Tua-183) to 14.0 ± 0.2 ka BP (12.70 ± 0.12 ^{14}C ka BP, AA-9458) indicate a significantly reduced ice sheet by this time [*Landvik et al.*, 1998]. Applying a larger reservoir correction of up to 1000 ^{14}C years to these records still does not shift the dates young enough for the BKIS to be a significant source of MWP-1A. Consequently, much of the BKIS deglaciation occurred prior to MWP-1A, and it therefore could not have made a significant contribution to this event.

[78] The history of the *Scandinavian Ice Sheet (SIS)* part of the EIS complex during MWP-1A is constrained by cosmogenic radionuclide and radiocarbon dates. Along its southeast margin, the SIS readvanced to the Pomeranian Moraine prior to MWP-1A with subsequent retreat beginning at 14.6 ± 0.3 ka based on ^{10}Be ages on moraine boulders (Figure 14b) [*Rinterknecht et al.*, 2005, 2006, 2007], corresponding to the start of MWP-1A. Ice only retreated ~100 km north, however, before depositing the Middle Lithuanian Moraine prior to 13.6 ± 0.3 ka [*Rinterknecht et al.*, 2006, 2007], suggesting little contribution from this sector of the SIS to MWP-1A. Cosmogenic and radiocarbon dates indicate that subsequent retreat of the southeastern SIS accelerated, retreating ~500 km north in ~600 years (Figure 14b) [*Rinterknecht et al.*, 2006], after the end of MWP-1A. Although the southwestern and western SIS margins retreated <50 km during MWP-1A [*Boulton et al.*, 2001], ^{10}Be boulder and bedrock dates suggest that some thinning occurred during MWP-1A, with decreases in ice surface elevation of 350–500 m between ~16.5 and 11.0 ka [*Brook et al.*, 1996; *Goehring et al.*, 2008; *Linge et al.*, 2006]. Planktonic and benthic δ^{18}O records from the adjacent Norwegian Sea show 0.4–0.5‰ and 0.2–0.5‰ decreases, respectively, at 14.5–14.0 ka (Figure 15a) [*Dokken and Jansen*, 1999; *Lehman et al.*, 1991; *Koc and Jansen*, 1994], which may reflect SIS

retreat during MWP-1A. Alternatively, this signal may record warming of the Norwegian Sea due to invigoration of the AMOC at the onset of the Bølling [*McManus et al.*, 2004; *Praetorius et al.*, 2008]. For example, *Karpuz and Jansen* [1992] documented coincident Norwegian Sea surface warming of 2–4°C, which could explain all of the observed planktonic $\delta^{18}O$ decrease and which could also have influenced the benthic record by advection of the warmer water mass to depth [*Skinner et al.*, 2003].

[79] The new compilation of the EIS area through the last deglaciation by the *Digital Atlas of the Eurasian Deglaciation (DATED) Project* (http://www.gyllencreutz.se/dated.html; R. Gyllencreutz and J. Mangerud, personal communication, 2010) shows that although these ice sheets retreated during MWP-1A, the rates of retreat were similar to rates prior to MWP-1A (Figure 14c). Scaling the area loss to ice volume [*Paterson*, 1994] suggests a sea level rise contribution from the EIS of 4.9 ± 0.8 m between ~15 and 14 ka, which is essentially the same as the preceding sea level rise contribution of 4.9 ± 1.8 between ~16 and 15 ka (Figure 16 and Table 1). These values agree with dynamic ice sheet model results that suggest 1–2 m of sea level rise from the SIS and BKIS between 14.5 and 14 ka at rates that are similar to the preceding 1 kyr (Figure 16 and Table 1) [*Siegert and Dowdeswell*, 2004].

5.3. Summary

[80] To summarize, our estimates for the sea level contributions of the LIS (6–8 m), the CIS (<1 m), and the SIS (1–3 m) suggest a combined Northern Hemisphere sea level contribution of 7–12 m over a 500–800 year period spanning MWP-1A. The contribution to this amount (7–12 m) above ongoing ice sheet retreat rates is, however, only 3–8 m of ice-equivalent sea level rise (Figure 16 and Table 1). Because the event is now constrained to have been 300 years in duration [*Deschamps et al.*, 2012], however, these amounts should be reduced by 40% to give 4–7 m for the total during MWP-1A and 2–5 m above ongoing ice sheet retreat rates. Accordingly, Northern Hemisphere ice sheets may have contributed at most 50% of the ice-equivalent sea level rise associated with MWP-1A (14 m total, 11.5 m anomalous), with the majority of this coming from the LIS.

6. MWP-1A: GEOLOGICAL CONSTRAINTS ON A SOURCE FROM ANTARCTICA

[81] In evaluating possible ice sheet sources for MWP-1A, *Clark et al.* [1996] were unable to identify any clear evidence that supported the prevailing argument for a substantial Northern Hemisphere contribution [*Fairbanks et al.*, 1992; *Keigwin et al.*, 1991; *Peltier*, 1994], with ice sheet models suggesting ~3 m of sea level sourced from the LIS [*Licciardi et al.*, 1998]. They thus concluded that the AIS was the only other plausible source, acknowledging that there were no high-resolution records available at the time to test that hypothesis. Since that time, a number of studies have constructed chronologies of AIS deglaciation, largely based on terrestrial records, with the majority of the work concluding that the AIS did not contribute significantly to MWP-1A, with most mass loss occurring afterward [*Ackert et al.*, 1999, 2007; *Baroni and Hall*, 2004; *Conway et al.*, 1999; *Harris and Beaman*, 2003; *Licht*, 2004; *Mackintosh et al.*, 2011; *Smith et al.*, 2010]. Nevertheless, there is also evidence for a change in AIS volume at the time of MWP-1A [*Bassett et al.*, 2007; *Heroy and Anderson*, 2007; *Price et al.*, 2007], and as discussed in section 7, geophysical modeling of far-field sea level records indicates that the geographic signature of the non-ice-equivalent sea level component of MWP-1A is most consistent with a contribution from the AIS [*Bassett et al.*, 2005; *Clark et al.*, 2002].

[82] In this section, we assess the chronological constraints that have been used to argue against a significant AIS contribution to MWP-1A. Although these data have significantly improved our understanding of the timing of the last deglaciation, we find that there is considerable uncertainty in the history of grounding line retreat, and little is known about the timing of ice surface lowering prior to the Holocene.

6.1. Issues in Developing Antarctic Geochronologies

6.1.1. Radiocarbon

[83] Two factors contribute to potentially large uncertainties in radiocarbon-based chronologies derived from marine sediments from the Antarctic continental shelves. The first is that the reservoir age of *dissolved inorganic carbon (DIC)* in the surface mixed layer in the Southern Ocean is much older than that of other oceans due to exchange with ^{14}C-depleted deep water and to the presence of sea ice which suppresses CO_2 exchange between the atmosphere and the ocean [*Gordon and Harkness*, 1992]. Most reservoir ages measured on twentieth century prebomb specimens range from 1000 to 1700 years, with the range likely representing some combination of vital effects and spatial variability in upwelling of deep waters [*Berkman and Forman*, 1996; *Ohkouchi and Eglinton*, 2008]. An average value of 1300 ± 100 years is commonly used for the reservoir age [*Berkman and Forman*, 1996], but the larger measured range becomes important when trying to establish chronologies at centennial resolution. Moreover, this correction is based only on samples from the early twentieth century, but it may have changed through time, especially during the deglaciation in association with large changes in ventilation and upwelling [*Anderson et al.*, 2009], sea ice extent [*Shemesh et al.*, 2002], and ice sheet meltwater fluxes [*Domack et al.*, 1989].

[84] The second factor is that because carbonate fossils are rare in Antarctic marine sediments, many constraints on deglaciation from the continental shelf are based on radiocarbon of the bulk *acid insoluble organic (AIO) carbon* fraction sub–ice shelf sediments. AIO ^{14}C ages from surface sediments, however, are consistently older than the ~1300 year reservoir age in modern DIC, with a range in any given region of as much as 26,000 ^{14}C years that largely reflects reworking of older organic matter [*Andrews et al.*, 1999b; *Harris and Beaman*, 2003; *Licht et al.*, 1999; *McKay et al.*, 2008; *Ohkouchi and Eglinton*, 2008]. Corresponding age corrections for each core site are conventionally established by subtracting the age of the AIO at the modern sediment-water interface [*Andrews et al.*, 1999b; *Domack et al.*, 1999;

Harris and Beaman, 2003; *Licht and Andrews*, 2002; *Mackintosh et al.*, 2011], but given the large spatial variability in the age of surface sediments, this makes the highly uncertain assumption that the amount of reworked organic matter has remained the same at each core site through time. AIO ^{14}C ages obtained from diatomaceous mud or ooze that may overlie sub–ice shelf sediments are more reliable [*Domack et al.*, 1999] and closely constrain the timing of the transition to open marine conditions, but they only provide limiting ages for grounding line retreat, and even these have been documented as containing old reworked carbon [*Leventer et al.*, 2006; *Mackintosh et al.*, 2011].

[85] *Ohkouchi and Eglinton* [2008] found that radiocarbon ages of solvent extractable, short-chain fatty acids isolated from surface sediments of the Ross Sea, Antarctica, are consistent with ^{14}C ages of the modern dissolved inorganic carbon reservoir age and that the radiocarbon ages of these fatty acids increase progressively with core depth. In contrast, as suggested from all previous work on AIO, *Ohkouchi and Eglinton* [2008] found that radiocarbon ages of bulk organic matter in the corresponding sediments are substantially older. These results suggest the possibility of significant improvements in developing future radiocarbon chronologies of Antarctic continental shelf sediments.

[86] Another important chronological constraint on deglaciation of the Ross Sea sector of the *West Antarctic Ice Sheet (WAIS)* is based on radiocarbon dating of lacustrine benthic algal mats [*Bockheim et al.*, 1989; *Hall and Denton*, 2000; *Stuiver et al.*, 1981]. Two issues may affect the reliability of these ages for constraining deglaciation. The first is that algal mats can grow in any standing body of water. When they are found in stratigraphic association with a former shoreline feature, in particular perched deltas associated with an ice-dammed lake, then they are likely contemporaneous with the former lake level, and their ages constrain the time of thicker ice responsible for damming the lake. In contrast, algal mats can also grow in small, ephemeral ponds that can form on former glaciated surfaces, and radiocarbon ages on the algal mats thus provide only limiting minimum ages for the underlying deposits. *Bockheim et al.* [1989] documented this latter case from ^{14}C ages measured on algal mats collected from the late Quaternary surfaces associated with deglaciation of the Hatherton and Darwin Glaciers in the Transantarctic Mountains. In particular, they found that not all ages were in stratigraphic order with elevation above the present ice surface, indicating that algal mats had grown at different times regardless of the initial time of deglaciation.

[87] An additional factor that introduces uncertainty in radiocarbon dating of algal mats is the potential that the lake water in which they lived had a reservoir age [*Stuiver et al.*, 1981]. *Doran et al.* [1999] attempted to systematically identify the ^{14}C ages of various carbon pools in the Antarctic Dry Valleys. The ^{14}C age of DIC of surface waters from three different lakes ranged from modern to 2100 years, while the age of DIC of bottom waters was as old as 10,000 years. *Doran et al.* [1999] also measured the ^{14}C age of glacial ice (7430 years) and of the DIC of stream water draining from the glacier (570 years), suggesting that the stream had largely equilibrated with the atmosphere. A ^{14}C age of an algal mat growing in a pool of the stream, however, dated to 1700 years, possibly suggesting a strong modern ^{14}C gradient between surface waters and the deeper waters of the pool. Stream water was modern by the time it reached a lake, as were algal mats living in that water. *Hall and Henderson* [2001] reported reservoir ages of ~3600 years and ~18,000 years based on paired dating of lacustrine carbonates by ^{14}C and U/Th, with the older age associated with carbonates deposited near the former grounding line of the Ross Sea ice sheet in the lake. *Hendy and Hall* [2006] found that most reservoir ages on water at the surface and at depth of two lakes in the Dry Valleys were 1900–2600 years, with one age on water adjacent to Taylor Glacier being 15,450 years. Algal mats from seasonally ice-free areas adjacent to the shoreline (moats) dated from 580 to 3600 years.

[88] *Doran et al.* [1999] and *Hendy and Hall* [2006] identified two possible explanations for these variable reservoir ages: (1) a source of old water from glaciers, which subsequently gets younger by exchange with the atmosphere if it drains as surface water but otherwise retains a significant reservoir age if it melts directly into the lake, and (2) aging of water that resides in the lake but is isolated from the atmosphere due to density stratification or ice cover. Based on the results reported by *Doran et al.* [1999], *Hall and Henderson* [2001, p. 567] concluded that "One key finding has been that algal mats growing on deltas located at the lake edge yield modern ages, as do streams entering the lakes. The present consensus drawn from this recent work is that radiocarbon ages of algae from deltas should be valid, but dates of material from deeper locations in the lakes probably will suffer from a reservoir effect which will vary both in space and time." The subsequent results by *Hendy and Hall* [2006], however, clearly demonstrate that algal mats from moat regions are subject to large reservoir ages. During the last glaciation, lakes in several Dry Valleys were much larger likely due to an increase in the meltwater contribution from glaciers and grounded ice in the Ross Sea [*Stuiver et al.*, 1981]. Because many of these ice masses were directly in contact with these lakes [*Hall and Denton*, 2000], their contributions to the ^{14}C balance in the lakes would have been greater, thus potentially increasing the reservoir age of the lakes.

6.1.2. In Situ Cosmogenic Nuclides

[89] Because of the extremely low erosion rates and the high cosmogenic nuclide production rates associated with the cold, dry, and high-latitude Antarctic environment, surface exposure dating with in situ cosmogenic nuclides provides a means of developing late Quaternary chronologies with potential centennial-scale resolution for events during the last deglaciation [*Stone et al.*, 2003]. *Brook et al.* [1995, 1993] developed the first such Antarctic glacial chronologies from the Dry Valleys in the Transantarctic Mountains. Several studies have since evaluated the last deglaciation of Antarctica with surface exposure dating, including the East Antarctic Ice Sheet [*Fink et al.*, 2006; *Mackintosh et al.*, 2007], the Antarctic Peninsula [*Bentley et al.*, 2006], and West Antarctica [*Ackert et al.*, 1999, 2007; *Bentley et al.*, 2010; *di Nicola et al.*, 2009; *Johnson et al.*, 2008; *Oberholzer et al.*,

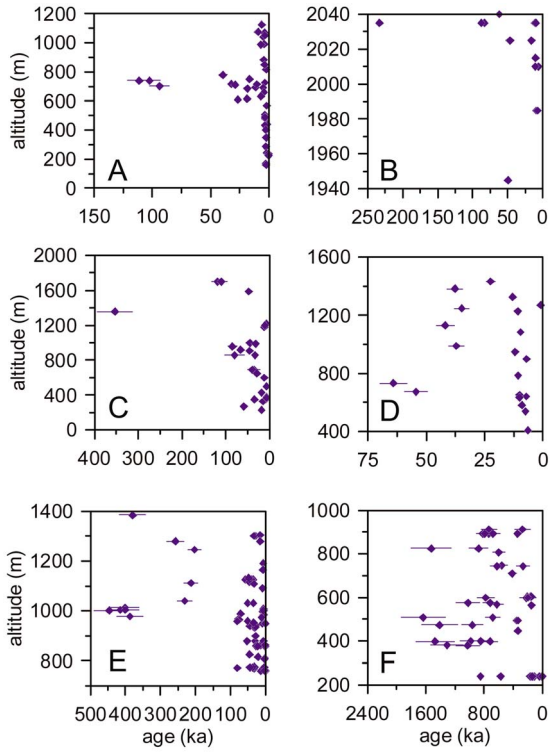

Figure 17. Cosmogenic nuclide data from glacial erratics exposed following the last deglaciation of Antarctica. (a) Data from *Stone et al.* [2003]. (b) Data from *Ackert et al.* [1999]. (c) Data from *Bentley et al.* [2006]. (d) Data from *Mackintosh et al.* [2007]. (e) Data from *Bentley et al.* [2010]. (f) Data from *Hein et al.* [2011].

2003; *Stone et al.*, 2003]. Whereas *Brook et al.* [1995, 1993] sampled boulders from glacial moraines, many subsequent studies have applied the so-called "dipstick" strategy of sampling single erratics along a vertical transect of a *nunatak* to constrain the history of ice sheet surface lowering. Here we discuss several general issues that these studies have revealed in using surface exposure dating in Antarctica.

[90] The first issue is *inheritance.* Figure 17 illustrates this problem by showing data from six studies that derived a history of ice surface lowering during the last deglaciation. Most of the samples are clearly older than the last deglaciation and are thus typically identified as outliers due to inheritance, but such decisions are not always straightforward when sample ages fall within the last glacial interval. This issue is further exacerbated by the fact that in many of these studies, only one erratic is sampled from any given location. Multiple independent measurements of the age of a single surface, however, are needed to identify anomalous samples due to issues such as inheritance. In particular, these anomalous samples may differ from the true age by only a few hundreds to thousands of years, as evident from the populations shown in Figure 17, which becomes significant when attempting to constrain events of the last deglaciation. Inheritance is also a widespread problem in many regions of the Arctic [*Briner et al.*, 2005; *Marsella et al.*, 2000; *Miller et al.*, 2006] and likely reflects transport by less erosive cold-based ice that fails to remove cosmogenic nuclides from previous exposure [*Kelly et al.*, 2008].

[91] A related issue in applying surface exposure dating to the deglacial history of Antarctic is the identification and interpretation of vertical zonation of a landscape according to differences in rock surface weathering. The significance of these so-called weathering zones to ice sheet history in Scandinavia and the eastern Canadian Arctic has been debated for over a century, with the upper limit of any given weathering zone interpreted as either a former ice surface [*Boyer and Pheasant*, 1974; *Ives*, 1978; *Nesje and Dahl*, 1990] or an englacial change in basal thermal regime from nonerosive cold-based ice above to erosive warm-based ice below the limit [*Sugden*, 1977; *Sugden and Watts*, 1977]. Surface exposure ages from upper weathered zones on Baffin Island [*Briner et al.*, 2005, 2006; *Miller et al.*, 2002] and Fennoscandia [*Fabel et al.*, 2006; *Goehring et al.*, 2008], however, have now conclusively demonstrated that the limit marks an englacial thermal boundary, whereby the upper, more weathered surface was covered by cold-based, largely nonerosive ice at the LGM. Recent work from Antarctica has similarly used exposure ages to demonstrate that highly weathered rock surfaces were preserved beneath cold-based ice during the last glaciation [*di Nicola et al.*, 2009; *Mackintosh et al.*, 2007; *Stone et al.*, 2003; *Strasky et al.*, 2009; *Sugden et al.*, 2005].

6.2. Regional Reconstructions of Antarctic Deglaciation

[92] In the following, we assess regional reconstructions of the deglacial history of the WAIS and *East Antarctic Ice Sheet (EAIS)* and their constraints on the ice sheet contribution to sea level. We begin by establishing the timing of the local LGM since this is important to understanding the timing of the sea level contribution of Antarctica during the last deglaciation, with particular emphasis on MWP-1A.

6.2.1. Ross Sea: Last Glacial Maximum

[93] Marine geological studies in the central and eastern Ross Sea demonstrate that grounded ice extended across the shelf toward the shelf edge at the LGM. *Shipp et al.* [1999] described a young unconformity covered by till, indicating advance of grounded ice across the shelf. Further evidence is provided by swath bathymetry and side-scan sonar records which show ice contact features on the shelf such as mega-scale glacial lineations and grounding zone sedimentary wedges that document grounded ice during the LGM [*Anderson et al.*, 2002; *Shipp et al.*, 1999]. The maximum extent of the LGM grounded ice margin is generally placed at or near the edge of the continental shelf in the eastern and central Ross Sea and either north [*Anderson et al.*, 2002; *Shipp et al.*, 1999] or south [*Licht et al.*, 1996] of Coulman Island in the western Ross Sea.

[94] Several lines of evidence constrain the timing of the initial LGM advance of WAIS in the inner Ross Sea as occurring between 31 and 28.5 cal ka (Figure 18). Reworked marine shells in glacial deposits on Ross Island and at the

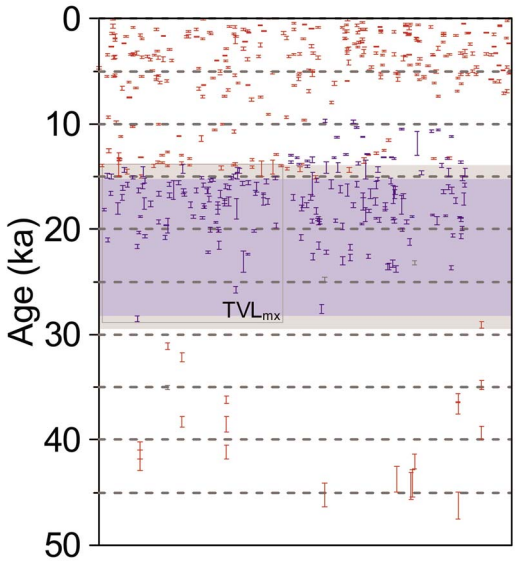

Figure 18. Compilation of calibrated ^{14}C ages used to identify the time of the local last glacial maximum for the Ross Sea area, West Antarctica. Calibrated ^{14}C ages are shown as 1σ range, with red symbols indicating ages that constrain there to be no ice at that time and location and blue symbols indicating limiting (maximum or minimum) ages that are stratigraphically associated with evidence for ice at the site. The horizontal blue bar with gray bars above and below represents the time of the LLGM and associated error, respectively. The calibrated ^{14}C ages (blue symbols) in the gray outlined box labeled TVL$_{mx}$ are on organic matter (algae) in sediments associated with high lake levels in Taylor Valley that require the WAIS ice margin to be at its maximum extent. The calibrated ^{14}C ages (blue symbols) immediately to the right of the gray outlined box are on organic matter associated with sediments that indicate an ice margin near the mouth of Taylor Valley but not at its maximum extent. Data from *Hall and Denton* [2000] and *Denton and Marchant* [2000]. Modified from *Clark et al.* [2009].

mouth of Taylor Valley indicate ice-free conditions from 31.2 ± 0.2 ka (28,160 ± 390 ^{14}C yr BP, UGA 6795) to 43.7 ± 1.0 ka (40,900 ± 1460 ^{14}C yr BP, AA 14058) [*Dochat et al.*, 2000; *Hall and Denton*, 2000]. These constraints on the timing of ice-free conditions are in excellent agreement with ^{14}C ages on fossil penguin eggshells at Cape Hickey on the western Ross Sea coast (30.8 ± 0.2 ka (27,170 ± 250 ^{14}C yr BP, NZA 20905) to 45.3 ± 1.1 ka (43,010 ± 1400 ^{14}C yr BP, BETA 204545)) [*Emslie et al.*, 2007]. The youngest shell and guano ages also constrain a limiting maximum age for the initial LGM advance as occurring after ~31 cal ka. *Licht and Andrews* [2002] reported a ^{14}C age on reworked benthic foraminifera which suggested that grounded ice advanced to its maximum extent on the outer continental shelf sometime after 16.8 ± 0.3 ka (14,970 ± 135 ^{14}C yr BP, AA 23222).

[95] Additional constraints on the timing of maximum grounded ice in the Ross Sea come from dating of proglacial lakes that were dammed by lobes of ice that projected partway up the Dry Valleys that are now open to the Ross Sea. The largest such lake (Lake Washburn) formed in Taylor Valley when a grounded ice lobe filled the mouth of the valley [*Stuiver et al.*, 1981]. The ^{14}C age on the oldest delta that formed in glacial Lake Washburn (28.6 ± 0.3 ka (23,800 ± 200 ^{14}C yr BP, QL-1708)) [*Hall and Denton*, 2000] thus provides a limiting minimum age for the onset of the local LGM. When the lake was at its largest, it extended up valley into the Lake Bonney basin and periodically reached a maximum elevation of 347 m, as indicated by dated deltas in the Lake Bonney basin [*Hall et al.*, 2010] (Figure 19). Although there is no discussion of what controlled this maximum elevation, we note that it is the same as the maximum elevation of the moraine on Hjorth Hill deposited by the grounded ice that dammed the lake [*Hall and Denton*, 2000], suggesting that when the lake filled to this level, it may have drained along the ice margin across Hjorth Hill. At this point, we hypothesize that the lake may have rapidly eroded its spillway and caused the rapid drops in lake level identified from shoreline features in the Taylor Valley [*Hall et al.*, 2010] (Figure 19).

[96] Extensive radiocarbon dating on benthic algal mats associated with proglacial lake sediments in the Taylor Valley and on adjacent Hjorth Hill provides key constraints on the termination of the LGM in the Ross Sea [*Hall and Denton*, 2000; *Stuiver et al.*, 1981]. In this case, the dating provides information on ice margin retreat associated with thinning of the grounded ice sheet in McMurdo Sound. (1) The youngest ^{14}C age (14.9 ± 0.3 ka (12,665 ± 120 ^{14}C yr BP, AA 20667)) constraining the time of the LGM ice margin at the Hjorth Hill moraine provides a limiting maximum age for retreat from the moraine. (2) Two ^{14}C ages on algae that grew in a local glacial lake that formed following initial ice margin retreat from the Hjorth Hill moraine provide limiting minimum ages for this retreat (15.0 ± 0.3 ka (12,708 ± 102 ^{14}C yr BP, AA 13576) and 15.0 ± 0.2 ka (12,739 ± 91 ^{14}C yr BP, AA 17342)). (3) Lacustrine deposits occur in a stream exposure cut into the moraine deposited by the LGM ice margin on the floor of Taylor Valley, with a ^{14}C age on algal mats requiring deglaciation from the moraine before 14.7 ± 0.2 ka (12,476 ± 97 ^{14}C yr BP, AA 17333). (4) Glaciolacustrine sediments containing dropstones occur along the distal side of the valley floor threshold moraine, indicating that the ice margin was at the moraine [*Hall and Denton*, 2000]. The youngest ^{14}C age from this unit (14.4 ± 0.8 ka (12,270 ± 500 ^{14}C yr BP, QL 1794)) provides a limiting maximum age for retreat from the moraine. These dating constraints thus suggest that the termination of the LGM in this region occurred between 14.4 and 15.0 ka based on the youngest limiting maximum ^{14}C age for ice margin retreat (14.4 ± 0.8 ka; QL 1794) and the oldest limiting minimum ^{14}C age for ice margin retreat (15.0 ± 0.3 ka; AA 13576).

[97] *Brook et al.* [1995] sampled erratics from four locations on the terminal moraine of Ross Sea drift that was deposited by grounded ice in the McMurdo Sound region [*Denton and Marchant*, 2000]. While the distribution of ^{3}He, ^{10}Be, and ^{26}Al cosmogenic ages suggests that inheritance is a problem at three locations, the ages from the Blue Glacier location are in good agreement, with a mean age of

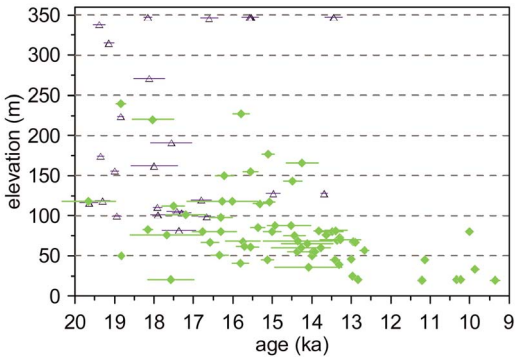

Figure 19. Calibrated ^{14}C ages on organic matter (algae) in deltas associated with high lake levels in Taylor Valley [*Hall et al.*, 2010]. Green symbols are from Fryxell Basin, and blue symbols are from Bonney Basin.

12.8 ± 2 ^{3}He ka (n = 5) and individual ages on the same boulder of 14 ± 2 ^{3}He ka, 14 ± 2 ^{10}Be ka, and 16 ± 2 ^{26}Al ka. Moreover, the moraine at this location abuts against an ice contact delta, which has algae dated to 14.2 ± 0.1 ka (12,330 ± 50 ^{14}C yr BP, QL 1146) [*Stuiver et al.*, 1981]. Insofar as we interpret in situ cosmogenic ages from moraines as dating the timing of ice retreat, this result is also in good agreement with the initial age of deglaciation suggested from the radiocarbon chronology in Taylor Valley.

6.2.2. Ross Sea: The Last Deglaciation

[98] The marine record of deglaciation of the Ross Sea is established by using the characteristic stratigraphic succession reflecting grounding line retreat as represented by the transition from subglacial facies to sub–ice shelf facies to open marine facies [*Anderson et al.*, 2002; *Domack et al.*, 1999]. AIO ^{14}C ages obtained from the diatomaceous mud or ooze that comprises the open marine facies provide the most reliable dating [*Andrews et al.*, 1999b; *Domack et al.*, 1999; *Licht et al.*, 1996] and thus closely constrain the timing of the transition from sub–ice shelf to open marine conditions but as such provide only limiting minimum ages for grounding line retreat, with estimated uncertainties of at least ±500 years [*Andrews et al.*, 1999b].

[99] Based on AMS ^{14}C ages on AIO from open marine sediments above the transition from subglacial sediments and assuming a 1200 year reservoir age correction, *Licht et al.* [1996] concluded that deglaciation of the Victoria Land coast near the Drygalski ice tongue occurred sometime before 13.3 ± 0.1 ka (11,440 ± 80 ^{14}C yr BP, CAMS 12581) and that the ice edge had retreated back to Ross Island sometime before 7.5 ± 0.1 ka (7830 ± 60 ^{14}C yr BP, AA 11876). By subtracting the age of surface sediment rather than the reservoir age, *Licht and Andrews* [2002] subsequently revised the minimum age for deglaciation of the Drygalski Trough from 13.3 ± 0.1 ka to 11.1 ± 0.1 ka.

[100] *Domack et al.* [1999] obtained ^{14}C ages on AIO from marine cores that were corrected for the age of the AIO at the sediment-water interface of each core. Although the ages were measured on samples from the full range of sediment facies, *Domack et al.* [1999] only used those ages from diatomaceous mud and ooze facies, which then only constrain the timing when open marine conditions became established. Accordingly, they argued that open marine conditions were established in the western Ross Sea by at least 13.0 ± 0.1 ka (11,060 ± 95 ^{14}C yr BP, AA 17360) in outer Drygalski Trough, by 11.3 ± 0.1 ka (9850 ± 95 ^{14}C yr BP, AA 17368) in inner Drygalski Trough off Cape Washington, and by at least 6.2 ± 0.1 ka (5480 ± 65 ^{14}C yr BP, AA 17370) east of Ross Island at Granite Harbor. *Licht and Andrews* [2002] were unable to construct a reliable deglaciation chronology for the central Ross Sea because the AIO ^{14}C ages on postglacial sediments were all apparently older than the age of deposition. *Licht* [2004] summarized the published ^{14}C ages on AIO in Ross Sea sediments. We note that although the timing of events is similar to that reconstructed by *Domack et al.* [1999], since it is largely based on the same ages, the interpretation of events is distinctly different. *Domack et al.* [1999] correctly recognized that the sediments from which the AIO ages were obtained represent open marine conditions and thus provide only limiting minimum ages for deglaciation, whereas *Licht* [2004] interpreted the ages to directly constrain "ice sheet retreat," from which she concluded that the ice sheet in the Ross Sea "is unlikely to have been a substantial contributor" to MWP-1A.

[101] Based on AIO ^{14}C ka ages from cores collected from near Ross Island, corrected for the age of surface sediments at each core site, *McKay et al.* [2008] concluded that the grounding line had retreated from its 11.3 ± 0.1 ka position in outer Drygalski Trough [*Domack et al.*, 1999] to Ross Island by 11.7 ± 0.1 ka (10,096 ± 85 ^{14}C yr BP, NZA 18140), or considerably earlier than previously inferred [*Conway et al.*, 1999; *Domack et al.*, 1999; *Licht*, 2004], and suggested that this rapid retreat may have contributed to MWP-1B.

[102] Radiocarbon ages from Taylor Valley and adjacent Hjorth Hill also provide key constraints on deglaciation of ice in McMurdo Sound following the LGM [*Stuiver et al.*, 1981; *Hall and Denton*, 2000]. Of the 18 radiocarbon ages obtained on algae from proximal positions relative to the terminal Hjorth Hill moraine, 16 fall within the range of ages constraining the age of the moraine, and 2 are younger. Most of the ages contemporaneous with moraine formation are from stratified sediments that may have been overridden, suggesting small fluctuations of the ice margin [*Hall and Denton*, 2000]. The two critical ^{14}C ages with respect to deglaciation (12.7 ± 0.1 ka (10,794 ± 148 yr BP, AA 17329) and 12.8 ± 0.1 ka (10,945 ± 80 yr BP, AA 20671)) are each on algal layers associated with recessional moraines that are within 500–700 m of the terminal moraine on Hjorth Hill. *Hall and Denton* [2000] described these algal layers as having colonized the surfaces of the recessional moraines, with the samples coming from 15 to 20 cm depth in fine laminated sand. They inferred that the algal layers are "integral parts of the moraines and therefore date their formation," and thus concluded that the ice margin remained close to its maximum position until at least 12.8 cal ka [see also *Mackintosh et al.*, 2011]. We note, however, that as documented by *Bockheim et al.* [1989] for similar

stratigraphic relations elsewhere in the Dry Valleys, algae that grew in local ponds on the surface of recessional moraines only provide limiting minimum ages for the moraines rather than dating their formation. We thus conclude that the position of the ice margin on Hjorth Hill at the time of algal growth associated with these two ages is unknown.

[103] The other constraint on deglaciation from Taylor Valley comes from the ages of proglacial lake deltas in Taylor Valley, with their continued existence requiring ice at the mouth of the valley to hold up the lakes. Dates on algal mats from deltas suggest that glacial Lake Washburn in Taylor Valley underwent substantial lake level fluctuations following its inception at more than ~28.5 cal ka [*Hall et al.*, 2010]. With respect to the youngest lake level fluctuation, *Hall et al.* [2010] reported one date of 13.4 ± 0.2 ka (11,560 ± 240 yr BP, QL-1937) on one delta at 347 m, with the first older delta at 45 m dated at 13.4 ± 0.1 ka (11,562 ± 115 ^{14}C yr BP, AA 14041) and the first younger delta at 69 m dated at 13.4 ± 0.1 ka (11,542 ± 85 ^{14}C yr BP, AA 18915), indicating that the lake nearly filled the Taylor Valley and then drained within perhaps decades (Figure 19). We note, however, that as first recognized by *Stuiver et al.* [1981], the only way the lake could have filled completely was if the ice dam was at its maximum extent on Hjorth Hill, yet all other dating constraints on the ice margin summarized above indicate that the margin had retreated from its maximum position ~500–1500 years earlier [*Denton et al.*, 1989; *Hall and Denton*, 2000] and could not have readvanced to its maximum extent without obliterating the older ages. *Hall et al.* [2010] did not provide any details on the stratigraphic relation of the dated algal mat to the high delta, but additional dating constraining this extraordinary lake level oscillation is necessary to replicate this result. Until then, we assume the dating of this high delta is in error.

[104] If we exclude the 13.4 ka age on the high-elevation delta, radiocarbon ages on Taylor Valley deltas suggest that the lake level permanently dropped to altitudes mostly below ~80 m after 14.2 ± 0.4 ka (12,250 ± 260 ^{14}C yr BP, AA 17314) (^{14}C age on youngest high-elevation delta) and before 14.0 ± 0.1 ka (12,140 ± 90 ^{14}C yr BP, QL 1707) (^{14}C age on oldest low-level delta after permanent drop) (Figure 19), which is consistent with the timing for onset of retreat of the ice margin from its maximum extent on Hjorth Hill and on the floor of Taylor Valley. There is one delta at 128 m dated to 13.7 ± 0.1 ka (11,820 ± 70 ^{14}C yr BP, QL 1576) [*Hall and Denton*, 2000] that may suggest a brief oscillation of the ice margin to cause the lake to partly fill at this time, but the remaining 31 dated deltas (with the exception of the high delta at 347 m) constrain lake levels to have remained at or below 80 m after 14.2 ± 0.4 cal ka until <9.4 ± 0.1 ka (8340 ± 120 ^{14}C yr BP, QL 993) (youngest delta age) [*Stuiver et al.*, 1981; *Hall and Denton*, 2000].

[105] A long-standing interpretation for the existence of this lower lake well after onset of deglaciation is that it required grounded ice at the mouth of Taylor Valley and that its final drainage constrains retreat of the grounding line in the Ross Sea south of the valley mouth [*Stuiver et al.*, 1981; *Denton et al.*, 1989; *Conway et al.*, 1999; *Hall and Denton*, 2000; *Mackintosh et al.*, 2011]. We suggest an alternative hypothesis whereby the drop in the lake level to ~80 m at ~14.2 ± 0.4 ka represents the passage of the grounding line south of the valley and that the ice dam required for the maintenance of this lake following this drop was associated with the *freeboard* of an ice shelf. An ice sheet model simulation of the last deglaciation of the Ross Sea demonstrated that the ice shelf proximal to the grounding line was sufficiently thick (order of 900–1000 m) to sustain a freeboard of >80 m [*Pollard and DeConto*, 2009]. We thus conclude that the lake level at ~80 m does not uniquely constrain the existence of grounded ice at the mouth of Taylor Valley until late in the deglaciation, with an ice shelf providing the dam for the lake being an equally viable hypothesis.

[106] Several additional lines of evidence have been used to reconstruct the timing of ice retreat in the western Ross Sea. *Dochat et al.* [2000] reported 15 radiocarbon ages from raised marine beaches on Cape Bird, which is on the western side of Ross Island. Of these, 11 are <4.0 ± 0.1 ka (4885 ± 95 ^{14}C yr BP, UGA 6809), while 4 ages are older, including an age on collagen from an abraded (reworked) penguin bone of 11.1 ± 0.1 ka (11,039 ± 74 ^{14}C yr BP, AA 15331). *Dochat et al.* [2000] argued that these four ages are anomalous, whereas *McKay et al.* [2008] suggested that the 11.1 ± 0.1 ka penguin bone may be reliable and indicates earlier open waters at this location.

[107] *Hall and Denton* [1999], *Hall et al.* [2004], and *Baroni and Hall* [2004] obtained multiple radiocarbon ages on raised marine beaches from sites north of Ross Island on the Scott and Victoria Land coasts, from which they constructed RSL curves of local emergence. *Hall and Denton* [1999] and *Hall et al.* [2004] focused on the southern Scott Coast between Cape Roberts and Marble Point. Although the elevation of the marine limit decreases southward along this coast, raised beaches of same age are at the same elevation along the coast, suggesting an equal amount of uplift. *Stuiver et al.* [1981], *Hall and Denton* [1999], and *Hall et al.* [2004] attributed the trend in the marine limit elevation to a progressive delay in beach formation as the ice shelf retreated southward but noted that the age of the marine limit at Cape Roberts (~7.4 ka, ~6.3–6.6 ^{14}C ka) closely constrains the age of grounded ice retreat from the Scott Coast. Farther north, *Baroni and Hall* [2004] developed the postglacial RSL history for Terra Nova Bay. They found that the age of the marine limit was several hundred years older (~8.0 ka, ~7.2 ^{14}C ka) than the Scott Coast, which they argued was consistent with a slow southward retreat of the grounding line during the middle Holocene. *Baroni and Hall* [2004, p. 377] concluded that "the presence of a significant amount of ice remaining in the Ross Sea embayment in Holocene time lessens the chance that Antarctica contributed significantly to meltwater pulse 1A."

[108] *Baroni and Orombelli* [1994] reported radiocarbon ages of 11.7 ± 0.5 ka (11,325 ± 360 ^{14}C yr BP, GX 16925) and 13.6 ± 0.5 ka (13,070 ± 405 ^{14}C yr BP, GX 18483) on penguin guano from Cape Hickey on the Scott coast, suggesting significantly earlier deglaciation than in any other reconstruction. *Hall et al.* [2004] further examined the

integrity of these and other old ages on penguin guano from Cape Hickey. First, they redated the older sample (13,070 ± 405 ^{14}C yr BP) as 12,250 ± 50 ^{14}C yr BP (OS 27351) (12.8 ± 0.1 ka, using a 1300 year reservoir age), which suggests agreement at 2 sigma. Redating of another sample and dates on a split of another sample, however, suggested that other old ages on penguin guano may be problematic. *Hall et al.* [2004] suggested that relict carbon may be the source of the problem and noted in support of this that stronger sample pretreatment yielded younger ages. Nevertheless, the younger pretreated guano ages are still considerably older than the age of final deglaciation suggested from the RSL records and are instead similar to the deglaciation age suggested by *McKay et al.* [2008]. There is currently no direct evidence to discount them.

[109] *Hall et al.* [2004] suggested one scenario for reconciling these records in which early grounding line retreat is followed by several thousand years of an ice shelf occupying the coast and inhibiting beach formation. In this scenario, the age of the marine limit records the retreat of the front of the ice shelf rather than the grounding line. On the other hand, *Hall et al.* [2004] argued that this scenario is inconsistent with their RSL records; if deglaciation had occurred earlier, they would not expect to see the upper, steep part of their curve. As noted by *Hall et al.* [2004], however, there are few constraints on the shape of the upper (older) part of the curve. Moreover, as discussed below, glacial isostatic modeling that evaluates an early and rapid thinning of Ross Sea grounded ice associated with MWP-1A provides good agreement with the RSL data from the Ross Sea coast [*Bassett et al.*, 2007].

[110] *Hall et al.* [2004, p. 260] also argued that deglaciation "could not have occurred significantly earlier because ice still occupied McMurdo Sound as late as 8300 ^{14}C years BP," as suggested by the lake levels in Taylor Valley at ~80 m, and "postglacial shells in McMurdo Sound dated so far are all younger than 6600 ^{14}C years BP. Older shells would be expected had deglaciation commenced prior to that time." As we have discussed, however, an ice shelf could have dammed the lakes in Taylor Valley, and final retreat of the ice shelf front would have allowed beach formation along the Scott coast and deposition of postglacial shells in McMurdo Sound at 6.2 ± 0.2 ka (6670 ± 200 ^{14}C yr BP, QL 191, with 1300 year reservoir age), consistent with the interpretation that the age of the marine limit on the southern Scott coast ~7.4 ka represents retreat of the ice shelf front.

[111] *Conway et al.* [1999] used the age of the marine limit on the Scott coast [*Hall and Denton*, 1999] and the age of lakes in the Dry Valleys that were dammed by ice in the Ross Sea [*Hall and Denton*, 2000] to reconstruct grounding line retreat. In their figure showing grounding line retreat during deglaciation, they inferred the grounding line was at Cape Ross on the Scott Coast at ~7.4 cal ka (~6.5 ^{14}C ka), which is based on the age of the marine limit on the coast as determined from the RSL curve [*Hall and Denton*, 2000]. In the text, however, *Conway et al.* [1999] suggested that retreat occurred sometime between 9.4 cal ka (8.3 ^{14}C ka), which corresponds to the youngest delta formed in a glacial lake in the Taylor Valley dammed by grounded Ross Sea ice [*Hall and Denton*, 2000], and the marine limit, which represents the time of open marine conditions. In any event, this result indicates an age for grounding line retreat from the McMurdo Sound region that is 2000 to 3000 years younger than suggested from the age of marine sediments near Ross Island [*McKay et al.*, 2008] and 3000 to 7000 years younger than suggested from the penguin remains at Cape Hickey.

6.2.3. Deglaciation of the WAIS Interior

[112] Several studies have used in situ cosmogenic nuclides measured in erratics from different elevations in a given region to constrain the history of lowering of the WAIS surface during the last deglaciation. *Ackert et al.* [1999] interpreted a lateral moraine on the flanks of Mount Waesche in Marie Byrd Land as being a composite landform, with the morphology of the upper part suggesting an older age than the lower part. Of course, the upper part must have been deposited before the lower part, so the question is whether there is a significant age difference. From their cosmogenic ^{3}He ages, *Ackert et al.* [1999, p. 278] concluded that "in general, the exposure ages increase with distance from and in elevation above the ice margin." Excluding outliers, the mean of the cosmogenic ^{3}He ages from the lower part of the moraine suggests deposition at 10.0 ± 0.6 ka. There are a number of pre-LGM ^{3}He ages from the upper part of the moraine, but one age (10.5 ± 0.1 ka) on the highest-elevation sample is the same (within error) as the mean age of the lower part of the moraine, and another sample also has a post-LGM age (16.1 ± 0.3 ka), indicating that the entire moraine was deposited after the LGM. For reasons that are unclear, however, *Ackert et al.* [1999] concluded that the lower part of the lateral moraine marks the maximum limit of the WAIS surface on Mount Waesche (45 m above present), although they then suggested that the young age (10.5 ka) on the sample from the upper moraine suggests that the WAIS surface may have been 85 m higher [*Ackert et al.*, 1999, p. 279] "during the last ice sheet high stand." In any event, *Ackert et al.* [1999] concluded that because thinning of the ice surface began at ~10 ka, the WAIS could not be a primary source for MWP-1B much less MWP-1A. Because there are no data to suggest that the flanks of Mount Waesche above the moraine remained unglaciated during the LGM, however, the actual elevation of the ice surface prior to ~10 ka is unconstrained, and an equally plausible interpretation is that the moraine is a recessional feature formed during deglaciation from a thicker LGM WAIS.

[113] Based on ^{10}Be ages on erratics from several nunataks in coastal mountains of Marie Byrd Land west of Mount Waesche, *Stone et al.* [2003] constrained 700 m of surface lowering of the WAIS over the last 10,000 years. All of the nunataks were covered by ice during the LGM, and *Stone et al.* [2003] concluded that the LGM ice sheet in this sector of WAIS may have been 1200 to 1500 m higher than present, similar to the ice sheet reconstruction by *Denton and Hughes* [2002]. In addition, *Stone et al.* [2003] found several pre-LGM age samples that came from upper elevation weathered surfaces that show no evidence of glacial erosion. Because their data demonstrate that these surfaces were covered by ice during the LGM, *Stone et al.* [2003, p. 100]

interpreted "the weathered surfaces, and the old glacially transported cobbles resting on them, as having survived glaciation beneath thin, cold based ice… and that the old 'ages' are artifacts of prior cosmic-ray exposure."

[114] *Sugden et al.* [2005] elaborated on the nature of the weathered surfaces described by *Stone et al.* [2003]. Of particular note are the following observations: There is an altitudinal zonation in preservation of glacial erosional landforms, with lower-elevation surfaces showing clear signs of glacial erosion, intermediate surfaces showing erosional landforms in "imperfect or embryo form," and the highest summits showing no signs of glacial erosion. In particular, the summit surface of Mount Rea (Figure 20a) has upstanding tors of granite bedrock, weathering pits up to 30 cm deep, tafoni on some steeper slopes, and rock surfaces [*Sugden et al.*, 2005, p. 325] "that are covered by a fragile layer of loose but not yet displaced crystals" (Figures 20c and 20d). Similar altitudinal zonation occurs on other peaks in the region. *Sugden et al.* [2005] also reported a decrease in the density of erratics with altitude. As shown by *Stone et al.* [2003], however, the cosmogenic data clearly demonstrate that all summits in the areas were covered by ice prior to 10.4 ka, indicating that weathered summit surfaces [*Sugden et al.*, 2005, p. 331] "are protected by cold-based ice during glacial periods."

[115] *Ackert et al.* [2007] argued that a *trimline* separating a highly weathered bedrock surface above from a surface below with glacial erratics recorded the maximum vertical extent of the WAIS in the Ohio Range near the WAIS divide (Figure 20b). In particular, *Ackert et al.* [2007] described evidence of this trimline as "granite bedrock exposed on the escarpment, and the nunataks exhibits cavernous weathering pits, with areas between pits reduced to delicate centimeters thick structures (tafoni). Along the escarpment face, up to 150 meters above the present day elevation of WAIS, the delicate tafoni have often been broken off, leaving sharp edges. We interpret a transition from surfaces that preserve the delicate tafoni, to those lacking it as a trimline that records the maximum highstand of the WAIS" (p. 2). *Ackert et al.* [2007] also interpreted the existence of a moraine on a bench on Discovery Ridge based on scattered granite erratics (Figure 20e), and argued that because the erratics are restricted to near the edge of the bench, "the ice margin barely overtopped the bench" (p. 3). Of the 45 samples of glacial erratics measured for cosmogenic ^{3}He, only two suggested no inheritance (supported by joint ^{10}Be ages). The elevations of the two ages (12.5 $\pm$ 0.9 ka and 10.5 $\pm$ 0.7 ka) are within 30 m of the inferred paleo–ice surface. From these results, *Ackert et al.* [2007] concluded that because the trimline formed at $\sim$11.5 ka, with $\sim$120 m of ice surface lowering since, the WAIS could not have been a primary source for MWP-1A.

[116] The interpretation by *Ackert et al.* [2007] for limited excess ice and late deglaciation in the Ohio Range hinges entirely on the interpretation that the trimline represents a former upper ice surface. As summarized above, however, *Stone et al.* [2003] and *Sugden et al.* [2005] demonstrated that identical features used by *Ackert et al.* [2007] to argue against ice coverage above the trimline (i.e., weathering pits, tafoni, and rare erratics) (Figure 20) were covered by cold-based (nonerosive) ice during the LGM in coastal mountains of Marie Byrd Land. Additional studies from the Antarctic [*Mackintosh et al.*, 2007; *di Nicola et al.*, 2009; *Strasky et al.*, 2009] and the Arctic [*Miller et al.*, 2002; *Briner et al.*, 2005; *Goehring et al.*, 2008] have similarly shown that such trimlines record englacial thermal boundaries, with upper, highly weathered bedrock surfaces preserved beneath nonerosive cold-based ice. We also question whether the distribution of erratics on the bench on Discovery Ridge (Figure 20e) is a moraine marking an ice limit on the bench. A moraine is conventionally defined as a constructional feature, whereas the feature shown by *Ackert et al.* [2007] appears to simply be a scattering of erratics on a bedrock bench. We thus conclude that an equally plausible interpretation of the trimline in the Ohio Range is that it represents an englacial thermal boundary, such as documented by *Stone et al.* [2003] and *Sugden et al.* [2005] for nearly identical landscapes on Marie Byrd Land, and that the mean age of the two erratics (11.5 ka) records the time of first exposure of the landscape after some unknown amount of ice thinning.

[117] *Bromley et al.* [2010] and *Todd et al.* [2010] reported on the glacial geology and chronology of deposits from the Reedy Glacier, which is a large outlet glacier of the EAIS that drains through the southern Transantarctic Mountains into the WAIS $\sim$1300 km south of Hjorth Hill. Similar to other EAIS outlet glaciers [*Bockheim et al.*, 1989; *Denton et al.*, 1989; *Denton and Marchant*, 2000], the Reedy Glacier thickened during the last glaciation, with maximum thickening occurring down glacier in response to thickening of the WAIS. Changes in the vertical surface of the glacier thus monitor changes in WAIS surface elevation. ^{10}Be ages on erratics associated with the limit of deposits from the last glaciation (Reedy III drift) suggest that the Reedy Glacier was at its thickest between 17.0 $\pm$ 1.5 ka and 14.1 $\pm$ 1.3 ka and then thinned rapidly, as indicated by ages of 14.4 $\pm$ 1.3 ka, 13.4 $\pm$ 1.2 ka, and 13.2 $\pm$ 1.2 ka from samples $\sim$100 m lower than the maximum ice limit [*Todd et al.*, 2010]. *Todd et al.* [2010] extrapolated the paleoglacier slope during the LGM to the mouth of the glacier where it merges with WAIS some 60 km down glacier by assuming that the surface slope from 7.5 ka, for which they have greater spatial control, was the same. In doing so, they recognized that the 7.5 ka surface slope was likely steeper than the glacial maximum slope and thus constrained the elevation of WAIS at that location to be at least 1060 m, or >500 m higher than present (Figure 21); *Bromley et al.* [2010] reached a similar conclusion. This elevation is $\sim$600 m lower than the elevation in the *Denton and Hughes* [2002] reconstruction of the LGM WAIS for this region, which was constrained at this location by *Mercer*'s [1968] reconstruction from the limit of Reedy drift (T. Hughes, personal communication, 2011), but the topographic maps used by *Mercer* [1968] were incorrect (B. Hall, personal communication, 2011). On the other hand, the reconstruction by *Todd et al.* [2010] is significantly higher than the reconstruction inferred by flow line modeling in *Ackert et al.* [2007]. There is nothing to prevent the extrapolated surface

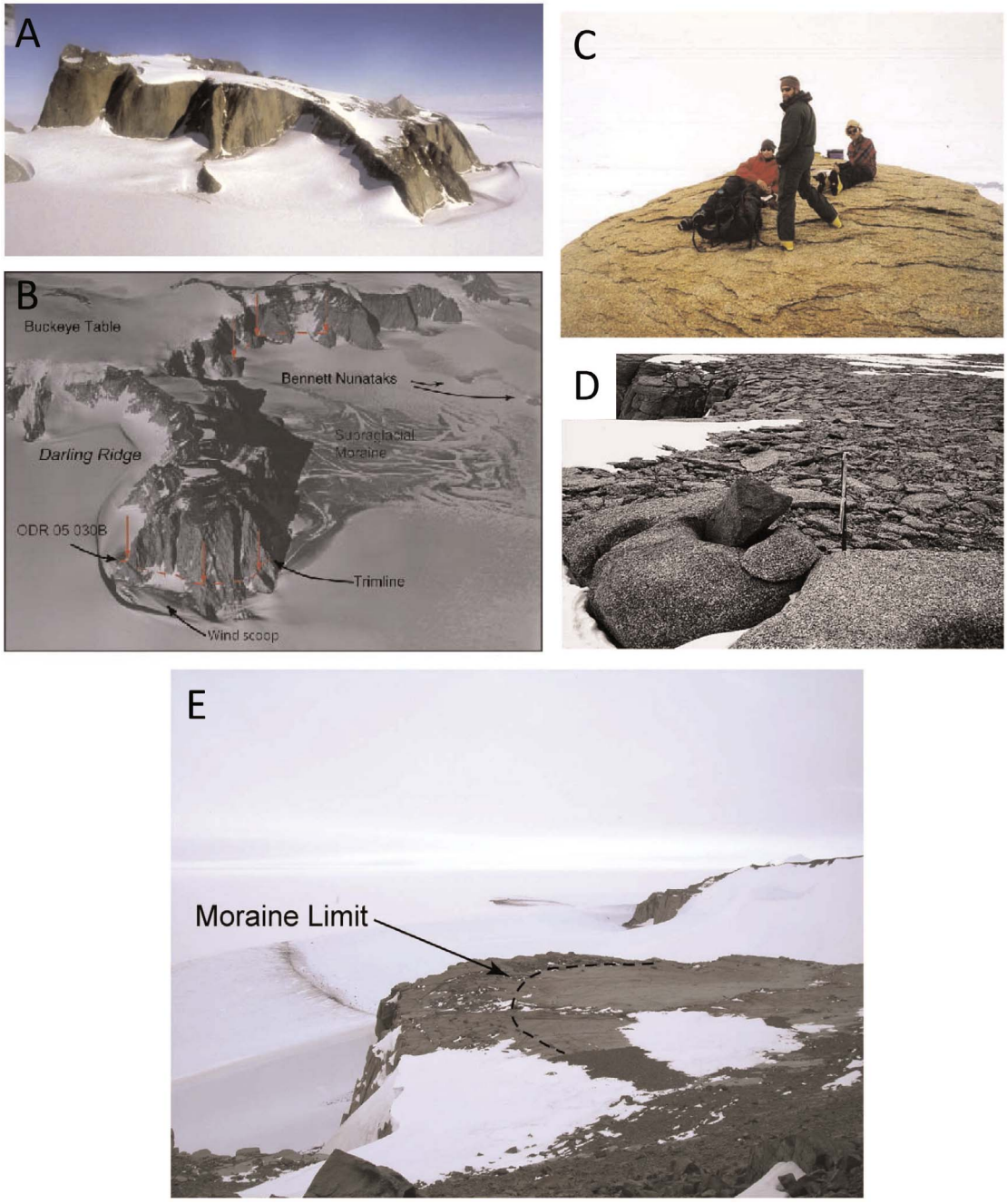

Figure 20. (a) Mount Rea, Sarnoff Mountains, Marie Byrd Land, showing the rolling upper surface on which there are tors, with ice-molded slopes at lower altitudes on the massif flanks [from *Sugden et al.*, 2005]. (b) Oblique air photograph of Darling Ridge, Ohio Range, showing an inferred trimline based on vertical differences in rock weathering [from *Ackert et al.*, 2007]. (c) The surface of a tor on Mount Rea, Marie Byrd Land [from *Sugden et al.*, 2005]. Cosmogenic nuclides ages show that this surface was covered by nonerosive, cold-based ice during the last glaciation. (d) An erratic lodged in a weathering pit on a tor from an upper surface of the Sarnoff Mountains, Marie Byrd Land [from *Sugden et al.*, 2005]. Cosmogenic nuclides ages show that this surface was covered by nonerosive, cold-based ice during the last glaciation. (e) Scattered erratics on a bedrock bench on Discovery Ridge, Ohio Range [from *Ackert et al.*, 2007]. *Ackert et al.* [2007] interpreted the erratics to be a moraine, with the inferred ice limit on the bedrock bench shown by the dashed line. Figures 20a, 20c, and 20d reprinted from *Sugden et al.* [2005], copyright 2005, with permission from Elsevier.

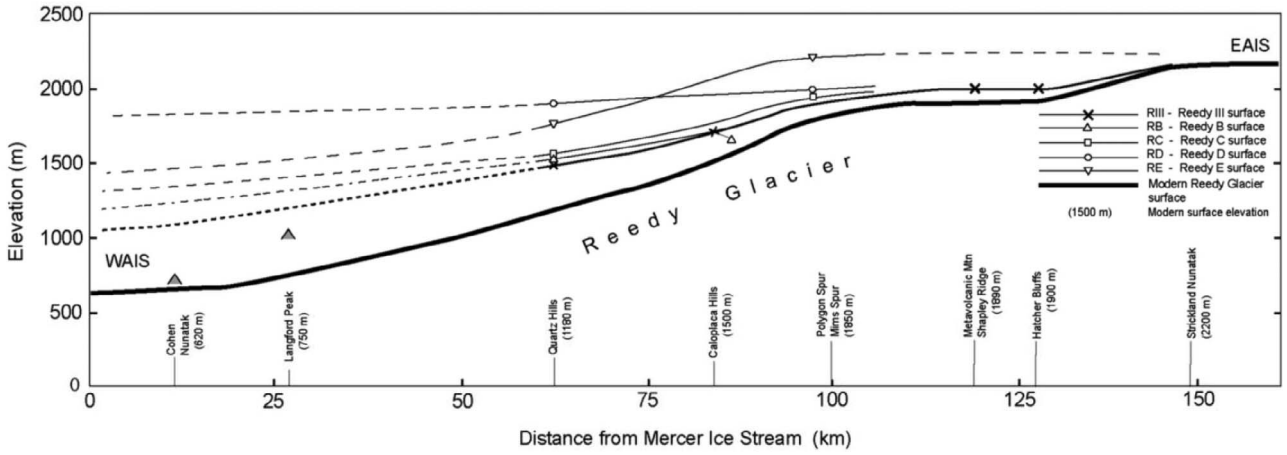

Figure 21. Present and reconstructed former longitudinal surface profiles of Reedy Glacier. Reprinted from *Bromley et al.* [2010]. Copyright 2010, with permission from Elsevier. Reconstructions are based on the upper limits of deposits at the glacier margins. Symbols denote the sites used in each reconstruction. Deposits of the local last glacial maximum are referred to as Reedy III. *Bromley et al.* [2010] extrapolated the profiles down glacier (dashed lines) to estimate surface elevations at the confluence of Reedy Glacier and Mercer Ice Stream.

slope from being nearly zero, however, in which case the surface elevation of WAIS would be ~1400 m, or 300 m lower than the *Denton and Hughes* [2002] reconstruction in this region. *Mercer* [1968] and *Denton et al.* [1989] reconstructed similar near-zero surface slopes for the distal portions of the Reedy Glacier as well as other EAIS outlet glaciers draining into WAIS during the LGM. Indeed, *Bromley et al.* [2010] recognized that the thickening of Reedy Glacier was time transgressive, such that maximum ice thickness occurred earlier near the mouth than at the head of the glacier, resulting in a shallower surface slope than used in their extrapolation. As such, *Bromley et al.* [2010] considered the former ice surface to have been 1100–1400 m.

[118] The Siple Dome ice core provides an additional constraint on LGM WAIS interior elevation and its subsequent lowering history. *Waddington et al.* [2005] used a time-dependent one-dimensional ice flow model constrained by the observed age-depth relationship from Siple Dome to reconstruct LGM surface elevations that were at most 200–400 m higher than present. *Price et al.* [2007] used a two-dimensional, full-stress, thermomechanical flow band model to investigate ice thickness histories. Their "favored" model suggested that nearly all of the deglacial thinning (350 m) occurred between 15 ka and 14 ka.

[119] The isotopic (δD and δ^{18}O) records from the Siple Dome ice core and the Taylor Dome ice core bordering the Ross Sea show an abrupt event at ~15 ka that, at face value, suggests an abrupt warming. *Mulvaney et al.* [2000] proposed an alternative age model for the Taylor Dome record, however, that suggests that more gradual warming occurred up until 14.5 ka, similar to other Antarctic ice cores, particularly the newer *TALDICE core* 550 km north of Taylor Dome [*Stenni et al.*, 2011]. Based on nitrogen and argon isotopes measured in the Siple Dome ice core, *Severinghaus et al.* [2003] concluded that there was an interval of ablation and resulting firn removal or low-to-no accumulation at 15 ka, suggesting that there is a short (<500 year) hiatus in the record at this time that makes the event appear more pronounced [*Brook et al.*, 2005]. *Severinghaus et al.* [2003] suggested that this event may be related to a similar low-accumulation event that produced the isotopic signal at Taylor Dome. Although these interpretations remain uncertain, it appears that the event at both ice core sites represents some combination of warming and low-to-no accumulation at ~15 ka, which may reflect ice surface lowering or some regional climate change induced by rapid ice surface lowering at this time [*Price et al.*, 2007].

[120] *Siddall et al.* [2012] used four WAIS ice core records (Byrd, Siple Dome, Taylor Dome, and Talos Dome) to evaluate elevation changes simulated in three different ice models for the last deglaciation. The ICE-5 G model [*Peltier*, 2004] has 17 m of excess sea level equivalent in the LGM Antarctic ice sheets, with the largest fraction distributed over WAIS, and onset of deglaciation occurring 12 ka. *Bassett et al.* [2007] used the model of Antarctic deglaciation from *Huybrechts* [2002], which has ~20 m of excess sea level equivalent in the LGM Antarctic ice sheets, again with the largest fraction being distributed over WAIS. *Bassett et al.* [2007] then altered the timing of mass loss from the original deglaciation history, with one ice history having rapid retreat and thinning of WAIS at ~14 ka to simulate a contribution of 14 m to MWP-1A, and another in which rapid deglaciation did not begin until 10 ka. *Siddall et al.* [2012] then computed the equivalent isotope (δD) signal that would be produced for the elevation changes simulated by the three different ice models. In all three cases, *Siddall et al.* [2012] found that the predicted deuterium histories substantially overestimated (100–200%) the observed records at the Byrd, Siple Dome, and Talos Dome sites, indicating that the modeled thinning may be an order of magnitude too large. There was reasonable agreement between the *Bassett et al.*

[2007] model for a large contribution to MWP-1A and the Taylor Dome record, but as discussed above, this record may be compromised.

6.2.4. Deglaciation of Other WAIS Sectors

[121] *Johnson et al.* [2008] used seven single cosmogenic ages to constrain the thinning history of the WAIS in the Pine Island Bay region, on the Amundsen Sea coast. Their oldest exposure age is also their highest, coming from within 12 m of the summit of the sampled nunatak, and suggests that the nunatak was covered by ice at the LGM. The LGM ice surface was thus at least 334 m higher than present, and it first became exposed at 14.4 ± 1.5 ^{10}Be ka.

[122] *Denton et al.* [1992] mapped a widespread erosional trimline throughout the Ellsworth Mountains which they interpreted to reflect a former ice surface that was 800 to >1000 m higher than present, although they could not discount an englacial thermal boundary for its origin. *Denton et al.* [1992, p. 419] also described just one *glacial drift* unit (Ellsworth drift) as occurring between this trimline and the present ice surface, with "no surface weathering differences or widespread morphologic breaks. Instead, [this] drift shows relatively uniform surface morphology and weathering characteristics over this entire elevation range." They also described unweathered bedrock with well-preserved striations from elevations just above the present ice surface to just below the trimline. They inferred a LGM age for this trimline in part based on the similarity in weathering characteristics of the Ellsworth drift and those developed in Ross Sea drift that have a known LGM age, but in the absence of numerical dating methods, *Denton et al.* [1992] could not exclude an older age.

[123] *Bentley et al.* [2010] distinguished a zone of less weathered drift and bedrock from a higher zone of more weathered drift and bedrock within the limits of the Ellsworth drift mapped by *Denton et al.* [1992], who did not identify such a distinction. *Bentley et al.* [2010] reported that in some places, a moraine is found at the upper limit of the lower drift, indicating that the limit marks an ice margin. They obtained 65 ^{10}Be ages from the lower drift and 4 ^{10}Be ages from the upper drift. Of the 65 ages from the lower drift, all but 11 were considered to be too old due to inheritance of ^{10}Be from previous exposure (Figure 17). Two ^{10}Be ages (15.4 ± 1.4 ka, 15.1 ± 1.3 ka) indicate that deglaciation from the moraine at the drift limit began at ~15 ka, and the ice surface subsequently slowly lowered to its present elevation by 1–2 kyr. The four ages from the upper drift are all >380 ka, and based on the greater degree of weathering of the drift and bedrock, *Bentley et al.* [2010] interpreted material above the limit as being substantially older than that below and stated that the limit of the lower drift thus represents the LGM position of the WAIS surface in this region. Given that the LGM ice sheet was at most 480 m thicker than present, *Bentley et al.* [2010] concluded that the Weddell sector of the ice sheet made little contribution to global sea level rise, including MWP-1A. They referred to two other lines of evidence in support of thinner ice in the Weddell Sea basin, including an unpublished ice core record and two cosmogenic ages on bedrock surfaces from the Shackleton Range that, however [*Fogwill et al.*, 2004, p. 267], "cannot rule out the possibility that the mountain has been covered intermittently for short periods by cold-based ice."

[124] *Clark* [2011] pointed to the possibility that the upper more weathered zone with old erratics had been preserved by cold-based LGM ice, as has been documented from elsewhere in Antarctica [*Stone et al.*, 2003; *Sugden et al.*, 2005] and the Arctic [*Briner et al.*, 2005, 2006; *Goehring et al.*, 2008]. In support of this are four ^{10}Be ages reported by *Todd and Stone* [2004] from the upper weathered surface described by *Bentley et al.* [2010] (range from 41 ± 3 to 67 ± 5 ka) that, given the likelihood of inheritance in these samples (e.g., Figure 17), provide plausible support for thicker LGM ice in this region. *Clark* [2011] thus proposed that thicker, cold-based LGM ice may have covered the upper, more highly weathered surface prior to 15 ka and that the 15 ka moraine represents a recessional phase during deglaciation after the LGM. A similar scenario has been established for the eastern Canadian Arctic, where unweathered glacial deposits and bedrock at lower elevations are separated from more highly weathered deposits and bedrock above by a well-defined moraine system, yet because ^{10}Be ages demonstrate that the upper surface was covered by cold-based ice at the LGM [*Briner et al.*, 2005, 2006], the moraine system must have formed during deglaciation.

[125] *Bentley et al.* [2011] replied by acknowledging that although Clark's argument cannot be ruled out, they reemphasized that they were unable to find unweathered erratics in the more weathered upper zone, such as those found in other localities that established overriding by cold-based ice. They also argued that if the depositional regime depositing moraines today has remained the same, all the glacial deposits they described were formed from supraglacial debris on marginal blue ice areas, and similar processes should have left similar deposits if thicker ice had thinned to the limiting moraine dated to ~15 ka. We note, however, that the characteristics of the glacial debris below the limiting moraine described by *Bentley et al.* [2010, p. 412] are typical of subglacial deposition: "continuous layer of drift that is dominated by fresh, unweathered clasts, with rarer weathered clasts. The drift is lithologically diverse… Many clasts are striated or faceted."

[126] We agree with *Bentley et al.* [2011] that the absence of unweathered material above their limit "raises the difficulty of interpreting negative evidence." We conclude that the discrepancy between the observations by *Denton et al.* [1992] for no weathering break up to their mapped higher trimline as opposed to the description by *Bentley et al.* [2010] of a weathering break well below the *Denton et al.* [1992] trimline remains a critical, unresolved question in the interpretation of LGM ice volume for this region that requires additional field investigation.

6.2.5. Deglaciation of the Antarctic Peninsula Ice Sheet

[127] *Heroy and Anderson* [2007] established a robust chronology of ice margin retreat of the *Antarctic Peninsula Ice Sheet (APIS)* across the adjacent continental shelf based on ^{14}C ages measured on carbonate fossils, thus avoiding the

large uncertainties associated with AIO ages. Ice margin retreat from its LGM extent on the shelf began at >18.2 ka, in good agreement with another study of APIS margin retreat based on ^{14}C ages measured on carbonate fossils [*Smith et al.*, 2010]. Expressed as a percentage of it maximum extent relative to the present-day margin, the ice margin then retreated gradually (~10%) until ~14 ka, when it retreated ~30% in a few hundred years, suggesting that the APIS contributed to MWP-1A [*Heroy and Anderson*, 2007]. The rate of ice margin retreat subsequently decelerated, and the margin reached the inner shelf at ~10 ka.

[128] Other studies have suggested that deglaciation from the Antarctic Peninsula shelf began at <12 ka based on the age of marine sediments from the inner shelf [*Mackintosh et al.*, 2011], but the APIS margin extended to the shelf edge during the LGM [*Heroy and Anderson*, 2007; *Smith et al.*, 2010], indicating that the inner shelf sites only record the final deglaciation and thus have no bearing on the onset of deglaciation from the shelf edge that occurred at least 7 kyr earlier.

6.2.6. EAIS: Deglaciation of Mac.Robertson Shelf and Land

[129] *Leventer et al.* [2006] reported 11 ^{14}C ages from a core (JPC43B) taken in a trough (Iceberg Alley) that is incised into the Mac.Robertson Shelf off the current EAIS margin. Five ages were on carbonate material, and six were on AIO matter; *Leventer et al.* [2006] applied a reservoir age of 1700 ± 200 years based on the radiocarbon age of surface sediments from nearby and regional box cores and karsten cores [*Mackintosh et al.*, 2011]. Age models based on the two types of dates show that AIO ages in the core are older than the carbonate ages. The lowest 4.83 m in the core is comprised of diatom-rich laminated sediments, which *Leventer et al.* [2006] interpreted as varves deposited in a calving embayment that formed in the trough. The notion of the existence of a calving bay is critical with respect to associating the timing of deposition of the laminated sediments with deglaciation and was based on a conceptual model developed by *Domack et al.* [2006, p. 138] for a trough (Palmer Deep) on the continental shelf off the Antarctic Peninsula, as follows: "We hypothesize that with the addition of basal water to the till system beneath the outer Hugo Island Trough, flow of the Palmer Deep (PD) outlet accelerated. With acceleration of drainage, via the PD ice stream, surface elevations of the surrounding ice sheet would have decreased, leading eventually to thinner ice within the ice stream and its drainage. Such a lowering of ice surface elevations following maximum conditions, when coupled with rising eustatic sea levels, would have provided sufficient instability to increase rates of calving. Hence, we envision a situation where calving bay reentrants were created along the entire front of the PD ice stream during deglaciation."

[130] The two (AIO) ages in the core from the basal diatom-rich laminated sediments suggest that they were deposited at 11.6 ± 0.3 ka (11,770 ± 45 ^{14}C yr BP, CAMS 99090). Based on the assumption that the conceptual model of a calving bay developed for the Antarctic Peninsula could be applied to the Mac.Robertson Shelf, *Leventer et al.* [2006] interpreted these sediments as having been deposited in a calving bay. On this basis, they interpreted these ages as constraining the age of onset of deglaciation from this shelf, from which they concluded that this margin of the EAIS did not contribute to MWP-1A. Seismic surveys, however, indicate that there is an additional ~6 m of postglacial sediment above a glacially scoured surface, suggesting that the age for deglaciation inferred by *Leventer et al.* [2006] is only a minimum-limiting age. *Mackintosh et al.* [2011] evaluated this issue by deriving an initial age for deglaciation from this core based on the following assumptions: (1) the 6 m of postglacial sediments below the depth of core penetration were deposited in the same way as the laminated sediments from the base of the core and (2) those sediments were deposited at the same rate as the sampled laminated sediments. *Mackintosh et al.* [2011] thus concluded that the 6 m of underlying sediments were deposited in ~100 years, so that initial age of deglaciation was ~11.7 ka.

[131] *Mackintosh et al.* [2011] also reported 13 ^{14}C ages from a core (JPC40) in the next trough to the east of Iceberg Alley on the Mac.Robertson Shelf. All ages were on AIO matter, and *Mackintosh et al.* [2011] used the same reservoir age as for JPC43B (1700 ± 200 years). The base of the core penetrated ~2.4 m of glacial sediments. These are overlain by 47 cm of rhythmically laminated sediments, similar to those in JPC43B that *Leventer et al.* [2006] interpreted to have also been deposited in a calving bay, which are then overlain by laminated biosiliceous ooze. The AIO ^{14}C age on the basal glaciogenic unit (25,230 ± 100 yr BP) is clearly too old, whereas the two ages from the laminated biosiliceous ooze are out of stratigraphic sequence and are older than the two from the underlying rhythmically laminated sediments. Of the five AIO ^{14}C ages from this section, *Mackintosh et al.* [2011] considered only the two from the rhythmically laminated sediments as reliable, citing their higher total organic content and diatom abundance as support for this selection. On this basis, they concluded that deglaciation at this site occurred at 14.0 ± 0.2 ka (13,895 ± 40 ^{14}C yr BP, CAMS 134392). On the basis of this age and that from JPC43B, as well as dates from elsewhere discussed below, *Mackintosh et al.* [2011] concluded that the initial retreat of the EAIS margin on the Mac.Robertson Shelf may have coincided with MWP-1A but that [*Mackintosh et al.*, 2011, p. 201] "most ice loss occurred significantly later."

[132] *Mackintosh et al.* [2007] reported 21 ^{10}Be ages from several ranges of the Framnes Mountains that protrude above the EAIS in Mac.Robertson Land, immediately adjacent to the Mac.Robertson Shelf. In three of the ranges, *Mackintosh et al.* [2007] identified an upper limit of unweathered erratics that occurs ~250 m above the present ice surface, whereas unweathered erratics were traced to the summits in the Masson Ranges (north and central) 350 m above the present ice surface, suggesting that ice overtopped these ranges. *Mackintosh et al.* [2007] interpreted the boulder limit as marking a former ice limit because its slope, as derived from Mount Henderson and Mount Horden, mimics the present-day ice surface profile. We note, however, that the Masson Ranges, where the unweathered boulders continue to the

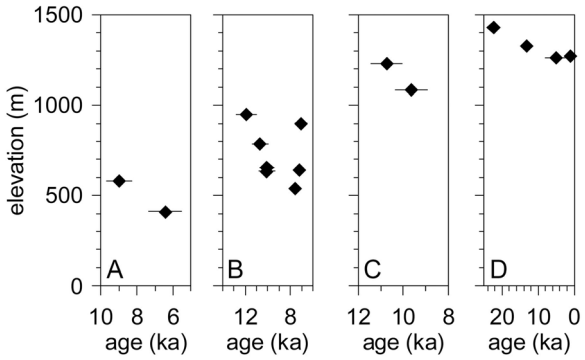

Figure 22. Cosmogenic ages on glacial erratics from the Framnes Mountains in Mac. Robertson Land, East Antarctica [*Mackintosh et al.*, 2007]. (a) Henderson Range. (b) North Masson Range. (c) Central Masson Range and Dunlop Peak. (d) Brown Range.

summits >350 m above the present ice surface, occur between the two ranges used by *Mackintosh et al.* [2007] to derive a former ice surface slope ~250 m above the present ice surface. Moreover, the Masson Ranges intersect the present ice surface at the same elevation (between 600 and 800 m) as the David Range, where *Mackintosh et al.* [2007] also reported a boulder limit 250 m above present ice surface. This raises the question of why an ice surface should be >350 m higher over the Masson Ranges, yet be restricted to 250 m up ice, down ice, and immediately to the west in these other ranges. In this regard, the boulder limit identified by *Mackintosh et al.* [2007] may not be defining a former ice surface and may instead mark a former thermal limit or a change in basal debris transport, possibilities which they also suggested.

[133] Of the 21 ^{10}Be ages, *Mackintosh et al.* [2007] discounted the 6 oldest as being too old due to inheritance and used the remaining 15 single-boulder ages to constrain the history of ice surface lowering during the last deglaciation. We summarize their results in Figure 22, which shows the ^{10}Be ages from each of the five ranges sampled. At Mount Henderson (Figure 22a), two ages constrain ~200 m of thinning between 8.9 and 6.6 ka. Two ages from the Central Masson Ranges and Dunlop Peak suggest ~300 m of ice surface lowering over the past ~9.5 ka (Figure 22c). *Mackintosh et al.* [2007] concluded that the ice surface in the Brown Range has not been more than 160 m higher than present in the last ~23 ka and has thinned 60 m in the last ~13 ka (Figure 22d). In doing so, *Mackintosh et al.* [2007] accepted a single boulder age of 22.9 ± 1.2 ka as being free of inherited ^{10}Be. Although this sample also had a concordant ^{26}Al age, older samples with concordant ^{10}Be/^{26}Al ages (35–65 ka) are clearly too old due to inheritance, indicating that this index does not necessarily preclude inheritance. Instead, given that the majority of published cosmogenic ages in Antarctica exhibit some amount of inheritance (Figure 17), replicating this age with multiple samples from the same site, as is the conventional practice in most studies using cosmogenic nuclides for surface exposure dating [*Gosse and Phillips*, 2001], is required. Finally, in excluding a 6.9 ka age at 900 m, *Mackintosh et al.* [2007] inferred ~350 m of ice surface lowering between ~12 and 7 ka in the North Masson Range, with ~250 m of that lowering occurring between 12 and 10 ka (Figure 22b). They considered an alternative interpretation whereby including the 6.9 ka age indicated that most surface lowering occurred after 7 ka but discounted this because it implied that [*Mackintosh et al.*, 2007, p. 553] "the remaining six samples with ages older than ca. 7 ka were deposited with a varying initial or inherited component of cosmogenic nuclides." We suggest an additional scenario whereby gradual surface lowering occurred between 12 and 7 ka and the two ages ~10 ka at ~650 m are too old due to inheritance. There is no independent, objective means to distinguish between these three scenarios, but we note that similar vertical age distributions with relatively small age differences (hundreds to thousands of years) among samples at similar elevations are common in other Antarctic data sets (Figure 17), where the protocol involves selecting the youngest erratic at any elevation to derive the ice thinning history [*Stone et al.*, 2003; *Bentley et al.*, 2010].

[134] *Mackintosh et al.* [2007, p. 553] concluded that their reconstructed ice surface for 12–13 ka, which is based on a single age of 13.1 ± 0.7 ka in the Brown Range (Figure 20d) and a single age of 12.0 ± 0.7 ka in the North Masson Range (Figure 20b), "is smaller than that predicted by recent ice-sheet models [*Denton and Hughes*, 2002; *Huybrechts*, 2002], which show ice as much as 1000 m thicker than present in this area." We note, however, that the modeled ice surface referred to is for the LGM and is thus not necessarily directly comparable since the reconstructed surface may represent one that has lowered since the LGM. This is particularly the case given the uncertainties in using a boulder limit to constrain an ice surface and in using single boulder ages to constrain chronologies where inheritance is a significant problem.

[135] In drawing the comparison to modeled LGM ice surfaces, *Mackintosh et al.* [2007, p. 553] noted that "The models simulate thicker ice because they assume that the EAIS advanced ~100 km to the continental shelf margin during the LGM. Seaward extension of our reconstructed ice-surface profile for this time period indicates that the EAIS could not have advanced more than 10–15 km to the edge of the inner continental shelf, where significant deepening occurs." *Mackintosh et al.* [2007], however, refer to the date from core JPC43B (11.6 ka) [*Leventer et al.*, 2006] as support for a late deglaciation age, thus neglecting the fact that this core was obtained from within 20 km of the continental shelf edge, far seaward of their postulated limit. In a subsequent paper using these same cosmogenic dating results to constrain ice history, *Mackintosh et al.* [2011] concluded that the maximum ice sheet extent at the LGM was in fact located near the edge of the continental shelf, some 100 km offshore.

[136] In noting that their results on the timing of deglaciation (12–13 ka) are similar to the *Leventer et al.* [2006] chronology for deglaciation of the Mac.Robertson Shelf at ~11.6 ka based on core JPC43B, *Mackintosh et al.* [2007, p. 553] concluded that the EAIS "is unlikely to have been a major contributor" to MWP-1A. As summarized above, however, *Mackintosh et al.*

[2011] subsequently found that deglaciation of the shelf began earlier, at ~14 ka, based on new AIO ^{14}C ages from core JPC40, and thus modified their conclusion as [*Mackintosh et al.*, 2011, p. 201] "although the initial retreat of the EAIS may have coincided with MWP 1a (within dating uncertainties), most ice loss occurred significantly later." The chronological basis for concluding that most mass loss occurred significantly later is (1) the age of ~11.7 ka established by extrapolating to the base of the unsampled 6 m of postglacial sediments at the site of core JPC43B (summarized above) and (2) the cosmogenic data from *Mackintosh et al.* [2007]. With respect to the cosmogenic data, a key constraint is derived from the data from the North Masson Range (Figure 22b), from which *Mackintosh et al.* [2007, 2011] concluded that ~200 m of surface lowering occurred between ~12 and 10 ka. As we have summarized above, however, the constraint on the height and age of the ice surface prior to 12 ka is highly uncertain, being based on a boulder limit and a single cosmogenic age. Moreover, *Mackintosh et al.* [2011] noted that recent work on the sea level high-latitude ^{10}Be production rate from *Putnam et al.* [2010] may be more applicable to the high southern latitudes than the production rate used in *Mackintosh et al.* [2007]. In using the new production rate, *Mackintosh et al.* [2011] recalculated the critical ^{10}Be age of 12.0 ± 0.7 ka as 14.1 ± 0.7 ka, using the CRONUS-Earth age calculator (http://hess.ess.washington.edu), which is the standard for computing exposure ages. *Mackintosh et al.* [2011, p. 198] thus concluded that they "cannot completely rule out the possibility that deglaciation of both troughs [on Mac.Robertson Shelf] began at ~14 kyr ago." This result is consistent with the calibrated AIO ^{14}C age of 11.6 ka from the base of core JPC43B being a minimum-limiting age and would imply that the initial emergence of the North Masson Range occurred at ~14 ka, assuming the validity of the single boulder age with the revised production rate.

6.2.7. Constraints From Antarctic Relative Sea Level Records

[137] *Bassett et al.* [2007] approached the question of an early and rapid AIS deglaciation associated with MWP-1A by using a GIA model to compute the near-field Antarctic sea level history for two scenarios, one in which MWP-1A was produced entirely from the Northern Hemisphere and one in which there was a dominant contribution from the AIS. *Bassett et al.* [2007] used the model of Antarctic deglaciation from *Huybrechts* [2002] but altered the timing of mass loss from the original deglaciation history, with one ice history having rapid deglaciation beginning at10 ka and another in which rapid retreat and thinning of WAIS occurred at ~14 ka to simulate a contribution of 14 m to MWP-1A. The former scenario would most closely correspond to the mid-Holocene deglaciation and retreat of the grounding line in the Ross Sea as interpreted by *Baroni and Hall* [2004] and *Hall et al.* [2004] from the Ross Sea RSL records, which are the best RSL records from Antarctica. In contrast, the latter scenario would test the hypothesis of whether AIS deglaciation associated with MWP-1A can be accommodated by the observed RSL histories. For both scenarios, there is a sea level rise at the Ross Sea sites associated with the Northern Hemisphere melting until this region deglaciates, after which there is a sea level fall resulting from the isostatic uplift. The combined effect of these two processes is a sea level highstand, which occurs earlier in the AIS source model and thus results in a more gradual sea level fall during the middle to late Holocene than is the case for the Northern Hemisphere source model. *Bassett et al.* [2007] concluded from this preliminary analysis that the more gradual sea level fall predicted by the Antarctic source model is more consistent with the data than the larger and steeper fall predicted by the Northern Hemisphere source model.

[138] As discussed in section 6.2.3, *Siddall et al.* [2012] used four WAIS ice core δD records to evaluate elevation changes simulated in the two *Bassett et al.* [2007] models. *Siddall et al.* [2012] found that the predicted δD histories substantially overestimated (100–200%) the observed records at the Byrd, Siple Dome, and Talos Dome sites, indicating that the modeled thinning may be an order of magnitude too large. There was reasonable agreement between the *Bassett et al.* [2007] model for a large contribution to MWP-1A and the Taylor Dome record, but as discussed above, this record may be compromised.

6.2.8. Synthesis

[139] The extensive geochronological constraints on the Ross Sea drainage system provide a record of this sector of the WAIS during the last glaciation that is comparable to the best dated records of the Northern Hemisphere ice sheets. In particular, these data establish that the last advance of grounded ice in the Ross Sea toward its LGM extent occurred at ~30 cal ka (Figure 18). There is similarly considerable information on the timing of the last deglaciation of the Ross Sea. The most reliable AIO ^{14}C ages from the Ross Sea are on sediments deposited in open marine conditions and thus only provide limiting minimum ages for ice shelf retreat [*Domack et al.*, 1999], although even these ages are subject to considerable uncertainties. In any event, they do not directly constrain the timing of grounding line retreat. The radiocarbon-dated record from Taylor Valley has provided one of the best dated records from Antarctica for the timing of the LGM and last deglaciation. The combination of dates constraining the onset of retreat of the ice margin from its terminal moraine on Hjorth Hill and the highstand of glacial Lake Washburn has long been used to infer the onset of deglaciation at ~14.5–15.0 cal ka [*Stuiver et al.*, 1981; *Denton et al.*, 1989], but the persistence of a lower lake level (<80 m) until ~9.3 cal ka and the two ages from recessional moraines on Hjorth Hill have been used to argue that the ice margin retreated slowly [*Hall et al.*, 2000; *Mackintosh et al.*, 2011] and that grounded ice remained in the mouth of Taylor Valley until final lake drainage sometime after 9.3 cal ka [*Denton et al.*, 1989; *Conway et al.*, 1999]. Along the Scott coast to the north of Taylor Valley, the age of the marine limit has been used to constrain the timing of retreat of the grounding line as occurring after 7.4 ka [*Conway et al.*, 1999; *Hall et al.*, 2004].

[140] We suggest an alternative hypothesis whereby the two ages on Hjorth Hill are simply limiting minimum ages for deglaciation and that ice thinned rapidly and the

grounding line of the Ross Sea ice sheet retreated to the south of the valley at ~14.4–15.0 ka, causing the lake to lower to a level (~80 m) dammed by an ice shelf (Figure 19). The AIO ages constraining open marine conditions (6.2 ka near Ross Island) [*Domack et al.*, 1999], the age of marine limit on the Scott coast (7.4 ka) [*Hall et al.*, 2004], and ages on raised marine shells in McMurdo Sound (6.2 ka) [*Stuiver et al.*, 1981] are all then consistent with the retreat of the ice shelf front, rather than the grounding line, as occurring during the early to middle Holocene.

[141] Elsewhere, the best constraints on onset of deglaciation and associated lowering of the WAIS surface come from the Siple Dome ice core, which suggests ~350 m of ice surface lowering between 14 and 15 ka [*Price et al.*, 2007], and deposits from the margin of the Reedy Glacier, which suggest at least 150 m of ice surface lowering also between 14 and 15 ka [*Bromley et al.*, 2010; *Todd et al.*, 2010]. Cosmogenic ages from mountains on the Amundsen Sea coast suggest that nunataks first emerged following WAIS thinning there at 14.4 ± 1.5 ^{10}Be ka [*Johnson et al.*, 2008]. Cosmogenic ages from the Ellsworth Mountains suggest that the Weddell Sea sector of WAIS began to thin from a moraine ~15 ka [*Bentley et al.*, 2010]. We suggest that these cosmogenic data do not uniquely constrain the LGM ice surface from having been thicker [*Clark*, 2011], with cosmogenic ages reported by *Todd and Stone* [2004] supporting this possibility. In addition, there remains a discrepancy in identifying a weathering limit below the trimline mapped by *Denton et al.* [1992] that needs to be resolved. In this regard, *Clark* [2011] proposed an alternative hypothesis whereby LGM ice was at the upper trimline mapped by *Denton et al.* [1992] with subsequent thinning to the moraine dated by *Bentley et al.* [2010] at ~15 ka.

[142] Radiocarbon ages on carbonate fossils from the continental shelf off the Antarctic Peninsula suggest that ice margin retreat from its LGM extent on the shelf began at >18.2 ka [*Heroy and Anderson*, 2007; *Smith et al.*, 2010], with an acceleration in retreat at ~14 ka, when it retreated ~30% in a few hundred years [*Heroy and Anderson*, 2007].

[143] How well constrained is the timing of deglaciation of Mac.Robertson Shelf and the adjacent Mac.Robertson Land? We first point to the uncertainty in the assumption that the conceptual model of a calving bay developed from the Antarctic Peninsula shelf also applies to the Mac.Robertson Shelf in order to explain the deposition of the rhythmically laminated sediments. We note that a similar facies (laminated diatomaceous ooze, subtle grading in distinct centimeter-scale intervals, and high *TOC*) is common in troughs developed on the floor of the Ross Sea, where *Domack et al.* [1999] interpreted it as having been deposited in open marine conditions following retreat of the ice shelf front. Second, the key dates for constraining deglaciation in both cores from Mac.Robertson Shelf are on AIO matter, which in other Antarctic marine sediments have large uncertainties, particularly with respect to the assumption that the age of surface sediments can be used to correct for the effect of old organic matter. In fact, *Leventer et al.* [2006, p. 8] dismissed AIO ^{14}C ages from a core off the Wilkes Land margin of the EAIS because of the "difficulties based on the presence of reworked organic material," although the problems do not appear to be any greater in this area than for sites elsewhere where dates are accepted and may be even less, as suggested by data in *Harris and Beaman* [2003]. Third, the calibrated AIO age of 11.6 ka from core JPC43B is only a minimum age; there are 6 m of underlying postglacial sediments that have no constraints on age or sedimentation rate. Fourth, the cosmogenic data do not uniquely constrain LGM ice surface elevations, and given the high probability of inheritance, single-boulder ages without replication are highly uncertain. *Mackintosh et al.* [2011] have also highlighted the uncertainties in high southern latitude production rates [*Putnam et al.*, 2010], which become critical when trying to establish millennial-scale resolution. We conclude that the hypothesis by *Mackintosh et al.* [2007, 2011] for the timing and rate of deglaciation of the Mac.Robertson sector of the EAIS being substantially after MWP-1A requires additional chronological constraints to be validated. In the meantime, the existing uncertainties in the chronology mean that a scenario for significant deglaciation of this margin coincident with MWP-1A cannot be excluded.

[144] These lines of direct evidence for Antarctic ice sheet thinning and retreat at the time of MWP-1A are consistent with geophysical modeling of the nonglobal mean component of the sea level rise during MWP-1A which suggests a large if not dominant source from Antarctica [*Clark et al.*, 2002; *Bassett et al.*, 2005; *Deschamps et al.*, 2012] (see section 7). In evaluating local RSL records from the Ross Sea, *Bassett et al.* [2007] also found that the more gradual sea level fall predicted by the Antarctic source model is generally more consistent with the data than the larger and steeper fall predicted by the Northern Hemisphere source model, although the imposed ice thinning histories for WAIS used in the model are likely overestimated [*Siddall et al.*, 2012].

[145] To summarize, one common signature in nearly all the records discussed here is for either the onset of or acceleration in deglaciation of all three Antarctic ice sheets between 14 and 15 ka (Figure 23). We thus conclude that although rates of deglaciation remain poorly constrained, the widespread signature of ice sheet retreat at 14–15 ka is consistent with an important contribution of the Antarctic ice sheets to MWP-1A.

7. FINGERPRINTING AND GIA MODELING OF THE SOURCE OF MWP-1A

[146] In the originally published ICE-4G model [*Peltier*, 1994], all of MWP-1A was sourced from the LIS (Figure 24a). A negligible amount of sea level rise came from the EIS, but that contribution was part of ongoing deglaciation and not explicitly associated with MWP-1A. In particular, *Peltier* [1994, pp. 198–199] stated that "The period of rapid sea level rise following the Y-D [Younger Dryas] is thought to be dominated by the disintegration of the Antarctic ice sheet. Because the marine ice sheets on the Barents and Kara seas are constrained to disappear rapidly following the LGM, the only viable source of the meltwater that is required

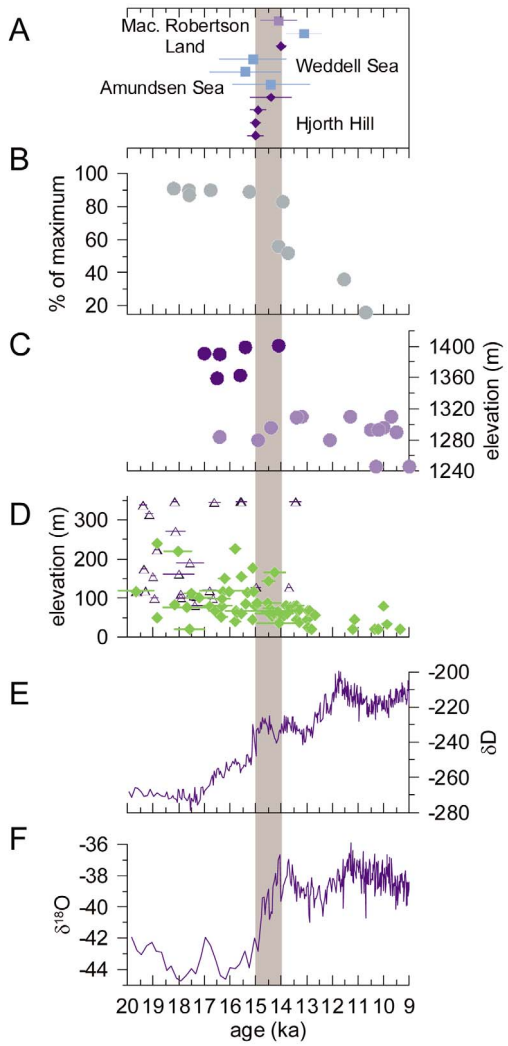

Figure 23. Summary of Antarctic records showing a signal of deglaciation between 15 to 14 ka (vertical gray bar). (a) Ages constraining deglaciation. Diamonds are calibrated radiocarbon ages, and squares are cosmogenic exposure ages. The cyan square from Mac. Robertson Land is from *Mackintosh et al.* [2007], whereas the light blue square is the same age but with a different production rate from *Putnam et al.* [2010], as discussed by *Mackintosh et al.* [2011]. The two cosmogenic ages from the Weddell Sea are from *Bentley et al.* [2010]. The cosmogenic age from the Amundsen Sea is from *Johnson et al.* [2008]. The four calibrated radiocarbon ages from Hjorth Hill are from *Hall and Denton* [2000]. (b) Calibrated radiocarbon ages on carbonate constraining the retreat of the Antarctic Peninsula ice sheet margin across the continental shelf, expressed as relative to maximum extent (100%) [*Heroy and Anderson*, 2007]. (c) Cosmogenic exposure ages constraining thinning of the Reedy Glacier surface [*Todd et al.*, 2010]. (d) Calibrated ^{14}C ages on organic matter (algae) in deltas associated with high lake levels in Taylor Valley [*Hall et al.*, 2010]. Green symbols are from Fryxell Basin, blue symbols are from Bonney Basin. (e) δD record from Siple Dome ice core [*Brook et al.*, 2005]. (f) $\delta^{18}O$ record from Taylor Dome ice core [*Steig et al.*, 1998].

to effect the rapid rise of sea level that precedes the Y-D is the Laurentian ice sheet… The main modification that I have made to the ICE-3G model in order to produce ICE-4G was therefore to incorporate a period of rapid Laurentide collapse."

[147] In a subsequent comment, *Edwards* [1995] noted that in comparing the ICE-4G prediction to the New Guinea sea level record, *Peltier* [1994] did not correct the New Guinea data for uplift rate (which *Peltier* [1994] also did not do for Barbados, but since it has a lower rate, this was less of an issue). *Edwards* [1995] pointed out that when compared to the corrected sea level data from New Guinea, there was a significant misfit between the New Guinea data and the model prediction of the data (Figure 24b). *Peltier* [1995] stated that this misfit was a "secondary aspect" of his study and that perhaps the assumption of constant uplift rate at New Guinea is wrong. *Peltier* [2002] invoked a similar argument to explain the "extremely large" (∼30 m) misfits between his model predictions and post-MWP-1A sea level data from New Guinea and Tahiti (Figure 24c).

[148] In looking at just the elastic solid Earth response as well as the gravitational and rotational effects associated with various possible mass loss scenarios for MWP-1A, *Clark et al.* [2002] showed that the greatest difference between Sunda Shelf and Barbados relative sea levels at the time of MWP-1A (i.e., the only two records of MWP-1A at the time) was for a LIS-only source, which was the basis for the ICE-4G scenario. Specifically, a LIS source would deliver ∼80% of ice-equivalent sea level at Barbados and ∼110% at Sunda. Accordingly, if MWP-1A was 25 m ice-equivalent sea level (as assumed by *Peltier* [2005]), then the Barbados sea level rise was 20 m versus 27.5 m at Sunda Shelf, corresponding to a 7.5 m difference. The difference was less if an all–Northern Hemisphere source was invoked (∼90% versus 110%, or 5 m difference for a 25 m ice-equivalent sea level event) and was least if the source was from the AIS (10%, or 2.5 m). *Clark et al.* [2002] suggested that the sea level constraints from Sunda Shelf and Barbados ruled out the large sea level difference associated with a LIS-only source.

[149] Further insight into identifying a source of MWP-1A was provided by *Bassett et al.* [2005], who used a GIA model through the deglaciation to look not only at the gravitational and rotational responses but also the full viscoelastic solid Earth response in sea level records following MWP-1A. The strength of this study was that the Tahiti and New Guinea records as well as Sunda and Barbados were now available for comparison to model predictions. When using an ice history like ICE-4G (an all-LIS source for MWP-1A), *Bassett et al.* [2005] found similar misfits in sea level histories at Tahiti and Sunda as well as the one at New Guinea that *Edwards* [1995] had first pointed out (Figure 24d). They noted that other work indicated that the lower mantle viscosity used in the nominal model was likely too low and showed that increasing it to 4×10^{22} Pa s reduced the misfit, but not entirely, and that further increasing it did not reduce the misfit any further. *Bassett et al.* [2005] next increased the contribution from the AIS to MWP-1A, with a compensating decrease in contribution from the Northern Hemisphere, and

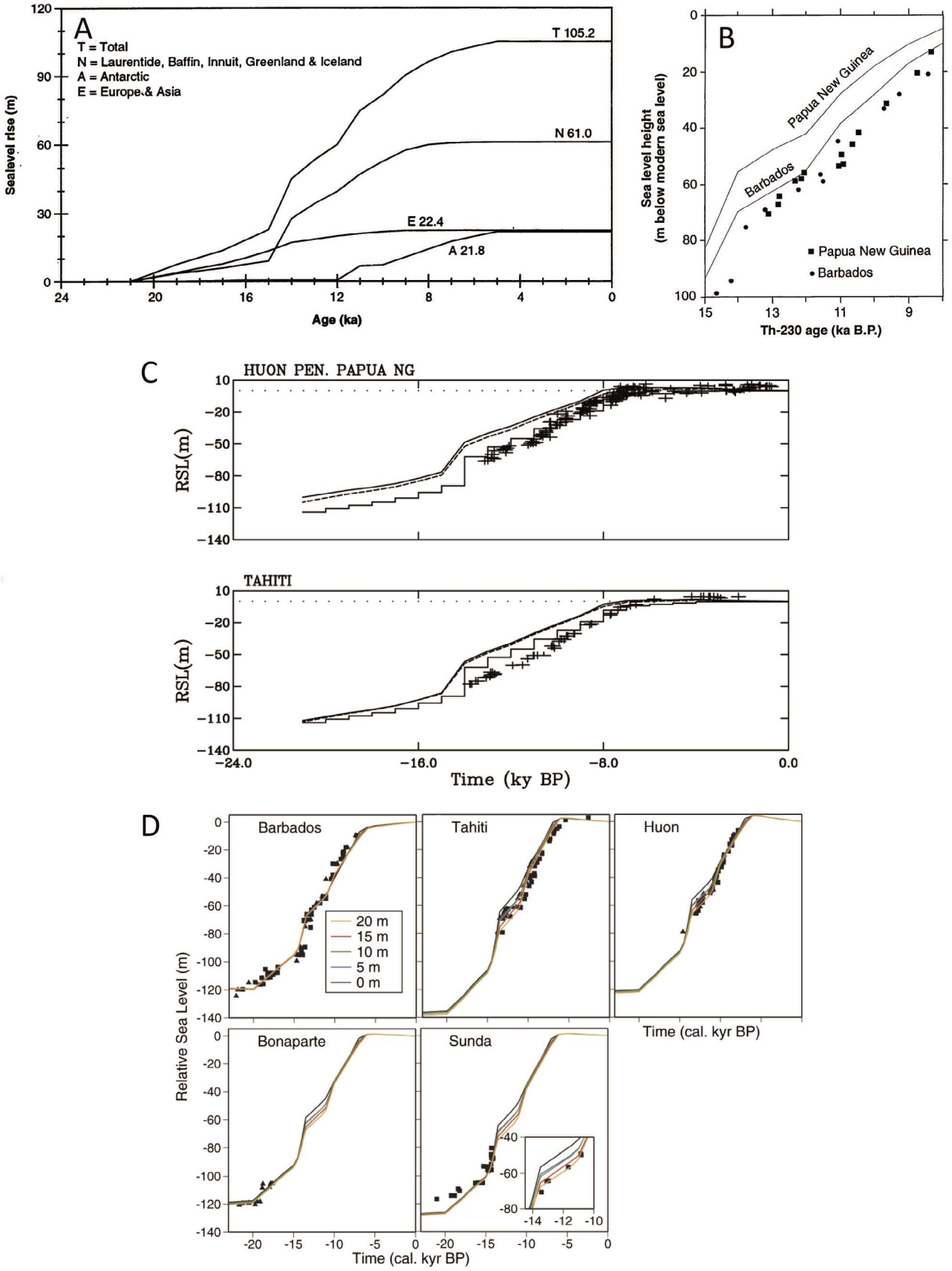
A
T = Total
N = Laurentide, Baffin, Innuit, Greenland & Iceland
A = Antarctic
E = Europe.& Asia
T 105.2
N 61.0
E 22.4
A 21.8
Sealevel rise (m)
Age (ka)
B
Papua New Guinea
Barbados
Sea level height (m below modern sea level)
Th-230 age (ka B.P.)
C
HUON PEN. PAPUA NG
TAHITI
RSL(m)
Time (ky BP)
D
Barbados
Tahiti
Huon
Bonaparte
Sunda
20 m
15 m
10 m
5 m
0 m
Relative Sea Level (m)
Time (cal. kyr BP)

Figure 24

found that the misfit was further reduced. Statistically, a 15 m AIS source with 8 m from the Northern Hemisphere (6 m from the LIS) provided a better fit than a 5 to 10 m AIS source (assuming a 23 m ice-equivalent sea level contribution) (Figure 24d). Similar results were shown for an all–Northern Hemisphere source (similar to LIS-only source) and a global ice sheet source (improved fit, but still misfits with New Guinea and Sunda that are resolved by increasing the AIS contribution to 15 m).

[150] In addressing the "hemispheric origins" of MWP-1A, *Peltier* [2005, pp. 1661–1662] stated that "the model of MWP1a that is embodied in the ICE-4G deglaciation history of *Peltier* [1994, 1996] is one which appears to deliver predictions of the amplitude of this event at Barbados and on the Sunda Shelf that are not sufficiently different so as to enable the difference to be employed to determine the geographical source(s) of the meltwater responsible for this episode of rapid sea level rise. One reason for this may have to do with the distributed nature of the northern hemisphere source assumed in the ICE-4G model." In *Peltier* [2005, Figure 5], contributions to MWP-1A include 4.6 m from the EIS and 3.6 m from the CIS as well as 16.5 m from the LIS, which *Peltier* [2005, p. 1662] stated that "This characteristic of the ICE-4G deglaciation model has not been described previously." As summarized above (Figure 24a), what *Peltier* [1994] had originally described for ICE-4G is that the LIS was "the only viable source." Moreover, as *Peltier* [1994] had originally identified, the BKIS had already deglaciated, and the geological record shows that the CIS could not have contributed 3.6 m of sea level equivalent at 14 ka [*Clague and James*, 2002]. It thus appears that *Peltier* [2005] uses a different ICE-4G history than the one that was originally published. Taking these results at face value, his "best" model results in a 7 m difference between Barbados and Sunda for a 25 m ice-equivalent sea level event, similar to what was found in *Clark et al.* [2002] for a LIS-only source. Because the geological records indicate that the ice sheet scenario used by *Peltier* [2005] is incorrect (no BKIS contribution possible and CIS contribution overestimated), the only remaining contributor for a substantial Northern Hemisphere source must be the LIS. Assuming that a similar response would apply for a LIS-only source as in *Clark et al.* [2002], the difference between Sunda and Barbados would be >7 m. Because of the amplification of the Sunda Shelf response relative to Barbados, such a response would cause the amplitude of the Sunda sea level to be greater than at Barbados, in contrast to the data, given uncertainties in the sea level records (section 4). Finally, we note that the post-MWP-1A predictions in *Peltier* [2005] continue to show the same model misfit to the Sunda Shelf data, such as *Bassett et al.* [2005] reproduced when assuming a Northern Hemisphere ice source (Figure 24d).

[151] Based on a GIA model similar to that used by *Bassett et al.* [2005] but now applied to the new Tahiti sea level data, *Deschamps et al.* [2012] obtained results that agree well with those found by *Bassett et al.* [2005], further supporting a substantial contribution from Antarctica. They pointed to the difficulty in constraining accurate amounts from these models given the depth uncertainties in the RSL data but suggested that [*Deschamps et al.*, 2012, p. 563] "it is probable that the AIS contributed at least half of the ∼14 m eustatic sea level rise observed during this event."

[152] In summary, both fingerprinting studies [*Clark et al.*, 2002] and GIA models [*Bassett et al.*, 2005; *Deschamps et al.*, 2012] support a substantial contribution of the AIS to MWP-1A. We note that *Clark et al.* [2002] based their analysis on a longer duration, and thus higher amplitude (25 m), definition of MWP-1A than has now been established from the Tahiti sea level record [*Deschamps et al.*, 2012] (section 4). With this new assessment of the ice-equivalent sea level amplitude associated with MWP-1A (∼14 m) and the newly assessed RSL amplitudes at Barbados (16–19 m), Sunda (16 m), and Tahiti (16–17 m), *Deschamps et al.* [2012] concluded that the similarity of all three RSL amplitudes with respect to the ice-equivalent sea level confirmed the conclusion by *Clark et al.* [2002] that precluded a sole contribution of the LIS. Given that the BKIS, SIS, and CIS contributed little if anything to MWP-1A (section 5), the remaining scenarios to explain similar RSL amplitudes at these three sites require an important Antarctic contribution. We agree with *Deschamps et al.* [2012] that the depth uncertainties in the RSL data preclude a robust conclusion from these models as to how much the AIS contributed but that it was substantial is supported by the likely contribution from the LIS derived from geological constraints and ice sheet models (section 5), which only account for ∼50% or less of the MWP-1A ice-equivalent sea level rise.

8. ALLERØD SEA LEVEL RISE AND ITS SOURCES

[153] Following the end of MWP-1A, RSL records suggest 7–10 m of sea level rise over the next ∼1 kyr (i.e., 7 to 10 mm yr^{-1}) [*Edwards et al.*, 1993; *Bard et al.*, 1996;

Figure 24. (a) Global sea level rise in the ICE-4G model of *Peltier* [1994], including contributions from individual ice sheet complexes (A, Antarctica; E, Eurasian; and N, North American) and their total (T). Reprinted with permission from *Peltier* [1994]. Copyright 1994 American Association for the Advancement of Science, http://www.sciencemag.org. (b) Comparison of ICE-4G model sea level predictions for New Guinea and Barbados with the relative sea level data from those localities, showing the mismatch between model and data at New Guinea. Reprinted with permission from *Edwards* [1995]. Copyright 1995 American Association for the Advancement of Science, http://www.sciencemag.org. (c) Comparison of ICE-4G model sea level predictions for New Guinea and Tahiti with the relative sea level data from those localities, showing the mismatch between the model and data. Reprinted from *Peltier* [2002]. Copyright 2002, with permission from Elsevier. (d) Comparison of sea level predictions with relative sea level data at five far-field sites (locations given in the plots), with varying contributions (0–20 m) of Antarctic ice to meltwater pulse 1A [*Bassett et al.*, 2005]. Note the significant mismatch between model and data at New Guinea, Tahit, and Sunda when there is no contribution from Antarctica and the improved agreement as the Antarctic contribution increases.

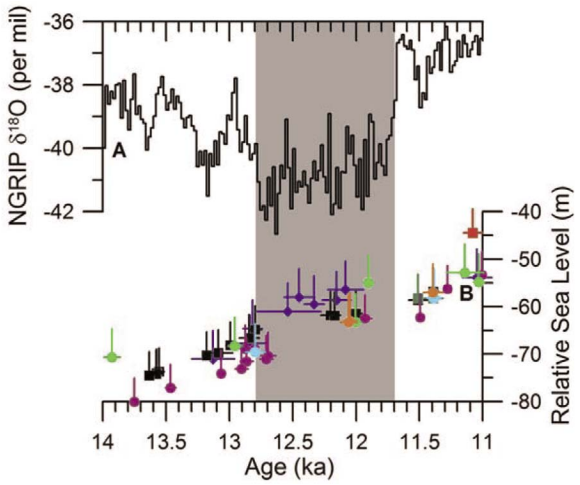

Figure 25. Younger Dryas and relative sea level. (a) NGRIP δ^{18}O [*Svensson et al.*, 2008]. (b) Relative sea level data (circles are from Tahiti [*Bard et al.*, 1996, 2010], squares from Barbados [*Peltier and Fairbanks*, 2006], and diamonds from New Guinea [*Edwards et al.*, 1993]). Age uncertainty is shown for all samples; where not visible, the uncertainty is less than the symbol size.

Peltier and Fairbanks, 2006], an interval of time encompassing the Allerød Warm Period from ~14.0 to 13.0 ka. The southern and southeastern LIS retreated rapidly during the early part of this interval as suggested by the growth of the Two Creeks Forest (Figure 13a). The southeastern LIS margin also retreated rapidly with New England and the St. Lawrence Valley deglaciating during the Allerød [*Rodrigues*, 1992; *Ridge*, 2003, 2004; *Rayburn et al.*, 2011]. This retreat led to the deglaciation of the eastern Great Lakes and eastward routing of LIS runoff for much of the Allerød that is recorded by decreased $\delta^{18}O_{sw}$ adjacent to the eastern outlets after ~14.2 ka, with the small fluctuations in $\delta^{18}O_{sw}$ explained by minor ice margin fluctuations in and out of the eastern Great Lakes (Figure 14c) [*Licciardi et al.*, 1999; *Clark et al.*, 2001; *Obbink et al.*, 2010]. The southwestern margin of the LIS also retreated rapidly during the Allerød, with the initial development of *Lake Agassiz* at ~14 ka [*Clayton and Moran*, 1982; *Dyke*, 2004; *Lepper et al.*, 2007]. This continued retreat of the southern LIS through the Allerød routed more of its meltwater eastward (Figure 1) [*Licciardi et al.*, 1999], which would explain declining AMOC strength and gradual North Atlantic cooling leading up to the Younger Dryas [*Clark et al.*, 2001; *Obbink et al.*, 2010]. Southwestern LIS meltwater was still routed through the Mississippi River, and this rapid retreat is reflected in peak deglacial $\delta^{18}O_{sw}$ depletions in the Gulf of Mexico at ~13.8 and 13.4 ka (Figure 14d) [*Flower et al.*, 2004]. The eastern margin of the LIS may have begun to retreat during the Allerød as suggested by cosmogenic radionuclide dates on moraines in northeast Labrador [*Clark et al.*, 2003], whereas the northern LIS margin continued its gradual retreat that began in the preceding Bølling (Figure 13a) [*Dyke*, 2004].

[154] Using the ice area-volume scaling method *Paterson* [1994], the area lost by the LIS at 14.0–13.0 ka would be equivalent to 10.9 ± 1.3 m of sea level rise, while the CIS may have added up to 1.1 ± 0.1 m of sea level rise equivalent volume. The combined estimated volume of 12 ± 1.3 m agrees with the ICE-5 G estimate of 11 m [*Peltier*, 2004] but is much larger than dynamic ice sheet model estimates of 4.5 ± 0.3 m to 2.9 ± 0.2 m of sea level rise from the LIS and CIS [*Tarasov and Peltier*, 2006]. The LIS area estimate is also larger than steady state flow line model results of 4.0–3.4 m of equivalent sea level rise from the LIS [*Licciardi et al.*, 1998]. The discrepancy between the area-volume and ice sheet model estimates may arise from overestimates of the ice volume in the LIS regions that were deglaciated during the Allerød by the *Paterson* [1994] method. This area-volume scaling does not account for the smaller volume of ice contained in the southern to southwestern LIS margins that had low ice surface slopes due to an underlying deformable, low-friction sediment substrate [*Clark*, 1992] relative to the predominately hard bedded AIS and GIS from which the scaling method was developed [*Paterson*, 1994].

[155] Retreat of the southeastern SIS margin accelerated during the Allerød, retreating ~500 km north (Figure 13b) [*Rinterknecht et al.*, 2006]. Although not as well dated, significant thinning continued along the southwestern SIS margin [*Goehring et al.*, 2008], and outer fjords may have deglaciated during this period [*Boulton et al.*, 2001]. Based on the DATED estimates (Figure 13c), the combined EIS contributed 3.6 ± 0.4 to 2.3 ± 0.3 m of equivalent sea level rise at 14–13 ka, which agree well with dynamic ice sheet model values of ~3 m of sea level rise sourced from the EIS during the Allerød [*Siegert and Dowdeswell*, 2002, 2004]. These estimates from the LIS and EIS thus suggest that much to all of the sea level rise that occurred during the Allerød can be explained by retreat of Northern Hemisphere ice sheets.

9. NORTH AMERICAN FRESHWATER DISCHARGE AND THE YOUNGER DRYAS COLD EVENT

[156] The Younger Dryas cold event (12.9 ± 0.1 to 11.7 ± 0.1 ka) [*Rasmussen et al.*, 2006] has long been viewed as the canonical abrupt climate change event [*Alley*, 2000; *Broecker*, 2003]. *Johnson and McClure* [1976] and *Rooth* [1982] hypothesized that the forcing of this event was northward retreat of the LIS out of the Great Lakes region that allowed the routing of Lake Agassiz runoff from the Mississippi River (southern outlet) to the St. Lawrence River (eastern outlet) (Figure 1). *Rooth* [1982] suggested that the attendant freshening of the North Atlantic caused a reduction in AMOC strength with cooling of the regional climate. Such a change in the location of freshwater runoff does not necessarily require a change in the rate of ice sheet retreat and would explain why sea level rise was minimal during a period of reduced AMOC (Figure 25) [*Fairbanks*, 1989; *Clark et al.*, 2001; *Bard et al.*, 2010]. Subsequent radiocarbon dating of sediment cores from the Gulf of Mexico confirmed the abandonment of the southern outlet at the start of the Younger Dryas [*Broecker et al.*, 1989; *Flower et al.*, 2004],

consistent with this hypothesis, but planktonic $\delta^{18}O$ records from the St. Lawrence estuary did not show a contemporaneous, large $\delta^{18}O$ decrease, which suggested that another forcing mechanism was required for the Younger Dryas [*Keigwin and Jones*, 1995; *de Vernal et al.*, 1996].

[157] More recently, emphasis for the cause of the Younger Dryas has switched from the routing of freshwater to a short (<1 year) flood that is assumed to have occurred from the abrupt lowering of Lake Agassiz as a lower outlet opened [*Broecker*, 2006; *Lowell et al.*, 2009; *Tarasov and Peltier*, 2005; *Teller et al.*, 2002, 2005; *Lowell et al.*, 2005; *Peltier et al.*, 2008]. Radiocarbon dates from the eastern Lake Agassiz outlet, however, have been interpreted as indicating that deep, erosional "flood" canyons were not open until well after the start of the Younger Dryas [*Teller et al.*, 2005; *Lowell et al.*, 2005, 2009]. Moreover, minimum-limiting radiocarbon dates that constrain the use of the southern outlet have also been interpreted to indicate abandonment several hundred years after the start of the Younger Dryas [*Fisher*, 2003; *Fisher and Lowell*, 2006; *Fisher et al.*, 2008], calling into question the flood hypothesis and eastward routing as the cause of the Younger Dryas. *Teller et al.* [2005] suggested that the northern outlet via the Mackenzie River opened at the start of the Younger Dryas, although the minimum-limiting radiocarbon record for this outlet can be interpreted as indicating an opening well after the end of the Younger Dryas [*Lowell et al.*, 2005; *Fisher et al.*, 2009]. The Lake Agassiz outlet chronology suggested by *Lowell et al.* [2005, 2009] and *Fisher et al.* [2008, 2009] has no outlet for the western Canadian Plains and Lake Agassiz during the Younger Dryas, with the Moorhead Low phase of Lake Agassiz suggested to be from enhanced evaporation. The evaporation rates required to sustain this low lake level, however, would be an order of magnitude greater than the highest evaporation rates anywhere on Earth and are thus untenable, requiring the existence of an outlet for Lake Agassiz lower than the southern outlet [*Carlson et al.*, 2009a]. Alternatively, in their Bayesian ice sheet modeling study, *Tarasov and Peltier* [2005, 2006] suggested that an abrupt, several centuries long melting of the northern LIS into the Arctic Ocean might have been the trigger for the Younger Dryas, which would not require either the northern or eastern outlets to be open at the start of the Younger Dryas.

[158] Because of these conflicting observations, interpretations, and ice sheet model simulations of LIS retreat and runoff, we assess the terrestrial and marine data that constrain the LIS history during this interval as well as place the ice sheet model simulations in the context of their climate forcings and AMOC responses. We do not discuss the bolide impact hypothesis for the Younger Dryas [*Firestone et al.*, 2007] because the evidence presented in support of the bolide hypothesis has not proven reproducible [*Marlon et al.*, 2009; *Surovell et al.*, 2009] and Younger Dryas–like events are observed during earlier deglaciations [*Carlson*, 2008, 2010].

9.1. Relative Sea Level During the Younger Dryas

[159] One of the first objections to a freshwater forcing hypothesis of the Younger Dryas was that it occurred during a period of minimal sea level change relative to before and after the event, raising the question as to how a reduced meltwater flux could explain the reduction in AMOC (Figure 25b). MWP-1A occurred at least 1000 years before the cold event and sea level rise accelerated after ~11.4 ka during what has been called MWP-1B [*Bard et al.*, 1996, 2010; *Edwards et al.*, 1993; *Fairbanks*, 1989]. Estimates of the rate of sea level rise during the Younger Dryas range from 5.6 ± 0.4 mm yr^{-1} to 10.4 ± 1.7 mm yr^{-1}, whereas the preceding 1 kyr had rates between ~10.9 mm yr^{-1} and 12.4 ± 1.1 mm yr^{-1} [*Bard et al.*, 2010]. These sea level records imply that global ice sheet retreat slowed during the Younger Dryas [*Bard et al.*, 2010], perhaps in response to regional cooling, but did not cease. Furthermore, they also indicate that a different mechanism than increased meltwater discharge to the oceans is required to explain this cold event, although elevated Northern Hemisphere ice sheet meltwater discharge during the Allerød (Figures 14 and 15) may have preconditioned the North Atlantic for the freshwater discharge that triggered the Younger Dryas [*Weaver et al.*, 2003].

9.2. Radiocarbon Age Control on Lake Agassiz Runoff Outlets

[160] Radiocarbon dates provide several constraints on the timing of occupation and abandonment of Lake Agassiz outlets. Basal radiocarbon dates from lake cores allow a minimum estimate of ice retreat and thus can provide a minimum estimate of when an outlet was open, whereas dates from organic material reworked in glacial sediment provide a maximum age for glacier advance to cover an outlet. Radiocarbon dates from channel gravel may constrain the timing of when the outlet was occupied or record channel abandonment with subsequent sediment slumping and reworking. Radiocarbon dates from terrestrial organic matter in beaches provide a maximum age of beach formation, whereas in situ terrestrial dates on lake sediment provide a minimum-limiting age for lake level fall and outlet abandonment.

9.2.1. The Southern Outlet Record

[161] The age of Lake Agassiz southern outlet abandonment was originally derived from a ^{14}C age on wood in beach sediment recording a drop in lake level below the southern outlet, presumably from the opening of a lower outlet, at 12.9 ± 0.3 ka (10.96 ± 0.30 ^{14}C ka BP, W-723) (Figure 26c) [*Moran et al.*, 1973], in good agreement with the onset of the Younger Dryas (Figures 26a and 26b). *Fisher and Lowell* [2006] questioned the validity of this date in constraining the abandonment of the southern outlet, however, suggesting that two radiocarbon dates from an alluvial fan in the southern outlet spillway provided better age control (red bars in Figure 26c) [*Fisher*, 2003]. These two dates are from a drill core into an alluvial fan built into the southern outlet spillway [*Fisher*, 2003], with a date of 12.6 ± 0.1 ka (10.68 ± 0.06 ^{14}C ka BP, AA-37029) in gravel overlain by a date of 12.8 ± 0.2 ka (10.87 ± 0.17 ^{14}C ka BP, AA-37030) in mud, which *Fisher* [2003] interpreted as constraining abandonment of the southern outlet at the start of the Younger Dryas. Assuming that the alluvial fan gravel records water flow through the outlet, *Fisher and Lowell* [2006] interpreted the

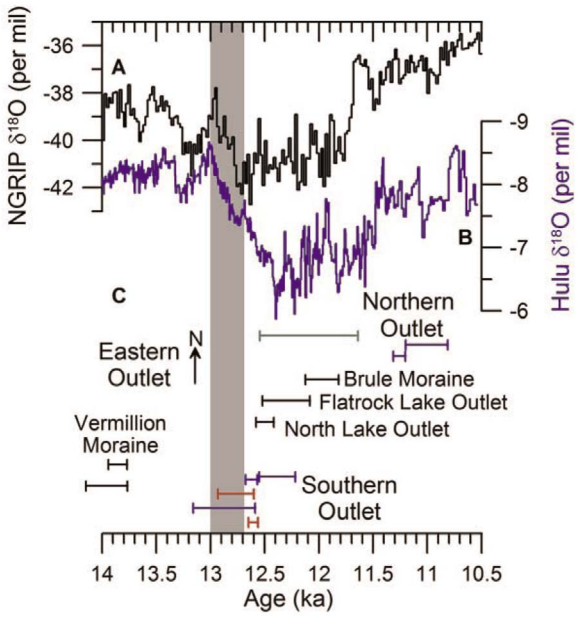

Figure 26. Radiocarbon constraints on the Lake Agassiz outlets compared with the (a) NGRIP and (b) Hulu Cave δ^{18}O records [*Wang et al.*, 2001; *Svensson et al.*, 2008] compared with (c) radiocarbon dates that constrain Lake Agassiz outlets. Southern outlet blue dates are minimum limiting for lake level drop [*Fisher et al.*, 2008]; red dates are from the gravel layer in the southern outlet [*Fisher*, 2003]. Eastern outlet dates are minimum limiting and arranged to progress northward with associated moraine or outlet indicated [*Lowell et al.*, 2009]. Northern outlet dates are from a gravel layer (green) [*Smith and Fisher*, 1993] or minimum limiting (blue) [*Fisher et al.*, 2009]. Gray bar denotes the timing of southern outlet abandonment.

lower gravel and radiocarbon date therein (AA-37029) as indicating that the southern outlet was active until after 12.6 ± 0.1 ka (10.68 ± 0.06 ^{14}C ka BP, AA-37029), and thus, the southern outlet was occupied until after the start of the Younger Dryas.

[162] The *Fisher and Lowell* [2006] and *Fisher et al.* [2008] argument depends on the interpretation of the gravel unit containing AA-37029 as being a direct deposit of Lake Agassiz overflow water rather than a reworked deposit following abandonment of Lake Agassiz overflow water. Because the drill core is in an alluvial fan built into the spillway, however, it seems unlikely that runoff from a large lake into the spillway of the highest lake outlet would be transporting large boulders and gravel as there is no obvious source for the coarse bed load. Instead, we suggest that the alluvial fan and incorporated organic materials were deposited after spillway abandonment, with slumping of the glacial sediments that make up the channel walls providing the coarse material deposited in the alluvial fan. An alternative hypothesis for these two dates, therefore, is that they provide minimum-limiting constraints on southern outlet abandonment.

[163] *Fisher et al.* [2008] also disregarded the oldest in situ root date of 12.6 ± 0.1 ka (10.71 ± 0.08 ^{14}C ka BP, ETH-32674) on lake sediment exposed upon abandonment of the southern outlet, which placed the drop in lake level to before 12.6 ± 0.1 ka (Figure 26c). Specifically, *Fisher et al.* [2008, p. 1129] stated that this date "appears to be anomalously old; 240 radiocarbon years older than the nearest root in stratigraphic context, nearly 200 radiocarbon years older than the oldest piece of wood, older than the maximum age for closing the southern outlet [*Fisher*, 2003; *Fisher and Lowell*, 2006], and thus is rejected." These authors chose another in situ root date of 12.4 ± 0.2 ka (10.47 ± 0.08 ^{14}C ka BP, ETH-32671) as a minimum-limiting constraint on the lake level drop. First, wood from ~12.6 ka does exist on Lake Agassiz sediment, such as the original *Moran et al.* [1973] wood date of 12.9 ± 0.3 ka (10.96 ± 0.30 ^{14}C ka BP, W-723). Second, *Fisher et al.* [2008] rejected this date based on their interpretations of the aforementioned radiocarbon dates from the southern outlet of *Fisher* [2003]. We suggest that an in situ date should hold more validity in constraining a lake level drop than a reworked date from a drill core in an ambiguous depositional setting [*Fisher*, 2003]. Comparison between the two dates from the southern outlet drill core (AA-37029 and AA-37030) that we suggest provide a minimum timing of outlet abandonment and the wood (W-723) and in situ root (ETH-32674) dates that constrain a drop in Lake Agassiz level with high-resolution, well-dated proxy records of the Younger Dryas (*North Greenland Ice Core Project (NGRIP)* and Hulu Cave δ^{18}O) [*Svensson et al.*, 2008; *Wang et al.*, 2001] indicates good agreement between the abandonment of the southern outlet, the beginning of the Moorhead lowstand, and the onset of the Younger Dryas (Figure 26).

9.2.2. The Eastern Outlet Record

[164] Unlike the southern outlet of the western Canadian Plains, the location of the eastern outlet is more ambiguous and likely shifted through the last deglaciation as the LIS margin retreat exposed successively isostatically depressed lower outlets [*Leverington and Teller*, 2003; *Teller et al.*, 2005]. *Teller et al.* [2002] suggested that a large flood would accompany the opening of the eastern outlet, which would presumably form a deep canyon [*Broecker*, 2006]. *Lowell et al.* [2005, 2009] and *Teller et al.* [2005] identified several erosional canyons near Lake Nipigon feeding into Lake Superior from the northwest (Figure 27) that could be the drainage route if deglaciated by the start of the Younger Dryas [*Lowell et al.*, 2005, 2009; *Teller et al.*, 2005]. Farther south of these canyons, *Teller et al.* [2005] also recognized five other incised outlets that could have carried Lake Agassiz runoff eastward once deglaciated (Figure 27).

[165] *Lowell et al.* [2009] attempted to constrain the recession of the LIS margin across this region using a series of lake cores with minimum-limiting radiocarbon ages. Based on their chronology, they postulated that the eastern outlet would have been through a low pass, which they mapped as having segments of the Steep Rock Moraine on both sides and being overlain by the Brule Moraine (Figure 27). This pass is also the headwaters of the Shebandowan Outlet of *Teller et al.* [2005], and the Brule Moraine does not overlay the lowest part of the outlet/pass. The Steep Rock Moraine has a minimum-limiting date of 12.3 ± 0.2 ka (Figure 26c) (10.40 ± 0.12 ^{14}C ka BP, ETH-31429). The oldest minimum-limiting age for the Brule Moraine of 12.0 ± 0.2 ka (10.25 ± 0.08 ^{14}C

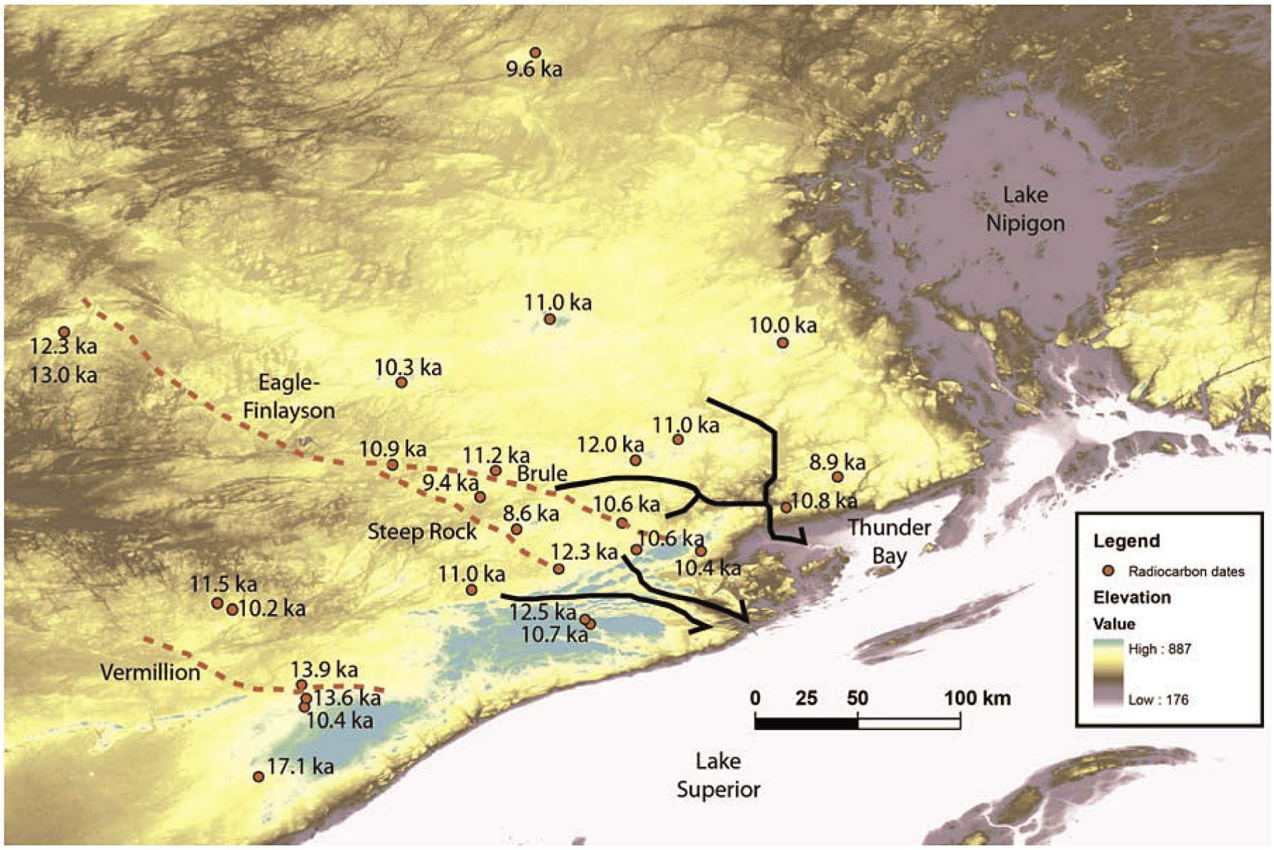

Figure 27. Digital elevation map in feet of the LIS eastern outlet near Thunder Bay. Calibrated radiocarbon dates from *Lowell et al.* [2009] are plotted along with the bulk age from Rattle Lake at ~13 ka. *Teller et al.* [2005] identified eastern outlets that could drain Lake Agassiz during the Younger Dryas (black lines). From south to north: North Lake, Flatrock Lake, Matawin River, Shebandowan, and Savanne. Moraines mentioned in text are denoted by dashed red lines.

ka BP, ETH-31430) is located tens of kilometers behind the moraine (Figure 27). In front of these two moraines, the oldest minimum-limiting macrofossil date is 12.5 ± 0.1 ka BP (10.55 ± 0.08 ^{14}C ka BP, ETH-28939). We note that in identifying eastern outlets across the continental divide, *Lowell et al.* [2005, 2009] did not account for isostatic uplift. As mentioned above, *Teller et al.* [2005] identified multiple potential eastern drainage routes for Lake Agassiz after correcting topography for differential isostatic uplift since deglaciation, two of which are south of the Brule Moraine (North Lake and Flatrock Lake Outlets) (Figure 27). The Steep Rock Moraine is absent from these two outlets [*Lowell et al.*, 2009].

[166] Based on these minimum-limiting dates, *Lowell et al.* [2009, p. 1597] postulated that "these ice margin reconstructions would not allow meltwater sourced in the Hudson Basin to drain into the Atlantic basin until after Younger Dryas time." This interpretation is based on the assumption that their minimum-limiting dates closely track ice margin recession with no readvances. An ice margin readvance following retreat would likely erode any organic material accumulated in the overrun lakes and relying only on minimum-limiting radiocarbon dates will only record an unknown temporal lag following the last retreat of ice from a region [*Carlson et al.*, 2009a; *Teller and Boyd*, 2006; *Teller et al.*, 2005]. Indeed, *Lowell et al.* [2005, p. 372] acknowledged this possibility, stating in regards to dating the opening of the eastern outlet that "an alternative interpretation has been that recession from a glacial re-advance associated with Younger Dryas cooling is being dated, not the original deglaciation." *Lowell et al.* [2009], however, assumed a simple ice margin retreat pattern, neglecting the possibility of an ice readvance that overrode and covered the eastern outlet [*Lowell et al.*, 2005; *Teller et al.*, 2005; *Teller and Boyd*, 2006; *Carlson et al.*, 2009a]. One such well-documented readvance of the Superior lobe across Lake Superior occurred during the Younger Dryas occurred just to the west of their study area [*Clayton*, 1984; *Lowell et al.*, 1999].

[167] A close examination of their lake core records further highlights the difficulty in actually dating the timing of ice retreat with minimum-limiting basal lake radiocarbon dates. For example, the critical basal dates for the *Lowell et al.* [2009] chronology are from their Sunbow Lake (~12.3 ka, ETH-31429) and Crawfish Lake (~12.0 ka, ETH-31430) records (Figure 27). Because these lake cores only penetrated sand and laminated silt, it is likely that there is the well-known lag between deglaciation and the accumulation of organic material in a lake [*Wright*, 1972, 1981]. Moreover, these sediments are not unique to ice marginal environments

in this region, as suggested from the Salo Lake core where there are multiple layers with grain sizes up to gravel occurring >1 m above the basal date of ~17.1 ± 0.2 ka (14.05 ± 0.10 ^{14}C ka BP, ETH-30180), further suggesting some unknown interval of time between ice retreat and the basal age.

[168] Radiocarbon dates from Bear Cub Lake that provide the minimum-limiting constraint for ice retreat north of the eastern outlets (Figure 27) are in reverse stratigraphic order outside the uncertainty of radiocarbon measurements, indicating that another lag exists between the arrival of vegetation to a region after deglaciation and when a lake actually preserves a datable macrofossil. The lowest radiocarbon date in Bear Cub Lake core is 11.4 ± 0.2 ka (9.97 ± 0.08 ^{14}C ka BP, ETH-28940), significantly younger than the oldest radiocarbon date of 12.5 ± 0.1 ka (10.55 ± 0.08 ^{14}C ka BP, ETH-28939) that is ~30 cm higher in the core. Consequently, the organic material dated at ~12.5 ka resided on the landscape for >1000 years before being deposited in Bear Cub Lake above the organic material dated at ~11.4 ka. Evidence of this lag is further seen in the basal radiocarbon dates from different lakes on the same moraine that range over thousands of years, indicating a variable timing in the onset of organic material accumulation in any given lake (Figure 27). Finally, regional cooling during the Younger Dryas may have slowed or halted the northward migration of the boreal forest [*Shuman et al.*, 2005], introducing another lag in the arrival of vegetation to a region following deglaciation. This additional lag may be reflected in the significant decrease in the number of basal radiocarbon dates in this region from the Younger Dryas interval (Figure 27) [*Lowell et al.*, 2009].

[169] *Lowell et al.* [2005, 2009] also argued that radiocarbon dates in front of a moraine provide a maximum-limiting age for deposition of that moraine. However, these moraine distal dates provide no actual stratigraphic control on the moraine and just represent a minimum-limiting age unless the date underlies proglacial sediment that is associated with the moraine. Therefore, a basal age from a lake in front of the moraine cannot be interpreted as necessarily older than the moraine, which is clearly indicated by the numerous basal radiocarbon dates in front of Steep Rock/Brule Moraines that are younger than the oldest minimum-limiting date on or behind these moraines.

[170] Given these caveats with minimum-limiting radiocarbon dates, we present a deglacial chronology for the eastern outlets that strictly interprets the radiocarbon dates in terms of their stratigraphic location (i.e., only a minimum-limiting age constraint) and also accounts for isostatic depression of the landscape [*Teller et al.*, 2005]. The oldest minimum-limiting date for northward retreat from the Vermillion Moraine is 13.9 ± 0.1 ka (12.00 ± 0.09 ^{14}C ka BP, ETH-28945) (Figure 26c). The minimum-limiting date from near the North Lake Outlet indicates that this outlet was ice free before 12.5 ± 0.1 ka (10.55 ± 0.08 ^{14}C ka BP, ETH-28939), confirming that Lake Agassiz runoff could drain eastward near the start of the Younger Dryas (Figure 26). Interestingly, just south of this outlet and the Steep Rock Moraine, there is the aforementioned gap in radiocarbon ages, with all basal dates younger than 11.5 ± 0.2 ka (10.00 ± 0.08 ^{14}C ka BP, ETH-28946), suggesting conditions not conducive to the accumulation of organic material in small lakes, possibly reflecting overflow of Lake Agassiz runoff. Continued northward recession of the LIS margin would have exposed the Flatrock Outlet prior to 12.3 ± 0.2 ka (10.40 ± 0.12 ^{14}C ka BP, ETH-31429), allowing sustained eastward discharge of Lake Agassiz runoff. Ice margin retreat north of the Brule Moraine before 12.0 ± 0.2 ka (10.25 ± 0.08 ^{14}C ka BP, ETH-31430) would open the even lower Matawin River, Shebandowan, and Savanne Outlets that would continue to drain Lake Agassiz eastward (Figure 27). Therefore, the current minimum-limiting radiocarbon chronology for the eastern Lake Agassiz outlets supports the original routing hypothesis of the Younger Dryas [*Johnson and McClure*, 1976; *Rooth*, 1982; *Broecker et al.*, 1989]. We note that the retreat/drainage chronology presented here is also supported by preliminary cosmogenic boulder ages from the eastern outlets that indicate that the LIS margin was north of the outlets around Thunder Bay by the start of the Younger Dryas and had retreated to Lake Nipigon by the end of the Younger Dryas [*Kelly et al.*, 2009].

9.2.3. The Northern Outlet Record

[171] Assuming that the southern outlet was abandoned at the start of the Younger Dryas [*Moran et al.*, 1973; *Broecker et al.*, 1989] and that the eastern outlet was still closed until near the end of the Younger Dryas based on minimum-limiting ^{14}C dates, *Teller et al.* [2005] suggested that Lake Agassiz freshwater was routed to the Arctic Ocean during the Younger Dryas. In contrast, based on minimum-limiting radiocarbon dates from the northern outlet, *Lowell et al.* [2005] and *Fisher et al.* [2009] argued that freshwater could not have drained north until 11.3 ± 0.1 ka (9.85 ± 0.07 ^{14}C ka BP, ETH-30590) to 11.0 ± 0.2 ka (9.67 ± 0.08 ^{14}C ka BP, ETH-30175) (Figure 26c). In doing so, they assumed that these dates date immediate deglaciation, which we argued above is unlikely, and that they did not consider older wood radiocarbon dates reworked in fluvial gravels from the northern outlet. *Carlson et al.* [2007b] suggested there may have been a short-lived northward routing of water during the Younger Dryas based on a radiocarbon date of 12.1 ± 0.5 ka (10.31 ± 0.29 ^{14}C ka BP, GX-5301-II) in fluvial gravels [*Smith and Fisher*, 1993], in agreement with two additional radiocarbon dates from the gravel layers [*Teller and Boyd*, 2006] and a light δ^{18}O anomaly in the Arctic Ocean at ~12 ka [*Andrews and Dunhill*, 2004] (Figures 28b and 28c).

[172] More recent research on the Mackenzie River delta identified a gravel layer overlying eroded aeolian sand, suggesting a flood event; fluvial sand overlies the gravel layer [*Murton et al.*, 2010]. *Optically stimulated luminescence (OSL)* dates on the lower aeolian sand units range from 13.4 ± 0.9 ka to 12.7 ± 0.8 ka (Figure 28c), although the oldest OSL date could be 17.5 ± 1.1 ka depending on the age model used to calculate its age [*Murton et al.*, 2010]. Two ages on the overlying fluvial sand are 11.9 ± 1.0 ka and 11.8 ± 1.0 ka. *Murton et al.* [2010] averaged the seven OSL dates from the lower sand unit and assumed that the erosion event and gravel deposition occurred shortly after 13.0 ± 0.2 ka.

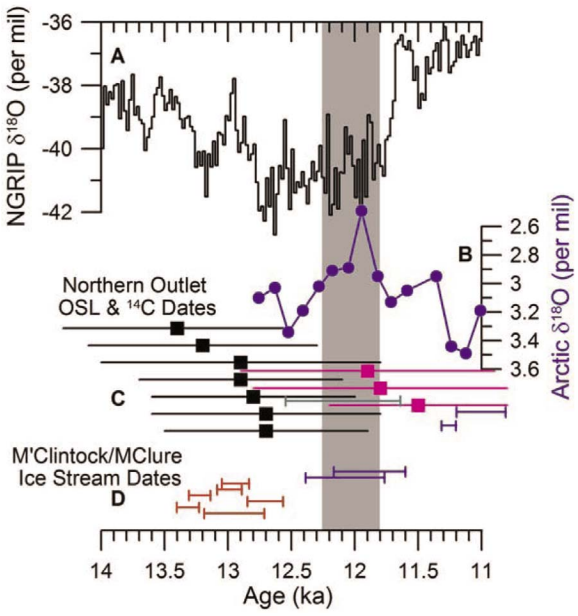

Figure 28. Arctic Younger Dryas records. (a) NGRIP δ^{18}O [*Svensson et al.*, 2008]. (b) Planktonic δ^{18}O from near the mouth of the Mackenzie River [*Andrews and Dunhill*, 2004]. (c) Optically stimulated luminescence (OSL) ages from the Mackenzie River delta that constrain the age of the erosion and gravel deposition event. Black symbols predate the event, and purple symbols postdate the event (note the 1σ error bars) [*Murton et al.*, 2010]. Green bar is the radiocarbon date from the northern outlet of Lake Agassiz [*Smith and Fisher*, 1993]. Blue bars are minimum-limiting radiocarbon dates for opening of the northern outlet [*Fisher et al.*, 2009]. (d) Radiocarbon constraints on the advance (red) and retreat (blue) of the M'Clintock/MClure Ice Stream in the Canadian Arctic [*Dyke*, 2004].

They attributed this flood to northward routing of Lake Agassiz water and proposed that it was the trigger for the Younger Dryas.

[173] The timing of this erosion event as inferred by *Murton et al.* [2010] assumes that deposition of the aeolian sediments below the erosion layer only slightly preceded the erosion event. Because the OSL dates on the aeolian sediment are distributed over an area of >100 km^2 and are most likely not from the same stratigraphic horizon, they should not be averaged together. Averaging assumes that these ages are all "geologically" the same and the uncertainty in the dating method is what makes their ages appear different. Second, the erosion event prior to the deposition of the gravel removed an unknown amount of aeolian sand, which also removes "time." Based upon the stratigraphic sequence of aeolian sand deposition, erosion, gravel deposition, and fluvial sand deposition, we suggest that the age of the erosion event is more likely close to the age of the overlying fluvial sand layer, the deposition of which should have closely followed the waning of the flood. This interpretation thus places the flood event closer to 11.9 ± 1.0 ka to 11.8 ± 1.0 ka. Within the errors of the OSL dates, our suggested timing of the flood corresponds with the three radiocarbon dates that imply the opening of the northern outlet of Lake Agassiz at ~12 ka [*Smith and Fisher*, 1993; *Teller and Boyd*, 2006], the decrease in planktonic δ^{18}O at ~12 ka off the mouth of the Mackenzie River [*Andrews and Dunhill*, 2004] (Figure 28), and the routing of Lake Agassiz water away from the eastern outlet at ~12 ka potentially from the opening of the northern outlet [*Carlson et al.*, 2007b].

9.2.4. Summary of the Terrestrial Radiocarbon Outlet Records

[174] We conclude that the Lake Agassiz southern outlet was abandoned before 12.6 ± 0.1 ka (ETH-32674) or 12.9 ± 0.3 ka (W-723), in good agreement with runoff records from the Gulf of Mexico [*Broecker et al.*, 1989; *Flower et al.*, 2004] and the onset of the Younger Dryas at ~12.9 ka in well-dated climate records (Figure 26) [*Wang et al.*, 2001; *Rasmussen et al.*, 2006; *Svensson et al.*, 2008]. The opening of the eastern outlet is not directly dated but occurred before 12.5 ± 0.1 ka (10.55 ± 0.08 ^{14}C ka BP, ETH-28939). Further northward retreat of the ice margin would have continued to open isostatically depressed outlets, allowing eastward drainage of Lake Agassiz freshwater until readvance of the Lake Superior lobe closed the outlet at the end of the Younger Dryas [*Clayton*, 1984; *Lowell et al.*, 1999]. There is also geologic evidence that Lake Agassiz runoff may have been briefly routed northward at ~12 ka [*Carlson et al.*, 2007b].

9.3. Rapid Melting of the Northwestern Laurentide Ice Sheet

[175] Another suggested cause of the Younger Dryas is that abrupt retreat and thinning of the northwestern LIS discharged meltwater to the Arctic Ocean that slowed the AMOC [*Tarasov and Peltier*, 2005, 2006]. This hypothesis stems from ice sheet model simulations rather than geologic data. The *Tarasov and Peltier* [2005, 2006] transient deglacial LIS model simulation produced an ~0.09 Sv increase in LIS Arctic discharge at 13.0–12.7 ka. In contrast, previous modeling studies did not produce a significant Arctic discharge from LIS melting until after the Younger Dryas [*Licciardi et al.*, 1999; *Marshall and Clarke*, 1999]. *Tarasov and Peltier* [2005] attributed this difference to the presence of a large Keewatin Dome in their simulations, although a Keewatin Dome existed in the two earlier simulations [*Licciardi et al.*, 1998, 1999; *Marshall and Clarke*, 1999].

[176] As discussed previously (section 5.1), there are large uncertainties in the climate forcing used in the *Tarasov and Peltier* [2004, 2005, 2006] ice sheet model. Furthermore, their climate forcing includes two additional scaling factors that enhance precipitation up to 3.5 × over the Keewatin Region between 30 and 10.6 ka to create and destroy a large Keewatin Dome, the latter of which is notably right around the time of the Younger Dryas. *Tarasov and Peltier* [2004, p. 366] argued that their use of precipitation enhancement factors was consistent with a high Keewatin Dome that "diverted the jet stream southward, and baroclinic instability along the southern margin of the ice sheet thereafter enhanced regional precipitation." However, fully coupled GCM experiments for the LGM indicated a reduction in precipitation over a high Keewatin Dome, not an enhancement, with decreasing

precipitation at higher altitudes [*Braconnot et al.*, 2007; *Otto-Bliesner et al.*, 2006]. Further information on the effects of these two parameters and the timing and manner of their manipulation is needed to fully assess the *Tarasov and Peltier* [2005, 2006] model results. We also note one apparent ambiguity in their results, however, whereby their model produces an increase in LIS discharge to the Arctic Ocean from melting when the cooling from the Bølling warm period to the Younger Dryas in their climate forcing (GRIP δ^{18}O) (Figure 25) would presumably reduce melting.

[177] Following *Tarasov and Peltier* [2005, 2006], *Stokes et al.* [2009] attempted to correlate flow patterns for a paleo–ice stream (M'Clintock/MClure Ice Stream) in the Canadian Arctic with the deglacial ice margin record for the region reconstructed by *Dyke et al.* [2003]. From this correlation, they suggested that glacial geologic evidence existed in support of an Arctic freshwater forcing of the Younger Dryas. The authors estimated that ~80,000 km^3 of ice was discharged to the Arctic between ~13.0 and 12.7 ka. This volume of ice, however, is small (~0.2 m of sea level rise) and constitutes a freshwater forcing of ~0.007 Sv for 300 years, which climate models demonstrate is too small to have caused a >1000 year reduction in the AMOC and the Younger Dryas cold event [*Liu et al.*, 2009; *Stouffer et al.*, 2006]. The correlation between flow patterns and ice margins is also difficult because of the unknown time lag between formation of flow pattern lineations and retreat of the ice margin over the lineations. Moreover, the timing of this ice stream event, which is constrained by maximum- and minimum-limiting radiocarbon dates [*Dyke*, 2004], does not support a forcing of the Younger Dryas cold event. Seven radiocarbon dates underlying till deposited during the ice margin advance indicate advance after 12.7 ± 0.2 ka (10.66 ± 0.16 ^{14}C ka BP, GSC-403), with two minimum-limiting radiocarbon dates indicating retreat before 12.1 ± 0.3 ka BP (10.29 ± 0.15 ^{14}C ka BP, S-2591) (Figure 28d) [*Dyke*, 2004]. Thus, this ice stream event occurred after the start of the Younger Dryas and ended in the middle of the Younger Dryas, indicating that meltwater discharge from the advance could not have caused the Younger Dryas.

[178] To summarize, the hypothesis of an Arctic LIS meltwater trigger for the Younger Dryas comes from a transient ice sheet model simulation [*Tarasov and Peltier*, 2005, 2006], but it has yet to be supported by terrestrial evidence. As such, the ice sheet model is only as good as its climate forcing, which *Tarasov and Peltier* [2004] suggested was a "significant limitation." In any event, the above discussed relative sea level records argue against a meltwater forcing of the Younger Dryas because the rates of ice sheet retreat slowed rather than accelerated during the event (Figure 25) [*Bard et al.*, 2010].

9.4. North American Runoff Records During the Younger Dryas

[179] Runoff records from North American outlets provide a continuous record of relative discharge and potentially the sources of freshwater. The most common proxy used is planktonic δ^{18}O, which is often interpreted to reflect the input of more ^{18}O-depleted terrestrial freshwater [*Broecker et al.*, 1989; *Keigwin and Jones*, 1995; *de Vernal et al.*, 1996; *Andrews and Dunhill*, 2004]. If changes in water temperature occur at the same time, they will diminish or amplify a given δ^{18}O signal, but these can be accounted for with independent temperature estimates, resulting in a signal of the salinity-dependent δ^{18}O of seawater ($\delta^{18}O_{sw}$) [*Flower et al.*, 2004; *Carlson et al.*, 2007b; *Obbink et al.*, 2010]. Other planktonic foraminifera proxies, such as δ^{13}C, provide independent evidence of the amount of terrestrial freshwater being discharged to the ocean [*Carlson et al.*, 2007b; *Polyak et al.*, 2000]. Proxies that are specific to a given bedrock terrain type/age are also useful as they track the water source region [*Carlson et al.*, 2007b]. These various proxy records can be converted into discharge estimates with a mixing model if the ocean and freshwater end-member values and the ocean fluxes are known [*Aharon*, 2003, 2006; *Carlson et al.*, 2007b; *Carlson*, 2009; *Obbink et al.*, 2010].

9.4.1. The Southern Outlet

[180] *Broecker et al.* [1989] dated a Gulf of Mexico planktonic δ^{18}O increase of ~3‰ at ~12.9 ka, or the start of the Younger Dryas, which they interpreted as a signal of the routing of Lake Agassiz water away from the southern outlet. After accounting for global ice volume effects, higher-resolution data suggest that this increase is ~1.8‰ (Figure 29d) [*Flower et al.*, 2004; *Leventer et al.*, 1982]. With the removal of the temperature effect on δ^{18}O, the $\delta^{18}O_{sw}$ increase is ~1.9‰ [*Flower et al.*, 2004]. The timing of this increase is well constrained by radiocarbon dates placing it between 13.2 ± 0.2 ka (11.29 ± 0.21 ^{14}C ka BP, ETH-number not reported) and 12.5 ± 0.2 ka (10.51 ± 0.16 ^{14}C ka BP, ETH-4769), with linear interpolation between the dates indicating a midpoint of ~12.9 ka [*Broecker and Andree*, 1988; *Broecker et al.*, 1989; *Flower et al.*, 2004].

9.4.2. The Eastern Outlet

[181] A planktonic δ^{18}O decrease of 0.5–0.7‰ found in cores near the mouth of the St. Lawrence River was interpreted to be too small to be the signal of runoff routed from the Gulf of Mexico [*Keigwin and Jones*, 1995; *de Vernal et al.*, 1996]. However, these studies neglected the effects of both global ice volume and temperature on planktonic δ^{18}O. Upon removal of the ice volume effect, planktonic δ^{18}O decreases by 0.8–0.9‰ at the start of the Younger Dryas (Figure 29c) [*Carlson et al.*, 2007b; *Obbink et al.*, 2010]. Although there is no direct Mg/Ca-temperature record from the planktonic foraminifera during the Younger Dryas due to the compromised relationship between Mg/Ca and temperature from the input of Mg-rich water [*Carlson et al.*, 2007b], there are several lines of evidence that indicate mixed layer cooling of the St. Lawrence estuary during the Younger Dryas. *de Vernal et al.* [1996] used *dinoflagellate* cysts to reconstruct an 8–10°C cooling of the upper 30 m of the water column during the Younger Dryas. Foraminifera census data suggest a cooling of ~5–7°C down to the pycnocline [*Keigwin and Jones*, 1995] at ~100 m water depth in the St. Lawrence estuary [*Dickie and Trites*, 1983]. Using the more conservative pycnocline cooling of ~5°C, the corresponding $\delta^{18}O_{sw}$ decrease in the St. Lawrence estuary is ~1.8‰, in

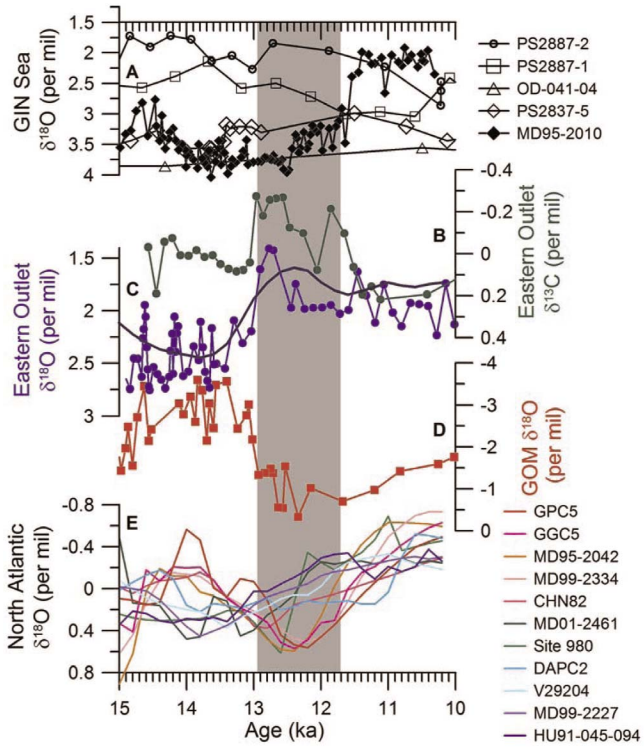

Figure 29. $\delta^{18}O$ (ice volume corrected) and $\delta^{13}C$ records for the outlets of the LIS and the North Atlantic. (a) Five records from the Greenland-Iceland-Norwegian (GIN) Sea (Fram Strait is indicated by open symbols, and Norwegian Sea is indicated by closed diamonds) [*Dokken and Jansen*, 1999; *Nørgaard-Pedersen et al.*, 2003]. (b) The $\delta^{13}C$ record from the St. Lawrence estuary [*de Vernal et al.*, 1996]. (c) High-resolution $\delta^{18}O$ record (blue) and stacked $\delta^{18}O$ records (dark blue) from St. Lawrence estuary [*Keigwin and Jones*, 1995; *Keigwin et al.*, 2005]. (d) The $\delta^{18}O$ record from the Gulf of Mexico [*Flower et al.*, 2004]. (e) Three-point smoothed North Atlantic planktonic $\delta^{18}O$ records that have been normalized to their mean: Bermuda Rise, GPC5 and GGC5; Iberian Margin, MD95-2042 and MD99-2334; North Atlantic, CHN82-20; Northeast Atlantic, ODP Site 980 and MD01-2461; Orphan Knoll, HU91-045-094; Eirik Drift, MD99-2227; Rockall Trough, DAPC2; and Iceland, V29204. Gray bar denotes the timing of the Younger Dryas [*Rasmussen et al.*, 2006].

agreement with the concurrent increase in Gulf of Mexico $\delta^{18}O_{sw}$ [*Flower et al.*, 2004]. The larger temperature cooling reconstructed from dinoflagellate cysts results in a greater decrease in $\delta^{18}O_{sw}$ [*Carlson et al.*, 2007b], but this is likely an overestimate.

[182] Planktonic $\delta^{13}C$ records also indicate an increase in freshwater discharge through the St. Lawrence at the onset of the Younger Dryas. An ~0.4‰ decrease in $\delta^{13}C$ indicates an increase in the discharge of terrestrially derived freshwater (Figure 29b) [*Carlson et al.*, 2007b], which derives its dissolved inorganic carbon predominately from plant biomass ($\delta^{13}C$ of approximately −11 to −25‰) [*Mook*, 1972; *Polyak et al.*, 2000]. Benthic faunal assemblages further indicate freshening of the Champlain Sea at 13.2–12.9 ka [*Rayburn et al.*, 2011], whereas Champlain Sea mollusk $\delta^{18}O$ show a 2–3‰ decrease reflecting increased freshwater discharge [*Brand and McCarthy*, 2005]. The deposition of the gray, silty Wilmette Bed contemporaneous with an *ostracode* $\delta^{18}O$ decrease of ~6‰ in Lake Michigan indicates Lake Agassiz inflow near or at the start of the Younger Dryas and provides additional support for eastward routing of Lake Agassiz [*Colman*, 2007; *Colman et al.*, 1994].

[183] *Carlson et al.* [2007b] used three independent geochemical tracers (planktonic ΔMg/Ca, *U/Ca*, and $^{87}Sr/^{86}Sr$) of freshwater sources that showed the addition of Lake Agassiz runoff to the St. Lawrence Basin at the start of the Younger Dryas. The increases in both Mg and U relative to Ca observed in the St. Lawrence estuary reflect the arrival of western Canadian Plains freshwater, which has Mg and U concentrations 6–10 and 10–20 times higher than the St. Lawrence system, respectively [*Carlson et al.*, 2007b; *Chabaux et al.*, 2003; *Yang et al.*, 1996]. Similarly, the Canadian Shield bedrock contained within the Lake Agassiz basin and the water that drains it are significantly more radiogenic than the bedrock of the St. Lawrence system [*Wadleigh et al.*, 1985], and thus, the observed increase in $^{87}Sr/^{86}Sr$ further confirms the arrival of western Canadian Plains freshwater. The $^{87}Sr/^{86}Sr$ record is also supported by $^{87}Sr/^{86}Sr$ measurements on Champlain Sea mollusk shells that show an increase in radiogenic Sr during the Younger Dryas [*Brand and McCarthy*, 2005]. An estuary mixing model that included inputs to the river end-member of all the bedrock terranes within the St. Lawrence and Lake Agassiz Basins suggested that the initial increase in discharge of ~0.06 Sv was required to explain these three independent changes in estuary geochemistry [*Carlson et al.*, 2007b], in agreement with earlier estimates from ice sheet–climate model results [*Licciardi et al.*, 1999] and of sufficient magnitude to cause a reduction in AMOC strength [*Clarke et al.*, 2009; *Liu et al.*, 2009; *Meissner*, 2007; *Meissner and Clark*, 2006; *Stouffer et al.*, 2006]. Discharge peaked at ~12.6 ka with a maximum base flow increase of ~0.12 Sv from the routing of Lake Agassiz runoff. A subsequent reduction in discharge was attributed to the northward routing of Lake Agassiz at ~12 ka (section 9.2.3), with a final discharge increase to ~0.06 Sv for the remainder of the Younger Dryas [*Carlson et al.*, 2007b].

[184] In their reply to the comment of *Carlson and Clark* [2008], *Peltier et al.* [2008] questioned the conclusions of *Carlson et al.* [2007b] based upon the sea surface salinity (SSS) record reconstructed from dinoflagellate cysts that did not show a decrease in SSS during the Younger Dryas [*de Vernal et al.*, 1996]. We note, however, that a more recent assessment of the dinoflagellate cyst transfer function methodology found that SSS explains only 2.4% of the variability in the modern distribution of dinoflagellates once the influence of temperature and sea ice are removed, indicating that this approach cannot reconstruct SSS [*Telford*, 2006]. Furthermore, dinoflagellates are euryhaline, and a distinct sensitivity to SSS has only been found below 12 *practical*

salinity units (psu) [*Dale*, 1996]. Thus, it is not surprising that the dinoflagellate cysts do not suggest any significant SSS change during the Younger Dryas because the St. Lawrence Estuary SSS was well above 12 psu, as indicated by the presence of planktonic foraminifera.

[185] *Peltier et al.* [2008] also suggested that the use of the dinoflagellate cyst temperature record to calculate $\delta^{18}O_{sw}$ and ΔMg/Ca was incorrect because the two planktonic foraminifera species used (*N. pachyderma* (s) and *G. bulloides*) live deeper than the photic zone habitat of dinoflagellates. *Carlson et al.* [2007b] specifically pointed out that both foraminifera live deeper than dinoflagellates and noted that the calculations using this temperature proxy likely overestimate mixed layer cooling. *Carlson et al.* [2007b] also noted the independent evidence for atmospheric [*Mott et al.*, 1986] and thermocline cooling of the St. Lawrence estuary during the Younger Dryas [*Keigwin and Jones*, 1995] and support the use of a temperature correction to the Mg/Ca and $\delta^{18}O$ records. Furthermore, the deeper dwelling species, *N. pachyderma* (s), can live in temperatures ranging between 17 and 0°C and salinities between 36.0 and 32.5 psu [*Hilbrecht*, 1996], which is within the likely range of temperatures and salinities of the St. Lawrence estuary before and during the Younger Dryas [*de Vernal et al.*, 1996]. *Peltier et al.* [2008] pointed out that *N. pachyderma* (s) occupies the pycnocline. In the St. Lawrence estuary, this is at ~100 m depth [*Dickie and Trites*, 1983], which is ~4 times closer to the surface of the ocean than in the Labrador Sea and only slightly shallower than the modern Arctic habitat of 100 to 200 m water depth [*Hillaire-Marcel and de Vernal*, 2008]. Therefore, in the St. Lawrence estuary, *N. pachyderma* (s) is more sensitive to changes in sea surface temperatures than in the open ocean. In any event, these criticisms are irrelevant because using a more conservative temperature estimate for the Younger Dryas still results in a large decrease in $\delta^{18}O_{sw}$.

[186] *Peltier et al.* [2008] additionally questioned the use of U/Ca as a freshwater tracer but did not provide insight into how this is not a proxy for the arrival of U-rich water. As *Carlson et al.* [2007b] discussed, the gradual increase in U/Ca during the Younger Dryas is due to increasing discharge and also the exponential relationship between colloidal release of U during freshwater discharge into saline water [*Swarzenski et al.*, 2003]. They also included the modern U and Ca concentrations of the St. Lawrence River in the calculations of the river end-member concentrations and noted that U is 10 to 20 times more concentrated in western Canadian Plains freshwater when compared to the St. Lawrence River (see above) [*Chabaux et al.*, 2003]. *Peltier et al.* [2008] also criticized the Sr isotope proxy and the discharge calculations derived there from but again did not provide a justification. As noted above, *Carlson et al.* [2007b] included the local bedrock Sr isotope ratios and Sr concentrations in their modeling of the river end-member Sr isotope ratios and noted that the western Canadian Shield has heavier Sr isotope ratios than the igneous/metamorphic terranes in the St. Lawrence River Basin [*Wadleigh et al.*, 1985].

9.4.3. The Northern Outlet

[187] Following on the modeling results of *Tarasov and Peltier* [2005, 2006], several studies have claimed to have found paleoceanographic evidence that supports an Arctic freshwater forcing of the Younger Dryas [*Peltier*, 2007; *Peltier et al.*, 2006, 2008; *Polyak et al.*, 2007]. However, paleoceanographic data in support of an Arctic source of freshwater at the start of the Younger Dryas at ~12.9 ka are scarce to nonexistent [*Carlson and Clark*, 2008].

[188] *Poore et al.* [1999] recorded a light planktonic $\delta^{18}O$ anomaly in the Beaufort Gyre of the Arctic Ocean concurrent with an increase in planktonic Ba/Ca [*Hall and Chan*, 2004], but these are dated between ~14.5 and 13.6 ka, well before the onset of the Younger Dryas (Figure 14b), and are more likely related to meltwater discharge during MWP-1A [*Poore et al.*, 1999; *Hall and Chan*, 2004]. *Hillaire-Marcel et al.* [2004] presented three planktonic $\delta^{18}O$ data points that may be from the Younger Dryas time period, but their age model is constrained by two radiocarbon dates at ~13.1 ka and ~7.5 ka, and these three data points actually show heavier $\delta^{18}O$ during the period inferred to be the Younger Dryas and thus at face value argue against an Arctic freshwater forcing. Likewise, *Hanslik et al.* [2010] did not find any Arctic planktonic $\delta^{18}O$ decreases between ~13.8 to 10.2 ka, regardless of the reservoir age applied. *Andrews and Dunhill* [2004] found a relatively brief (~300 year duration) $\delta^{18}O$ decrease off the mouth of the Mackenzie River at ~11.5 ka, at the end of the Younger Dryas. Using a revised reservoir age from *Dyke* [2004] still places the light $\delta^{18}O$ anomaly well after the start of the Younger Dryas (Figure 28b) [*Carlson et al.*, 2007b]. On the Chukchi Margin, *Polyak et al.* [2007] identified a light $\delta^{18}O$ anomaly at ~12.6 ka but did not use an additional regional reservoir correction [*Dyke*, 2004] which, when accounted for, places the anomaly at ~12.1 ka. These authors also identified an earlier and larger $\delta^{18}O$ decrease dated at ~13.7 ka, which is still prior to the Younger Dryas after accounting for an additional reservoir effect [*Dyke*, 2004]. *Darby et al.* [2002] documented an ice rafting event in the Arctic Ocean at ~15.0 ka. *Spielhagen et al.* [2005] recognized a light planktonic $\delta^{18}O$ anomaly at ~12.9 ka in the Laptev Sea, which they attributed to the release of freshwater from an ice-dammed lake routed through the Lena or Yana Rivers of northeastern Russia, specifically noting that this event was not related to Lake Agassiz discharge or the LIS. *Spielhagen et al.* [2005] also indicated that they used a 400 year reservoir age, and when the more recent reservoir age of *Björck et al.* [2003] was used, the light $\delta^{18}O$ anomaly occurred well within the Younger Dryas rather than at the start. We emphasize that reservoir ages for radiocarbon dates in the Arctic Ocean are relatively well known, and thus, it is highly unlikely that these paleoceanographic data can be shifted to the onset of the Younger Dryas by the application of a larger reservoir age [*Dyke*, 2004]. For example, after accounting for an even higher reservoir age, as has been suggested for the Norwegian Sea [*Björck et al.*, 2003], these light $\delta^{18}O$ anomalies and ice rafting events still occur at least 350 ^{14}C years prior to the start of the Younger Dryas.

[189] In contrast, *Not and Hillaire-Marcel* [2012] documented an increase in detrital carbonate deposition in the sand and silt fraction during the deglaciation in the central Arctic Ocean. Based on their chronologic assumption of a 1400 year reservoir age, *Not and Hillaire-Marcel* [2012] placed this detrital carbonate event during the Younger Dryas and argued that it represented increased discharge of Lake Agassiz runoff through the Mackenzie River to the Arctic Ocean following *Murton et al.* [2010]. However, this linkage depends solely on the assumed reservoir age, for which there is little constraint. *Hanslik et al.* [2010] produced the radiocarbon chronology for the core, and a standard reservoir age of 400 years dates the detrital carbonate event to ~14 ka. This event in the core is concurrent with a low in planktonic foraminifera concentration. If one assumes that this low is due to Younger Dryas cooling rather than, say, dilution from detrital carbonate deposition, then it can be correlated to the Younger Dryas and suggests an additional reservoir age of 1000 years [*Hanslik et al.*, 2010]. In addition to the conundrum of attributing the foraminifera concentration low to cooling rather than dilution, a similar decrease in planktonic foraminifera concentration occurs 15 cm higher in the core, well after the Younger Dryas. This demonstrates that the assumption of low foraminifera concentration corresponding to hemispheric cold events is incorrect and suggests that the assumed additional 1000 year reservoir age used by *Not and Hillaire-Marcel* [2012] is too large and that this detrital carbonate event does not correspond to the Younger Dryas. Indeed, as we discussed in section 9.2.3, the *Murton et al.* [2010] Mackenzie River erosion event likely occurred well after the start of the Younger Dryas, arguing against the detrital carbonate source suggested by *Not and Hillaire-Marcel* [2012]. It seems more likely that the detrital carbonate layer records the breakup of the LIS on the Canadian Arctic Archipelago that started before ~14.1 ka and was completed before ~13.3 ka (see section 5.1 and Figure 14a) [*Dyke*, 2004; *England et al.*, 2009], which is recorded in multiple Arctic Ocean cores as detrital carbonate layers [*Darby et al.*, 2002] as well as decreased in planktonic foraminifera $\delta^{18}O$ and increased in Ba/Ca (Figure 15b) [*Poore et al.*, 1999; *Hall and Chan*, 2004]. *Stokes et al.* [2009] also suggested greater ice streaming and iceberg discharge during this event relative to the small readvance that occurred during the Younger Dryas.

[190] Multiple sediment cores collected from Fram Strait, through which Arctic freshwater would presumably pass to affect AMOC, do not show a planktonic $\delta^{18}O$ decrease during the Younger Dryas (Figure 29a) [*Nørgaard-Pedersen et al.*, 2003], nor does $\delta^{18}O_{sw}$ significantly decrease off of southern Greenland in the pathway of Arctic freshwater discharged through Fram Strait [*Holliday et al.*, 2007; *Winsor et al.*, 2012], refuting the Arctic forcing hypothesis. The highest-resolution planktonic $\delta^{18}O$ record from the Norwegian Sea also does not show any significant change during the Younger Dryas (Figure 29a) [*Dokken and Jansen*, 1999]. Conversely, *Maccali et al.* [2012] documented an increase in detrital $^{206}Pb/^{204}Pb$ in one sample from central Fram Strait. No radiocarbon dates are near enough in the core to constrain the age of the sample beyond that it is of deglacial age. *Maccali et al.* [2012] therefore assumed that the age of the increase corresponded with the detrital carbonate event of the *Not and Hillaire-Marcel* [2012] study using their age model, along with an ash layer several centimeters above the sample that they suggest to be Vedde Ash from ~12.1 ka. With an assumed Younger Dryas age based on these correlations, *Maccali et al.* [2012] suggested that this detrital event reflected detrital rainout from icebergs discharged from the Arctic due to northward LIS drainage. The LIS source was based on two river sediment Pb analyses from the Red and Mackenzie Rivers [*Millot et al.*, 2004]. However, as we discussed, the chronology of *Not and Hillaire-Marcel* [2012] is dependent on the assumed reservoir age, and existing data suggest that the detrital carbonate layer is older than the Younger Dryas. The ash layer has no published geochemical record that would identify it as the Vedde Ash. Likewise, with only one tephra and no closely constraining radiocarbon dates, it is not possible to document a tephra as the Vedde Ash because at least four widespread tephras with the same chemistry as the Vedde were erupted from Katla during the deglacial period [*Lane et al.*, 2012], with the potential for even more tephras [*Thornalley et al.*, 2011a]. Thus, without more precise radiocarbon age constraints or the documentation of these four major eruptions, the age of this tephra can only be constrained to the deglacial period. We would note that an ice rafting event has previously been documented in Fram Strait at ~14 ka, to which this detrital event may correspond [*Darby et al.*, 2002]. Alternatively, the higher Th/Zr ratio of this sample from *Maccali et al.* [2012] relative to other samples in the core used to document a detrital flux is equivalent to the Th/Zr ratios of late Holocene samples from a core in eastern Fram Strait, where the higher Th/Zr ratios reflect the inflow of Atlantic waters. The $^{206}Pb/^{204}Pb$ ratio for this one sample is the same as those from the late Holocene multicore record and plots in the same $^{206}Pb/^{204}Pb$-$^{208}Pb/^{206}Pb$ isotope space, which could mean that the anomalous sample in central Fram Strait possibly reflects a greater incursion of Atlantic waters into central Fram Strait during the deglacial period relative to modern.

9.4.4. Summary of Runoff Records

[191] In Figure 29e, we summarize 11 ice volume corrected planktonic $\delta^{18}O$ records that span the North Atlantic and are of high enough resolution to assess changes in $\delta^{18}O$ during the Younger Dryas, in addition to the above discussed records from the Norwegian and Greenland Seas and the Gulf of Mexico (Figures 29a and 29d). None of these records show a decrease in $\delta^{18}O$ at the start of the Younger Dryas. In fact, the only $\delta^{18}O$ decrease observed in the North Atlantic at the start of the Younger Dryas is adjacent to the St. Lawrence estuary (Figure 29c), confirming this as the source of the freshwater discharge that caused the Younger Dryas. We would note that no decreases are observed near Iceland and farther north into the Nordic Seas, in conflict with the Arctic freshwater forcing hypothesis. We conclude that the existing LIS runoff records support the original routing hypothesis as the cause of the Younger Dryas.

9.5. Floods, Ice Discharge, and Routing Effects on AMOC

[192] As noted in section 1, much attention as of late has been given to the hypothesis that a short-lived flood or ice discharge event caused the Younger Dryas rather than a sustained, yet smaller-magnitude routing event. The length of the Younger Dryas flood is estimated to be ≤1 year in duration based on modern glaciological observations and hydrological modeling [*Teller et al.*, 2002; *Clarke et al.*, 2004], with estimated 1 year fluxes of 0.54–1.08 Sv; a longer duration simply reduces the flux accordingly. The modeled increase in Arctic LIS discharge is ~300 years in duration with a flux of ~0.09 Sv [*Tarasov and Peltier*, 2005, 2006]. On the other hand, the eastward routing of Lake Agassiz runoff spans the Younger Dryas with estimated discharge increases of ~0.07 Sv based on ice sheet–climate model results [*Licciardi et al.*, 1999] and 0.06 to 0.12 Sv based on four independent geochemical runoff proxies [*Carlson et al.*, 2007b]. For comparison, a 1 year flood with a flux of 1 Sv is equivalent to 3.15×10^{13} m^3 of freshwater, whereas a 1200 year routing event with a flux of 0.07 Sv is equivalent to 2.65×10^{15} m^3 of freshwater, or two orders of magnitude larger than a flood.

9.5.1. Floods

[193] Despite the focus on identifying a flood at the start of the Younger Dryas, floods of an even larger magnitude than suggested for the Younger Dryas fail to cause the 1200 year long reduction in AMOC strength as has been reconstructed by proxies [*McManus et al.*, 2004; *Praetorius et al.*, 2008; *Robinson et al.*, 2005]. In one Earth system model of intermediate complexity (EMIC) with a full ocean GCM, a Younger Dryas flood failed to affect the AMOC [*Meissner and Clark*, 2006]. In fully coupled GCMs, a 5 to 8 Sv flood either produces only a 40 year reduction in AMOC strength [*LeGrande and Schmidt*, 2008; *LeGrande et al.*, 2006] or produces no AMOC reduction [*Clarke et al.*, 2009]. Models thus indicate that a flood is most likely not the cause of the Younger Dryas, and a longer-duration freshwater forcing is required to explain the event.

9.5.2. Rapid Ice-Discharge Events

[194] A centuries-long ice discharge event would presumably cause a longer AMOC reduction [*Tarasov and Peltier*, 2005]. In this regard, *Peltier et al.* [2006] used a fully coupled GCM to simulate the effects of an Arctic freshwater forcing from a 300 year long increase in meltwater/iceberg discharge from the LIS. To cause a reduction in AMOC strength, however, the authors required a significantly larger freshwater forcing to the Arctic than suggested by the *Tarasov and Peltier* [2005, 2006] ice sheet model. In particular, *Peltier et al.* [2006] applied a forcing of 1 Sv for 100 years (equivalent to 8 m of sea level rise) to the Arctic Ocean and produced a 300 year reduction in AMOC. Given this relationship between Arctic discharge, duration and the AMOC response, a volume of freshwater equivalent to 32 m of sea level would have to be discharged into the Arctic Ocean to explain the 1200 year long Younger Dryas AMOC reduction. This scenario is negated, however, because sea level rose <5 m during the Younger Dryas (Figure 25b) [*Tarasov and Peltier*, 2005; *Bard et al.*, 2010]. The actual meltwater forcing of *Tarasov and Peltier* [2005, 2006] was ~0.09 Sv for only 300 years, which, according to the fully coupled GCMs, is too short to explain the 1200 year event [*Clarke et al.*, 2009; *LeGrande and Schmidt*, 2008; *LeGrande et al.*, 2006; *Liu et al.*, 2009; *Otto-Bliesner and Brady*, 2010; *Peltier et al.*, 2006; *Stouffer et al.*, 2006].

[195] We note that suggestions of an iceberg discharge event from Hudson Strait as the forcing of the Younger Dryas [*Broecker et al.*, 2010; *Thornalley et al.*, 2011b] also fall under these constraints. While there is clear evidence for increased iceberg discharge during the Younger Dryas, iceberg discharge began after the start of the Younger Dryas [*Andrews and Tedesco*, 1992; *Bond et al.*, 1997; *Hillaire-Marcel and Bilodeau*, 2000]. Furthermore, the volume of icebergs discharged must be <5 m of equivalent sea level rise (Figure 25b), and thus a freshwater forcing of <0.05 Sv, assuming that the entire Younger Dryas sea level rise was sourced only from Hudson Strait. As this assumption is clearly wrong and only a fraction of the Younger Dryas sea level rise was sourced from Hudson Strait ice, the actual freshwater forcing from this iceberg discharge event is likely too small to have caused the Younger Dryas AMOC reduction.

9.5.3. Routing Events

[196] In contrast to these shorter freshwater forcings, an EMIC with a full ocean GCM simulated an ~30% reduction in AMOC strength for the duration of the Younger Dryas when forced with 0.07 Sv of freshwater for 1200 years through the St. Lawrence [*Meissner and Clark*, 2006], in agreement with the magnitude of AMOC reduction indicated by AMOC proxies [*McManus et al.*, 2004; *Robinson et al.*, 2005]. The same EMIC was also forced with the time varying St. Lawrence discharge estimates of *Carlson et al.* [2007b] (0.06 to 0.12 Sv) [*Meissner*, 2007], reproducing not only the magnitude of the AMOC reduction but also the centennial-scale structure of the event, with a century-long increase in AMOC at ~12 ka [*Carlson et al.*, 2007b; *Eltgroth et al.*, 2006; *McManus et al.*, 2004]. In fully coupled GCMs (with or without glacial boundary conditions), a freshwater discharge of 0.1 Sv to the North Atlantic produces an ~30% reduction in AMOC strength that persists for the duration of the freshwater forcing [*Stouffer et al.*, 2006; *Clarke et al.*, 2009; *Liu et al.*, 2009].

9.5.4. Summary of Freshwater Delivery Mechanisms

[197] In summary, climate model simulations refute claims that because incised channels near the eastern outlet (presumably from floods) were not open until after the Younger Dryas, another mechanism is needed to explain the event [*Lowell et al.*, 2005, 2009; *Teller et al.*, 2005; *Steig*, 2006; *Tarasov and Peltier*, 2005, 2006; *Peltier et al.*, 2008]. Instead, they show that a flood is inconsequential to the forcing of the Younger Dryas, rather requiring a sustained discharge of freshwater to the North Atlantic to suppress AMOC and cause a millennia-long cold event like the Younger Dryas [*Liu et al.*, 2009; *Singarayer and Valdes*, 2010; *Valdes*, 2011]. The lack of an identifiable large incised channel from a flood therefore

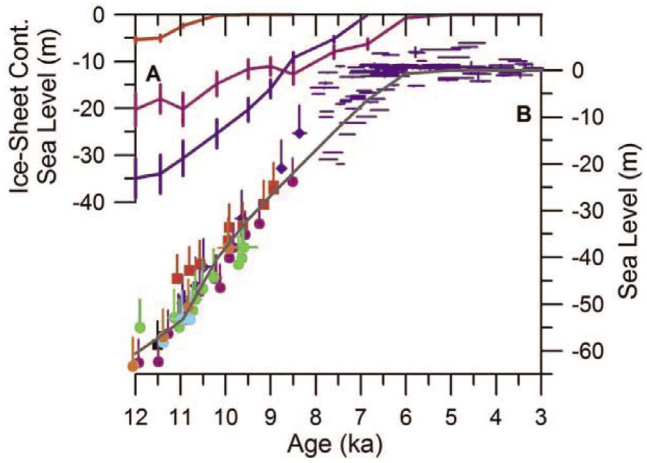

Figure 30. Holocene ice sheet volume and relative sea level. (a) Ice sheet contributions. Blue line is the LIS [*Carlson et al.*, 2008], red line is the SIS [*Boulton et al.*, 2001], and purple line is the AIS (this study). AIS volume is calculated by the remainder between the LIS, SIS, and ice-equivalent sea level. Vertical lines indicate estimated volume error (12% for the LIS and SIS and 17% for the AIS). (b) Relative sea level: circles are from Tahiti [*Bard et al.*, 1996, 2010], squares are from Barbados [*Peltier and Fairbanks*, 2006], diamonds are from New Guinea [*Edwards et al.*, 1993], and blue lines are from *Fleming et al.* [1998]. Age uncertainty is shown for all samples; where not visible, the uncertainty is less than the symbol size. Ice-equivalent sea level is denoted by the gray line [*Clark et al.*, 2009].

does not preclude eastward routing as the forcing of the Younger Dryas. Freshwater may have just drained east through the less incised yet still substantial outlets identified by *Teller et al.* [2005] [*Carlson and Clark*, 2008]. Based on these climate model simulations, the routing of freshwater to the St. Lawrence remains the only known forcing mechanism that can explain the timing, magnitude and duration of the Younger Dryas cold event.

10. HOLOCENE ICE SHEET RETREAT AND SEA LEVEL RISE

[198] At the start of the Holocene 11.7 ka [*Rasmussen et al.*, 2006], most of the remaining ~60 m of global sea level rise [*Fairbanks*, 1989; *Bard et al.*, 1990] (Figure 30b) came from retreat of the LIS, SIS, and AIS, with model estimates suggesting that the LIS contributed 25–35 m [*Carlson et al.*, 2008; *Licciardi et al.*, 1998; *Peltier*, 2004; *Tarasov and Peltier*, 2004] and the SIS contributed 3–5 m [*Boulton et al.*, 2001; *Siegert and Dowdeswell*, 2004] of sea level rise. Sea level rise was not constant, with a possible meltwater pulse (MWP-1B) at ~11.3 ka [*Fairbanks*, 1989; *Bard et al.*, 1990] and two possible periods of increased sea level rise at ~9.0–8.5 ka [*Cronin et al.*, 2007] and ~7.6 ka [*Bird et al.*, 2007; *Blanchon and Shaw*, 1995; *Cronin et al.*, 2007; *Horton et al.*, 2005; *Yu et al.*, 2007], indicating intervals of rapid ice sheet retreat. The final abrupt climate event recorded by Greenland $\delta^{18}O$ occurred at ~8.2 ka (the 8.2 ka event) [*Alley et al.*, 1997], likely from a reduction in AMOC strength [*Ellison et al.*, 2006; *Kleiven et al.*, 2008]. In this section, we review the sources of these increases in the rate of sea level rise, the locations of meltwater discharge, and their effect on climate.

10.1. Sources of Holocene Sea Level Rise

10.1.1. MWP-1B and Its Sources

[199] *Fairbanks* [1989] defined MWP-1B in the Barbados coral record as an abrupt ~13 m rise in sea level in <500 years (>2 cm yr^{-1} of sea level rise) at ~11.3 ka [*Bard et al.*, 1990]. This sea level rise occurred at a break between two cores, the top of one core dated at ~11.4 ka (core 12) and the bottom of the second at ~11.1 ka (core 7) (Figures 5b and 30b). The first Tahiti coral records suggest that there may have been an acceleration of sea level rise at ~11.3 ka, though this was not statistically different from a constant rate sea level rise spanning 11.5 to 10.2 ka [*Bard et al.*, 1996]. Three new Tahiti coral records show acceleration in relative sea level rise after the Younger Dryas but not an abrupt jump in sea level (Figure 30b) [*Bard et al.*, 2010]. *Bard et al.* [2010] suggested that part of the discrepancy between the Tahiti and Barbados coral records could arise from MWP-1B being at a break in the Barbados cores. The two Barbados cores that constrain MWP-1B lie on different sides of a tectonic structure extending seaward of Barbados (Figure 5) and thus may be subject to different uplift rates (see discussion in section 2.1), which *Bard et al.* [2010] proposed would explain the larger increase in RSL at Barbados relative to Tahiti. Sea level rise thus likely accelerated in the early Holocene but did not constitute a large MWP like MWP-1A.

[200] *Peltier* [1994, 2004] assumed a predominant AIS source for MWP-1B (Figure 24a), although the justification for this assumption is not provided. The existing chronology for the AIS is limited to only a few locations (see section 6 for further discussion), however, precluding confirmation of the *Peltier* [1994, 2004] assumption. Cosmogenic dating records for the EAIS may indicate increased thinning during the early Holocene with attendant sea level rise contributions [*Mackintosh et al.*, 2007] (Figure 22), although the actual amount of thinning is small (50 to 200 m) and likely too gradual and too late, thus not constituting the rapid and large sea level rise required for MWP-1B in the *Peltier* [1994, 2004] model. In contrast, cosmogenic dating records for the WAIS suggest ice sheet retreat and thinning accelerating only after ~7 ka and continuing until present [*Stone et al.*, 2003], arguing against a large MWP-1B contribution. We note, however, that these land-based chronologies of the AIS are localized to the available nunataks, which may not reflect the behavior of the entire ice sheet nor constrain the ice sheet chronology prior to the exposure of the nunataks.

[201] *Conway et al.* [1999] also suggested an acceleration of ice retreat in the Ross Sea after ~7 ka, but this assumed that the Ross Sea radiocarbon dates constrain grounding line retreat. As we discussed previously (section 6.2.2), however, these ages may just as likely date retreat of the ice shelf edge with retreat of the grounding line occurring significantly

earlier, perhaps during MWP-1A. Other attempts have been made to constrain the behavior of the marine portion of the AIS [*Licht et al.*, 1996; *Domack et al.*, 1999; *Mackintosh et al.*, 2011], but the resulting chronologies are limited by several factors (section 6.1.1). For example, the most reliable radiocarbon ages can only be assigned to the onset of marine sedimentation, providing only a minimum age for the retreat of the grounding line. Furthermore, the highly variable corrections for the radiocarbon age of the AIO carbon fraction that is commonly used for dating lead to highly uncertain chronologies [*Anderson et al.*, 2002]. Given these uncertainties, we conclude that there are insufficient data to constrain the contribution of the AIS to MWP-1B.

[202] The existing SIS chronology for the Holocene is based largely on the varve records from Sweden and Finland from the Baltic Sea/Ice Lake [*Cato*, 1985; *Fromm*, 1985], several minimum-limiting radiocarbon dates on bulk organic matter and macrofossils from northern Sweden [*Andersen*, 1981; *Karlen*, 1979], and cosmogenic radionuclide dates from northern Sweden [*Stroeven et al.*, 2011]. The oldest macrofossil radiocarbon date on wood from northern Sweden places deglaciation of this region ice-free before 9.5 ± 0.2 ka (8.48 ± 0.16 ^{14}C ka BP, ST-4507) [*Karlen*, 1979]. Using this date and the well-documented extent of the SIS at the end of the Younger Dryas [*Andersen et al.*, 1995; *Boulton et al.*, 2001], the SIS contributed 3–5 m of sea level rise over 1.5–2.0 kyr (Figure 30a) at a rate of 0.2–0.3 cm yr^{-1}, thus constituting only a small fraction of the sea level rise following the Younger Dryas. These data are of insufficient resolution to constrain changes in the rate of SIS retreat or determine if retreat accelerated during MWP-1B, but any such contribution to MWP-1B must have been small.

[203] We suggest that the majority of the increase in the rate of sea level rise following the Younger Dryas was sourced from the LIS, with a minor component from the SIS, though not at rates that would constitute a MWP. Following a readvance of the southern LIS margin during the Younger Dryas [*Lasalle and Elson*, 1975; *Lasalle and Shilts*, 1993; *Lowell et al.*, 1999], the LIS began to retreat [*Dyke*, 2004], contributing to a sea level rise of 0.4–0.9 cm yr^{-1} from 11.5 to 10.0 ka [*Peltier*, 2004; *Tarasov and Peltier*, 2006; *Carlson et al.*, 2008]. Combining the LIS contribution with the SIS contribution of ~0.2 cm yr^{-1} explains much of the sea level rise of the early Holocene of ~0.7 cm yr^{-1} (Figure 30). The range in LIS volume estimates and retreat rates allows for an AIS contribution to the initial increase in sea level rise following the Younger Dryas of 0–2 m, thus largely ruling out the hypothesized AIS source for MWP-1B (Figure 30a).

10.1.2. Increases in the Rate of Holocene Sea Level Rise

[204] Following MWP-1B, coral records suggest that Holocene sea level rise averaged ~1 cm yr^{-1} for the remainder of the main phase of deglaciation (until ~6 ka) (Figure 30b) [*Fairbanks*, 1989; *Edwards et al.*, 1993; *Bard et al.*, 1996; *Fleming et al.*, 1998]. Higher-resolution RSL records suggest two periods of increased rates of sea level rise (herein referred to as "sea level events") between ~9.0 and 8.5 ka [*Cronin et al.*, 2007; *Hori and Saito*, 2007] and ~7.6 ka [*Bird et al.*, 2007; *Cronin et al.*, 2007; *Yu et al.*, 2007], with the latter rise possibly recorded by some coral communities [*Blanchon and Shaw*, 1995]. As the SIS had deglaciated by ~9.0 ka [*Karlen*, 1979; *Andersen*, 1981; *Boulton et al.*, 2001], the only two possible sources for these sea level events are the LIS and AIS.

[205] *Cronin et al.* [2007] documented the ~9.0 ka sea level event in the Chesapeake Bay with a rate of >1.2 cm yr^{-1} of RSL rise and suggested a LIS source, concurrent with infilling of incised valleys in Southeast Asia at 9.0–8.5 ka [*Hori and Saito*, 2007]. The precise increase in the rate of GMSL rise above the ~1 cm yr^{-1} early Holocene average may be difficult to determine from the Chesapeake Bay record; gravitational adjustment from LIS melting would reduce RSL rise relative to GMSL rise by >80% while ongoing rebound would cause gradual RSL rise [*Kendall et al.*, 2008], but the latter would not cause an abrupt increase in RSL rise. Thus, the increase in the rate or RSL is likely a shorter-lived event imprinted on ongoing GIA. The LIS margin chronology [*Dyke*, 2004] indicates rapid retreat along the southwestern and northwestern margins at ~9.0 ka (gray bars in Figure 31) [*Carlson et al.*, 2008, 2009c], leading up to the collapse of ice over Hudson Bay at ~8.5 ka [*Barber et al.*, 1999]. Based on the change in LIS area, *Carlson et al.* [2008] estimated a LIS sea level rise contribution of ~1.3 cm yr^{-1} at 9–8.5 ka, explaining much of the 9 ka sea level event and in agreement with the ice sheet model results of *Licciardi et al.* [1998] and *Gregoire et al.* [2012]. Alternatively, another ice sheet model [*Tarasov and Peltier*, 2006] and an Earth model [*Peltier*, 2004] predict slower and earlier maximum LIS sea level contributions at ~11.5–10 ka of up to ~0.9 cm yr^{-1} and ~11.0–10.0 at ~0.8 cm yr^{-1}, respectively. These two model results do not agree, however, with Labrador Sea records that indicate decreased δ^{18}O and $\delta^{18}O_{sw}$ beginning at 10–9.5 ka with minima at ~9 ka (Figures 31b–31d) [*Andrews et al.*, 1999a; *Hillaire-Marcel and Bilodeau*, 2000; *Hillaire-Marcel et al.*, 2007; *Keigwin et al.*, 2005]. The timing of the δ^{18}O decrease supports a later peak in LIS retreat and a significant LIS contribution to the 9 ka sea level rise event [*Carlson et al.*, 2008].

[206] The ~7.6 ka sea level event has been documented in near- [*Cronin et al.*, 2007; *Yu et al.*, 2007], intermediate- [*Blanchon and Shaw*, 1995], and far-field [*Bird et al.*, 2007] RSL records, indicating an increase in the rate of sea level rise to ~1.0 cm yr^{-1} following a period of slower sea level rise at ~8.4–7.8 ka. Other intermediate- and far-field records suggest rather sustained high rates of sea level rise at 0.8–1.0 cm yr^{-1} up to 7.5–7 ka with no inflection points [*Horton et al.*, 2005; *Törnqvist et al.*, 2004b, 2006]. This event was originally attributed to the AIS, assuming a largely deglaciated LIS [*Blanchon and Shaw*, 1995; *Horton et al.*, 2005; *Cronin et al.*, 2007]. However, ^{10}Be surface exposure ages indicate that a large Labrador Dome of the LIS still remained after the opening of Hudson Bay and could explain much of the sea level rise for this event up to ~7.6 ka when this dome deglaciated [*Carlson et al.*, 2007a]. Minimum-limiting radiocarbon dates for the Keewatin Dome show deglaciation prior to ~7.2 ka, implying persistent ice up to ~7.6 ka [*Dyke*,

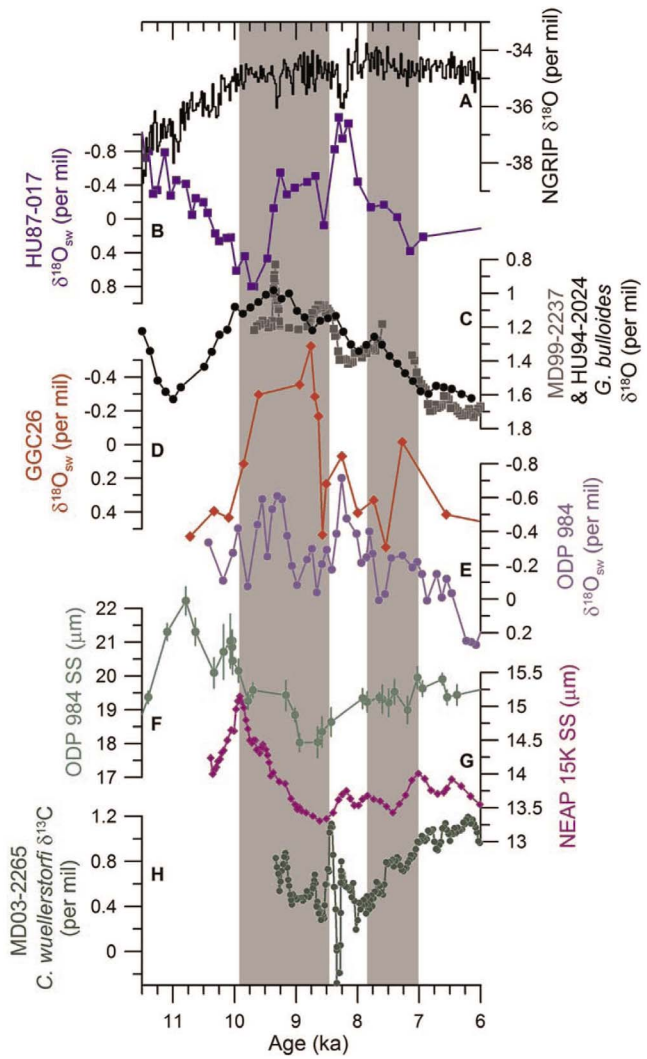

Figure 31. North Atlantic $\delta^{18}O$ and AMOC proxies. (a) NGRIP [*Svensson et al.*, 2008]. (b) Cartwright Saddle $\delta^{18}O_{sw}$ [*Hoffman et al.*, 2012]. (c) Ice volume corrected Orphan Knoll $\delta^{18}O$ [*Hillaire-Marcel and Bilodeau*, 2000; *Hillaire-Marcel et al.*, 2007]. (d) Laurentian Fan $\delta^{18}O_{sw}$ [*Keigwin et al.*, 2005]. (e) Northeast Atlantic $\delta^{18}O_{sw}$ [*Came et al.*, 2007]. (f) Northeast Atlantic sortable silt monitoring Iceland-Scotland overflow strength at 1650 m water depth [*Praetorius et al.*, 2008]. (g) Northeast Atlantic sortable silt monitoring Iceland-Scotland overflow strength at 2850 m water depth [*Bianchi and McCave*, 1999]. (h) Eirik Drift benthic $\delta^{13}C$ record of NADW volume at 3440 m water depth [*Kleiven et al.*, 2008]. Gray bars denote periods of inferred rapid LIS retreat [*Carlson et al.*, 2007a, 2008].

2004]. Given the extent of ice after the opening of Hudson Bay, the LIS likely contributed ~0.7 cm yr^{-1} [*Carlson et al.*, 2007a] to this interval of rapid sea level rise, suggesting an AIS contribution of <0.3 cm yr^{-1} (Figure 30a).

10.1.3. Summary

[207] New coral records rule out a large MWP-1B and rather indicate an increase in the rate of RSL at the end of the Younger Dryas. Contrary to previous assertions [e.g., *Peltier*, 1994, 2004], the geologic record indicates that much of the MWP-1B sea level rise was sourced from the LIS and SIS rather than the AIS. Subsequent increases in the rate of sea level rise at ~9 ka and potentially at ~7.6 ka were mainly sourced from the LIS. The AIS may also have contributed to the 7.6 ka sea level event.

10.2. The 8.2 ka Event

[208] The last abrupt climate event recorded in the Greenland ice cores is the 8.2 ka event (Figure 31a). *Alley et al.* [1997] first identified the ~160 year long cold event in the GISP2 ice core and attributed it to a slowing of the AMOC that was subsequently supported by proxy records [*Bianchi and McCave*, 1999; *Ellison et al.*, 2006; *Kleiven et al.*, 2008; *Oppo et al.*, 2003; *Praetorius et al.*, 2008]. *Klitgaard-Kristensen et al.* [1998] hypothesized that the drainage of Lake Agassiz into the Labrador Sea from collapse of ice over Hudson Bay caused the AMOC reduction. *Barber et al.* [1999] showed that indeed Lake Agassiz drainage corresponded with the 8.2 ka event after correcting for additional reservoir effects on carbonate shell dates from the Hudson and James Bay regions. The drainage of Lake Agassiz deposited a red detrital carbonate layer in Hudson Strait [*Kerwin*, 1996] that can be traced into the northwest Labrador Sea [*Andrews et al.*, 1999a; *Hillaire-Marcel et al.*, 2007].

[209] Concurrent with the drainage of Lake Agassiz, *Törnqvist et al.* [2004a] documented a 0.99–1.39 m jump in RSL in Louisiana between ~8.3 and 8.1 ka, which *Li et al.* [2012] recently revised to a RSL jump of 0.1 to 0.56 m between ~8.3 and 8.2 ka. In the Netherlands, RSL jumped by 1.22–3.00 m between ~8.5 and 8.2 ka [*Hijma and Cohen*, 2010]. After accounting for gravimetric effects for meltwater released from the LIS [*Kendall et al.*, 2008], the amount of GMSL rise increases to 0.8–2.2 m for Louisiana [*Li et al.*, 2012] and 1.6–3.9 m for the Netherlands [*Hijma and Cohen*, 2010], or 0.09–0.25 Sv for 0.1 kyr and 0.06–0.15 Sv for 0.3 kyr, respectively [*Törnqvist and Hijma*, 2012]. These increases in sea level likely reflect both the drainage of Lake Agassiz and the discharge of ice as the LIS deglaciated Hudson Bay [*Törnqvist and Hijma*, 2012; *Gregoire et al.*, 2012; *Hoffman et al.*, 2012]. The potentially larger rise in RSL in the Netherlands may reflect the longer interval of rapid sea level rise and record the end of the 9 ka increase in sea level rise.

[210] Several issues, however, still surround the 8.2 ka event forcing. First, could a short-lived flood cause the century- to centuries-long climate anomalies that surround the event, or are additional climate forcings required, such as reduced solar radiation [*Alley and Ágústsdóttir*, 2005; *Bond et al.*, 2001; *Rohling and Pälike*, 2005] or a longer-lived freshwater forcing [*Carlson et al.*, 2009b; *Clark et al.*, 2001]? Second, a freshwater signal has yet to be found in the Labrador Sea during the event [*Keigwin et al.*, 2005; *Hillaire-Marcel et al.*, 2007], questioning the Lake Agassiz freshwater discharge path and if it would reach regions of convection and slow AMOC [*Condron and Winsor*, 2011; *Wunsch*, 2010].

10.2.1. Lake Agassiz Flood and AMOC

[211] Estimates of the total Lake Agassiz flood volume range from 1.6 to 15.0 × 10^{14} m^3 [*Barber et al.*, 1999; *Leverington et al.*, 2002; *Li et al.*, 2012; *Törnqvist et al.*,

2004a], which may also include contributions from the breakup of the LIS over Hudson Bay. Using a glaciohydrologic model, *Clarke et al.* [2004] estimated that Lake Agassiz drained in ~0.5 years with an ~5.0 Sv flood. Fully coupled GCMs have failed, however, to produce the length of the climate anomaly when forced only with the flood. When forced with the 0.5 Sv flood discharge, one fully coupled GCM produced the magnitude of the 8.2 ka event as recorded by proxy records but not the centennial length of the event [*LeGrande et al.*, 2006; *LeGrande and Schmidt*, 2008]. Another GCM failed to show an AMOC response to the flood forcing, requiring an additional freshwater forcing [*Clarke et al.*, 2009]. The *UVic* EMIC also showed a similar response, where a 2.5 Sv flood for 1 year failed to produce a long-lived reduction in AMOC strength [*Meissner and Clark*, 2006].

[212] *Clark et al.* [2001] suggested that the routing of western Canadian Plains freshwater that accompanied the opening of Hudson Bay might provide an additional, longer-lived freshwater forcing. Recent U/Ca geochemical runoff records from Hudson Strait confirm the routing of western Canadian Plains freshwater through Hudson Strait with a discharge of 0.13 ± 0.03 Sv for several hundred years [*Carlson et al.*, 2009b]. When forced with this smaller but longer-lived routing discharge, both an EMIC and an *AOGCM* produced a longer reduction in AMOC strength [*Meissner and Clark*, 2006; *Clarke et al.*, 2009], in agreement with proxy evidence [*Bianchi and McCave*, 1999; *Oppo et al.*, 2003; *Ellison et al.*, 2006; *Kleiven et al.*, 2008; *Praetorius et al.*, 2008], and a longer climate anomaly [*Alley and Ágústsdóttir*, 2005; *Rohling and Pälike*, 2005]. It thus appears that the century-long routing of Lake Agassiz runoff may have played a larger role in forcing the 8.2 ka event than the short-lived flood [*Clark et al.*, 2001; *Clarke et al.*, 2009; *Carlson et al.*, 2009b].

10.2.2. Path of Lake Agassiz Runoff

[213] Despite evidence for a reduction in $\delta^{18}O_{sw}$ in the northeast Atlantic during the 8.2 ka event [*Came et al.*, 2007; *Ellison et al.*, 2006; *Thornalley et al.*, 2010], the pathway of freshwater discharge from Hudson Strait to regions of deep water formation in the Nordic and Labrador Seas has been questioned based on the lack of a freshwater signal in the Labrador Sea [*Keigwin et al.*, 2005; *Hillaire-Marcel et al.*, 2007] and results of one high-resolution eddy-resolving ocean-only model [*Condron and Winsor*, 2011]. The *MITgcm* simulated that a 1 year, 5 Sv flood released from Hudson Strait would hug the Labrador coastline and ultimately end up in the subtropical gyre, where it would have little to no impact on AMOC [*Condron and Winsor*, 2011]. *Condron and Winsor* [2011] did not test the impact of the longer-lived associated routing event on AMOC [*Carlson et al.*, 2009b], which EMICs and fully coupled GCMs have shown to be capable of forcing an 8.2 ka–like event, rather than the flood [*Meissner and Clark*, 2006; *Clarke et al.*, 2009]. *Condron and Winsor* [2011] also only ran the MITgcm for 10 years, which may be too short a period of time for freshwater to reach deep water convection regions. Moreover, another high-resolution eddy-resolving ocean model that included a simplified atmosphere showed that freshwater discharge through Hudson Strait would be transported to North Atlantic convection sites and slow AMOC [*Spence et al.*, 2008]. This latter study also demonstrated that the AMOC response was insensitive to model resolution.

[214] A recent $\delta^{18}O_{sw}$ record adjacent to the Labrador Coast provides conclusive evidence for freshwater discharge to the Labrador Sea during the 8.2 ka event [*Hoffman et al.*, 2012]. Western Labrador Sea $\delta^{18}O_{sw}$ decreases by 0.7–1.3‰ (Figure 31b), coincident with the deposition of detrital carbonate and red sediment indicative of the discharge of Lake Agassiz runoff into the Labrador Sea [*Barber et al.*, 1999; *Kerwin*, 1996]. This $\delta^{18}O_{sw}$ decrease had been masked in the planktonic $\delta^{18}O$ record by 3–4°C of contemporaneous cooling. The Lake Agassiz runoff $\delta^{18}O_{sw}$ signal can be traced eastward as it decreases in magnitude to ~0.4‰ in the northeast Atlantic near regions of deep water convection [*Came et al.*, 2007; *Thornalley et al.*, 2009]. Water isotope enabled AOGCM simulations document this path and thus confirm the drainage of Lake Agassiz and attendant routing of runoff as the forcing of the 8.2 ka event [*LeGrande and Schmidt*, 2008; *Hoffman et al.*, 2012].

10.2.3. Early Holocene Runoff Routing

[215] Prior to the 8.2 ka event and the opening of Hudson Bay, Lake Agassiz runoff and much of the LIS meltwater were routed through the St. Lawrence River to the North Atlantic [*Carlson et al.*, 2009b; *Licciardi et al.*, 1999], and rerouting of this runoff to Hudson Strait would therefore seem to not have much of an impact on AMOC [*Clarke et al.*, 2009]. *Clarke et al.* [2009] suggested that Lake Agassiz runoff might have entered the North Atlantic as a hyperpycnal flow through the St. Lawrence prior to the opening of Hudson Bay. However, this runoff is recorded as decreased planktonic $\delta^{18}O_{sw}$ near the Gulf of St. Lawrence that subsequently increases by ~1.0‰ (Figure 31d) when runoff is routed to Hudson Strait at the start of the 8.2 ka event (Figure 31b) [*Keigwin et al.*, 2005; *Carlson et al.*, 2009b; *Hoffman et al.*, 2012]. Because planktonic foraminifera record the pre–8.2 ka event discharge through the St. Lawrence, Lake Agassiz runoff likely did not enter the ocean as a hyperpycnal flow, which is further supported by sedimentary records that show no change in sedimentology when Lake Agassiz runoff is routed away from the Gulf of St. Lawrence [*Keigwin and Jones*, 1995].

[216] We suggest one possible solution to this apparent conundrum whereby the AMOC response to the routing event depends on the location of deep water formation relative to the discharge location of Lake Agassiz runoff. At the end of the Younger Dryas, AMOC abruptly increased [*McManus et al.*, 2004; *Praetorius et al.*, 2008]. *Sortable silt* records from the northeast Atlantic suggest peak Iceland-Scotland Overflow (*North Atlantic Deep Water (NADW)* component formed in the Nordic Seas) strength at ~10.8 ka with a subsequent decline to a minimum at ~8.5 ka (Figures 31f and 13g) [*Bianchi and McCave*, 1999; *Praetorius et al.*, 2008]. North Atlantic benthic $\delta^{13}C$ from 3440 m water depth also shows a reduction in NADW volume after ~9.5 ka (Figure 31h) [*Kleiven et al.*, 2008]. We attribute this decrease in NADW to

freshwater input from increased LIS retreat [*Carlson et al.*, 2008], the majority of which would have been routed through the St. Lawrence Estuary (Figure 31d) [*Licciardi et al.*, 1999; *Keigwin et al.*, 2005; *Carlson et al.*, 2009c] and advected in the North Atlantic Current to the Northeast Atlantic where planktonic foraminifera record a decrease in $\delta^{18}O_{sw}$ at ~9 ka (Figure 31e) [*Came et al.*, 2007; *Thornalley et al.*, 2009]. With transport in the North Atlantic Current, it is possible that LIS runoff may have had less of an effect on convection in the Labrador Sea.

[217] We suggest that the subsequent breakup of ice over Hudson Bay and the associated routing of Lake Agassiz runoff to the Labrador Sea reduced deep water formation in the Labrador Sea [*Clark et al.*, 2001; *Carlson et al.*, 2009b; *Hoffman et al.*, 2012] and caused the century-long 8.2 ka event observed in the Greenland ice cores. Indeed, an AOGCM simulation for 9 ka found that Greenland Summit precipitation had an increased Labrador Sea source at the expense of the present Asian source [*LeGrande and Schmidt*, 2009], making Greenland ice core $\delta^{18}O$ records more sensitive to changes in the Labrador Sea and also providing an explanation for why Greenland $\delta^{18}O$ increases between 10 and 8.5 ka when NADW strength is decreasing (Figure 31). The routed freshwater would still be capable of advection to the northeast Atlantic and sustaining a reduction in NADW [*LeGrande et al.*, 2006; *LeGrande and Schmidt*, 2008; *Hoffman et al.*, 2012] as observed in proxy records [*Bianchi and McCave*, 1999; *Kleiven et al.*, 2008; *Praetorius et al.*, 2008]. NADW strength and volume only starts to recover at ~8 ka when present North American freshwater routing is established [*Clark et al.*, 2001; *Carlson et al.*, 2009b; *Hoffman et al.*, 2012] but do not reach mid-Holocene levels until ~7 ka, when the LIS was finally deglaciated (Figures 31f–31h) [*Carlson et al.*, 2007a]. Although it has been argued that Labrador Sea convection did not begin until well after the 8.2 ka event [*Hillaire-Marcel et al.*, 2001], this hypothesis relied largely on SSS reconstructions by dinoflagellate cysts which, as discussed previously (see section 9.4.2), are not able to independently reconstruct SSS and are insensitive to changes in SSS above 12 psu [*Dale*, 1996; *Telford*, 2006]. Therefore, we suggest that until independent Labrador Sea deep water formation records become available, the timing of changes in Labrador Sea convection remains uncertain.

10.2.4. Summary

[218] In summary, the 8.2 ka event is more complex than the simple Lake Agassiz flood hypothesis would suggest and likely resulted from a combination of factors. Rapid retreat of the LIS up to the drainage of Lake Agassiz slowed the formation of NADW in the Nordic Seas prior to the 8.2 ka event. The subsequent flood and routing of much of the LIS meltwater through Hudson Strait may have further reduced NADW formation as well as Labrador Sea convection, causing the century-long cold event.

11. CONCLUSIONS

[219] We return to the primary question presented in the introduction regarding the relationship between MWPs, ice sheet retreat, runoff routing, and climate change in light of the geological evidence presented here. We frame our conclusions in the context of unresolved questions and potential future research directions.

[220] The Northern Hemisphere ice sheet contribution to the initial sea level rise at ~19–19.5 ka from its LGM lowstand was likely responsible for the start of a prolonged reduction of the AMOC [*Clark et al.*, 2004, 2012; *Liu et al.*, 2009; *Shakun et al.*, 2012; *Stanford et al.*, 2011a]. While the onset of Northern Hemisphere ice retreat that caused the initial sea level rise from the LGM lowstand was likely due to increasing high northern latitude summer insolation [*Clark et al.*, 2009], the cause of nearly coeval retreat of sectors of the AIS remains to be fully explained [*Weber et al.*, 2011]. Subsequent eastward routing of LIS meltwater followed by H1 iceberg discharge sustained a reduction in the AMOC, with the combined freshwater forcing and its impact on the AMOC causing the Oldest Dryas cold event [*Clark et al.*, 2012]. Sea level rise of 8–20 m from ~19 to 14.5 ka can be attributed to continued retreat of the LIS and EIS, with an additional freshwater forcing of an uncertain but likely small amount contributed by H1. Existing model estimates of the contributions of Northern Hemisphere ice sheets to sea level during this interval bracket the upper end of the estimates from the RSL records (maximum is 20.8 m), suggesting that the AIS may have gained mass to balance the sea level budget. In general, the volume contributions of individual ice sheets to sea level change between 19.5 ka and 14.6 ka, which are required to specify freshwater fluxes and their entry points to the ocean, need to be better determined.

[221] The geologic record of global ice sheets indicates that MWP-1A had sources in both hemispheres, but our understanding of what caused this event remains poorly understood. Much of the LIS chronology during MWP-1A is well constrained, and models have successfully reproduced the climate changes from the Oldest Dryas into the Bølling. An informative new approach to this issue would be to force a dynamic/energy balance ice sheet model with the full climate forcing of the Bølling warming and require it to match the known position of the LIS (and other ice sheets) to more tightly constrain the Northern Hemisphere contribution to this MWP. This would allow a more comprehensive conversion of the geologic record of ice sheet extent and discharge into a sea level rise estimate. Previous attempts at this have not matched the actual extent of the LIS, used oversimplified climate forcings, or included assumed dynamic processes that are not supported by the geologic record.

[222] Current estimates of the AIS contribution to MWP-1A largely depend on the difference between the Northern Hemisphere contribution and the actual amount of ice-equivalent sea level rise that occurred during this MWP. Most estimates of Northern Hemisphere ice sheet contributions explain less than half of the total ice-equivalent sea level rise (~14 m) during MWP-1A, requiring the remainder to be sourced from Antarctic ice. Such a large Antarctic contribution is consistent with GIA model studies that examine the sea level response to ice mass changes at far-

field RSL sites [*Clark et al.*, 2002; *Bassett et al.*, 2005; *Deschamps et al.*, 2012], but the uncertainties in these RSL records need to be reduced before these approaches can yield conclusive results [*Deschamps et al.*, 2012]. A comprehensive effort is also needed to directly date changes in the extent of the AIS not only during the timing of MWP-1A but also through the last deglaciation. Such an approach should carefully assess the various assumptions now used to constrain ice limits, including that weathering limits define ice sheet limits; that local valley lake level records constrain grounding line locations; and that in the absence of other field evidence, minimum-limiting marine dates are closely related to ice margin locations.

[223] A smaller Northern Hemisphere contribution to MWP-1A than inferred in previous studies may explain why the AMOC remained relatively strong and North Atlantic climate warmed during MWP-1A at the onset of the Bølling. Some studies suggest that a large freshwater forcing in the Southern Ocean at this time may in fact have helped trigger the Bølling [*Weaver et al.*, 2003], but not all models simulate this response [*Stouffer et al.*, 2007], and additional modeling is required to evaluate the impacts of freshwater forcing of both oceans during MWP-1A.

[224] More rapid LIS retreat with increasing eastward meltwater discharge after MWP-1A during the Allerød may have gradually slowed the AMOC leading up to the Younger Dryas cold event. At this point, all existing data suggest that the most likely means of causing the Younger Dryas is through the routing of LIS runoff through Lake Agassiz eastward into the St. Lawrence River. Other hypotheses or arguments against eastward routing have been based on ice sheet models with poorly constrained climate forcings or misinterpretations of geologic data or are inconsistent with sea level constraints on meltwater discharge. Using cosmogenic nuclide ages to directly date when the ice margin retreated from the multiple eastern outlets south of the LIS would confirm hypotheses based on minimum-limiting radiocarbon dates and more distal runoff records. Similarly, directly dating when the northern LIS outlet opened is key to understanding late deglacial runoff routing and AMOC/climate evolution. In particular, the direction that LIS runoff was routed at the end of the Younger Dryas is poorly constrained. Its identification would provide a critical constraint for understanding the response of the AMOC and climate system to changes in the North Atlantic hydrologic cycle.

[225] After the Younger Dryas, the geologic record indicates that early Holocene increases in the rate of sea level rise appear to be predominately sourced from Northern Hemisphere ice sheets. However, the retreat of the AIS is poorly constrained to unconstrained through this interval, and documenting its retreat history will be important for better understanding the global sea level budget as well as for placing current mass changes in the AIS in a longer-term context. Meltwater from retreat of Northern Hemisphere ice sheets may have slowed the AMOC, preconditioning the North Atlantic so that when deglaciation of Hudson Bay occurred, the associated final LIS routing event triggered the 8.2 ka event. Nevertheless, a significant remaining question is why this large volume of freshwater that clearly discharged to the North Atlantic had a smaller impact on the AMOC than earlier freshwater discharge events. Future research should focus on better constraining the location, timing, and volume of freshwater discharge from the remaining Northern Hemisphere ice sheets during the early to middle Holocene, which will improve our understanding of the Earth system response to cryospheric change under a climate state somewhat analogous to the coming century. In particular, the Holocene retreat chronology of the northwest sector of the LIS is at present based only on minimum-limiting radiocarbon dates. Dating when and at what rate this portion of the LIS retreated would not only evaluate a potential source of Holocene sea level rise but also aid in determining the impact that freshwater discharge to Arctic Ocean has on the AMOC and climate.

GLOSSARY

^{10}Be: A cosmogenic radionuclide isotope of beryllium. The accumulation of ^{10}Be in quartz can be used to date how long a rock surface has been exposed to bombardment by cosmic radiation, thus determining the time since ice sheet retreat exposed the boulder or bedrock surface. Potential issues may arise if ^{10}Be from previous exposure still remains in the rock, which would make the apparent age older than the true timing of ice margin retreat.

^{14}C: A cosmogenic radionuclide isotope of carbon. It is produced in the atmosphere from the replacement of a proton for a neutron in ^{14}N. The decay of ^{14}C in organic material dates the time since the organic material died and ceased to exchange carbon with the atmosphere or ceased to secrete a carbonate shell from ocean water. Because of changes in ^{14}C production and carbon reservoirs, it necessary to calibrate a ^{14}C age to a calendar age.

8.2 ka event: The last abrupt climate event of the last deglaciation. It was first defined in the Summit Greenland GISP2 ice core δ^{18}O record and was likely caused by a reduction in Atlantic meridional overturning circulation strength.

^{87}Sr/^{86}Sr: The ratio of the radiogenic ^{87}Sr isotope relative to stable ^{86}Sr. In rocks it varies mainly as a function of age, with higher ratios reflecting older rocks. It can be used to track the source of runoff because stream ^{87}Sr/^{86}Sr ratios reflect that of the underlying bedrock.

A events: Short for Antarctic events. These represent the pattern of temperature change observed in Antarctic ice cores during glacial periods, with gradual warming and cooling occurring on multimillennia-long cycles. Peak warmth in an A event corresponds with the abrupt warming observed in Greenland ice core records.

Accelerator mass spectrometer (AMS): A technique of mass spectrometry where ions are first accelerated before separation, which allows the analysis of rare isotopes like ^{14}C and ^{10}Be.

Acid insoluble organic (AIO) carbon: The total organic matter of sediments in which the sample is pretreated with acid to remove the carbonate fraction.

Allerød: A relatively warm period of the last deglaciation in the Northern Hemisphere, originally defined by

European pollen records. It lasted from ~13.9 to 12.9 ka and occurred between the Older and Younger Dryas cold events.

Antarctic Peninsula Ice Sheet (APIS): A separate mass of ice on the Antarctica peninsula.

AOGCM: Atmosphere-ocean general circulation model.

Atlantic meridional overturning circulation (AMOC): The northward flow of warm salty surface waters in the Atlantic basin. Subsequent cooling in the high latitude Nordic and Labrador Seas results in the sinking of these cold-salty waters and their southward return flow at depth. Perturbation of this process is thought to result in Northern Hemisphere cooling and Southern Hemisphere warming.

Barents-Kara Ice Sheet (BKIS): A portion of the Eurasian Ice Sheet located north of Europe in the Barents and Kara Seas.

Benthic: A descriptor for bottom dwelling organisms in the ocean, here used to denote the habitat of foraminifera.

Bipolar seesaw: The climate pattern caused by reductions in Atlantic meridional overturning circulation, with Northern Hemisphere cooling and Southern Hemisphere warming. Increases in meridional overturning result in an opposite climate pattern.

Bølling: A Northern Hemisphere warm event of the last deglaciation with an abrupt onset. Originally defined by European pollen records and likely caused by an increase in Atlantic meridional overturning circulation, it lasted from ~14.6 to 14.1 ka and occurred between the Oldest and Older Dryas cold events.

British Irish Ice Sheet (BIIS): A small ice sheet over the British Isles that at glacial maximums connected with the larger Eurasian Ice Sheet.

Cordilleran Ice Sheet (CIS): An ice sheet in western Canada and the northwest United States the resulted from the coalescence of valley glaciers over the Canadian Rockies. At glacial maxima, it abutted the larger Laurentide Ice Sheet.

Cosmogenic nuclide date: An age determined by the accumulation of a cosmogenic nuclide in a rock surface. In the case of ice sheets, this accumulation reflects the period since ice retreated, exposing the boulder or bedrock surface, and thus dates the time of ice retreat. Complications include the potential for nuclides persisting through the period of ice cover if the ice sheet is not effective enough to erode and remove the surface that contains these inherited nuclides from previous exposure.

δ^{13}C: A stable isotope of carbon, expressed as the ratio to ^{12}C relative to a standard and multiplied by 1000 (δ notation). δ^{13}C can be used as a tracer of terrestrial runoff to the ocean because stream δ^{13}C reflects ratios in terrestrial biomass, which is significantly depleted relative to the ocean. δ^{13}C also reflects the amount of nutrients in a water mass and thus can be used as a proxy of the volume of deep waters from northern and southern sources, with northern sources having higher δ^{13}C values due to their young age and low nutrient content.

Δ^{14}C: The amount of ^{14}C in a reservoir relative to the ^{14}C it should contain if in equilibrium with the atmosphere. It can be used to date how long a water mass has been isolated from exchange with the atmosphere.

δ^{18}O: A stable isotope of oxygen, expressed as the ratio to ^{16}O relative to a standard and multiplied by 1000 (δ notation). δ^{18}O is fractionated in the atmosphere with respect to temperature and thus can be used as a temperature proxy in ice core records. This can be complicated, however, by changes in the source of moisture to the ice core site. In the ocean, δ^{18}O is used in foraminifera calcite shells as a proxy of temperature because it is fractionated during calcite precipitation. These shells also record the δ^{18}O of the water mass they are precipitating in, which reflects precipitation/runoff/evaporative effects on the water mass. Thus, if the temperature component is independently known, one can calculate the δ^{18}O of seawater, which is a salinity proxy. δ^{18}O is further affected by continental ice volume, which preferentially accumulates ^{16}O as ice grows.

Database on Eurasian Deglaciation Dates (DATED) Project: A European project reconstructing the deglacial history of the Eurasian Ice Sheet. Information is available at http://www.gyllencreutz.se/research.html.

Dinoflagellate: A eukaryote that can occur in fresh and saltwater conditions. Their speciation depends on the surrounding environmental conditions, and thus, assemblages of dinoflagellate remains (cysts) can be used to reconstruct paleoceanographic climate, such as sea surface temperature.

Dissolved inorganic carbon (DIC): Component of inorganic carbon that is dissolved in water.

East Antarctic Ice Sheet (EAIS): The much larger, eastern part of the Antarctic Ice Sheet.

EDC: EPICA Dome C.

Eurasian Ice Sheet (EIS): The amalgamated ice sheet that covered northern Eurasia, consisting of the Barents-Kara, Scandinavian, and British Irish Ice Sheets.

Foraminifera: Amoeboid protists that secrete a calcite shell called a test. These shells can record past changes in ocean conditions with δ^{18}O and δ^{13}C isotopes, temperature in the shell Mg/Ca ratios, and other tracers of continental runoff. Their speciation can also be used as a proxy of past environmental changes. Surface dwelling foraminifera are referred to as planktonic, whereas bottom dwellers are referred to as benthic.

Freeboard: The height of the surface of a less dense mass resting in a more dense mass. In isostatic equilibrium, is proportional to the ratio of the density of the less dense to the more dense masses.

General circulation model (GCM): A computer model of atmospheric or oceanic circulation. GCMs can also be coupled together to form an Earth system model or atmosphere-oceanic general circulation model.

Greenland Ice Sheet Project 2 (GISP2): The name of the U.S. ice core recovered from Summit Greenland.

Glacial drift: A term that refers to sediment deposited directly by an ice sheet or glacier.

Glacial isostatic adjustment (GIA): The isostatic response of the solid Earth to a redistribution of surface mass during glaciations. GIA includes both an elastic and viscous component of deformation.

Greenland Ice Core Project (GRIP): The name of the European ice core recovered from Summit Greenland.

Heinrich event: The time when a detrital carbonate layer is deposited in the North Atlantic by icebergs that were sourced from Hudson Bay.

Holocene: The geologic epoch of the last 11,700 years.

Hyperpycnal: A descriptor of water-saturated debris flows that are denser than the surrounding medium (i.e., ocean water) and thus move along the ocean floor.

Ice-rafted debris (IRD): Refers to debris transported into the ocean by icebergs discharged by a marine-terminating ice sheet or glacier.

Inheritance: The incomplete erosion of a surface by ice that was exposed during a previous ice-free period. This results in a greater amount of cosmogenic nuclides in the surface than would have accumulated during the period of its most recent ice-free exposure, resulting in cosmogenic ages that are too old.

IntCal09: The name of the ^{14}C calibration data set used to convert ^{14}C years into calendar years (http://www.radiocarbon.org/IntCal09.htm).

Interstadial: The term used to describe relatively warm intervals on millennial time scales during the glacial periods. They are usually associated with ice margin recession.

Isostasy: The state of gravitational equilibrium between two masses of different densities.

Lake Agassiz: A large proglacial lake that formed along the southwest margin of the Laurentide Ice Sheet.

Last Glacial Maximum (LGM): The interval of maximum global ice volume during the last glacial period. This lasted from ~26 to 19 ka, as indicated by a sea level lowstand.

Laurentide Ice Sheet (LIS): The ice sheet that covered much of Canada and extended down into the northern part of central to eastern United States.

Lowstand: Low in relative or global mean sea level.

Meltwater pulses (MWPs): Abrupt jumps in ice-equivalent of relative sea level of many meters on the timescale of centuries.

Mg/Ca: The ratio of magnesium ions to calcium ions in a foraminifera calcite shell, with units of mmol/mol. This is used as a proxy of temperature but can also detect increased discharge of Mg-rich waters to the ocean in estuarine environments.

MITgcm: An ocean general circulation model developed at the Massachusetts Institute of Technology.

North Greenland Ice Core Project (NGRIP): The name of the European ice core recovered from northwest Greenland.

North Atlantic Deep Water (NADW): Part of the Atlantic meridional overturning circulation. It forms in the Nordic and Labrador Seas due to loss of heat to the atmosphere and subsequent sinking of the cooler/salty water mass and flows southward at depth in the Atlantic Ocean basin.

Nunatak: A mountain peak that rises above an ice sheet surface.

Oldest Dryas: A Northern Hemisphere cold event that followed the end of the Last Glacial Maximum, lasting from ~18.5 to 14.6 ka.

Optically stimulated luminescence (OSL): A dating technique that measures the excitement of electrons in a crystal (usually quartz or feldspar), which determines the time since the sediment was last stimulated by sunlight and thus dates deposition of the sediment.

Ostracode: A class of small crustaceans. Their calcite shells can be used to document water mass temperature and salinity with $\delta^{18}O$, similar to foraminifera shells.

Pa/Th: The ratio between ^{231}Pa and ^{230}Th in marine sediments. In the North Atlantic, Th is scavenged by particles to the ocean floor at a faster rate than Pa. Thus, if Atlantic meridional overturning circulation slows, there is a longer interval for Pa to be scavenged and the Pa/Th ratio in sediments increases, making the Pa/Th a proxy of Atlantic meridional overturning circulation strength.

Planktonic: A descriptor for near surface dwelling organisms in the ocean, here used to denote the habitat of foraminifera.

Practical salinity units (psu): The measure of water mass salinity, with average ocean water being 35 and freshwater 0.

Relative sea level (RSL): The height of the ocean surface at any given location, or sea level, measured with respect to the surface of the solid Earth.

Reservoir age: The amount of decay that has occurred to ^{14}C in a water mass since its last equilibration with the atmosphere, which needs to be accounted for in ^{14}C dating of marine carbonates because it will lead toward apparently older ages. It is denoted by ΔR. Carbon supplied to water from dissolved carbonate bedrock can also add to the reservoir age, requiring corrections for terrestrial carbonate dates that are from samples on carbonate terranes.

Scandinavian Ice Sheet (SIS): The portion of the Eurasian Ice Sheet that resided over northern Europe and the Baltic Sea.

Sortable silt: A proxy for local bottom current speed in the ocean that analyzes the grain size distribution of the silt size fraction. A coarser fraction denotes greater winnowing of the finer fraction and thus faster bottom current speed.

Stadial: The term used to describe relatively cold intervals on millennial time scales during the glacial periods. They are usually associated with ice margin advance.

Sverdrups (Sv): A unit of discharge used to describe ocean circulation magnitude volumes and rates, with units of 10^6 m^3 s^{-1}.

TALDICE core: The name of a European ice core collected from Talos Dome, Antarctica, as part of the Talos Dome Ice Core Project.

TOC: Total organic content.

Trimline: A weathering limit in mountainous regions that can denote former ice surfaces or a change in thermal regime in a glacier/ice sheet from an erosive, wet bed to a nonerosive, frozen bed.

U/Ca: The ratio of uranium ions to calcium ions in a foraminifera calcite shell, with units of μmol/mol. This is used to detect increased discharge of U-rich waters to the ocean in estuarine environments.

U/Th ages: Measures the accumulation of ^{230}Th in a calcium carbonate crystal matrix from the decay of ^{234}U, which allows for dating of the age of the aragonite-forming organism (usually corals) or in a calcite speleothem.

UVic: University of Victoria.

Varve: A sediment layer deposited in one year, which usually contains a distinct layering that reflects changes in the seasonal cycle of the lake or marine setting.

West Antarctic Ice Sheet (WAIS): The smaller, western part of the Antarctic Ice Sheet.

Younger Dryas: A cold event during the last deglaciation first defined by European pollen records. It followed the Allerød warm period, with its end denoting the transition into the Holocene, and lasted from ~12.9 to 11.7 ka.

[226] **ACKNOWLEDGMENTS.** The authors contributed equally to this work. We thank Glenn Milne, Eelco Rohling, Mark Siddall, and Jenny Stanford for their reviews which helped clarify a number of issues and George Denton and Brenda Hall for discussions. George Denton and Aaron Putnam provided the base map used in Figure 1. A.E.C. is supported by the NSF Paleoclimate Program. P.U.C. is supported by the NSF Paleoclimate Program for the Paleovar Project through grant AGS-0602395 and by the NSF Antarctic Glaciology Program.

[227] The Editor on this paper was Eelco Rohling. He thanks Mark Siddall and two anonymous reviewers for their review assistance on this manuscript.

REFERENCES

Ackert, R. P., D. J. Barclay, H. W. Borns, P. E. Calkin, M. D. Kurz, J. L. Fastook, and E. J. Steig (1999), Measurements of past ice sheet elevations in interior West Antarctica, *Science*, *286*(5438), 276–280, doi:10.1126/science.286.5438.276.

Ackert, R. P., S. Mukhopadhyay, B. R. Parizek, and H. W. Borns (2007), Ice elevation near the West Antarctic Ice Sheet divide during the Last Glaciation, *Geophys. Res. Lett.*, *34*, L21506, doi:10.1029/2007GL031412.

Aharon, P. (2003), Meltwater flooding events in the Gulf of Mexico revisited: implications for rapid climate changes during the last deglaciation, *Paleoceanography*, *18*(4), 1079, doi:10.1029/2002PA000840.

Aharon, P. (2006), Entrainment of meltwaters in hyperpycnal flows during deglaciation superfloods in the Gulf of Mexico, *Earth Planet. Sci. Lett.*, *241*(1–2), 260–270, doi:10.1016/j.epsl.2005.10.034.

Alley, R. B. (2000), The Younger Dryas cold interval as viewed from central Greenland, *Quat. Sci. Rev.*, *19*(1–5), 213–226.

Alley, R. B., and A. M. Ágústsdóttir (2005), The 8 k event: Cause and consequences of a major Holocene abrupt climate change, *Quat. Sci. Rev.*, *24*(10–11), 1123–1149, doi:10.1016/j.quascirev.2004.12.004.

Alley, R. B., and P. U. Clark (1999), The deglaciation of the Northern Hemisphere: A global perspective, *Annu. Rev. Earth Planet. Sci.*, *27*, 149–182, doi:10.1146/annurev.earth.27.1.149.

Alley, R. B., and D. R. MacAyeal (1994), Ice-rafted debris associated with binge/purge oscillations of the Laurentide Ice Sheet, *Paleoceanography*, *9*, 503–511, doi:10.1029/94PA01008.

Alley, R. B., P. A. Mayewski, T. Sowers, M. Stuiver, K. C. Taylor, and P. U. Clark (1997), Holocene climate instability: A prominent, widespread event 8200 years ago, *Geology*, *25*, 483–486, doi:10.1130/0091-7613(1997)025<0483:HCIAPW>2.3.CO;2.

Alley, R. B., S. Anandakrishnan, T. K. Dupont, B. R. Parizek, and D. Pollard (2007), Effect of sedimentation on ice-sheet grounding-line stability, *Science*, *315*(5820), 1838–1841, doi:10.1126/science.1138396.

Alvarez-Solas, J., S. Charbit, C. Ritz, D. Paillard, G. Ramstein, and C. Dumas (2010), Links between ocean temperature and iceberg discharge during Heinrich events, *Nat. Geosci.*, *3*(2), 122–126, doi:10.1038/ngeo752.

Andersen, B. G. (1981), Late Weichselian ice sheets in Eurasia and Greenland, in *The Last Great Ice Sheets*, edited by G. H. Denton and T. J. Hughes, pp. 1–65, John Wiley, New York.

Andersen, B., J. Mangerud, R. Sorenson, A. Reite, H. Sveian, M. Thoresen, and B. Bergstrom (1995), Younger Dryas ice-marginal deposits in Norway, *Quat. Int.*, *28*, 147–169, doi:10.1016/1040-6182(95)00037-J.

Anderson, J. B., S. S. Shipp, A. L. Lowe, J. S. Wellner, and A. B. Mosola (2002), The Antarctic Ice Sheet during the Last Glacial Maximum and its subsequent retreat history: A review, *Quat. Sci. Rev.*, *21*(1–3), 49–70, doi:10.1016/S0277-3791(01)00083-X.

Anderson, R. F., S. Ali, L. I. Bradtmiller, S. H. H. Nielsen, M. Q. Fleisher, B. E. Anderson, and L. H. Burckle (2009), Wind-driven upwelling in the Southern Ocean and the deglacial rise in atmospheric CO_2, *Science*, *323*(5920), 1443–1448, doi:10.1126/science.1167441.

Andrews, J. T., and G. Dunhill (2004), Early to mid-Holocene Atlantic water influx and deglacial meltwater events, Beaufort Sea slope, Arctic Ocean, *Quat. Res.*, *61*(1), 14–21, doi:10.1016/j.yqres.2003.08.003.

Andrews, J. T., and K. Tedesco (1992), Detrital carbonate-rich sediments, northwestern Labrador Sea: Implications for ice-sheet dynamics and iceberg rafting (Heinrich) events in the North Atlantic, *Geology*, *20*, 1087–1090, doi:10.1130/0091-7613(1992)020<1087:DCRSNL>2.3.CO;2.

Andrews, J. T., L. Keigwin, F. Hall, and A. E. Jennings (1999a), Abrupt deglaciation events and Holocene palaeoceanography from high-resolution cores, Cartwright Saddle, Labrador Shelf, Canada, *J. Quat. Sci.*, *14*, 383–397, doi:10.1002/(SICI)1099-1417(199908)14:5<383::AID-JQS464>3.0.CO;2-J.

Andrews, J. T., E. W. Domack, W. L. Cunningham, A. Leventer, K. J. Licht, A. J. T. Jull, D. J. DeMaster, and A. E. Jennings (1999b), Problems and possible solutions concerning radiocarbon dating of surface marine sediments, Ross Sea, Antarctica, *Quat. Res.*, *52*(2), 206–216, doi:10.1006/qres.1999.2047.

Balco, G., J. Briner, R. C. Finkel, J. A. Rayburn, J. C. Ridge, and J. M. Schaefer (2009), Regional beryllium-10 production rate calibration for late-glacial northeastern North America, *Quat. Geochronol.*, *4*(2), 93–107, doi:10.1016/j.quageo.2008.09.001.

Barbante, C., et al. (2006), One-to-one coupling of glacial climate variability in Greenland and Antarctica, *Nature*, *444*(7116), 195–198, doi:10.1038/nature05301.

Barber, D. C., et al. (1999), Forcing of the cold event of 8,200 years ago by catastrophic drainage of Laurentide lakes, *Nature*, *400*, 344–348, doi:10.1038/22504.

Bard, E., M. Arnold, P. Maurice, J. Duprat, J. Moyes, and J. C. Duplessey (1987), Retreat velocity of the North Atlantic polar front during the last deglaciation determined by ^{14}C accelerator mass spectrometry, *Nature*, *328*(6133), 791–794, doi:10.1038/328791a0.

Bard, E., B. Hamelin, and R. G. Fairbanks (1990), U-Th ages obtained by mass spectrometry in corals from Barbados: Sea level during the past 130,000 years, *Nature*, *346*, 456–458, doi:10.1038/346456a0.

Bard, E., M. Arnold, J. Mangerud, M. Paterne, L. Labeyrie, J. Duprat, M. A. Melieres, E. Sonstegaard, and J.-C. Duplessey

(1994), The North Atlantic atmosphere-sea surface ^{14}C gradient during the Younger Dryas climatic event, *Earth Planet. Sci. Lett.*, *126*, 275–287, doi:10.1016/0012-821X(94)90112-0.

Bard, E., B. Hamelin, M. Arnold, L. Montaggioni, G. Cabioch, G. Faure, and F. Rougerie (1996), Deglacial sea-level record from Tahiti corals and the timing of global meltwater discharge, *Nature*, *382*, 241–244, doi:10.1038/382241a0.

Bard, E., F. Rostek, J.-L. Turon, and S. Gendreau (2000), Hydrological impact of Heinrich Events in the subtropical northeast Atlantic, *Science*, *289*, 1321–1324.

Bard, E., B. Hamelin, and D. Delanghe-Sabatier (2010), Deglacial meltwater pulse 1B and Younger Dryas sea levels revisited with boreholes at Tahiti, *Science*, *327*(5970), 1235–1237, doi:10.1126/science.1180557.

Barnett, P. J. (1985), Glacial retreat and lake levels, north central Lake Erie basin, Ontario, in *Quaternary Evolution of the Great Lakes*, edited by P. F. Karrow and P. E. Calkin, *Geol. Assoc. Can. Spec. Pap.*, *30*, 185–194.

Baroni, C., and B. L. Hall (2004), A new Holocene relative sea-level curve for Terra Nova Bay, Victoria Land, Antarctica, *J. Quat. Sci.*, *19*, 377–396, doi:10.1002/jqs.825.

Baroni, C., and G. Orombelli (1994), Abandoned penguin rookeries as Holocene paleoclimatic indicators in Antarctica, *Geology*, *22*(1), 23–26, doi:10.1130/0091-7613(1994)022<0023:APRAHP>2.3.CO;2.

Bassett, S. E., G. A. Milne, J. X. Mitrovica, and P. U. Clark (2005), Ice sheet and solid earth influences on far-field sea-level histories, *Science*, *309*(5736), 925–928, doi:10.1126/science.1111575.

Bassett, S. E., G. A. Milne, M. J. Bentley, and P. Huybrechts (2007), Modelling Antarctic sea-level data to explore the possibility of a dominant Antarctic contribution to meltwater pulse IA, *Quat. Sci. Rev.*, *26*(17–18), 2113–2127, doi:10.1016/j.quascirev.2007.06.011.

Bentley, M. J., C. J. Fogwill, P. W. Kubik, and D. E. Sugden (2006), Geomorphological evidence and cosmogenic Be-10/Al-26 exposure ages for the Last Glacial Maximum and deglaciation of the Antarctic Peninsula Ice Sheet, *Geol. Soc. Am. Bull.*, *118*(9–10), 1149–1159, doi:10.1130/B25735.1.

Bentley, M. J., C. J. Fogwill, A. M. Le Brocq, A. L. Hubbard, D. E. Sugden, T. J. Dunai, and S. Freeman (2010), Deglacial history of the West Antarctic Ice Sheet in the Weddell Sea embayment: Constraints on past ice volume change, *Geology*, *38*(5), 411–414, doi:10.1130/G30754.1.

Bentley, M. J., D. E. Sugden, C. J. Fogwill, A. M. Le Brocq, A. L. Hubbard, T. J. Dunai, and S. Freeman (2011), Deglacial history of the West Antarctic Ice Sheet in the Weddell Sea embayment: Constraints on past ice volume change: Reply, *Geology*, *39*(5), E240–e240, doi:10.1130/G32140Y.1.

Berkman, P. A., and S. L. Forman (1996), Pre-bomb radiocarbon and the reservoir correction for calcareous marine species in the Southern Ocean, *Geophys. Res. Lett.*, *23*(4), 363–366, doi:10.1029/96GL00151.

Bettis, E. A., Jr., D. J. Quade, and T. J. Kemmis (1996), Hogs, bogs, and logs: Quaternary deposits and environmental geology of the Des Moines lobe, in *Geological Survey Bureau Guidebook*, vol. 18, pp. 1–170, Iowa Dep. of Nat. Resour., Des Moines.

Bianchi, G. G., and I. N. McCave (1999), Holocene periodicity in North Atlantic climate and deep-ocean flow south of Iceland, *Nature*, *397*(6719), 515–517, doi:10.1038/17362.

Birchfield, G. E., and W. S. Broecker (1990), A salt oscilator in the glacial Atlantic? 2. A "scale analysis" model, *Paleoceanography*, *5*, 835–843, doi:10.1029/PA005i006p00835.

Bird, M. I., L. K. Fifield, T. S. Teh, C. H. Chang, N. Shirlaw, and K. Lambeck (2007), An inflection in the rate of early mid-Holocene eustatic sea-level rise: A new sea-level curve from Singapore, *Estuarine Coastal Shelf Sci.*, *71*(3–4), 523–536, doi:10.1016/j.ecss.2006.07.004.

Björck, S., N. Koc, and G. Skog (2003), Consistently large marine reservoir ages in the Norwegian Sea during the last deglaciation, *Quat. Sci. Rev.*, *22*, 429–435, doi:10.1016/S0277-3791(03)00002-7.

Blanchon, P., and J. Shaw (1995), Reef drowning during the last deglaciation: Evidence for catastrophic sea-level rise and ice-sheet collapse, *Geology*, *23*, 4–8, doi:10.1130/0091-7613(1995)023<0004:RDDTLD>2.3.CO;2.

Blunier, T., and E. J. Brook (2001), Timing of millennial-scale climate change in Antarctica and Greenland during the last glacial period, *Science*, *291*, 109–112, doi:10.1126/science.291.5501.109.

Blunier, T., et al. (1998), Asynchrony of Antarctic and Greenland climate change during the last glacial period, *Nature*, *394*, 739–743, doi:10.1038/29447.

Bockheim, J. G., S. C. Wilson, G. H. Denton, B. G. Andersen, and M. Stuiver (1989), Late Quaternary ice-surface fluctuations of Hatherton Glacier, Transantarctic Mountains, *Quat. Res.*, *31*(2), 229–254, doi:10.1016/0033-5894(89)90007-0.

Bond, G. C., et al. (1992), Evidence for massive discharges of icebergs into the North Atlantic ocean during the last glacial period, *Nature*, *360*, 245–249, doi:10.1038/360245a0.

Bond, G. C., W. S. Broecker, S. Johnsen, J. McManus, L. Labeyrie, J. Jouzel, and G. Bonani (1993), Correlations between climate records from North Atlantic sediments and Greenland ice, *Nature*, *365*, 143–147, doi:10.1038/365143a0.

Bond, G., W. Showers, M. Cheseby, R. Lotti, P. Almasi, P. deMenocal, P. Priore, H. Cullen, I. Hajdas, and G. Bonani (1997), A pervasive millennial-scale cycle in North Atlantic Holocene and glacial climates, *Science*, *278*, 1257–1266, doi:10.1126/science.278.5341.1257.

Bond, G. C., W. Showers, M. Elliot, M. Evans, R. Lotti, I. Hajdas, G. Bonani, and S. Johnsen (1999), The North Atlantic's 1–2 kyr climate rhythm: Relation to Heinrich events, Dansgaard/Oeschger cycles and the Little Ice Age, in *Mechanisms of Global Climate Change at Millennial Time Scales*, *Geophys. Monogr. Ser.*, vol. 112, edited by U. Clark, S. Webb, and D. Keigwin, pp. 35–58, AGU, Washington, D. C., doi:10.1029/GM112p0035.

Bond, G. C., B. Kromer, J. Beer, R. Muscheler, M. N. Evans, W. Showers, S. Hoffmann, R. Lotti-Bond, I. Hajdas, and G. Bonani (2001), Persistent solar influence on North Atlantic climate during the Holocene, *Science*, *294*, 2130–2136, doi:10.1126/science.1065680.

Bondevik, S., J. Mangerud, H. H. Birks, S. Gulliksen, and P. Reimer (2006), Changes in North Atlantic radiocarbon reservoir ages during the Allerod and Younger Dryas, *Science*, *312*(5779), 1514–1517, doi:10.1126/science.1123300.

Boulton, G. S., P. Dongelmans, M. Punkari, and M. Broadgate (2001), Palaeoglaciology of an ice sheet through a glacial cycle: The European ice sheet through the Weichselian, *Quat. Sci. Rev.*, *20*, 591–625, doi:10.1016/S0277-3791(00)00160-8.

Bowen, D. Q., F. M. Phillips, A. M. McCabe, P. C. Knutz, and G. A. Sykes (2002), New data for the Last Glacial Maximum in Great Britain and Ireland, *Quat. Sci. Rev.*, *21*, 89–101, doi:10.1016/S0277-3791(01)00102-0.

Boyer, S. J., and D. R. Pheasant (1974), Delimitation of weathering zone in the fiord area of eastern Baffin Island, Canada, *Geol. Soc. Am. Bull.*, *85*, 805–810, doi:10.1130/0016-7606(1974)85<805:DOWZIT>2.0.CO;2.

Boyle, E. A., and L. Keigwin (1987), North Atlantic thermohaline circulation during the past 20,000 years linked to high-latitude surface temperature, *Nature*, *330*, 35–40.

Braconnot, P., et al. (2007), Results of PMIP2 coupled simulations of the Mid-Holocene and Last Glacial Maximum—Part 1: Experiments and large-scale features, *Clim. Past*, *3*(2), 261–277, doi:10.5194/cp-3-261-2007.

Brand, U., and F. M. G. McCarthy (2005), The Allerod-Younger Dryas-Holocene sequence in the west-central Champlain Sea, eastern Ontario: A record of glacial, oceanographic, and climatic changes, *Quat. Sci. Rev.*, *24*(12–13), 1463–1478, doi:10.1016/j.quascirev.2004.11.002.

Briner, J. P., G. H. Miller, P. T. Davis, and R. C. Finkel (2005), Cosmogenic exposure dating in arctic glacial landscapes:

Implications for the glacial history of northeastern Baffin Island, Arctic Canada, *Can. J. Earth Sci.*, *42*(1), 67–84, doi:10.1139/e04-102.

Briner, J. P., G. H. Miller, P. T. Davis, and R. C. Finkel (2006), Cosmogenic radionuclides from fiord landscapes support differential erosion by overriding ice sheets, *Geol. Soc. Am. Bull.*, *118*(3–4), 406–420, doi:10.1130/B25716.1.

Broecker, W. S. (1990), Salinity history of the Northern Atlantic during the last deglaciation, *Paleoceanography*, *5*, 459–467, doi:10.1029/PA005i004p00459.

Broecker, W. S. (1994), Massive iceberg discharges as triggers for global climate change, *Nature*, *372*, 421–424.

Broecker, W. S. (1998), Paleocean circulation during the last deglaciation: A bipolar seesaw?, *Paleoceanography*, *13*, 119–121, doi:10.1029/97PA03707.

Broecker, W. S. (2003), Does the trigger for abrupt climate change reside in the ocean or in the atmosphere?, *Science*, *300*, 1519–1522, doi:10.1126/science.1083797.

Broecker, W. S. (2006), Was the Younger Dryas triggered by a flood?, *Science*, *312*(5777), 1146–1148, doi:10.1126/science.1123253.

Broecker, W. S., and M. Andree (1988), The chronology of the last deglaciation: Implications to the cause of the Younger Dryas event, *Paleoceanography*, *3*, 1–19, doi:10.1029/PA003i001p00001.

Broecker, W. S., J. P. Kennett, B. P. Flower, J. T. Teller, S. Trumbore, G. Bonani, and W. Wolfli (1989), Routing of meltwater from the Laurentide ice sheet during the Younger Dryas cold episode, *Nature*, *341*, 318–321, doi:10.1038/341318a0.

Broecker, W. S., G. Bond, M. Klas, E. Clark, and J. McManus (1992), Origin of the northern Atlantic's Heinrich events, *Clim. Dyn.*, *6*, 265–273, doi:10.1007/BF00193540.

Broecker, W. S., G. H. Denton, R. L. Edwards, H. Cheng, R. B. Alley, and A. E. Putnam (2010), Putting the Younger Dryas cold event into context, *Quat. Sci. Rev.*, *29*(9–10), 1078–1081, doi:10.1016/j.quascirev.2010.02.019.

Bromley, G. R. M., B. L. Hall, J. O. Stone, H. Conway, and C. E. Todd (2010), Late Cenozoic deposits at Reedy Glacier, Transantarctic Mountains: Implications for former thickness of the West Antarctic Ice Sheet, *Quat. Sci. Rev.*, *29*(3–4), 384–398, doi:10.1016/j.quascirev.2009.07.001.

Brook, E. J., M. D. Kurz, R. P. J. Ackert, G. H. Denton, E. T. Brown, G. M. Raisbeck, and F. Yiou (1993), Chronology of Taylor Glacier advances in Arena Valley, Antarctica, using *in situ* cosmogenic ^{3}He and ^{10}Be, *Quat. Res.*, *39*, 11–23, doi:10.1006/qres.1993.1002.

Brook, E. J., M. D. Kurz, R. P. J. Ackert, G. M. Raisbeck, and F. Yiou (1995), Cosmogenic nuclide exposure ages and glacial history of late Quaternary Ross Sea drift in McMurdo Sound, Antarctica, *Earth Planet. Sci. Lett.*, *131*, 41–56, doi:10.1016/0012-821X(95)00006-X.

Brook, E. J., A. Nesje, S. J. Lehman, G. M. Raisbeck, and F. Yiou (1996), Cosmogenic nuclide exposure ages along a vertical transect in western Norway: Implications for the height of the Fennoscandian ice sheet, *Geology*, *24*, 207–210, doi:10.1130/0091-7613(1996)024<0207:CNEAAA>2.3.CO;2.

Brook, E. J., J. W. C. White, A. S. M. Schilla, M. L. Bender, B. Barnett, J. P. Severinghaus, K. C. Taylor, R. B. Alley, and E. J. Steig (2005), Timing of millennial-scale climate change at Siple Dome, West Antarctica, during the last glacial period, *Quat. Sci. Rev.*, *24*(12–13), 1333–1343, doi:10.1016/j.quascirev.2005.02.002.

Calkin, P. E., and B. H. Feenstra (1985), Evolution of the Erie-Basin Great Lakes, in *Quaternary Evolution of the Great Lakes*, edited by P. F. Karrow and P. E. Calkin, *Geol. Assoc. Can. Spec. Pap.*, *30*, 149–170.

Came, R. E., D. W. Oppo, and J. F. McManus (2007), Amplitude and timing of temperature and salinity variability in the subpolar North Atlantic over the past 10 k.y., *Geology*, *35*(4), 315–318, doi:10.1130/G23455A.1.

Carlson, A. E. (2008), Why there was not a Younger Dryas-like event during the Penultimate Deglaciation, *Quat. Sci. Rev.*, *27*(9–10), 882–887, doi:10.1016/j.quascirev.2008.02.004.

Carlson, A. E. (2009), Geochemical constraints on the Laurentide Ice Sheet contribution to meltwater pulse 1A, *Quat. Sci. Rev.*, *28*(17–18), 1625–1630, doi:10.1016/j.quascirev.2009.02.011.

Carlson, A. E. (2010), What caused the Younger Dryas cold event?, *Geology*, *38*(4), 383–384, doi:10.1130/focus042010.1.

Carlson, A. E., and P. U. Clark (2008), Rapid climate change and Arctic Ocean freshening: Comment, *Geology*, *36*, e177, doi:10.1130/G24786C.1.

Carlson, A. E., P. U. Clark, G. M. Raisbeck, and E. J. Brook (2007a), Rapid Holocene deglaciation of the Labrador sector of the Laurentide Ice Sheet, *J. Clim.*, *20*(20), 5126–5133, doi:10.1175/JCLI4273.1.

Carlson, A. E., P. U. B. A. Haley, G. P. Klinkhammer, K. Simmons, E. J. Brook, and K. J. Meissner (2007b), Geochemical proxies of North American freshwater routing during the Younger Dryas cold event, *Proc. Natl. Acad. Sci. U. S. A.*, *104*(16), 6556–6561, doi:10.1073/pnas.0611313104.

Carlson, A. E., A. N. Legrande, D. W. Oppo, R. E. Came, G. A. Schmidt, F. S. Anslow, J. M. Licciardi, and E. A. Obbink (2008), Rapid early Holocene deglaciation of the Laurentide ice sheet, *Nat. Geosci.*, *1*(9), 620–624, doi:10.1038/ngeo285.

Carlson, A. E., P. U. Clark, and S. W. Hostetler (2009a), Comment: Radiocarbon deglaciation chronology of the Thunder Bay, Ontario area and implications for ice sheet retreat patterns, *Quat. Sci. Rev.*, *28*(23–24), 2546–2547, doi:10.1016/j.quascirev.2009.05.005.

Carlson, A. E., P. U. Clark, B. A. Haley, and G. P. Klinkhammer (2009b), Routing of western Canadian Plains runoff during the 8.2 ka cold event, *Geophys. Res. Lett.*, *36*, L14704, doi:10.1029/2009GL038778.

Carlson, A. E., F. S. Anslow, E. A. Obbink, A. N. LeGrande, D. J. Ullman, and J. M. Licciardi (2009c), Surface-melt driven Laurentide Ice Sheet retreat during the early Holocene, *Geophys. Res. Lett.*, *36*, L24502, doi:10.1029/2009GL040948.

Carlson, A. E., D. J. Ullman, F. S. Anslow, F. He, P. U. Clark, Z. Liu, and B. L. Otto-Bliesner (2012), Modeling the surface mass-balance response of the Laurentide Ice Sheet to Bølling warming and its contribution to meltwater pulse 1A, *Earth Planet. Sci. Lett.*, *315–316*, 24–29, doi:10.1016/j.epsl.2011.07.008.

Cato, I. (1985), The definitive connection of the Swedish geochronological time scale with the present, and the new date of the zero year in Doviken, northern Sweden, *Boreas*, *14*, 117–122, doi:10.1111/j.1502-3885.1985.tb00901.x.

Chabaux, F., J. Riotte, and O. Dequincey (2003), U-Th-Ra fractionation during weathering and river transport, in *Uranium-Series Geochemistry*, *Rev. in Mineral. and Geochem.*, vol. 52, edited by B. Bourdon et al., pp. 533–576, Mineral. Soc. of Am., Washington, D. C., doi:10.2113/0520533.

Cheng, H., R. L. Edwards, J. A. Hoff, C. D. Gallup, D. A. Richards, and Y. Asmerom (2000), The half-lives of uranium-234 and thorium-230, *Chem. Geol.*, *169*, 17–33, doi:10.1016/S0009-2541(99)00157-6.

Cheng, H., R. L. Edwards, W. S. Broecker, G. H. Denton, X. G. Kong, Y. J. Wang, R. Zhang, and X. F. Wang (2009), Ice age terminations, *Science*, *326*(5950), 248–252, doi:10.1126/science.1177840.

Clague, J. J., and T. S. James (2002), History and isostatic effects of the last ice sheet in southern British Columbia, *Quat. Sci. Rev.*, *21*(1–3), 71–87, doi:10.1016/S0277-3791(01)00070-1.

Clark, J. A., W. Farrel, and W. R. Peltier (1978), Global changes in postglacial sea level: A numerical calculation, *Quat. Res.*, *9*, 265–287, doi:10.1016/0033-5894(78)90033-9.

Clark, P. U. (1992), Surface form of the southern Laurentide Ice Sheet and its implications to ice-sheet dynamics, *Geol. Soc. Am. Bull.*, *104*, 595–605, doi:10.1130/0016-7606(1992)104<0595:SFOTSL>2.3.CO;2.

Clark, P. U. (2011), Deglacial history of the West Antarctic Ice Sheet in the Weddell Sea embayment: Constraints on past ice volume change: Comment, *Geology*, *39*(5), e239, doi:10.1130/G31533C.1.

Clark, P. U., and A. C. Mix (2002), Ice sheets and sea level of the Last Glacial Maximum, *Quat. Sci. Rev.*, *21*, 1–7.

Clark, P. U., R. B. Alley, L. D. Keigwin, J. M. Licciardi, S. J. Johnsen, and H. Wang (1996), Origin of the global meltwater pulse following the last glacial maximum, *Paleoceanography*, *11*(5), 563–577, doi:10.1029/96PA01419.

Clark, P. U., S. J. Marshall, G. K. C. Clarke, S. W. Hostetler, J. M. Licciardi, and J. T. Teller (2001), Freshwater forcing of abrupt climate change during the last glaciation, *Science*, *293*, 283–287, doi:10.1126/science.1062517.

Clark, P. U., J. X. Mitrovica, G. A. Milne, and M. E. Tamisiea (2002), Sea-level fingerprinting as a direct test for the source of global meltwater pulse 1A, *Science*, *295*, 2438–2441.

Clark, P. U., E. J. Brook, G. M. Raisbeck, F. Yiou, and J. Clark (2003), Cosmogenic ^{10}Be ages of the Saglek Moraines, Torngat Mountains, Labrador, *Geology*, *31*, 617–620, doi:10.1130/0091-7613(2003)031<0617:CBAOTS>2.0.CO;2.

Clark, P. U., A. M. McCabe, A. C. Mix, and A. J. Weaver (2004), Rapid rise of sea level 19,000 years ago and its global implications, *Science*, *304*(5674), 1141–1144, doi:10.1126/science.1094449.

Clark, P. U., S. W. Hostetler, N. G. Pisias, A. Schmittner, and K. J. Meisner (2007), Mechanisms for an ~7-kyr climate and sea-level oscillation during marine isotope stage 3, in *Ocean Circulation: Mechanisms and Impacts—Past and Future Changes of Meridional Overturning*, *Geophys. Monogr. Ser.*, vol. 173, edited by A. Schmittner, J. C. H. Chiang, and S. R. Hemming, pp. 209–246, AGU, Washington, D. C., doi:10.1029/173GM15.

Clark, P. U., A. S. Dyke, J. D. Shakun, A. E. Carlson, J. Clark, B. Wohlfarth, J. X. Mitrovica, S. W. Hostetler, and A. M. McCabe (2009), The Last Glacial Maximum, *Science*, *325*(5941), 710–714, doi:10.1126/science.1172873.

Clark, P. U., et al. (2012), Global climate evolution during the last deglaciation, *Proc. Natl. Acad. Sci. U. S. A.*, *109*(19), E1134–E1142, doi:10.1073/pnas.1116619109.

Clarke, G. K. C., D. W. Leverington, J. T. Teller, and A. S. Dyke (2004), Paleohydraulics of the last outburst flood from the Lake Agassiz and the 8200 BP cold event, *Quat. Sci. Rev.*, *23*, 389–407, doi:10.1016/j.quascirev.2003.06.004.

Clarke, G. K. C., A. B. G. Bush, and J. W. M. Bush (2009), Freshwater discharge, sediment transport, and modeled climate impacts of the final drainage of glacial Lake Agassiz, *J. Clim.*, *22*, 2161–2180, doi:10.1175/2008JCLI2439.1.

Clayton, L. (1984), *Pleistocene Geology of the Superior Region, Wisconsin*, 40 pp., Wisc. Geol. and Nat. Hist. Surv., Madison.

Clayton, L., and S. R. Moran (1982), Chronology of late Wisconsinan glaciation in middle North America, *Quat. Sci. Rev.*, *1*, 55–82, doi:10.1016/0277-3791(82)90019-1.

Colman, S. M. (2007), Conventional wisdom and climate history, *Proc. Natl. Acad. Sci. U. S. A.*, *104*(16), 6500–6501, doi:10.1073/pnas.0701952104.

Colman, S. M., L. D. Keigwin, and R. M. Forester (1994), Two episodes of meltwater influx from glacial Lake Agassiz into the Lake Michigan basin and their climatic contrasts, *Geology*, *22*(6), 547–550, doi:10.1130/0091-7613(1994)022<0547:TEOMIF>2.3.CO;2.

Condron, A., and P. Winsor (2011), A subtropical fate awaited freshwater discharged from glacial Lake Agassiz, *Geophys. Res. Lett.*, *38*, L03705, doi:10.1029/2010GL046011.

Conway, H., B. L. Hall, G. H. Denton, A. M. Gades, and E. D. Waddington (1999), Past and future grounding-line retreat of the West Antarctic Ice Sheet, *Science*, *286*(5438), 280–283, doi:10.1126/science.286.5438.280.

Cronin, T. M., P. R. Vogt, D. A. Willard, R. Thunell, J. Halka, M. Berke, and J. Pohlman (2007), Rapid sea level rise and ice sheet response to 8,200-year climate event, *Geophys. Res. Lett.*, *34*, L20603, doi:10.1029/2007GL031318.

Crowley, T. J. (1992), North Atlantic Deep Water cools the Southern Hemisphere, *Paleoceanography*, *7*, 489–497, doi:10.1029/92PA01058.

Cutler, K. B., R. L. Edwards, F. W. Taylor, H. Cheng, J. F. Adkins, C. D. Gallup, P. M. Cutler, G. S. Burr, J. Chappell, and A. L. Bloom (2003), Rapid sea-level fall and deep-ocean temperature change since the last interglacial, *Earth Planet. Sci. Lett.*, *206*, 253–271, doi:10.1016/S0012-821X(02)01107-X.

Dale, B. (1996), Dinoflagellate cyst ecology: Modeling and geological applications, in *Palynology: Principles and Applications*, edited by J. Jansonius and D. G. McGregor, pp. 1249–1275, AASP Found., College Station, Tex.

Darby, D. A., J. F. Bischof, R. F. Spielhagen, S. A. Marshall, and S. W. Herman (2002), Arctic ice export events and their potential impact on global climate during the late Pleistocene, *Paleoceanography*, *17*(2), 1025, doi:10.1029/2001PA000639.

De Angelis, H., and P. Skvarca (2003), Glacier surge after ice shelf collapse, *Science*, *299*, 1560–1562, doi:10.1126/science.1077987.

De Deckker, P., and Y. Yokoyama (2009), Micropalaeontological evidence for Late Quaternary sea-level changes in Bonaparte Gulf, Australia, *Global Planet. Change*, *66*(1–2), 85–92, doi:10.1016/j.gloplacha.2008.03.012.

Denton, G. H., and T. J. Hughes (2002), Reconstructing the Antarctic Ice Sheet at the Last Glacial Maximum, *Quat. Sci. Rev.*, *21*(1–3), 193–202, doi:10.1016/S0277-3791(01)00090-7.

Denton, G. H., and D. R. Marchant (2000), The geologic basis for a reconstruction of a grounded ice sheet in McMurdo Sound, Antarctica, at the last glacial maximum, *Geogr. Ann., Ser. A Phys. Geogr.*, *82A*(2–3), 167–211.

Denton, G. H., J. G. Bockheim, S. C. Wilson, and M. Stuiver (1989), Late Wisconsin and Early Holocene Glacial History, Inner Ross Embayment, Antarctica, *Quat. Res.*, *31*(2), 151–182, doi:10.1016/0033-5894(89)90004-5.

Denton, G. H., J. G. Bockheim, R. H. Rutford, and B. G. Andersen (1992), Glacial history of the Ellsworth Mountains, West Antarctica, in *Geology and Paleontology of the Ellsworth Mountains, West Antarctica*, edited by G. F. Webers, C. Craddock, and J. F. Splettstoesser, pp. 403–432, Geol. Soc. of Am., Boulder, Colo.

Denton, G. H., R. F. Anderson, J. R. Toggweiler, R. L. Edwards, J. M. Schaefer, and A. E. Putnam (2010), The Last Glacial Termination, *Science*, *328*(5986), 1652–1656, doi:10.1126/science.1184119.

Deschamps, P., N. Durand, E. Bard, B. Hamelin, G. Camoin, A. L. Thomas, G. M. Henderson, J. Okuno, and Y. Yokoyama (2012), Ice-sheet collapse and sea-level rise at the Bolling warming 14,600 years ago, *Nature*, *483*(7391), 559–564, doi:10.1038/nature10902.

de Vernal, A., C. Hillaire-Marcel, and G. Bilodeau (1996), Reduced meltwater outflow from the Laurentide ice margin during the Younger Dryas, *Nature*, *381*, 774–777, doi:10.1038/381774a0.

Dickie, L. M., and R. W. Trites (1983), The Gulf of St. Lawrence, in *Estuaries and Enclosed Seas*, edited by B. H. Ketchum, pp. 403–425, Elsevier, New York.

di Nicola, L., S. Strask, C. Schluchter, M. C. Salvatore, N. Akcar, P. W. Kubik, M. Christl, H. U. Kasper, R. Wieler, and C. Baroni (2009), Multiple cosmogenic nuclides document complex Pleistocene exposure history of glacial drifts in Terra Nova Bay (northern Victoria Land, Antarctica), *Quat. Res.*, *71*(1), 83–92, doi:10.1016/j.yqres.2008.07.004.

Dochat, T. M., D. R. Marchant, and G. H. Denton (2000), Glacial geology of Cape Bird, Ross Island, Antarctica, *Geogr. Ann., Ser. A Phys. Geogr.*, *82A*(2–3), 237–247.

Dokken, T., and E. Jansen (1999), Rapid changes in the mechanism of ocean convection during the last glacial period, *Nature*, *401*, 458–461, doi:10.1038/46753.

Domack, E. W., A. J. T. Jull, J. B. Anderson, T. W. Linick, and C. R. Williams (1989), Application of tandem accelerator mass-spectrometer dating to late Pleistocene-Holocene sediments of the East Antarctic continental shelf, *Quat. Res.*, *31*, 277–287, doi:10.1016/0033-5894(89)90009-4.

Domack, E. W., E. A. Jacobson, S. Shipp, and J. B. Anderson (1999), Late Pleistocene-Holocene retreat of the West Antarctic Ice-Sheet system in the Ross Sea: Part 2—Sedimentologic and stratigraphic signature, *Geol. Soc. Am. Bull.*, *111*(10), 1517–1536, doi:10.1130/0016-7606(1999)111<1517:LPHROT>2.3.CO;2.

Domack, E. W., D. Amblas, R. Gilbert, S. Brachfeld, A. Camerlenghi, M. Rebesco, M. Canals, and R. Urgeles (2006), Subglacial morphology and glacial evolution of the Palmer deep outlet system, Antarctic Peninsula, *Geomorphology*, *75*(1–2), 125–142, doi:10.1016/j.geomorph.2004.06.013.

Doran, P. T., G. W. Berger, W. B. Lyons, R. A. Wharton, M. L. Davisson, J. Southon, and J. E. Dibb (1999), Dating Quaternary lacustrine sediments in the McMurdo Dry Valleys, Antarctica, *Palaeogeogr. Palaeoclimatol. Palaeoecol.*, *147*(3–4), 223–239, doi:10.1016/S0031-0182(98)00159-X.

Dowdeswell, J. A., M. A. Maslin, J. T. Andrews, and I. N. McCave (1995), Iceberg production, debris rafting, and the extent and thickness of Heinrich layers (H-1, H-2) in North Atlantic sediments, *Geology*, *23*, 301–304, doi:10.1130/0091-7613(1995)023<0297:IPDRAT>2.3.CO;2.

Dyke, A. S. (2004), An outline of North American deglaciation with emphasis on central and northern Canada, in *Quaternary Glaciations: Extent and Chronology*, edited by J. Ehlers and P. L. Gibbard, pp. 373–424, Elsevier, Amsterdam, doi:10.1016/S1571-0866(04)80209-4.

Dyke, A. S., and V. K. Prest (1987), Late Wisconsinan and Holocene history of the Laurentide Ice Sheet, *Geogr. Phys. Quat.*, *XLI*(2), 237–263.

Dyke, A. S., A. Moore, and L. Robertson (2003), *Deglaciation of North America*, *Geol. Surv. Can. Open File*, *1574*, doi:10.4095/214399.

Edwards, R. L. (1995), Paleotopography of glacial-age ice sheets, *Science*, *267*(5197), 536–538, doi:10.1126/science.267.5197.536.

Edwards, R. L., J. W. Beck, G. S. Burr, D. J. Donahue, J. M. A. Chappell, A. L. Bloom, E. R. M. Druffel, and F. W. Taylor (1993), A large drop in atmospheric $^{14}C/^{12}C$ and reduced melting in the Younger Dryas, documented with ^{230}Th ages of corals, *Science*, *260*, 962–968, doi:10.1126/science.260.5110.962.

Ellison, C. R. W., M. R. Chapman, and I. R. Hall (2006), Surface and deep ocean interactions during the cold climate event 8200 years ago, *Science*, *312*(5782), 1929–1932, doi:10.1126/science.1127213.

Eltgroth, S. F., J. F. Adkins, L. F. Robinson, J. Southon, and M. Kashgarian (2006), A deep-sea coral record of North Atlantic radiocarbon through the Younger Dryas: Evidence for intermediate water/deepwater reorganization, *Paleoceanography*, *21*, PA4207, doi:10.1029/2005PA001192.

Emslie, S. D., L. Coats, and K. Licht (2007), A 45,000 yr record of Adelie penguins and climate change in the Ross Sea, Antarctica, *Geology*, *35*(1), 61–64, doi:10.1130/G23011A.1.

England, J. H., M. F. A. Furze, and J. P. Doupe (2009), Revision of the NW Laurentide Ice Sheet: Implications for paleoclimate, the northeast extremity of Beringia, and Arctic Ocean sedimentation, *Quat. Sci. Rev.*, *28*, 1573–1596, doi:10.1016/j.quascirev.2009.04.006.

Fabel, D., D. Fink, O. Fredin, J. Harbor, M. Land, and A. P. Stroeven (2006), Exposure ages from relict lateral moraines overridden by the Fennoscandian ice sheet, *Quat. Res.*, *65*(1), 136–146, doi:10.1016/j.yqres.2005.06.006.

Fairbanks, R. G. (1989), A 17,000-year glacio-eustatic sea level record: Influence of glacial melting rates on the Younger Dryas event and deep-ocean circulation, *Nature*, *342*, 637–642, doi:10.1038/342637a0.

Fairbanks, R. G., C. D. Charles, and J. D. Wright (1992), Origin of global meltwater pulses, in *Radiocarbon After Four Decades*, edited by R. E. Taylor, A. Long, and R. S. Kra, pp. 473–500, Springer, New York.

Fairbanks, R. G., R. A. Mortlock, T.-C. Chiu, L. Cao, A. Kaplan, T. P. Guilderson, T. W. Fairbanks, A. L. Bloom, P. M. Grootes, and M.-J. Nadeau (2005), Radiocarbon calibration curve spanning 0 to 50,000 years BP based on paired $^{230}Th/^{234}U/^{238}U$ and ^{14}C dates on pristine corals, *Quat. Sci. Rev.*, *24*, 1781–1796, doi:10.1016/j.quascirev.2005.04.007.

Fink, D., B. McKelvey, M. J. Hambrey, D. Fabel, and R. Brown (2006), Pleistocene deglaciation chronology of the Amery Oasis and Radok Lake, northern Prince Charles Mountains, Antarctica, *Earth Planet. Sci. Lett.*, *243*(1–2), 229–243, doi:10.1016/j.epsl.2005.12.006.

Firestone, R. B., et al. (2007), Evidence for an extraterrestrial impact 12,900 years ago that contributed to the megafaunal extinctions and the Younger Dryas cooling, *Proc. Natl. Acad. Sci. U. S. A.*, *104*(41), 16,016–16,021, doi:10.1073/pnas.0706977104.

Fisher, T. G. (2003), Chronology of glacial Lake Agassiz meltwater routed to the Gulf of Mexico, *Quat. Res.*, *59*(2), 271–276, doi:10.1016/S0033-5894(03)00011-5.

Fisher, T. G., and T. V. Lowell (2006), Questioning the age of the Moorhead Phase in the glacial Lake Agassiz basin, *Quat. Sci. Rev.*, *25*(21–22), 2688–2691, doi:10.1016/j.quascirev.2006.05.007.

Fisher, T. G., C. H. Yansa, T. V. Lowell, K. Lepper, I. Hajdas, and A. Ashworth (2008), The chronology, climate, and confusion of the Moorhead Phase of glacial Lake Agassiz: New results from the Ojata Beach, North Dakota, USA, *Quat. Sci. Rev.*, *27*(11–12), 1124–1135, doi:10.1016/j.quascirev.2008.02.010.

Fisher, T. G., N. Waterson, T. V. Lowell, and I. Hajdas (2009), Deglaciation ages and meltwater routing in the Fort McMurray region, northeastern Alberta and northwestern Saskatchewan, Canada, *Quat. Sci. Rev.*, *28*(17–18), 1608–1624, doi:10.1016/j.quascirev.2009.02.003.

Fleming, K., P. Johnston, D. Zwartz, Y. Yokoyama, K. Lambeck, and J. Chappell (1998), Refining the eustatic sea-level curve since the Last Glacial Maximum using far- and intermediate-field sites, *Earth Planet. Sci. Lett.*, *163*, 327–342.

Flower, B. P., D. W. Hastings, H. W. Hill, and T. M. Quinn (2004), Phasing of deglacial warming and Laurentide Ice Sheet meltwater in the Gulf of Mexico, *Geology*, *32*(7), 597–600, doi:10.1130/G20604.1.

Flückiger, J., R. Knutti, and J. W. C. White (2006), Oceanic processes as potential trigger and amplifying mechanisms for Heinrich events, *Paleoceanography*, *21*, PA2014, doi:10.1029/2005PA001204.

Fogwill, C. J., M. J. Bentley, D. E. Sugden, A. R. Kerr, and P. W. Kubik (2004), Cosmogenic nuclides Be-10 and Al-26 imply limited Antarctic Ice Sheet thickening and low erosion in the Shackleton Range for >1 m.y., *Geology*, *32*(3), 265–268, doi:10.1130/G19795.1.

Fromm, E. (1985), Chronological calculation of the varve zero in Sweden, *Boreas*, *14*, 123–125, doi:10.1111/j.1502-3885.1985.tb00902.x.

Fullerton, D. S. (1980), Preliminary correlation of post-Erie interstadial events (16,000–10,000 radiocarbon years before present), central and eastern Great Lakes region, and Hudson, Champlain, and St. Lawrence lowlands, United States and Canada, *U.S. Geol. Surv. Prof. Pap.*, *1089*, 1–52.

Ganopolski, A., and S. Rahmstorf (2001), Rapid changes of glacial climate simulated in a coupled climate model, *Nature*, *409*, 153–158, doi:10.1038/35051500.

Gill, J. L., J. W. Williams, S. T. Jackson, K. B. Lininger, and G. S. Robinson (2009), Pleistocene megafaunal collapse, novel plant communities, and enhanced fire regimes in North America, *Science*, *326*, 1100–1103.

Goehring, B. M., E. J. Brook, H. Linge, G. M. Ralsbeck, and F. Yiou (2008), Beryllium-10 exposure ages of erratic boulders in southern Norway and implications for the history of the

Fennoscandian Ice Sheet, *Quat. Sci. Rev.*, *27*(3–4), 320–336, doi:10.1016/j.quascirev.2007.11.004.

Gomez, N., J. X. Mitrovica, P. Huybers, and P. U. Clark (2010), Sea level as a stabilizing factor for marine-ice-sheet grounding lines, *Nat. Geosci.*, *3*(12), 850–853, doi:10.1038/ngeo1012.

Gomez, N., D. Pollard, J. X. Mitrovica, P. Huybers, and P. U. Clark (2012), Evolution of a coupled marine ice sheet–sea level model, *J. Geophys. Res.*, *117*, F01013, doi:10.1029/2011JF002128.

Gonzales, L. M., and E. C. Grimm (2009), Synchronization of late-glacial vegetation changes at Crystal Lake, Illinois, USA with the North Atlantic event stratigraphy, *Quat. Res.*, *72*, 234–245.

Gordon, J. E., and D. D. Harkness (1992), Magnitude and geographic variation of the radiocarbon content in Antarctic marine life: Implications for reservoir corrections in radiocarbon dating, *Quat. Sci. Rev.*, *11*(7–8), 697–708, doi:10.1016/0277-3791(92)90078-M.

Gosse, J. C., and F. M. Phillips (2001), Terrestrial in situ cosmogenic nuclides: Theory and application, *Quat. Sci. Rev.*, *20*, 1475–1560, doi:10.1016/S0277-3791(00)00171-2.

Gravenor, C. P., and M. Stupavsky (1976), Magnetic, physical, and lithologic properties and age of till exposed along the east coast of Lake Huron, Ontario, *Can. J. Earth Sci.*, *13*, 1655–1666, doi:10.1139/e76-175.

Gregoire, L. J., A. J. Payne, and P. J. Valdes (2012), Deglacial rapid sea level rises caused by ice-sheet saddle collapses, *Nature*, *487*, 219–222, doi:10.1038/nature11257.

Grimm, E. C., L. J. Maher, and D. M. Nelson (2009), The magnitude of error in conventional bulk-sediment radiocarbon dates from central North America, *Quat. Res.*, *72*, 301–308.

Grousset, F. E., E. Cortijo, S. Huon, L. Herve, T. Richter, D. Burdloff, J. Duprat, and O. Weber (2001), Zooming in on Heinrich layers, *Paleoceanography*, *16*(3), 240–259, doi:10.1029/2000PA000559.

Gutjahr, M., and J. Lippold (2011), Early arrival of Southern Source Water in the deep North Atlantic prior to Heinrich event 2, *Paleoceanography*, *26*, PA2101, doi:10.1029/2011PA002114.

Gutjahr, M., B. A. A. Hoogakker, M. Frank, and I. N. McCave (2010), Changes in North Atlantic Deep Water strength and bottom water masses during marine isotope stage 3 (45–35 ka BP), *Quat. Sci. Rev.*, *29*(19–20), 2451–2461, doi:10.1016/j.quascirev.2010.02.024.

Gwiazda, R. H., S. R. Hemming, and W. S. Broecker (1996), Tracking the sources of icebergs with lead isotopes: The provenance of ice-rafted debris in Heinrich layer 2, *Paleoceanography*, *11*, 77–93, doi:10.1029/95PA03135.

Hall, B. L., and G. H. Denton (1999), New relative sea-level curves for the southern Scott Coast, Antarctica: Evidence for Holocene deglaciation of the western Ross Sea, *J. Quat. Sci.*, *14*(7), 641–650, doi:10.1002/(SICI)1099-1417(199912)14:7<641::AID-JQS466>3.0.CO;2-B.

Hall, B. L., and G. H. Denton (2000), Radiocarbon chronology of Ross Sea drift, eastern Taylor Valley, Antarctica: Evidence for a grounded ice sheet in the Ross Sea at the last glacial maximum, *Geogr. Ann., Ser. A Phys. Geogr.*, *82A*(2–3), 305–336.

Hall, B. L., and G. M. Henderson (2001), Use of uranium-thorium dating to determine past C-14 reservoir effects in lakes: Examples from Antarctica, *Earth Planet. Sci. Lett.*, *193*(3–4), 565–577, doi:10.1016/S0012-821X(01)00524-6.

Hall, B. L., G. H. Denton, and C. H. Hendy (2000), Evidence from Taylor Valley for a grounded ice sheet in the Ross Sea, Antarctica, *Geogr. Ann.*, *28*, 275–303.

Hall, B. L., C. Baroni, and G. H. Denton (2004), Holocene relative sea-level history of the Southern Victoria Land Coast, Antarctica, *Global Planet. Change*, *42*(1–4), 241–263, doi:10.1016/j.gloplacha.2003.09.004.

Hall, B. L., G. H. Denton, A. G. Fountain, C. H. Hendy, and G. M. Henderson (2010), Antarctic lakes suggest millennial reorganizations of Southern Hemisphere atmospheric and oceanic circulation, *Proc. Natl. Acad. Sci. U. S. A.*, *107*(50), 21,355–21,359, doi:10.1073/pnas.1007250107.

Hall, I. R., S. B. Moran, R. Zahn, P. C. Knutz, C. C. Shen, and R. L. Edwards (2006), Accelerated drawdown of meridional overturning in the late-glacial Atlantic triggered by transient pre-H event freshwater perturbation, *Geophys. Res. Lett.*, *33*, L16616, doi:10.1029/2006GL026239.

Hall, J. M., and L. H. Chan (2004), Ba/Ca in Neogloboquadrina as an indicator of deglcial meltwater discharge into the western Arctic Ocean, *Paleoceanography*, *19*, PA1017, doi:10.1029/2003PA000910.

Hanebuth, T., K. Stattegger, and P. M. Grootes (2000), Rapid flooding of the Sunda Shelf: A late-glacial sea-level record, *Science*, *288*, 1033–1035, doi:10.1126/science.288.5468.1033.

Hanebuth, T., K. Stattegger, and A. Bojanowski (2009), Termination of the Last Glacial Maximum sea-level lowstand: The Sunda-Shelf data revisited, *Global Planet. Change*, *66*(1–2), 76–84, doi:10.1016/j.gloplacha.2008.03.011.

Hansel, A. K., and D. M. Mickelson (1988), A reevaluation of the timing and causes of high lake phases in the Lake Michigan basin, *Quat. Res.*, *29*, 113–128, doi:10.1016/0033-5894(88)90055-5.

Hanslik, D., M. Jakobsson, J. Backman, S. Bjorck, E. Sellen, M. O'Regan, E. Fornaciari, and G. Skog (2010), Quaternary Arctic Ocean sea ice variations and radiocarbon reservoir age corrections, *Quat. Sci. Rev.*, *29*(25–26), 3430–3441, doi:10.1016/j.quascirev.2010.06.011.

Harris, P. T., and R. J. Beaman (2003), Processes controlling the formation of the Mertz Drift, George Vth continental shelf, East Antarctica: Evidence from 3.5 kHz sub-bottom profiling and sediment cores, *Deep Sea Res., Part II*, *50*(8–9), 1463–1480, doi:10.1016/S0967-0645(03)00070-5.

Hein, A. S., C. J. Fogwill, D. E. Sugden, and S. Xu (2011), Glacial/interglacial ice-stream stability in the Weddell Sea embayment, Antarctica, *Earth Planet. Sci. Lett.*, *307*, 211–221.

Hemming, S. R. (2004), Heinrich events: Massive late Pleistocene detritus layers of the North Atlantic and their global climate imprint, *Rev. Geophys.*, *42*, RG1005, doi:10.1029/2003RG000128.

Hemming, S. R., W. S. Broecker, W. D. Sharp, G. C. Bond, R. H. Gwiazda, J. F. McManus, M. Klas, and I. Hajdas (1998), Provenance of Heinrich layers in core V28-82, Northeastern Atlantic: $^{40}Ar/^{39}Ar$ ages of ice-rafted hornblende, Pb isotopes in feldspar grains, and Nd-Sr-Pb isotopes in the fine sediment fraction, *Earth Planet. Sci. Lett.*, *164*, 317–333, doi:10.1016/S0012-821X(98)00224-6.

Hendy, C. H., and B. L. Hall (2006), The radiocarbon reservoir effect in proglacial lakes: Examples from Antarctica, *Earth Planet. Sci. Lett.*, *241*(3–4), 413–421, doi:10.1016/j.epsl.2005.11.045.

Heroy, D. C., and J. B. Anderson (2007), Radiocarbon constraints on Antarctic Peninsula Ice Sheet retreat following the Last Glacial Maximum (LGM), *Quat. Sci. Rev.*, *26*(25–28), 3286–3297, doi:10.1016/j.quascirev.2007.07.012.

Hijma, M. P., and K. M. Cohen (2010), Timing and magnitude of the sea-level jump preluding the 8200 yr event, *Geology*, *38*(3), 275–278, doi:10.1130/G30439.1.

Hilbrecht, H. (1996), Extant planktic foraminifera and the physical environment in the Atlantic and Indian Oceans, report, 98 pp., Geol. Inst. der Eidgen. Tech. Hochschule und der Univ. Zurich, Zurich, Switzerland.

Hillaire-Marcel, C., and G. Bilodeau (2000), Instabilities in the Labrador Sea water mass structure during the last climatic cycle, *Can. J. Earth Sci.*, *37*(5), 795–809, doi:10.1139/e99-108.

Hillaire-Marcel, C., and A. de Vernal (2008), Comment on "Mixed-layer deepening during Heinrich events: A multi-planktonic foraminiferal delta O-18 approach," *Science*, *320*(5880), 1161, doi:10.1126/science.1153316.

Hillaire-Marcel, C., A. de Vernal, G. Bilodeau, and A. J. Weaver (2001), Absence of deep-water formation in the Labrador Sea during the last interglacial period, *Nature*, *410*, 1073–1077, doi:10.1038/35074059.

Hillaire-Marcel, C., A. de Vernal, L. Polyak, and D. Darby (2004), Size-dependent isotopic composition of planktic foraminifers

from Chukchi Sea vs. NW Atlantic sediments: Implications for the Holocene paleoceanography of the western Arctic, *Quat. Sci. Rev.*, *23*(3–4), 245–260, doi:10.1016/j.quascirev.2003.08.006.

Hillaire-Marcel, C., A. de Vernal, and D. J. W. Piper (2007), Lake Agassiz Final drainage event in the northwest North Atlantic, *Geophys. Res. Lett.*, *34*, L15601, doi:10.1029/2007GL030396.

Hoffman, J. S., A. E. Carlson, K. Winsor, G. P. Klinkhammer, A. N. LeGrande, J. T. Andrews, and J. C. Strasser (2012), Linking the 8.2 ka event and its freshwater forcing in the Labrador Sea, *Geophys. Res. Lett.*, *39*, L18703, doi:10.1029/2012GL053047.

Holland, D. M., R. H. Thomas, B. De Young, M. H. Ribergaard, and B. Lyberth (2008), Acceleration of Jakobshavn Isbrae triggered by warm subsurface ocean waters, *Nat. Geosci.*, *1*(10), 659–664, doi:10.1038/ngeo316.

Holliday, N. P., A. Meyer, S. Bacon, S. G. Alderson, and B. de Cuevas (2007), Retroflection of part of the east Greenland current at Cape Farewell, *Geophys. Res. Lett.*, *34*, L07609, doi:10.1029/2006GL029085.

Hori, K., and Y. Saito (2007), An early Holocene sea-level jump and delta initiation, *Geophys. Res. Lett.*, *34*, L18401, doi:10.1029/2007GL031029.

Horton, B. P., P. L. Gibbard, G. M. Milne, R. J. Morley, C. Purintavaragul, and J. M. Stargardt (2005), Holocene sea levels and palaeoenvironments, Malay-Thai Peninsula, southeast Asia, *Holocene*, *15*(8), 1199–1213, doi:10.1191/0959683605hl891rp.

Hostetler, S., N. Pisias, and A. Mix (2006), Sensitivity of Last Glacial Maximum climate to uncertainties in tropical and subtropical ocean temperatures, *Quat. Sci. Rev.*, *25*(11–12), 1168–1185, doi:10.1016/j.quascirev.2005.12.010.

Huybrechts, P. (2002), Sea-level changes at the LGM from ice-dynamic reconstructions of the Greenland and Antarctic ice sheets during the glacial cycles, *Quat. Sci. Rev.*, *21*, 203–231, doi:10.1016/S0277-3791(01)00082-8.

Ives, J. D. (1978), Maximum extent of Laurentide Ice Sheet along east coast of North America during last glaciation, *Arctic*, *31*(1), 24.

Johnson, J. S., M. J. Bentley, and K. Gohl (2008), First exposure ages from the Amundsen Sea embayment, West Antarctica: The late Quaternary context for recent thinning of Pine Island, Smith, and Pope Glaciers, *Geology*, *36*(3), 223–226, doi:10.1130/G24207A.1.

Johnson, R. G., and B. T. McClure (1976), A model for Northern Hemisphere continental ice sheet variation, *Quat. Res.*, *6*, 325–353, doi:10.1016/0033-5894(67)90001-4.

Jones, G. A., and L. D. Keigwin (1988), Evidence from Fram Strait (78°N) for early deglaciation, *Nature*, *336*, 56–59, doi:10.1038/336056a0.

Kaiser, K. F. (1994), Two Creeks Interstade dated through dendrochronology and AMS, *Quat. Res.*, *42*, 288–298, doi:10.1006/qres.1994.1079.

Karlen, W. (1979), Deglaciation dates from northern Swedish Lapland, *Geogr. Ann., Ser. A Phys. Geogr.*, *61*, 203–210.

Karpuz, N. K., and E. Jansen (1992), A high-resolution diatom record of the last deglaciation from the SE Norwegian Sea: Documentation of rapid climatic changes, *Paleoceanography*, *7*(4), 499–520, doi:10.1029/92PA01651.

Keigwin, L. D., and G. A. Jones (1995), The marine record of deglaciation from the continental margin off Nova Scotia, *Paleoceanography*, *10*, 973–985, doi:10.1029/95PA02643.

Keigwin, L. D., G. A. Jones, S. J. Lehman, and E. A. Boyle (1991), Deglacial meltwater discharge, North Atlantic deep circulation, and abrupt climate change, *J. Geophys. Res.*, *96*, 16,811–16,826, doi:10.1029/91JC01624.

Keigwin, L. D., J. P. Sachs, Y. Rosenthal, and E. A. Boyle (2005), The 8200 year B.P. event in the slope water system, western subpolar North Atlantic, *Paleoceanography*, *20*, PA2003, doi:10.1029/2004PA001074.

Kelly, M. A., T. V. Lowell, B. L. Hall, J. M. Schaefer, R. C. Finkel, B. M. Goehring, R. B. Alley, and G. H. Denton (2008), A Be-10 chronology of late glacial and Holocene mountain glaciation in the Scoresby Sund region, east Greenland: Implications for seasonality during lateglacial time, *Quat. Sci. Rev.*, *27*(25–26), 2273–2282, doi:10.1016/j.quascirev.2008.08.004.

Kelly, M. A., T. G. Fisher, T. Lowell, P. Barnett, J. M. Schaefer, and R. Schwartz (2009), ^{10}Be ages of glacial and meltwater features northwest of Lake Superior: A chronology of Laurentide Ice Sheet deglaciation and eastward flooding from Glacial Lake Agassiz, *Eos Trans. AGU*, *90*(52), Fall Meet. Suppl., Abstract PP21A-1329.

Kendall, R. A., J. X. Mitrovica, G. A. Milne, T. E. Törnqvist, and Y. X. Li (2008), The sea-level fingerprint of the 8.2 ka climate event, *Geology*, *36*(5), 423–426, doi:10.1130/G24550A.1.

Kerwin, M. W. (1996), A regional stratigraphic isochron (ca 8000 C-14 yr BP) from final deglaciation of Hudson Strait, *Quat. Res.*, *46*(2), 89–98, doi:10.1006/qres.1996.0049.

Kleiven, H. F., C. Kissel, C. Laj, U. S. Ninnemann, T. O. Richter, and E. Cortijo (2008), Reduced North Atlantic Deep Water coeval with the glacial Lake Agassiz freshwater outburst, *Science*, *319*(5859), 60–64, doi:10.1126/science.1148924.

Klitgaard-Kristensen, D., H. P. Sejrup, H. Haflidason, S. Johnsen, and M. Spurk (1998), A regional 8200 cal. yr BP cooling event in northwest Europe, induced by final stages of the Laurentide ice-sheet deglaciation?, *J. Quat. Sci.*, *13*, 165–169, doi:10.1002/(SICI)1099-1417(199803/04)13:2<165::AID-JQS365>3.0.CO;2-#.

Knutti, R., J. Flückiger, T. F. Stocker, and A. Timmermann (2004), Strong hemispheric coupling of glacial climate through freshwater discharge and ocean circulation, *Nature*, *430*(7002), 851–856, doi:10.1038/nature02786.

Koc, N., and E. Jansen (1994), Response of the high-latitude Northern Hemisphere to orbital climate forcing: evidence from the Nordic Seas, *Geology*, *22*, 523–526.

Kopp, R. E. (2012), Tahitian record suggests Antarctic collapse, *Nature*, *483*, 549–550.

Lambeck, K., and J. Chappell (2001), Sea level change through the last glacial cycle, *Science*, *292*(5517), 679–686, doi:10.1126/science.1059549.

Landvik, J. Y., S. Bondevik, A. Elverhoi, W. Fjeldskaar, J. Mangerud, O. Salvigsen, M. J. Siegert, J. I. Svendsen, and T. O. Vorren (1998), The last glacial maximum of Svalbard and the Barents Sea area: Ice sheet extent and configuration, *Quat. Sci. Rev.*, *17*(1–3), 43–75, doi:10.1016/S0277-3791(97)00066-8.

Lane, C. S., S. P. E. Blockley, J. Mangerud, V. C. Smith, O. S. Lohne, E. L. Tomlinson, I. P. Matthews, and A. F. Lotter (2012), Was the 12.1 ka Icelandic Vedde Ash one of a kind?, *Quat. Sci. Rev.*, *33*, 87–99, doi:10.1016/j.quascirev.2011.11.011.

Larson, G. J., T. V. Lowell, and N. E. Ostrom (1994), Evidence for the Two Creeks interstade in the Lake Huron basin, *Can. J. Earth Sci.*, *31*, 793–797, doi:10.1139/e94-072.

Lasalle, P., and J. A. Elson (1975), Emplacement of St. Narcisse moraine as a climatic event in eastern Canada, *Quat. Res.*, *5*, 621–625, doi:10.1016/0033-5894(75)90018-6.

Lasalle, P., and W. W. Shilts (1993), Younger Dryas age readvance of Laurentide ice into the Champlain Sea, *Boreas*, *22*, 25–37, doi:10.1111/j.1502-3885.1993.tb00161.x.

Lea, D. W., D. K. Pak, and H. J. Spero (2000), Climate impact of late Quaternary equatorial Pacific sea surface temperature variations, *Science*, *289*, 1719–1724, doi:10.1126/science.289.5485.1719.

LeGrande, A. N., and G. A. Schmidt (2008), Ensemble, water isotope–enabled, coupled general circulation modeling insights into the 8.2 ka event, *Paleoceanography*, *23*, PA3207, doi:10.1029/2008PA001610.

LeGrande, A. N., and G. A. Schmidt (2009), Sources of Holocene variability of oxygen isotopes in paleoclimate archives, *Clim. Past*, *5*(3), 441–455, doi:10.5194/cp-5-441-2009.

LeGrande, A. N., G. A. Schmidt, D. T. Shindell, C. V. Field, R. L. Miller, D. M. Koch, G. Faluvegi, and G. Hoffmann (2006), Consistent simulations of multiple proxy responses to an abrupt

climate change event, *Proc. Natl. Acad. Sci. U. S. A.*, *103*(4), 837–842, doi:10.1073/pnas.0510095103.

Lehman, S. J., et al. (1991), Initiation of Fennoscandian ice-sheet retreat during the last deglaciation, *Nature*, *349*, 513–516, doi:10.1038/349513a0.

Lemieux-Dudon, B., E. Blayo, J. R. Petit, C. Waelbroeck, A. Svensson, C. Ritz, J. M. Barnola, B. M. Narcisi, and F. Parrenin (2010), Consistent dating for Antarctic and Greenland ice cores, *Quat. Sci. Rev.*, *29*(1–2), 8–20, doi:10.1016/j.quascirev.2009.11.010.

Lepper, K., T. G. Fisher, I. Hajdas, and T. V. Lowell (2007), Ages for the Big Stone Moraine and the oldest beaches of glacial Lake Agassiz: Implications for deglaciation chronology, *Geology*, *35*(7), 667–670, doi:10.1130/G23665A.1.

Leventer, A., D. F. Williams, and J. P. Kennett (1982), Dynamics of the Laurentide ice sheet during the last deglaciation: Evidence from the Gulf of Mexico, *Earth Planet. Sci. Lett.*, *59*, 11–17, doi:10.1016/0012-821X(82)90112-1.

Leventer, A., E. Domack, R. Dunbar, J. Pike, C. Stickley, E. Maddison, S. Brachfeld, P. Manley, and C. McClennen (2006), Marine sediment record from the East Antarctic margin reveals dynamics of ice sheet recession, *GSA Today*, *16*, 4–10.

Leverington, D. W., and J. Teller (2003), Paleotopographic reconstructions of the eastern outlets of glacial Lake Agassiz, *Can. J. Earth Sci.*, *40*(9), 1259–1278, doi:10.1139/e03-043.

Leverington, D. W., J. D. Mann, and J. T. Teller (2002), Changes in the bathymetry and volume of glacial Lake Agassiz between 9200 and 7700 C-14 yr BP, *Quat. Res.*, *57*(2), 244–252, doi:10.1006/qres.2001.2311.

Li, Y.-X., T. E. Törnqvist, J. M. Nevitt, and B. Kohl (2012), Synchronizing a sea-level jump, final Lake Agassiz drainage, and abrupt cooling 8200 years ago, *Earth Planet. Sci. Lett.*, *315–316*, 41–50, doi:10.1016/j.epsl.2011.05.034.

Licciardi, J. M., P. U. Clark, J. W. Jenson, and D. R. MacAyeal (1998), Deglaciation of a soft-bedded Laurentide Ice Sheet, *Quat. Sci. Rev.*, *17*, 427–448, doi:10.1016/S0277-3791(97)00044-9.

Licciardi, J. M., J. T. Teller, and P. U. Clark (1999), Freshwater routing by the Laurentide Ice Sheet during the last deglaciation, in *Mechanisms of Global Climate Change at Millennial Time Scales*, *Geophys. Monogr. Ser.*, vol. 112, edited by U. Clark, S. Webb, and D. Keigwin, pp. 177–201, AGU, Washington, D. C., doi:10.1029/GM112p0177.

Licht, K. J. (2004), The Ross Sea's contribution to eustatic sea level during meltwater pulse 1A, *Sediment. Geol.*, *165*(3–4), 343–353, doi:10.1016/j.sedgeo.2003.11.020.

Licht, K. J., and J. T. Andrews (2002), The C-14 record of Late Pleistocene ice advance and retreat in the central Ross Sea, Antarctica, *Arct. Antarct. Alp. Res.*, *34*(3), 324–333, doi:10.2307/1552491.

Licht, K. J., A. E. Jennings, J. T. Andrews, and K. M. Williams (1996), Chronology of late Wisconsin ice retreat from the western Ross Sea, Antarctica, *Geology*, *24*(3), 223–226, doi:10.1130/0091-7613(1996)024<0223:COLWIR>2.3.CO;2.

Licht, K. J., N. W. Dunbar, J. T. Andrews, and A. E. Jennings (1999), Distinguishing subglacial till and glacial marine diamictons in the western Ross Sea, Antarctica: Implications for a last glacial maximum grounding line, *Geol. Soc. Am. Bull.*, *111*(1), 91–103, doi:10.1130/0016-7606(1999)111<0091:DSTAGM>2.3.CO;2.

Linge, H., E. J. Brook, A. Nesje, G. M. Raisbeck, F. Yiou, and H. Clark (2006), In situ Be-10 exposure ages from southeastern Norway: Implications for the geometry of the Weichselian Scandinavian ice sheet, *Quat. Sci. Rev.*, *25*(9–10), 1097–1109, doi:10.1016/j.quascirev.2005.10.007.

Lippold, J., J. Grutzner, D. Winter, Y. Lahaye, A. Mangini, and M. Christl (2009), Does sedimentary ^{231}Pa/^{230}Th from the Bermuda Rise monitor past Atlantic Meridional Overturning Circulation?, *Geophys. Res. Lett.*, *36*, L12601, doi:10.1029/2009GL038068.

Liu, Z., et al. (2009), Transient simulation of last deglaciation with a new mechanism for Bolling-Allerod warming, *Science*, *325*(5938), 310–314, doi:10.1126/science.1171041.

Lowell, T. V., G. Larson, J. D. Hughes, and G. Denton (1999), Age verification of the Lake Gribben forest bed and the Younger Dryas advance of the Laurentide Ice Sheet, *Can. J. Earth Sci.*, *36*, 383–393, doi:10.1139/e98-095.

Lowell, T., et al. (2005), Testing the Lake Agassiz meltwater trigger for the Younger Dryas, *Eos Trans. AGU*, *86*(40), 365, doi:10.1029/2005EO400001.

Lowell, T. V., T. G. Fisher, I. Hajdas, K. Glover, H. Loope, and T. Henry (2009), Radiocarbon deglaciation chronology of the Thunder Bay, Ontario area and implications for ice sheet retreat patterns, *Quat. Sci. Rev.*, *28*(17–18), 1597–1607, doi:10.1016/j.quascirev.2009.02.025.

MacAyeal, D. R. (1993), Binge/purge oscillations of the Laurentide Ice Sheet as a cause of the North Atlantic's Heinrich events, *Paleoceanography*, *8*, 775–784, doi:10.1029/93PA02200.

Maccali, J., C. Hillarie-Marcel, J. Carignan, and L. C. Reisberg (2012), Pb isotopes and geochemical monitoring of Arctic sedimentary supplies and water mass export through Fram Strait since the Last Glacial Maximum, *Paleoceanography*, *27*, PA1201, doi:10.1029/2011PA002152.

Mackintosh, A., D. White, D. Fink, D. B. Gore, J. Pickard, and P. C. Fanning (2007), Exposure ages from mountain dipsticks in Mac. Robertson Land, East Antarctica, indicate little change in ice-sheet thickness since the Last Glacial Maximum, *Geology*, *35*(6), 551–554, doi:10.1130/G23503A.1.

Mackintosh, A., et al. (2011), Retreat of the East Antarctic ice sheet during the last glacial termination, *Nat. Geosci.*, *4*, 195–202, doi:10.1038/ngeo1061.

Maher, L. J., N. G. Miller, R. G. Baker, B. B. Curry, and D. M. Mickelson (1998), Paleobiology of the sand beneath the Valders diamicton at Valders, Wisconsin, *Quat. Res.*, *49*(2), 208–221, doi:10.1006/qres.1997.1957.

Manabe, S., and R. J. Stouffer (1995), Simulation of abrupt climate change induced by freshwater input to the North Atlantic Ocean, *Nature*, *378*, 165–167, doi:10.1038/378165a0.

Mangini, A., J. M. Godoy, M. L. Godoy, R. Kowsmann, G. M. Santos, M. Ruckelshausen, A. Schroeder-Ritzrau, and L. Wacker (2010), Deep sea corals off Brazil verify a poorly ventilated Southern Pacific Ocean during H2, H1 and the Younger Dryas, *Earth Planet. Sci. Lett.*, *293*(3–4), 269–276, doi:10.1016/j.epsl.2010.02.041.

Marchitto, T. M., and K. Wei (1995), History of Laurentide meltwater flow to the Gulf of Mexico during the last deglaciation, as revealed by reworked calcareous nannofossils, *Geology*, *23*, 779–782, doi:10.1130/0091-7613(1995)023<0779:HOLMFT>2.3.CO;2.

Marcott, S. A., et al. (2011), Ice-shelf collapse from subsurface warming as a trigger for Heinrich events, *Proc. Natl. Acad. Sci. U. S. A.*, *108*(33), 13,415–13,419, doi:10.1073/pnas.1104772108.

Marlon, J. R., et al. (2009), Wildfire responses to abrupt climate change in North America, *Proc. Natl. Acad. Sci. U. S. A.*, *106*(8), 2519–2524, doi:10.1073/pnas.0808212106.

Marsella, K. A., P. R. Bierman, P. T. Davis, and M. W. Caffee (2000), Cosmogenic Be-10 and Al-26 ages for the Last Glacial Maximum, eastern Baffin Island, Arctic Canada, *Geol. Soc. Am. Bull.*, *112*(8), 1296–1312, doi:10.1130/0016-7606(2000)112<1296:CBAAAF>2.0.CO;2.

Marshall, S. J., and G. K. C. Clarke (1997), A continuum mixture model of ice stream thermomechanics in the Laurentide Ice Sheet: 2. Application to the Hudson Strait ice stream, *J. Geophys. Res.*, *102*, 20,615–20,637, doi:10.1029/97JB01189.

Marshall, S. J., and G. K. C. Clarke (1999), Modeling North American freshwater runoff through the Last Glacial Cycle, *Quat. Res.*, *52*, 300–315, doi:10.1006/qres.1999.2079.

Marshall, S. J., and M. R. Koutnik (2006), Ice sheet action versus reaction: Distinguishing between Heinrich events and

Dansgaard-Oeschger cycles in the North Atlantic, *Paleoceanography*, *21*, PA2021, doi:10.1029/2005PA001247.

McCabe, A. M. (1986), Glaciomarine facies deposited by retreating tidewater glaciers: An example from the late Pleistocene of Northern Ireland, *J. Sediment. Petrol.*, *56*, 880–894.

McCabe, A. M., P. U. Clark, and J. Clark (2005), AMS C-14 dating of deglacial events in the Irish Sea Basin and other sectors of the British-Irish ice sheet, *Quat. Sci. Rev.*, *24*(14–15), 1673–1690, doi:10.1016/j.quascirev.2004.06.019.

McCabe, A. M., J. A. G. Cooper, and J. T. Kelley (2007), Relative sea-level changes from NE Ireland during the last glacial termination, *J. Geol. Soc., 164, 1059–1063, doi:10.1144/0016-76492006-164.*

McKay, R. M., G. B. Dunbar, T. R. Naish, P. J. Barrett, L. Carter, and M. Harper (2008), Retreat history of the Ross Ice Sheet (Shelf) since the Last Glacial Maximum from deep-basin sediment cores around Ross Island, *Palaeogeogr. Palaeoclimatol. Palaeoecol.*, *260*(1–2), 245–261, doi:10.1016/j.palaeo.2007.08.015.

McManus, J. F., R. F. Ardison, W. S. Broecker, M. Q. Fleisher, and S. M. Higgins (1998), Radiometrically determined sedimentary fluxes in the sub-polar North America during the last 140,000 years, *Earth Planet. Sci. Lett.*, *155*, 29–43, doi:10.1016/S0012-821X(97)00201-X.

McManus, J. F., R. Francois, J. M. Gherardi, L. D. Keigwin, and S. Brown-Leger (2004), Collapse and rapid resumption of Atlantic meridional circulation linked to deglacial climate changes, *Nature*, *428*(6985), 834–837, doi:10.1038/nature02494.

Meissner, K. J. (2007), Younger Dryas: A data to model comparison to constrain the strength of the overturning circulation, *Geophys. Res. Lett.*, *34*, L21705, doi:10.1029/2007GL031304.

Meissner, K. J., and P. U. Clark (2006), Impact of floods versus routing events on the thermohaline circulation, *Geophys. Res. Lett.*, *33*, L15704, doi:10.1029/2006GL026705.

Menviel, L., A. Timmermann, A. Mouchet, and O. Timm (2008), Meridional reorganizations of marine and terrestrial productivity during Heinrich events, *Paleoceanography*, *23*, PA1203, doi:10.1029/2007PA001445.

Mercer, J. H. (1968), Glacial geology of Reedy Glacier area, Antarctica, *Geol. Soc. Am. Bull.*, *79*, 471–486, doi:10.1130/0016-7606(1968)79[471:GGOTRG]2.0.CO;2.

Mickelson, D. M., L. Clayton, D. S. Fullerton, and H. W. Borns Jr. (1983), The late Wisconsin glacial record of the Laurentide ice sheet in the United States, in *Late Quaternary Environments of the Western United States*, vol. 1, *The Late Pleistocene*, edited by S. C. Porter, pp. 3–37, Univ. of Minn. Press, Minneapolis.

Mickelson, D. M., T. S. Hooyer, B. J. Socha, and C. Winguth (2007), Late-glacial ice advances and vegetation changes in east-central Wisconsin, in *Late-Glacial History of East-Central Wisconsin, Guide Book for the 53rd Midwest Friends of the Pleistocene Field Conference*, edited by T. S. Hooyer, *Open File Rep.*, *2007-01*, pp. 73–87, Wis. Geol. and Nat. Hist. Surv., Madison.

Miller, G. H., A. P. Wolfe, E. J. Steig, P. E. Sauer, M. R. Kaplan, and J. P. Briner (2002), The Goldilocks dilemma: Big ice, little ice, or "just-right" ice in the eastern Canadian Arctic, *Quat. Sci. Rev.*, *21*(1–3), 33–48, doi:10.1016/S0277-3791(01)00085-3.

Miller, G. H., J. P. Briner, N. A. Lifton, and R. C. Finkel (2006), Limited ice-sheet erosion and complex in situ cosmogenic Be-10, Al-26, and C-14 on Baffin Island, Arctic Canada, *Quat. Geochronol.*, *1*(1), 74–85, doi:10.1016/j.quageo.2006.06.011.

Millot, R., C. J. Allegre, J. Gaillardet, and S. Roy (2004), Lead isotopic systematics of major river sediments: A new estimate of the Pb isotopic composition of the upper continental crust, *Chem. Geol.*, *203*(1–2), 75–90, doi:10.1016/j.chemgeo.2003.09.002.

Milne, G. A., and J. X. Mitrovica (2008), Searching for eustasy in deglacial sea-level histories, *Quat. Sci. Rev.*, *27*(25–26), 2292–2302, doi:10.1016/j.quascirev.2008.08.018.

Milne, G. A., W. R. Gehrels, C. W. Hughes, and M. E. Tamisiea (2009), Identifying the causes of sea-level change, *Nat. Geosci.*, *2*(7), 471–478, doi:10.1038/ngeo544.

Mitrovica, J. X., M. E. Tamisiea, J. L. Davis, and G. A. Milne (2001), Recent mass balance of polar ice sheets inferred from patterns of global sea-level change, *Nature*, *409*(6823), 1026–1029, doi:10.1038/35059054.

Mix, A. C., W. F. Ruddiman, and A. McIntyre (1986), Late Quaternary paleoceanography of the tropical Atlantic: 1. Spatial variability of annual mean sea-surface temperatures, 0–20,000 years B.P., *Paleoceanography*, *1*, 43–66, doi:10.1029/PA001i001p00043.

Monaghan, G. W., and A. K. Hansel (1990), Evidence for the intra-Glenwood (Mackinaw) low-water phase of glacial Lake Chicago, *Can. J. Earth Sci.*, *27*, 1236–1241, doi:10.1139/e90-131.

Montaggioni, L. F., G. Cabioch, G. F. Camoinau, E. Bard, A. Ribaud Laurenti, G. Faure, P. Dejardin, and J. Recy (1997), Continuous record of reef growth over the past 14 ky on the mid-Pacific island of Tahiti, *Geology*, *25*(6), 555–558, doi:10.1130/0091-7613(1997)025<0555:CRORGO>2.3.CO;2.

Mook, W. G. (1972), Application of natural isotopes in ground water hydrology, *Biol. Mijnbouw*, *51*, 131–136.

Moran, S. R., L. Clayton, M. Scott, and J. Brophy (1973), Catalog of North Dakota radiocarbon dates, *Misc. Ser. N. D. Geol. Surv.*, *53*, 1–51.

Mörner, N.-A., and A. Dreimanis (1973), The Erie interstade, in *The Wisconsinan Stage*, edited by R. F. Black, R. P. Goldthwait, and H. B. Willman, *Mem. Geol. Soc. Am.*, *136*, 107–134.

Mott, R. J., D. R. Grant, R. R. Stea, and S. Occhietti (1986), Late-glacial climatic oscillation in Atlantic Canada equivalent to the Allerod/Younger Dryas event, *Nature*, *323*, 247–250, doi:10.1038/323247a0.

Motyka, R. J., M. Truffer, M. Fahnestock, J. Mortensen, S. Rysgaard, and I. Howat (2011), Submarine melting of the 1985 Jakobshavn Isbræ floating tongue and the triggering of the current retreat, *J. Geophys. Res.*, *116*, F01007, doi:10.1029/2009JF001632.

Muller, E. H., and P. E. Calkin (1993), Timing of Pleistocene glacial events in New York State, *Can. J. Earth Sci.*, *30*, 1829–1845, doi:10.1139/e93-161.

Mulvaney, R., R. Rothlisberger, E. W. Wolff, S. Sommer, J. Schwander, M. A. Hutteli, and J. Jouzel (2000), The transition from the last glacial period in inland and near-coastal Antarctica, *Geophys. Res. Lett.*, *27*(17), 2673–2676, doi:10.1029/1999GL011254.

Murton, J. B., M. D. Bateman, S. R. Dallimore, J. T. Teller, and Z. R. Yang (2010), Identification of Younger Dryas outburst flood path from Lake Agassiz to the Arctic Ocean, *Nature*, *464*(7289), 740–743, doi:10.1038/nature08954.

Nesje, A., and S. O. Dahl (1990), Autochthonous block fields in southern Norway: Implications for the geometry, thickness, and isostatic loading of the Late Weichselian Scandinavian ice sheet, *J. Quat. Sci.*, *5*, 225–234.

Neumann, A. C., and I. G. Macintyre (1985), Reef response to sea-level rise: Keep-up, catch-up, or give-up, paper presented at International Coral Reef Congress, Int. So. for Reef Stud., Papeete, Tahiti.

Nørgaard-Pedersen, N., R. F. Spielhagen, H. Erlenkeuser, P. M. Grootes, J. Heinemeier, and J. Knies (2003), Arctic Ocean during the Last Glacial Maximum: Atlantic and polar domains of surface water mass distribution and ice cover, *Paleoceanography*, *18*(3), 1063, doi:10.1029/2002PA000781.

Not, C., and C. Hillaire-Marcel (2012), Enhanced sea-ice export from the Arctic during the Younger Dryas, *Nat. Commun.*, *3*, 647.

Obbink, E. A., A. E. Carlson, and G. P. Klinkhammer (2010), Eastern North American freshwater discharge during the Bolling-Allerod warm periods, *Geology*, *38*(2), 171–174, doi:10.1130/G30389.1.

Oberholzer, P., C. Baroni, J. M. Schaefer, G. Orombelli, S. I. Ochs, P. W. Kubik, H. Baur, and R. Wieler (2003), Limited Pliocene/Pleistocene glaciation in Deep Freeze Range, northern Victoria Land, Antarctica, derived from in situ cosmogenic nuclides, *Antarct. Sci.*, *15*(4), 493–502, doi:10.1017/S0954102003001603.

Ohkouchi, N., and T. I. Eglinton (2008), Compound-specific radiocarbon dating of Ross Sea sediments: A prospect for constructing chronologies in high-latitude oceanic sediments, *Quat. Geochronol.*, *3*(3), 235–243, doi:10.1016/j.quageo.2007.11.001.

Okazaki, Y., A. Timmermann, L. Menviel, N. Harada, A. Abe-Ouchi, M. O. Chikamoto, A. Mouchet, and H. Asahi (2010), Deepwater formation in the North Pacific during the last glacial termination, *Science*, *329*(5988), 200–204, doi:10.1126/science.1190612.

Oppo, D. W., J. F. McManus, and J. L. Cullen (2003), Palaeoceanography: Deepwater variability in the Holocene epoch, *Nature*, *422*(6929), 277–278, doi:10.1038/422277b.

Otto-Bliesner, B. L., and E. C. Brady (2010), The sensitivity of the climate response to the magnitude and location of freshwater forcing: Last glacial maximum experiments, *Quat. Sci. Rev.*, *29*(1–2), 56–73, doi:10.1016/j.quascirev.2009.07.004.

Otto-Bliesner, B. L., E. C. Brady, G. Clauzet, R. Tomas, S. Levis, and Z. Kothavala (2006), Last Glacial Maximum and Holocene climate in CCSM3, *J. Clim.*, *19*(11), 2526–2544, doi:10.1175/JCLI3748.1.

Paterson, W. S. B. (1994), *The Physics of Glaciers*, 3rd ed., 480 pp., Pergamon, New York.

Peltier, W. R. (1994), Ice age paleotopography, *Science*, *265*, 195–201, doi:10.1126/science.265.5169.195.

Peltier, W. R. (1995), Paleotopography of glacial-age ice sheets: Reply, *Science*, *267*(5197), 536–538, doi:10.1126/science.267.5197.536-a.

Peltier, W. R. (1996), Mantle viscosity and ice-age ice sheet topography, *Science*, *273*(5280), 1359–1364, doi:10.1126/science.273.5280.1359.

Peltier, W. R. (2002), On eustatic sea level history: Last Glacial Maximum to Holocene, *Quat. Sci. Rev.*, *21*(1–3), 377–396, doi:10.1016/S0277-3791(01)00084-1.

Peltier, W. R. (2004), Global glacial isostasy and the surface of the ice-age Earth: The ICE-5 G (VM2) model and GRACE, *Annu. Rev. Earth Planet. Sci.*, *32*, 111–149, doi:10.1146/annurev.earth.32.082503.144359.

Peltier, W. R. (2005), On the hemispheric origins of meltwater pulse 1a, *Quat. Sci. Rev.*, *24*(14–15), 1655–1671, doi:10.1016/j.quascirev.2004.06.023.

Peltier, W. R. (2007), Rapid climate change and Arctic Ocean freshening, *Geology*, *35*(12), 1147–1148, doi:10.1130/focus122007.1.

Peltier, W. R., and R. G. Fairbanks (2006), Global glacial ice volume and Last Glacial Maximum duration from an extended Barbados sea level record, *Quat. Sci. Rev.*, *25*, 3322–3337, doi:10.1016/j.quascirev.2006.04.010.

Peltier, W. R., G. Vettoretti, and M. Stastna (2006), Atlantic meridional overturning and climate response to Arctic Ocean freshening, *Geophys. Res. Lett.*, *33*, L06713, doi:10.1029/2005GL025251.

Peltier, W. R., A. de Vernal, and C. Hillaire-Marcel (2008), Rapid climate change and Arctic Ocean freshening: Reply, *Geology*, *36*, e178, doi:10.1130/G24971Y.1.

Pisias, N. G., P. U. Clark, and E. J. Brook (2010), Modes of global climate variability during marine isotope stage 3 (60–26 ka), *J. Clim.*, *23*(6), 1581–1588, doi:10.1175/2009JCLI3416.1.

Pollard, D., and R. M. DeConto (2009), Modelling West Antarctic ice sheet growth and collapse through the past five million years, *Nature*, *458*(7236), 329–332, doi:10.1038/nature07809.

Polyak, L., M. Levitan, V. Gataullin, T. Khusid, V. Mikhailov, and V. Mukhina (2000), The impact of glaciation, river-discharge and sea-level change on Late Quaternary environments in the southwestern Kara Sea, *Int. J. Earth Sci.*, *89*(3), 550–562, doi:10.1007/s005310000119.

Polyak, L., D. A. Darby, J. F. Bischof, and M. Jakobsson (2007), Stratigraphic constraints on late Pleistocene glacial erosion and deglaciation of the Chukchi margin, Arctic Ocean, *Quat. Res.*, *67*(2), 234–245, doi:10.1016/j.yqres.2006.08.001.

Poore, R. Z., L. Osterman, W. B. Curry, and R. L. Phillips (1999), Late Pleistocene and Holocene meltwater events in the western Arctic Ocean, *Geology*, *27*(8), 759–762, doi:10.1130/0091-7613(1999)027<0759:LPAHME>2.3.CO;2.

Praetorius, S. K., J. F. McManus, D. W. Oppo, and W. B. Curry (2008), Episodic reductions in bottom-water currents since the last ice age, *Nat. Geosci.*, *1*(7), 449–452, doi:10.1038/ngeo227.

Price, S. F., H. Conway, and E. D. Waddington (2007), Evidence for late Pleistocene thinning of Siple Dome, West Antarctica, *J. Geophys. Res.*, *112*, F03021, doi:10.1029/2006JF000725.

Putnam, A. E., J. M. Schaefer, D. J. A. Barrell, M. Vandergoes, G. H. Denton, M. R. Kaplan, R. C. Finkel, R. Schwartz, B. M. Goehring, and S. E. Kelley (2010), In situ cosmogenic ^{10}Be production-rate calibration from the Southern Alps, New Zealand, *Quat. Geochronol.*, *5*(4), 392–409, doi:10.1016/j.quageo.2009.12.001.

Rasmussen, S. O., et al. (2006), A new Greenland ice core chronology for the last glacial termination, *J. Geophys. Res.*, *111*, D06102, doi:10.1029/2005JD006079.

Rayburn, J. A., T. M. Cronin, D. A. Franzi, P. L. K. Knuepfer, and D. A. Willard (2011), Timing and duration of North American glacial lake discharges and the Younger Dryas climate reversal, *Quat. Res.*, *75*(3), 541–551, doi:10.1016/j.yqres.2011.02.004.

Rech, J. A., J. C. Nekola, and J. S. Pigati (2012), Radiocarbon ages of terrestrial gastropods extend duration of ice-free conditions at the Two Creeks forest bed, Wisconsin, USA, *Quat. Res.*, *77*(2), 289–292, doi:10.1016/j.yqres.2011.11.007.

Reimer, P. J., et al. (2009), Intcal09 and Marine09 radiocarbon age calibration curves, 0–50,000 years cal BP, *Radiocarbon*, *51*(4), 1111–1150.

Ridge, J. C. (2003), The last deglaciation of the northeastern United States: A combined varve, paleomagnetic, and calibrated ^{14}C chronology, in *Geoarchaeology of Landscapes in the Glaciated Northeast U.S.*, edited by J. P. Hart and D. L. Cremeens, *N. Y. State Mus. Bull.*, *497*, 15–45.

Ridge, J. C. (2004), The Quaternary glaciation of western New England with correlations to surrounding areas, in *Quaternary Glaciations: Extent and Chronology. Part II: North America*, edited by J. Ehlers and P. L. Gibbard, pp. 212–231, Elsevier, Amsterdam, doi:10.1016/S1571-0866(04)80196-9.

Rignot, E., and S. S. Jacobs (2002), Rapid bottom melting widespread near Antarctic Ice Sheet grounding lines, *Science*, *296*, 2020–2023, doi:10.1126/science.1070942.

Rignot, E., G. Casassa, P. Gogineni, W. Krabill, A. Rivera, and R. Thomas (2004), Accelerated ice discharge from the Antarctic Peninsula following the collapse of Larsen B ice shelf, *Geophys. Res. Lett.*, *31*, L18401, doi:10.1029/2004GL020697.

Rignot, E., M. Koppes, and I. Velicogna (2010), Rapid submarine melting of the calving faces of West Greenland glaciers, *Nat. Geosci.*, *3*(3), 187–191, doi:10.1038/ngeo765.

Rinterknecht, V. R., L. Marks, J. A. Piotrowski, G. M. Raisbeck, F. Yiou, E. J. Brook, and P. U. Clark (2005), Cosmogenic Be-10 ages on the Pomeranian Moraine, Poland, *Boreas*, *34*(2), 186–191, doi:10.1080/03009480510012926.

Rinterknecht, V. R., et al. (2006), The last deglaciation of the southeastern sector of the Scandinavian Ice Sheet, *Science*, *311*(5766), 1449–1452, doi:10.1126/science.1120702.

Rinterknecht, V. R., I. E. Pavlovskaya, P. U. Clark, G. M. Raisbeck, F. Yiou, and E. J. Brook (2007), Timing of the last deglaciation in Belarus, *Boreas*, *36*, 307–313, doi:10.1111/j.1502-3885.2007.tb01252.x.

Robinson, L. F., J. F. Adkins, L. D. Keigwin, J. Southon, D. P. Fernandez, S.-L. Wang, and D. S. Scheirer (2005), Radiocarbon variability in the western North Atlantic during the last deglaciation, *Science*, *310*, 1469–1473, doi:10.1126/science.1114832.

Roche, D., D. Paillard, and E. Cortijo (2004), Constraints on the duration and freshwater release of Heinrich event 4 through isotope modelling, *Nature*, *432*(7015), 379–382, doi:10.1038/nature03059.

Rodrigues, C. G. (1992), Succession of invertebrate microfossils and the late Quaternary deglaciation of the central St. Lawrence

lowland, Canada and United States, *Quat. Sci. Rev.*, *11*, 503–534, doi:10.1016/0277-3791(92)90010-6.

Rohling, E. J., and H. Pälike (2005), Centennial-scale climate cooling with a sudden cold event around 8,200 years ago, *Nature*, *434*(7036), 975–979, doi:10.1038/nature03421.

Rooth, C. (1982), Hydrology and ocean circulation, *Prog. Oceanogr.*, *11*, 131–149, doi:10.1016/0079-6611(82)90006-4.

Scambos, T. A., J. A. Bohlander, C. A. Shuman, and P. Skvarca (2004), Glacier acceleration and thinning after ice shelf collapse in the Larsen B embayment, Antarctica, *Geophys. Res. Lett.*, *31*, L18402, doi:10.1029/2004GL020670.

Severinghaus, J. P., and E. J. Brook (1999), Abrupt climate change at the end of the last glacial period inferred from trapped air in polar ice, *Science*, *286*, 930–934.

Severinghaus, J. P., A. Grachev, B. Luz, and N. Caillon (2003), A method for precise measurement of argon 40/36 and krypton/argon ratios in trapped air in polar ice with applications to past firn thickness and abrupt climate change in Greenland and at Siple Dome, Antarctica, *Geochim. Cosmochim. Acta*, *67*(3), 325–343, doi:10.1016/S0016-7037(02)00965-1.

Shaffer, G., S. M. Olsen, and C. J. Bjerrum (2004), Ocean subsurface warming as a mechanism for coupling Dansgaard-Oeschger climate cycles and ice-rafting events, *Geophys. Res. Lett.*, *31*, L24202, doi:10.1029/2004GL020968.

Shakun, J. D., and A. E. Carlson (2010), A global perspective on Last Glacial Maximum to Holocene climate change, *Quat. Sci. Rev.*, *29*(15–16), 1801–1816, doi:10.1016/j.quascirev.2010.03.016.

Shakun, J. D., P. U. Clark, F. He, S. A. Marcott, A. C. Mix, Z. Y. Liu, B. Otto-Bliesner, A. Schmittner, and E. Bard (2012), Global warming preceded by increasing carbon dioxide concentrations during the last deglaciation, *Nature*, *484*(7392), 49, doi:10.1038/nature10915.

Shemesh, A., D. A. Hodell, X. Crosta, S. Kanfoush, C. D. Charles, and T. Guilderson (2002), Sequence of events during the last deglaciation in Southern Ocean sediments and Antarctic ice cores, *Paleoceanography*, *17*(4), 1056, doi:10.1029/2000PA000599.

Shennan, I., and G. A. Milne (2003), Sea-level observations around the Last Glacial Maximum from the Bonaparte Gulf, NW Australia, *Quat. Sci. Rev.*, *22*, 1543–1547.

Shipp, S., J. B. Anderson, and E. Domack (1999), Late Pleistocene-Holocene retreat of the West Antarctic Ice-Sheet system in the Ross Sea: Part 1—Geophysical results, *Geol. Soc. Am. Bull.*, *111*(10), 1486–1516, doi:10.1130/0016-7606(1999)111<1486:LPHROT>2.3.CO;2.

Shuman, B., P. J. Bartlein, and T. Webb III (2005), The magnitudes of millennial- and orbital-scale climatic change in eastern North America during the Late Quaternary, *Quat. Sci. Rev.*, *24*(20–21), 2194–2206, doi:10.1016/j.quascirev.2005.03.018.

Siddall, M., E. J. Rohling, W. G. Thompson, and C. Waelbroeck (2008), Marine isotope stage 3 sea level fluctuations: Data synthesis and new outlook, *Rev. Geophys.*, *46*, RG4003, doi:10.1029/2007RG000226.

Siddall, M., G. A. Milne, and V. Masson-Delmotte (2012), Uncertainties in elevation changes and their impact on Antarctic temperature records since the end of the last glacial period, *Earth Planet. Sci. Lett.*, *315–316*, 12–23, doi:10.1016/j.epsl.2011.04.032.

Siegert, M. J., and J. A. Dowdeswell (2002), Late Weichselian iceberg, surface-melt and sediment production from the Eurasian Ice Sheet: results from numerical ice-sheet modelling, *Mar. Geol.*, *188*, 109–127.

Siegert, M. J., and J. A. Dowdeswell (2004), Numerical reconstructions of the Eurasian ice sheet and climate during the Late Weichselian, *Quat. Sci. Rev.*, *23*(11–13), 1273–1283, doi:10.1016/j.quascirev.2003.12.010.

Singarayer, J. S., and P. J. Valdes (2010), High-latitude climate sensitivity to ice-sheet forcing over the last 120 kyr, *Quat. Sci. Rev.*, *29*(1–2), 43–55, doi:10.1016/j.quascirev.2009.10.011.

Skinner, L. C., N. J. Shackleton, and H. Elderfield (2003), Millennial-scale variability of deep-water temperature and $\delta^{18}O_{dw}$ indicating deep-water source variations in the Northeast Atlantic, 0–34 cal. ka BP, *Geochem. Geophys. Geosyst.*, *4*(12), 1098, doi:10.1029/2003GC000585.

Smith, D. G., and T. G. Fisher (1993), Glacial Lake Agassiz: the northwestern outlet and paleoflood, *Geology*, *21*, 9–12.

Smith, J. A., C. D. Hillenbrand, C. J. Pudsey, C. S. Allen, and A. G. C. Graham (2010), The presence of polynyas in the Weddell Sea during the Last Glacial Period with implications for the reconstruction of sea-ice limits and ice sheet history, *Earth Planet. Sci. Lett.*, *296*(3–4), 287–298, doi:10.1016/j.epsl.2010.05.008.

Spence, J. P., M. Eby, and A. J. Weaver (2008), The sensitivity of the Atlantic meridional overturning circulation to freshwater forcing at eddy-permitting resolutions, *J. Clim.*, *21*(11), 2697–2710, doi:10.1175/2007JCLI2103.1.

Spielhagen, R. F., H. Erlenkeuser, and C. Siegert (2005), History of freshwater runoff across the Laptev Sea (Arctic) during the last deglaciation, *Global Planet. Change*, *48*(1–3), 187–207, doi:10.1016/j.gloplacha.2004.12.013.

Stanford, J. D., E. J. Rohling, S. E. Hunter, A. P. Roberts, S. O. Rasmussen, E. Bard, J. McManus, and R. G. Fairbanks (2006), Timing of meltwater pulse 1a and climate responses to meltwater injections, *Paleoceanography*, *21*, PA4103, doi:10.1029/2006PA001340.

Stanford, J. D., E. J. Rohling, S. Bacon, A. P. Roberts, F. E. Grousset, and M. Bolshaw (2011a), A new concept for the paleoceanographic evolution of Heinrich event 1 in the North Atlantic, *Quat. Sci. Rev.*, *30*(9–10), 1047–1066, doi:10.1016/j.quascirev.2011.02.003.

Stanford, J. D., R. Hemingway, E. J. Rohling, P. G. Challenor, M. Medina-Elizade, and A. J. Lester (2011b), Sea-level probability for the last deglaciation: A statistical analysis of far-field records, *Global Planet. Change*, *79*, 193–203, doi:10.1016/j.gloplacha.2010.11.002.

Steig, E. (2006), Climate may not be linked with circulation slowdowns, *Nature*, *439*, 660.

Steig, E. J., E. Brook, J. White, C. M. Sucher, M. Bender, S. J. Lehman, D. L. Morse, E. D. Waddington, and G. D. Clow (1998), Synchronous climate changes in Antarctica and the North Atlantic, *Science*, *282*, 92–95, doi:10.1126/science.282.5386.92.

Stenni, B., et al. (2011), Expression of the bipolar see-saw in Antarctic climate records during the last deglaciation, *Nat. Geosci.*, *4*, 46–49, doi:10.1038/ngeo1026.

Stocker, T. F., and S. J. Johnsen (2003), A minimum thermodynamic model for the bipolar seesaw, *Paleoceanography*, *18*(4), 1087, doi:10.1029/2003PA000920.

Stocker, T. F., and D. Wright (1991), Rapid transitions of the ocean's deep circulation induced by changes in surface water fluxes, *Nature*, *351*, 729–732, doi:10.1038/351729a0.

Stocker, T. F., A. Timmermann, M. Renold, and O. Timm (2007), Effects of salt compensation on the climate model response in simulations of large changes of the Atlantic meridional overturning circulation, *J. Clim.*, *20*(24), 5912–5928, doi:10.1175/2007JCLI1662.1.

Stokes, C. R., and L. Tarasov (2010), Ice streaming in the Laurentide Ice Sheet: A first comparison between data-calibrated numerical model output and geological evidence, *Geophys. Res. Lett.*, *37*, L01501, doi:10.1029/2009GL040990.

Stokes, C. R., C. D. Clark, and R. Storrar (2009), Major changes in ice stream dynamics during deglaciation of the north-western margin of the Laurentide Ice Sheet, *Quat. Sci. Rev.*, *28*(7–8), 721–738, doi:10.1016/j.quascirev.2008.07.019.

Stone, J. O., G. A. Balco, D. E. Sugden, M. W. Caffee, L. C. Sass III, S. G. Cowdery, and C. Siddoway (2003), Holocene deglaciation of Marie Byrd Land, West Antarctica, *Science*, *299*, 99–102, doi:10.1126/science.1077998.

Stoner, J. S., J. E. T. Channell, C. Hillaire-Marcel, and C. Kissel (2000), Geomagnetic paleointensity and environmental record from Labrador Sea core MD95-2024: Global marine sediment and ice

core chronostratigraphy for the last 110 kyr, *Earth Planet. Sci. Lett.*, *183*(1–2), 161–177, doi:10.1016/S0012-821X(00)00272-7.

Stott, L., A. Timmermann, and R. Thunell (2007), Southern Hemisphere and deep-sea warming led deglacial atmospheric CO_2 rise and tropical warming, *Science*, *318*(5849), 435–438, doi:10.1126/science.1143791.

Stouffer, R. J., et al. (2006), Investigating the causes of the response of the thermohaline circulation to past and future climate changes, *J. Clim.*, *19*(8), 1365–1387, doi:10.1175/JCLI3689.1.

Stouffer, R. J., D. Seidov, and B. J. Haupt (2007), Climate response to external sources of freshwater: North Atlantic versus the Southern Ocean, *J. Clim.*, *20*(3), 436–448, doi:10.1175/JCLI4015.1.

Strasky, S., L. di Nicola, C. Baroni, M. C. Salvatore, H. Baur, P. W. Kubik, C. Schluchter, and R. Wieler (2009), Surface exposure ages imply multiple low-amplitude Pleistocene variations in East Antarctic Ice Sheet, Ricker Hills, Victoria Land, *Antarct. Sci.*, *21*(1), 59–69, doi:10.1017/S0954102008001478.

Stroeven, A. P., D. Fabel, J. M. Harbor, D. Fink, M. W. Caffee, and T. Dahlgren (2011), Importance of sampling across an assemblage of glacial landforms for interpreting cosmogenic ages of deglaciation, *Quat. Res.*, *76*(1), 148–156, doi:10.1016/j.yqres.2011.04.004.

Stuiver, M., G. Denton, T. J. Hughes, and J. Fastook (1981), History of the marine ice sheet in West Antarctica during the last glaciation: A working hypothesis, in *The Last Great Ice Sheets*, edited by G. H. Denton and T. J. T. J. Hughes, pp. 319–436, John Wiley, New York.

Sugden, D. E. (1977), Reconstruction of the morphology, dynamics, and thermal characteristics of the Laurentide Ice Sheet at its maximum, *Arct. Alp. Res.*, *9*, 21–47, doi:10.2307/1550407.

Sugden, D. E., and S. H. Watts (1977), Tors, felsenmeer, and glaciation in northern Cumberland Peninsula, Baffin Island, *Can. J. Earth Sci.*, *14*(12), 2817–2823, doi:10.1139/e77-248.

Sugden, D. E., G. Balco, S. G. Cowdery, J. O. Stone, and L. C. Sass (2005), Selective glacial erosion and weathering zones in the coastal mountains of Marie Byrd Land, Antarctica, *Geomorphology*, *67*(3–4), 317–334, doi:10.1016/j.geomorph.2004.10.007.

Surovell, T. A., V. T. Holliday, J. A. M. Gingerich, C. Ketron, C. V. Haynes, I. Hilman, D. P. Wagner, E. Johnson, and P. Claeys (2009), An independent evaluation of the Younger Dryas extra-terrestrial impact hypothesis, *Proc. Natl. Acad. Sci. U. S. A.*, *106*(43), 18,155–18,158, doi:10.1073/pnas.0907857106.

Svensson, A., et al. (2008), A 60,000 year Greenland stratigraphic ice core chronology, *Clim. Past*, *4*(1), 47–57, doi:10.5194/cp-4-47-2008.

Swarzenski, P. W., D. Porcelli, P. S. Andersson, and J. M. Smoak (2003), The behavior of U- and Th-series nuclides in the estuarine environment, *Rev. Mineral. Geochem.*, *52*, 577–606, doi:10.2113/0520577.

Tarasov, L., and W. R. Peltier (2004), A geophysically constrained large ensemble analysis of the deglacial history of the North American ice-sheet complex, *Quat. Sci. Rev.*, *23*(3–4), 359–388, doi:10.1016/j.quascirev.2003.08.004.

Tarasov, L., and W. R. Peltier (2005), Arctic freshwater forcing of the Younger Dryas cold reversal, *Nature*, *435*(7042), 662–665, doi:10.1038/nature03617.

Tarasov, L., and W. R. Peltier (2006), A calibrated deglacial drainage chronology for the North American continent: Evidence of an Arctic trigger for the Younger Dryas, *Quat. Sci. Rev.*, *25*(7–8), 659–688, doi:10.1016/j.quascirev.2005.12.006.

Tarasov, L., A. S. Dyke, R. M. Neal, and W. R. Peltier (2012), A data-calibrated distribution of deglacial chronologies for the North American ice complex from glaciological modeling, *Earth Planet. Sci. Lett.*, *315–316*, 30–40, doi:10.1016/j.epsl.2011.09.010.

Taylor, F. W., and P. Mann (1991), Late Quaternary folding of coral-reef terraces, Barbados, *Geology*, *19*, 103–106, doi:10.1130/0091-7613(1991)019<0103:LQFOCR>2.3.CO;2.

Telford, R. J. (2006), Limitations of dinoflagellate cyst transfer functions, *Quat. Sci. Rev.*, *25*(13–14), 1375–1382, doi:10.1016/j.quascirev.2006.02.012.

Teller, J. T., and M. Boyd (2006), Two possible routings for overflow from Lake Agassiz during the Younger Dryas: A reply to comment by T. Fisher, T. Lowell, H. Loope on "Alternative routing of Lake Agassiz overflow during the Younger Dryas: New dates, paleotopography, a re-evaluation", *Quat. Sci. Rev.*, *25*(9–10), 1142–1145, doi:10.1016/j.quascirev.2006.01.011.

Teller, J. T., D. W. Leverington, and J. D. Mann (2002), Freshwater outbursts to the oceans from glacial Lake Agassiz and their role in climate change during the last deglaciation, *Quat. Sci. Rev.*, *21*(8–9), 879–887, doi:10.1016/S0277-3791(01)00145-7.

Teller, J. T., M. Boyd, Z. R. Yang, P. S. G. Kor, and A. M. Fard (2005), Alternative routing of Lake Agassiz overflow during the Younger Dryas: New dates, paleotopography, and a re-evaluation, *Quat. Sci. Rev.*, *24*(16–17), 1890–1905, doi:10.1016/j.quascirev.2005.01.008.

Thompson, W. B., C. B. Griggs, N. G. Miller, R. E. Nelson, T. K. Weddle, and T. M. Kilian (2011), Associated terrestrial and marine fossils in the late-glacial Presumpscot Formation, southern Maine, USA, and the marine reservoir effect on radiocarbon ages, *Quat. Res.*, *75*(3), 552–565, doi:10.1016/j.yqres.2011.02.002.

Thornalley, D. J. R., H. Elderfield, and I. N. McCave (2009), Holocene oscillations in temperature and salinity of the surface subpolar North Atlantic, *Nature*, *457*, 711–714.

Thornalley, D. J. R., I. N. McCave, and H. Elderfield (2010), Freshwater input and abrupt deglacial climate change in the North Atlantic, *Paleoceanography*, *25*, PA1201, doi:10.1029/2009PA001772.

Thornalley, D. J. R., I. N. McCave, and H. Elderfield (2011a), Tephra in deglacial ocean sediments south of Iceland: Stratigraphy, geochemistry and oceanic reservoir ages, *J. Quat. Sci.*, *26*(2), 190–198, doi:10.1002/jqs.1442.

Thornalley, D. J. R., S. Barker, W. S. Broecker, H. Elderfield, and I. N. McCave (2011b), The deglacial evolution of North Atlantic deep convection, *Science*, *331*(6014), 202–205, doi:10.1126/science.1196812.

Timmermann, A., U. Krebs, F. Justino, H. Goosse, and T. Ivanochko (2005), Mechanisms for millennial-scale global synchronization during the last glacial period, *Paleoceanography*, *20*, PA4008, doi:10.1029/2004PA001090.

Todd, C., and J. Stone (2004), Deglaciation of the southern Ellsworth Mountains, Weddell Sea sector of the West Antarctic Ice Sheet, paper presented at 11th Annual WAIS Workshop, West Antarct. Ice Sheet Initiative, Sterling, Va.

Todd, C., J. Stone, H. Conway, B. Hall, and G. Bromley (2010), Late Quaternary evolution of Reedy Glacier, Antarctica, *Quat. Sci. Rev.*, *29*, 1328–1341.

Toggweiler, J. R. (2008), Origin of the 100,000-year timescale in Antarctic temperatures and atmospheric CO_2, *Paleoceanography*, *23*, PA2211, doi:10.1029/2006PA001405.

Törnqvist, T., and M. P. Hijma (2012), Links between early Holocene ice-sheet decay, sea-level rise and abrupt climate change, *Nat. Geosci.*, *5*, 601–606.

Törnqvist, T. E., S. J. Bick, J. L. Gonzalez, K. van der Borg, and A. F. M. de Jong (2004a), Tracking the sea-level signature of the 8.2 ka cooling event: New constraints from the Mississippi Delta, *Geophys. Res. Lett.*, *31*, L23309, doi:10.1029/2004GL021429.

Törnqvist, T. E., J. L. Gonzalez, L. A. Newsom, K. van der Borg, A. F. M. de Jong, and C. W. Kurnik (2004b), Deciphering Holocene sea-level history on the US Gulf Coast: A high-resolution record from the Mississippi Delta, *Geol. Soc. Am. Bull.*, *116*(7), 1026–1039, doi:10.1130/B2525478.1.

Törnqvist, T. E., S. J. Bick, K. van der Borg, and A. F. M. de Jong (2006), How stable is the Mississippi Delta?, *Geology*, *34*(8), 697–700, doi:10.1130/G22624.1.

Valdes, P. (2011), Built for stability, *Nat. Geosci.*, *4*(7), 414–416, doi:10.1038/ngeo1200.

Waddington, E. D., H. Conway, E. J. Steig, R. B. Alley, E. J. Brook, K. C. Taylor, and J. W. C. White (2005), Decoding the dipstick: Thickness of Siple Dome, West Antarctica, at the Last Glacial Maximum, *Geology*, *33*(4), 281–284, doi:10.1130/G21165.1.

Wadleigh, M. A., J. Veizer, and C. Brooks (1985), Strontium and its isotopes in Canadian rivers - fluxes and global implications, *Geochim. Cosmochim. Acta*, *49*, 1727–1736, doi:10.1016/0016-7037(85)90143-7.

Waelbroeck, C., J.-C. Duplessy, E. Michel, L. Labeyrie, D. Paillard, and J. Duprat (2001), The timing of the last deglaciation in North Atlantic climate records, *Nature*, *412*, 724–727, doi:10.1038/35089060.

Wang, Y. J., H. Cheng, R. L. Edwards, Z. S. An, J. Y. Wu, C.-C. Shen, and J. A. Dorale (2001), A high-resolution absolute-dated late Pleistocene monsoon record from Hulu Cave, China, *Science*, *294*, 2345–2348, doi:10.1126/science.1064618.

Weaver, A. J., O. A. Saenko, P. U. Clark, and J. X. Mitrovica (2003), Meltwater pulse 1A from Antarctica as a trigger of the Bolling-Allerod warm interval, *Science*, *299*(5613), 1709–1713, doi:10.1126/science.1081002.

Weber, M. E., P. U. Clark, W. Ricken, J. X. Mitrovica, S. W. Hostetler, and G. Kuhn (2011), Interhemispheric ice-sheet synchronicity during the Last Glacial Maximum, *Science*, *334*(6060), 1265–1269, doi:10.1126/science.1209299.

Winsor, K., A. E. Carlson, G. P. Klinkhammer, J. S. Stoner, and R. G. Hatfield (2012), Evolution of the northeast Labrador Sea during the last interglaciation, *Geochem. Geophys. Geosyst.*, *13*, Q11006, doi:10.1029/2012GC004263.

Wright, H. E., Jr. (1972), Interglacial and postglacial climates: The pollen record, *Quat. Res.*, *2*, 274–282, doi:10.1016/0033-5894(72)90048-8.

Wright, H. E., Jr. (1981), Vegetation east of the Rocky Mountains 18,000 years ago, *Quat. Res.*, *15*, 113–125, doi:10.1016/0033-5894(81)90099-5.

Wunsch, C. (2010), Towards understanding the Paleocean, *Quat. Sci. Rev.*, *29*(17–18), 1960–1967, doi:10.1016/j.quascirev.2010.05.020.

Yang, C., K. Telmer, and J. Veizer (1996), Chemical dynamics of the "St Lawrence" riverine system: δD_{H2O}, $\delta^{18}O_{H2O}$, $\delta^{13}C_{DIC}$, $\delta^{34}S_{sulfate}$, and dissolved $^{87}Sr/^{86}Sr$, *Geochim. Cosmochim. Acta*, *60*, 851–866, doi:10.1016/0016-7037(95)00445-9.

Yokoyama, Y., K. Lambeck, P. De Deckker, P. Johnston, and L. K. Fifield (2000), Timing of the Last Glacial Maximum from observed sea-level minima, *Nature*, *406*, 713–716, doi:10.1038/35021035.

Yokoyama, Y., P. De Deckker, K. Lambeck, P. Johnston, and L. K. Fifield (2001), Sea-level at the Last Glacial Maximum: Evidence from northwestern Australia to constrain ice volumes for oxygen isotope stage 2, *Palaeogeogr. Palaeoclimatol. Palaeoecol.*, *165*(3–4), 281–297, doi:10.1016/S0031-0182(00)00164-4.

Yokoyama, Y., P. De Deckker, and K. Lambeck (2003), Reply to "Sea-level observations around the Last Glacial Maximum from the Bonaparte Gulf, NW Australia" by I. Shennan and G. Milne, *Quat. Sci. Rev.*, *22*(14), 1549–1550, doi:10.1016/S0277-3791(03)00089-1.

Yu, S. Y., B. E. Berglund, P. Sandgren, and K. Lambeck (2007), Evidence for a rapid sea-level rise 7600 yr ago, *Geology*, *35*(10), 891–894, doi:10.1130/G23859A.1.

Zahn, R., J. Schonfeld, H. R. Kudrass, M. H. Park, H. Erlenkeuser, and P. Grootes (1997), Thermohaline instability in the North Atlantic during meltwater events: Stable isotope and ice-rafted detritus records from core SO75-26KL, *Paleoceanography*, *12*, 696–710, doi:10.1029/97PA00581.